Universidade de Aveiro Departamento de Química
Ano 2014

Maria Elisabete Alves Maciel

Oxidação e glicoxidação da fosfatidilserina e os seus efeitos na resposta imune: uma abordagem lipidómica

Oxidation and glycoxidation of phosphatidylserine and their effect in immune response: a lipidomic approach

Universidade de Aveiro Departamento de Química
Ano 2014

Maria Elisabete Alves Maciel

Oxidação e glicoxidação da fosfatidilserina e os seus efeitos na resposta imune: uma abordagem lipidómica

Oxidation and glycoxidation of phosphatidylserine and their effect in immune response: a lipidomic approach

Tese apresentada à Universidade de Aveiro para cumprimento dos requisitos necessários à obtenção do grau de Doutor em Bioquímica, realizada sob a orientação científica da Doutora Maria do Rosário Gonçalves dos Reis Marques Domingues, Professora auxiliar com Agregação do Departamento de Química da Universidade de Aveiro e do Doutor Pedro Miguel Dimas Neves Domingues, Professor auxiliar com Agregação do Departamento de Química da Universidade de Aveiro.

Apoio financeiro do POPH-QREN no âmbito do III Quadro Comunitário de Apoio.

Apoio financeiro da FCT e do FSE no âmbito do III Quadro Comunitário de Apoio.

Dedico este trabalho aos meus pais e ao meu irmão pelo incansável apoio.

o júri

presidente

Prof. Doutor Carlos Manuel Martins da Costa
Professor Catedrático da Universidade de Aveiro

vogais

Prof. Doutor Jorge Eduardo da Silva Azevedo
Professor Catedrático do Instituto de Ciências Biomédicas Abel Salazar, instituto de Biologia Molecular e Celular da Universidade do Porto

Prof. Doutora Maria do Rosário Gonçalves Reis Marques Domingues
Professora Auxiliar com Agregação da universidade de Aveiro. (Orientadora)

Prof. Doutora Maria Amália da Silva Jurado
Professora Auxiliar do Centro de Neurociências e Biologia celular da Faculdade de Ciências e Tecnologia da Universidade de Coimbra

Prof. Doutora Maria Teresa Teixeira Cruz Rosete
Professora auxiliar do Centro de Neurociências e Biologia celular da Faculdade de Farmácia da Universidade de Coimbra

Prof. Doutora Rita Maria Pinho Ferreira
Professora Auxiliar da Universidade de Aveiro

agradecimentos

Em primeiro lugar gostaria de agradecer à minha orientadora, a Doutora Rosário Domingues, por ter acreditado em mim, por todo o apoio que me prestou e pela motivação e incentivo constantes, nunca me deixando sem rumo e nem ir a baixo quando as coisas corriam menos bem.

Agradeço ao Doutor Pedro Domingues pela orientação, disponibilidade e principalmente por todo o conhecimento que me transmitiu.

Agradeço à Doutora Corinne Spickett por me ter recebido no seu laboratório na Universidade de Aston e a Doutora Ana Reis que me ajudou no desenvolvimento do trabalho nesse laboratório contribuindo não só para o enriquecimento deste trabalho mas também a nível pessoal.

Agradeço ao João Martins e ao Doutor Bruno Neves pela grande ajuda que me prestaram e pelos conhecimentos que me transmitiram, agradeço também à Professora Doutora Teresa Cruz que me recebeu no seu laboratório e pela colaboração.

Queria também agradecer à Juliana Felgueiras pela incansável ajuda e à Doutora Margarida Fardilha pela colaboração.

Agradeço a todos as minhas colegas de laboratório à Cláudia, à Ana, à Tânia, à Rita, à Elisabete e ao André por todo o companheirismo, pelas horas do café e pelo bom ambiente no laboratório que sempre proporcionaram. Agradeço também a todas as pessoas do grupo de espectrometria de massa que me receberam e que sempre me trataram bem, um agradecimento especial à Dra. Cristina Barros que me acompanhou e que me ouvi em todos os momentos ao longo destes anos.

Agradeço a todos os meus amigos, em especial à Joana que sempre me acompanhou e apoiou e que teve sempre um tempinho para me ouvir nos momentos menos bons.

Queria fazer um agradecimento especial ao Daniel pelo apoio e pela paciência que teve ao longo deste anos que nem sempre foram fáceis, mas que esteve sempre do meu lado.
Um grandíssimo obrigado à minha família em especial aos meus pais, ao meu irmão e aos meus avós que sempre acreditaram em mim e que sempre me deram forças para continuar.

Agradeço à FCT pelo financiamento através de uma bolsa de doutoramento (SFRH/BD/73203/2010
Agradeço à Unidade de Investigação QOPNA da Universidade de Aveiro.
Agradeço o apoio aos projetos PTDC/QUI-BIQ/104968/2008 e PTDC/SAL/OSM/099762/2008 financiados por FCT, do projeto COMPETE-Programa Operacional Fatores de competitividade (FEDER)

palavras-chave

Fosfatidilserina, fosfolipidos, espectrometria de massa, stress oxidativo, glicação, macrofagos,inflamação

resumo

A fosfatidilserina (PS) é um fosfolípido que se encontra em todas as células de mamíferos e desempenha um papel importante em processos biológicos, tais como, a coagulação sanguínea e a apoptose. A externalização da PS em células apoptóticas é reconhecida pelos recetores dos macrófagos, sendo uma via de sinalização essencial para a eliminação destas células. Nos últimos anos, tem sido proposto que a externalização da PS pode estar associada oxidação, e que a PS oxidada (oxPS) parece ser mais facilmente reconhecida pelos macrófagos do que a PS não oxidada. No entanto as modificações geradas pela oxidação da PS, assim como os seus efeitos biológicos são ainda pouco conhecidas. A PS, tal como outros fosfolípidos, pode ser facilmente oxidada em especial quando tem na sua composição ácidos gordos polinsaturados. Por outro lado, o grupo amina livre do aminoácido serina do grupo polar da PS pode sofrer glicação por reação com o grupo carbonilo da glucose, aumentando assim a sua suscetibilidade à oxidação. O principal objetivo deste trabalho foi caracterizar e identificar produtos de oxidação e glicação de PS e desta forma contribuir para a compreensão do seu papel biológico especialmente na resposta imune e inflamatória.

Para alcançar o objetivo proposto, procedeu-se à oxidação da PS. Para este fim, foram selecionados compostos modelo de PS com diferentes composições de ácidos gordos: 1-palmitoil-2-oleoil-sn-glicero-3-fosfo-L-serina (POPS); 1,2-dipalmitoil-sn-glicero-3-fosfo-L-serina (DPPS); 1-palmitoil-2-linoleoil-sn-glicero-3-fosfo-L-serina (PLPS) e 1-palmitoil-2-araquidonoil-sn-glicero-3-fosfo-L-serina (PAPS). De modo a completar o estudo procedeu-se também à oxidação da PAPS e POPS glicadas. As reações de oxidação foram realizadas em sistemas modelo usando diferentes reagentes oxidantes: HO• e dicloridrato de 2,2'-azo-bis- (2-amidinopropano) (AAPH). A caracterização estrutural detalhada dos produtos obtidos nas diversas reações foi realizada por espectrometria de massa (MS) com ionização por *electrospray* (ESI) ESI-MS e por espectrometria se massa tandem (MS/MS) acoplada a técnicas de separação como cromatografia de camada fina (TLC) (off-line TLC-MS) e cromatografia líquida (LC) (on line LC-MS).

Os resultados obtidos neste trabalho permitiram identificação dos vários produtos de oxidação de PS e PS glicada, observando-se modificações na cadeia acilo insaturada. Observaram-se também produtos de oxidação formados devido a alterações estruturais no grupo polar com formação de produtos com terminais: acetamida, hidroperoxiacetaldeido e ácido acético (ácido glicerofosfoacetico, GPAA). A caracterização por MS/MS permitiu identificar as vias de fragmentação específicas de cada tipo de produto de oxidação. Com base nas vias de fragmentação identificadas anteriormente, foi realizada uma análise de lipidómica direcionada "targeted lipidomic" para detetar os produtos resultantes da oxidação do grupo polar da PS em queratinócitos HaCaT tratados com AAPH, como estímulo de stress oxidativo.

Com esta abordagem direcionada foi possível detetar derivados GPAA nos extratos lipídicos obtidos destas células HaCaT, confirmando a possibilidade de oxidação de cabeça de PS em sistemas biológicos. Os estudos de oxidação de PS glicadas mostraram que as PS glicadas oxidam mais facilmente que as suas congéneres não glicadas. Durante a oxidação de PS glicada, além da oxidação nas cadeias acilo foram identificadas novos produtos de oxidação devido a degradação oxidativa na molécula de glucose ligada á PS, identificados como PS-AGES (do inglês, PS- Advanced glycation end products).

Com o objetivo de investigar o efeito da radiação UVA na membrana fosfolipídica e, em particular, no perfil de fosfatidilserinas, foi realizado um estudo com linhas celulares de melanoma (SK-MEL-28). Após a exposição à radiação UVA das linhas SK-MEL-28, os extratos lipídicos foram analisados por LC-MS e MS/MS e GC-MS. Os resultados não revelaram diferenças significativas no teor de PS após a exposição. A nível molecular, apenas a PS (18:0/18:1) diminuiu no momento da irradiação, sugerindo algum dano oxidativo, mas que foi revertido nos tempos seguintes. As mudanças mais significativas no teor de fosfolípidos ocorreram nas classes da fosfatidilcolina e fosfatidilinositol, observando-se um aumento da concentração relativa de ácidos gordos monoinsaturados (MUFA). As alterações observadas nos lípidos parecem estar relacionadas com a lipogénese e com desenvolvimento e progressão do cancro. Curiosamente, apesar do UVA estar associado ao dano oxidativo, não foi possível observar neste estudo a presença fosfolípidos oxidados. Para o estudo das propriedades anti- e pró-inflamatórias da PLPS oxidada (oxPLPS) e PLPS não oxidados foi avaliada a produção de óxido nítrico (NO) por macrófagos na presença e na ausência do estímulo inflamatório, o lipopolissacarídeo (LPS). Os resultados obtidos mostraram que não houve alteração na produção de NO em macrófagos estimulados com PS e oxPS na ausência de LPS. Por outro lado observou-se que no caso de macrófagos estimulados com LPS, o oxPLPS inibiu significativamente a produção de NO induzida por LPS, enquanto que o PLPS não mostrou qualquer efeito significativo. A nível molecular, observou-se que a diminuição de NO foi mediada pela inibição da fosforilação da c-Jun-N-terminal quinase (JNK) e na translocação nuclear do p65 NF-$_k$B. Em geral estes dados sugerem que oxPLPS, mas não PLPS, reduz a sinalização pró-inflamatória em macrófagos, contribuindo para a contenção de inflamação durante apoptose celular.

Os resultados obtidos nesta dissertação fornecem nova informação sobre as modificações da PS, facilitando a sua identificação em amostras complexas, nomeadamente em condições fisiopatológicas e também, informação que permite uma melhor compreensão sobre o papel da oxPS e PS na resposta inflamatória, no processo de apoptose e em outras funções biológicas.

keywords

Phosphatidylserine, phospholipids, mass spectrometry, oxidative stress, glycation, macrophages, inflammation.

abstract

Phosphatidylserine (PS) is a member of the class of phospholipids, and is distributed among all cells of mammalians, playing important roles in diverse biological processes, including blood clotting and apoptosis. When externalized, PS is a ligand that is recognized on apoptotic cells. It has been considered that before externalization PS is oxidized and oxPS enhance the recognition by macrophages receptors, however the knowledge about oxidation of PS is still limited. PS, like others phospholipids, has two fatty acyl chains and one polar head group, in this case is the amino acid serine. The modifications in PS structure can occur by oxidation of the unsaturated fatty acyl chains and by glycation of the polar head group, due to free amine group, thus increasing the susceptibility to oxidative events. The main goal of this work was to characterize and identify oxidized and glycoxidized PS, contributing to the knowledge of the biological role of oxidation products of PS, as well as of glycated PS, in immune and inflammatory processes.

To achieve this goal, PS standards (1-palmitoyl-2-oleoyl-sn-glycero-3-phospho-L-serine (POPS), 1,2-dipalmitoyl-sn-glycero-3-phospho-L-serine (DPPS), 1-palmitoyl-2-linoleoyl-sn-glycero-3-phospho-L-serine (PLPS) and 1-palmitoyl-2-arachidonoyl-sn-glycero-3-phospho-L-serine (PAPS)) and glycated PS (PAPS and POPS) were induced to oxidize in model systems, using different oxidant reagents: HO• and 2,2'-azobis-2-methyl-propanimidamide dihydrochloride (AAPH) . The detailed structural characterization of the oxidative products was performed by ESI-MS and MS/MS coupled to separation techniques such as off line TLC-MS and on line LC-MS, in order to obtained better characterization of the larger number of PS and glycated PS oxidation products.

The results obtained in this work allowed to identify several oxidation products of PS and glycated PS with modifications in unsaturated fatty acyl chain. Also, oxidation products formed due to structural changes in the serine polar head with formation of terminal acetamide, terminal hydroperoxyacetaldehyde.and terminal acetic acid (glycerophosphacetic acid, GPAA) were identified. The mass spectrometric specific fragmentation pathway of each type of oxidation product was determined using different mass spectrometry approaches. Based on the identified fragmentation pathways, targeted lipidomic analysis was performed to detect oxidation products modified in serine polar head in HaCaT cell line treated with AAPH. The GPAA was detected in HaCaT cells treated with AAPH to induce oxidative stress, thus confirming that modifications in PS polar head is possible to occur in biological systems. Furthermore, it was found that glycated PS species are more prone to oxidative modifications when compared with non glycated PS. During oxidation of glycated PS, besides the oxidation in acyl chains, new oxidation products due to oxidation of the glucose moiety were identified, including PS advanced glycation end products (PS-AGES).

To investigate if UVA oxidative stress exerted changes in the lipidome of melanoma cell lines, particularly in PS profile, a lipidomic analysis was performed. The lipid profile was obtained using HILIC-LC-MS and GC-MS analysis of the total lipid extracts obtained from human melanoma cell line (SK-MEL-28) after UVA irradiation at 0, 2 and 24 hours. The results did not showed significant differences in PS content. At molecular level, only PS (18:0:18:1) decreased at the moment of irradiation. The most significant changes in phospholipids content occurred in phosphatidylcholines (PC) and phosphatidylinositol (PI) classes, with an increase of mono-unsaturated fatty acid (MUFA), similarly as observed for the fatty acid analysis. Overall, these data indicate that the observed membrane lipid changes associated with lipogenesis after UVA exposure may be correlated with malignant transformations associated with cancer development and progression. Despite of UVA radiation is associated with oxidative damage, in this work was not possible observe oxidation phospholipids.

The anti/pro-inflammatory properties of the oxidized PLPS (oxPLPS) versus non-oxidized PLPS were tested on LPS stimulated RAW 264.7 macrophages. The modulation of intracellular signaling pathways such as NF-kB and MAPK cascades by oxPLPS and PS was also examined in this study. The results obtained from evaluation of anti/pro-inflammatory properties showed that neither PLPS or oxPLPS species activated the macrophages. Moreover only oxidized PLS were found to significantly inhibit NO production and iNOS and il1β gene transcription induced by LPS. The analysis at molecular level showed that this was the result of the attenuation of LPS-induced c-Jun-N-terminal kinase (JNK) and p65 NF-$_k$B nuclear translocation. Overall these data suggest that oxPLPS, but not native PLPS, mitigates pro-inflammatory signaling in macrophages, contributing to containment of inflammation during apoptotic cell engulfment.

The results obtained in this work provides new information on the modifications of PS, facilitating the identification of oxidized species in complex samples, namely under physiopathologic conditions and also contributes to a better understanding of the role of oxPS and PS in the inflammatory response, in the apoptotic process and other biological functions

Publicações

Publicações em Revistas Cientificas Internacionais com Referee:

E. Maciel, J. Felgueiras, E.M.P Silva., A.S.P Moreira, M. Fardilha, P. Domingues, M.R.M. Domingues, UVA exposure induces changes in the lipid profile of human melanoma cells, submitted to Journal of Cellular Physiology.

E. Maciel, R.N. da Silva, C. Simoes, P. Domingues, M.R.M. Domingues, Structural Characterization of Oxidized Glycerophosphatidylserine: Evidence of Polar Head Oxidation, J. Am. Soc. Mass Spectrom., 22 (2011) 1804-1814.

E. Maciel, R. Faria, D. Santinha, M.R.M. Domingues, P. Domingues, Evaluation of oxidation and glyco-oxidation of 1-palmitoyl-2-arachidonoyl-phosphatidylserine by LC–MS/MS, J. Chromatogr. B, 929 (2013) 76-83.

E. Maciel, R.N. da Silva, C. Simões, T. Melo, R. Ferreira, P. Domingues, M.R.M. Domingues, Liquid chromatography–tandem mass spectrometry of phosphatidylserine advanced glycated end products, Chem. Phys. Lipids, 174 (2013) 1-7.

E. Maciel, B.M. Neves, D. Santinha, A. Reis, P. Domingues, M. Teresa Cruz, A.R. Pitt, C.M. Spickett, M.R.M. Domingues, Detection of phosphatidylserine with a modified polar head group in human keratinocytes exposed to the radical generator AAPH, Arch. Biochem. Biophys., 548 (2014) 38-45.

Abstracts de Comunicações em Encontros científicos

E. Maciel, B.M. Neves, T. Cruz, P. Domingues, M.R.M. Domingues, Identification of phosphatidylserine oxidized/glycated/glyco-oxidized products by LC-MS and the study of their anti-inflammatory properties, XIII Congress of the Iberian Society of Cytometry, 9-11 May 2013, University of Aveiro.

E. Maciel, C. Simões, P. Domingues, M.R.M. Domingues. Study of influence of glycation on phosphatidylserine modifications under oxidative stress conditions by LC-MS/MS. XVII. Lipid-Meeting, 8-10 Dezembro 2011, Leipzig, Germany.

E. Maciel, R. N. da Silva, P. Domingues, M.R.M. Domingues. Identification of oxidative modifications in phosphatidylserine polar head using lipidómica approach. Lipid Maps annual meeting 2011" Lipidomics Impact on Cell Biology, Cancer, and Metabolic Diseases", 2 - 3 May 2011, La Jolla, CA.

Comunicações Orais em Encontros Científicos

E. Maciel, Identification oxidized phosphatidylserine by LC-MS. Evaluation of their effects on the inflammatory process. 1st Workshop-Lipidomics, 16 May 2012. University of Aveiro;

E. Maciel, Phosphatidylserine oxidation by Fenton Reaction: Recognition of oxidation of serine polar head by TLC and Mass Spectrometry, V Journeys of biochemistry "metabolic changes in disease", 27 April 2011. University of Aveiro;

Table of contents

List of Figures

List of Schemes

List of Tables

List of Abbreviations

AAPH	2,2′-azobis(2-methylpropionamidine) dihydrochloride
AD	Alzheimer's disease
AGEs	Advanced glycation end products
APT	Aminophospholipid translocase
CL	Cardiolipin
CDP	Cytidine diphosphate
DHB	2,5-dihydroxybenzoic acid
DPPS	1,2-dipalmitoyl-phosphatidylserine
ER	Endoplasmatic Reticulum
ESI	Electrospray ionization
FA	Fatty acids
GC-MS	Gas chromatography-mass spectrometry
gluPE	Glycated phosphatidylethanolamine
gluPS	Glycated phosphatidylserine
GPAA	glycerophosphoacetic acid
HPLC	High performance liquid chromatography
IL	Interleukin
LC	Liquid chromatography
LDL	Low-density lipoprotein
LPS	Lipopolysaccharide
MALDI	Matrix-assisted laser desorption ionization
MPO	Myeloperoxidase
MS	Mass spectrometry
MS/MS	Tandem mass spectrometry
MUFA	Mono-unsaturated fatty acids
oxPS	Oxidized PS
oxgluPS	Oxidized glycated PS
PA	Phosphatidic acid
PAPS	1-palmitoyl-2- arachidonoyl- phosphatidylserine
PC	Phosphatidylcholine
PE	Phosphatidylethanolamine

PG	phosphatidylglycerol
PI	Phosphatidylinositol
PL	Phospholipid
PLPS	1-palmitoyl-2- linoleoyl- phosphatidylserine
PLSCR1	phospholipid scramblase-1
POPS	1-palmitoyl-2- oleoyl- phosphatidylserine
PPS1	Phosphatidylserine synthase 1
PPS2	Phosphatidylserine synthase 2
PS	Phosphatidylserine
PSD	Phosphatidylserine decarboxylase
PUFA	Polyunsaturated fatty acids
Q	Quadrupole
RA	Relative abundance
ROS	Reactive oxygen species
RIC	Reconstructed ion chromatogram
RT-PCR	Real time - polymerase chain reaction
SFA	Saturated fatty acids
SM	Sphingomyelin
TGF-β	Transforming growth factor-β
TLC	Thin layer chromatography
TNFα	Tumor necrosis factor α
TOF	Time of flight
UVA	Ultraviolet A

Chapter I

General Introduction

1.1 Introduction to phospholipids structure and functions

Lipids are one of the most important group of biomolecules that embrace structurally quite heterogeneous molecules. The structural diversity of the lipid species is side by side with their different roles in living systems. In fact, lipids can fulfill a variety of biological functions, such as energy source (e.g. triglycerides and fatty acids), constituents of cell membranes and subcellular compartments (e.g. mitochondria) or as bioactive molecules with important role in several signaling events (e.g. phosphatidic acid, sphingosine-1-phosphate, ceramides) [1,2,3,4]. To understand these diversified structures and functions, a new omics field has emerged. In fact, lipidomics became during the last decade a growing research discipline, positioned between proteomics and metabolomics, aiming at the global characterization of lipids and lipids metabolites and their functions in biological systems [5,6].

Among lipids, the phospholipids (PL) are a major class present in high abundance in all organisms, from the *arcobacter* to plants and humans. These hydrophobic molecules have a diversity of functions: building blocks of cell membranes, compartmentalization of the cytoplasm, storage of proteins involved in cell signaling, intercellular adhesion and cytoskeleton support [7]. They also serve as a precursor for lipid's biologically active mediators [8]. The major groups of PLs are glycerophospholipids and sphingolipids.

The glycerophospholipids are the most abundant PLs; they have a key role in energy storage as well as in cell structure, since they are the main components of cell membrane. They are also involved in cell signaling, cell proliferation and may serve as potential biomarkers for several diseases. Glycerophospholipids usually consist of a glycerol molecule linked to two fatty acids and a phosphate group that can bind a polar molecule by an ester bond. This portion of the PL molecule is called the head group of the PL, as is the base to define several classes of PLs [9] (Figure 1).

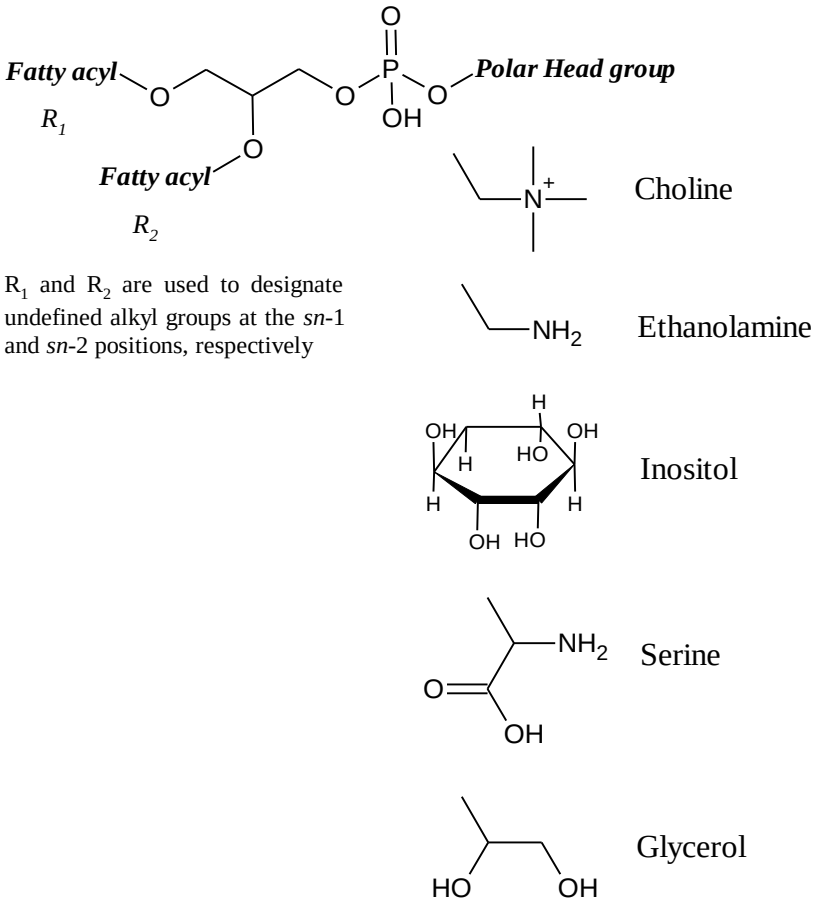

R_1 and R_2 are used to designate undefined alkyl groups at the *sn*-1 and *sn*-2 positions, respectively

Figure 1: Structure of glycerophospholipids. Typical glycerophospholipids consist of two fatty acyl chains, a glycerol backbone, and a phosphophodiester linked to a head group. The most common phospholipid classes are: Phosphatidylcholine (PC); phosphatidylethanolamine (PE), phosphatidylinositol (PI); phosphatidylserine (PS); phosphatidylglycerol (PG); phosphatidic acid (PA).

The composition of the head group of glycerophospholipids is primordial in dividing the PL in distinct classes. For example, if the head group is a serine, then the PL belongs to the phosphatidylserines (PS) class. Other classes include phosphatidylcholine (PC), phosphatidylethanolamine (PE), phosphatidylglycerols (PG) and phosphatidylinositols (PI) (Figure 1). When the phosphate group is not substituted the PL class is called PA. All these classes paring with Cardiolipin (CL) are the main classes of polar PLs. The cardiolipin is an odd PL, since it is a dimeric PL that presents two phosphatidic acids linked together through an additional glycerol molecule and thus bearing four fatty acyl chains. Glycerophospholipids are a group of biomolecules that is abundant in cells, presenting

very diverse in structural forms. This structural variety is due to the presence of different combinations of lipids that vary according to the composition of the polar head group and also with different combination of fatty acyl chains that can have linked to the glycerol fatty acids. The fatty acyl chains that bind to the glycerol backbone encompass variation in their length, degree of unsaturation of acyl chains and in the positions of the glycerol backbone (*sn*-1 and *sn*-2 positions) [10]. In mammalian tissues it is possible to find between 30-60 different fatty acids, that can have chain length between 12-26 carbons and can be saturated or unsaturated, with up to 6 double bonds, and the double bonds can be located in different positions. In general, the saturated fatty acids are attached to glycerol at *sn*-1 position while unsaturated fatty acids are at *sn*-2 position. The *sn*-2 fatty acids are usually attached through an acyl bond, however the *sn*-1 fatty chain can be either acyl, alkyl ether or alkyl-1'-enyl ether linked, called respectively diacyl, plasmanyl and plasmenyl (also called plasmalogen) PLs [11]. The possibility of different combination of polar head, fatty acyl structure and position, makes several combinations possible. It is estimated that glycerophospholipids comprise around 600 detectable molecular species, but theoretical has been estimated to be in order of ~10000 glycerophospholipids (as reviewed in [12].

Each tissue, type of cell or biofluid has specific combinations of PL classes and a proper fatty acyl distribution [13]. PC is the most abundant class comprising around 50% of total PL classes in almost all tissues and cells [14]. PE is the second most abundant PL, but the percentage is very diverse among tissues; For example, in the brain it represents around 45% and in the liver around 20% of the total of PLs. PE is also present in higher proportions in mitochondria than in other organelles [15]. PI is present in all tissues, but in the brain is present with more abundance than in other tissues (~10%) [16]. CL has been found to be present exclusively in mitochondria membrane, representing 15% of total PL content in this organelle [17]. Lipids in plasma membranes of eukaryotic cells are asymmetrically distributed between the inner and outer membrane leaflet. PC and sphingomyelin (SM) are primarily located on the external leaflet, while PS, PE, and PI are concentrated in the internal leaflet. This odd distribution is crucial for cell homeostasis and it is maintained and regulated by numerous enzymes and proteins [18]. It is assumed that the temporal and spatial distribution of different classes of lipids in the cytoplasmic membranes and organelles has an important biological significance. The disturbance of

lipid distribution have been thoroughly investigated and are the topic of many areas of biomedical research, mainly due to their correlation with several pathological conditions such as cancer, diabetes or atherosclerosis. The deviation in the distribution and concentration of lipid molecules are associated with the development of diseases and suggest that these biomolecules can be biomarkers for diversified pathologies [19]. As an example, a panel of PC has recently been used as signaling molecules for Alzheimer disease [20,21].

One of the causes that can affect lipid homeostasis and distribution is the induced modifications associated with oxidative injure. Under oxidative conditions, PLs are very prone to suffer oxidative modifications mainly due to the presence of unsaturated fatty acids in their structure. Oxidation of PLs causes changes in their structure, resulting in a vast number of structurally different oxidation products. In biological systems, these changes may occur through radical reactions involving non-enzymatic (•OOH, •OH, Fe^{2+}, Cu^{+}, radiation) or enzymatic systems, leading to a diversity of oxidation products. Depending on the predominating oxidative process, different PLs oxidation products can be formed. Oxidized PLs can acquire novel biological activities, which are distinct from the non-oxidized PLs. These oxidized PLs have been described to participate in several biological processes such as the immune response, inflammation, apoptosis and age-related diseases, but little is known about the relationship between specific oxidation products and distinct biological effects. These biological effects have been described both *in vitro* and *in vivo*, and may have deleterious effects, as for example exhibiting potent pro-inflammatory activities, or beneficial and protective effects, for example the ones with anti-inflammatory properties [22]. These oxidative modifications have been extensively studied for the PC, since it is the most abundant class of PL. Several studies suggested that oxidized PC are important mediators in inflammation and are assumed that they are involved in LDL oxidation and the process of atherosclerosis formation by the uptake of oxidized LDL [22,23].

Aminophospholipids, namely PS and PE, can also be modified by glycation and glycated PE have been identified in plasma, LDL and erythrocytes of diabetic patients with hyperglycemia [24,25,26,27,28,29]. In fact, amino PLs have a primary amine and are a target of modifications such as glycation, which contributes to increased oxidative stress. Recently, in attempt to explain the high plasma levels of PC hydroperoxides (PC-OOH) in

patients with type 2 diabetes, Suzuki *et al* correlated the presence of Amadori-PE with PC-OOH, relating the involvement of lipid glycation and lipid oxidation in the development of diabetes [30]. Although glycated PE has already been detected *in vivo*, the glycated derivatives PS were only produced in laboratory using in model conditions that mimic hyperglycemia. Thus, PS glycation *in vivo* was just hypothesized and most probably has never been identified because PS exist in very low abundance in plasma and the correspondent glycated derivatives, should be very difficult to detect.

Oxidized PS (oxPS) has already been detect in some tissues and has been correlated with important regulatory functions. PS have been correlated with CL oxidation in a process that seems to be essential in apoptotic, during controlled cell death [31]. Oxidized CL in mitochondria is proposed to facilitate the release of cytochrome *c* into the cytosol, that may further contribute to the formation of oxPS, culminating in its externalization to the outside of the plasma membrane [31]. PS itself has significant roles in several biological processes, which is outweighed by its physiological importance. These importance is attributable to its unique physical and biochemical properties, as we will explain in detail in the following sections.

1.2 Phosphatidylserine: structure and localization

Phosphatidylserine (PS) was first isolated in 1941 by Folch and coworkers from brain lipid extracts [32]. In 1948 they proposed the chemical structure of PS [32,33], but the exact structure was describe later by Baer and Maurukas in 1955 [34]. As described earlier, PS contains two acyl chains at the *sn*-1 and *sn*-2 positions of the glycerol moiety, and attached to position *sn*-3 the phosphate group linked to the amino acid serine, the polar head of the class of lipids. PS is dissimilar from other PLs by the polar head group features, being considered an anionic PL (Figure 2), while PC and PE are zwitterionic PLs. PS, like the other PLs, is found in nature in the form of salt.

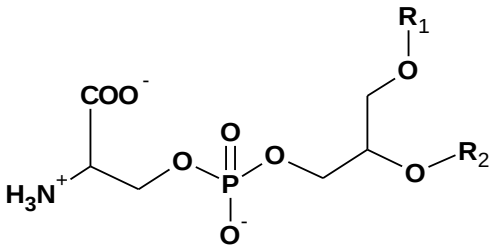

Figure 2: Structure of phosphatidylserine. Note that at physiological pH the head-group bears one net negative charge, thus being called anionic phospholipid.

PS is found preferentially in the inner leaflet of the plasma membrane and in endocytic membranes [35]. When present in relatively high amounts in membrane, there is an accumulation of negative charges, allowing the binding of polycationic proteins. This effect may be important in movement and recruitment of proteins at the cellular level. [36].

The maintenance of PS in this specific location and thus maintaining the membrane lipid asymmetry is mediated by the interplay of different transporters, including aminophospholipid translocases (APT) or ‘‘flippase’’, which transports PS and PE from the outer leaflet to the inner leaflet and ‘‘floppases’’ that transport lipids in the opposite direction, from inside to outside [18] (Figure 3). The transbilayer movement of PS in plasma membrane may also be mediated by Ca^{2+}-dependent scramblase-1 (PLSCR1), which can random distribute PS across membrane bilayers [37].

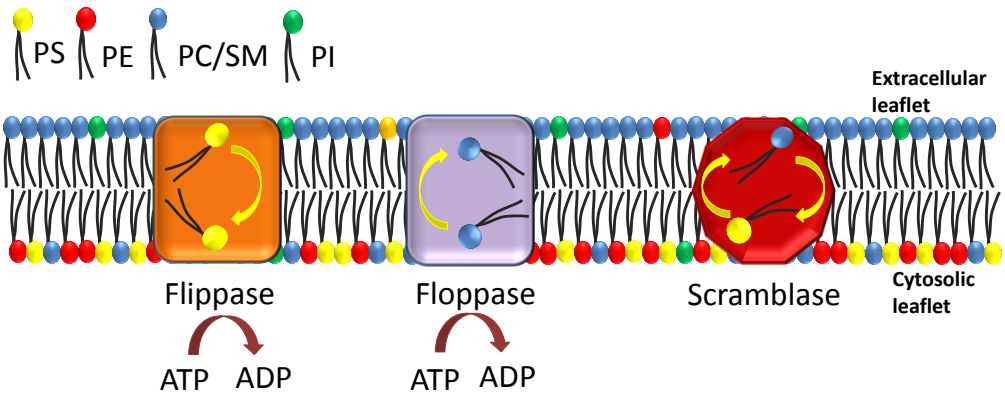

Figure 3: Asymmetric membrane regulated by aminophospholipid translocases. Adapted from Pennings [18].

PS is present in biological membranes in various relative abundances when considered other membrane lipids or protein content. The plasma membrane is, of the biological membranes, the most enriched in PS, followed by early endosomes, while mitochondria membranes contain the lowest mole fraction of PS [38]. PS is also present in higher proportions in brain and central nervous system, representing about 15% of total PL pool in human brain [39]. Other tissues usually contain a smaller amount of PS; in rat liver, for example, the PS content is around 3% [40,41].

PS molecular species present in the cell membranes consist of many different molecular species because of the combination of several fatty acids bonded at the *sn*-1 and *sn*-2 position of glycerol moiety. Although the acyl chains in PS vary among cell types and organelles, the saturated fatty acids of 16 and 18 or more carbons are generally attached to the *sn*-1 position, whereas unsaturated and mostly polyunsaturated fatty acids are generally found at the *sn*-2 position. The most abundant PS molecular specie contains at *sn*-1 position almost exclusively stearic acid (FA 18:0) and docosahexaenoic acid (FA 22:6) at sn-2 position (PS-18:0/22:6). The FA 22:6 accounts for more than 36% of the fatty acyl species of PS in brain. This is probably related to the fact that FA 22:6 is essential for the normal development and functioning of the nervous system [42,43].

1.3 Biosynthesis of phosphatidylserine

In mammalian cells, PS is synthesized by calcium dependent reaction in which the polar head group of an existing PL is replaced by L-serine (Figure 4) [44,45]. In prokaryotes and yeast, PS is synthesized by conjugation of serine to CDP-diacylglycerol. The CDP-diacylglycerol pathway for PS synthesis has not been detected in mammalian cells [38,45,46].

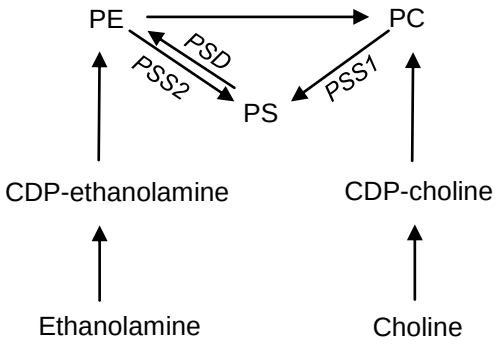

Figure 4: Phosphatidylserine (PS) synthesis and metabolism in mammalian cells. (PS) is synthetized by replacement of the choline group of PC by serine in a reaction catalyzed by PSS1. The PSS2 is responsible for the replacement of ethanolamine group of PE by serine [36].

Synthesis of PS occurs in the endoplasmic reticulum (ER), mediated by two base-exchange enzymes, PS synthase-1 (PSS1) and PS synthase-2 (PSS2), that exchange choline and ethanolamine head groups of PC and PE respectively for serine [36,38,44,46]. The brain, testis and kidney are the tissues that have higher capacity to synthesize PS. Studies in brain suggested PC-(18:0/22:6) molecular specie is the preferred substrate for PS synthesis [41]. Although PC-(16:0:22:6) molecular specie is present in large amount is not utilized efficiently by PSS1 [41]. In the other hand, recent studies demonstrate that PSS2 utilizes PE containing FA16:0 and FA18:0 at *sn*-1 position equally well. However PSS2 prefers PE with FA22:6 in the *sn*-2 position to either FA20:4 or FA18:1 [47]. Thus, both PSS1 and PSS2 contribute to the higher amount of PS containing FA22:6 in the Brain [41].

1.4 Functions of phosphatidylserine

Although PS is only a quantitatively minor PL in most biological membranes, it is required for specific functions in addition to its assumed structural role in membranes. PS play important roles in diverse biological processes with emphasis in blood clotting and apoptosis. The involvement of this aminophospholipid in signaling pathways is correlated with the asymmetric transbilayer distribution. Externalization of PS occurs in apoptotic cells, being an important signal in apoptosis and an important modulator of the immune response. PS asymmetry has been associated with clinical situations where apoptosis plays

a relevant role, like in cancer, chronic autoimmunity, and infections. PS participate both in intracellular and extracellular cellular functions, as we will describe latter.

1.4.1 Intracellular functions of PS

Among intracellular function of PS, a key function is of being the precursor of PE, via the mitochondrial enzyme PS decarboxylase (Figure 4) [36,44]. PS is involved in signaling pathways such as Raf1 kinase, neutral sphingomyelinase and protein kinase C pathways and in localizing intracellular proteins to cytosolic membrane leaflets [36,44]. PS also promotes Ca^{2+}-induced membrane fusion events such occur during exocytosis [48,49,50].

PS has also important roles in maintaining brain and central nervous system homeostasis. PS plays an important role in neuronal modulation and excitability, signal transduction and neurotransmitter activity. It is well known its effect in the improvement in the NA^{+}/K^{+}-ATPase activity, and its effects in memory recovery [51]. This PL has shown to provide many benefits in physical and mental performances, being recognized to improve the cerebral function, including attention and memory, especially in elderly people [51,52], thus being used as a nutritional supplement. Alteration in PS profile and in PS structure (e.g. due to oxidation) have been considered as important players in the pathological process in several brain diseases, including depression, neurodegenerative diseases, aging and many other neuronal disorders [53,54].

Some studies reported other important roles of PS since it increases procollagen synthesis and inhibits metalloproteinase-1 induction in both UV-irradiated skin and intrinsically aged skin *in vivo* [55,56]. Due to these beneficial effects in skin, PS is also being considered as having therapeutical benefits in the treatment of a variety of cutaneous disorders.

1.4.2 Extracellular functions of PS

PS is normally localized in membrane leaflets that face the cytosol, however, in certain physiologically relevant circumstances, PS redistribution from the inner to the outer surface of the plasma membrane of mammalian cells can occur. This redistribution to the outer surface may initiate and participate in humoral and cellular processes [57]. Cell surface localization of PS has been found in erythrocytes and platelets from patients with

diabetes mellitus [58,59,60], aging erythrocytes [61], activated platelets, activated macrophages, undifferentiated tumor cells and apoptotic cells [48] and also in tumor cells [62]. The PS externalization can play a different roles. For example, this process is important in the activation of platelets, which is critical for the efficient propagation and control of coagulation and thrombosis. In erythrocytes and other cells is also an important and necessary signal for apoptotic cell removal by phagocytes [63,64].

Translocation of PS to the cell surface has also been shown to occur independently of the apoptotic process in the case of tumor cells. In fact, several studies indicated that malignant cells showed surface exposure of PS, such as in the case of leukemia and neuroblastoma cells [65], malignant melanoma [62,66,67] and gastric carcinoma [68], as well as in surface of endothelial cells in tumor blood vessels [69]. In all of these cases no apoptotic events occurred. Tumor cells, although exposing PS, seems to find a way around apoptosis and prevent the recognition by macrophages [70,71]. The investigators believed that PS could serve as uniform marker of tumor cells and metastases as well as a target for a novel therapeutic approaches based on membrane-active peptides, since positively charged peptides specifically interact with negative charge of PS on their target cell membrane [62,65,72]. However, the real role of PS in tumor cell surface are far from being completely elucidated. In the next section, we will describe in detail the functions of PS in clotting and apoptosis.

PS in blood clotting

PS is a key signal in the coagulation cascade [57,73]. In normal blood circulation, the coagulation factors in plasma do not contact with PS, since PS is absent from the surface blood cells and endothelial cells that line the vessel wall. When activated, blood platelets expose PS on their outer surface. The exposure of extracellular PS triggers the activation of several clotting factors, notably factors V, VIII, X, and prothrombin [57,74,75,76,77,78]. The recruitment of these proteins to the surface of platelets is mediated by specialized recognition modules, such as discoidin-type C2 or gamma-carboxyglutamic acid domains that bind PS with a high degree of selectivity and stereospecificity. The tenase and prothrombinase complexes that promote coagulation become fully active only after binding PS on the surface of activated platelets [57,76].

In blood platelets from diabetic patients, a 3-7 times enhanced capacity to catalyze prothrombinase activity has been observed [79], which is most likely due to increased surface exposure of PS. Erythrocytes and platelets from patients with diabetes mellitus have been found to exhibit a partial collapse of membrane asymmetry with increased surface exposure of PS [58,59,60]. These observations suggest that in diabetic conditions, besides a partial loss of PL asymmetry, these events also reflect a destabilization of the erythrocyte membranes [48].

PS in apoptotic cell removal by phagocytes

During apoptosis the asymmetric transbilayer distribution of PS is lost, bringing PS to the surface where it acts as a signal for engulfment by phagocytes [48,80,81,82,83]. Several studies showed that apoptotic cells are recognized and phagocytized by macrophages through a PS-dependent mechanism, suggesting that externalization of PS is the "eat-me" signal that macrophages recognize to initiate the clearance of apoptotic cells [48,84,85,86].

Kagan and colleagues attempted to explain the proper context by which PS is recognized as an "eat-me" signal. These investigators pointed out that fatty acyl oxidation of PS are a prerequisite for PS externalization and recognition as an apoptotic signal [87,88]. APT is responsible for the maintenance of PS in the inner leaflet of the plasma membrane [89,90] and the mechanisms for PS exposure on surface of apoptotic cells appears to involve the down-regulation of APT [91,92]. Earlier, it was established that apoptosis and PS externalization were associated with reactive oxygen species (ROS) generation [93,94]. Thus, appearance of PS in outer monolayer of the plasma membrane can be related to its oxidation in membrane of apoptotic cells, and that oxPS may fail to be recognized by APT, preventing its translocation to the inner leaflet of plasma membrane [95,96]. Kagan and co-workers proposed that oxidation of PS preceded its externalization during apoptosis [95,97,98,99,100,101] and they found that recognition of the cells with externalized PS was strongly facilitated when oxPS was also present on the surface of target cells [98]. They also, demonstrated that oxPS exist both within and on the surface of apoptotic cells [102]. In Figure 5 it is illustrated the participation of oxPS in its externalization and recognition and engulfment of apoptotic cells.

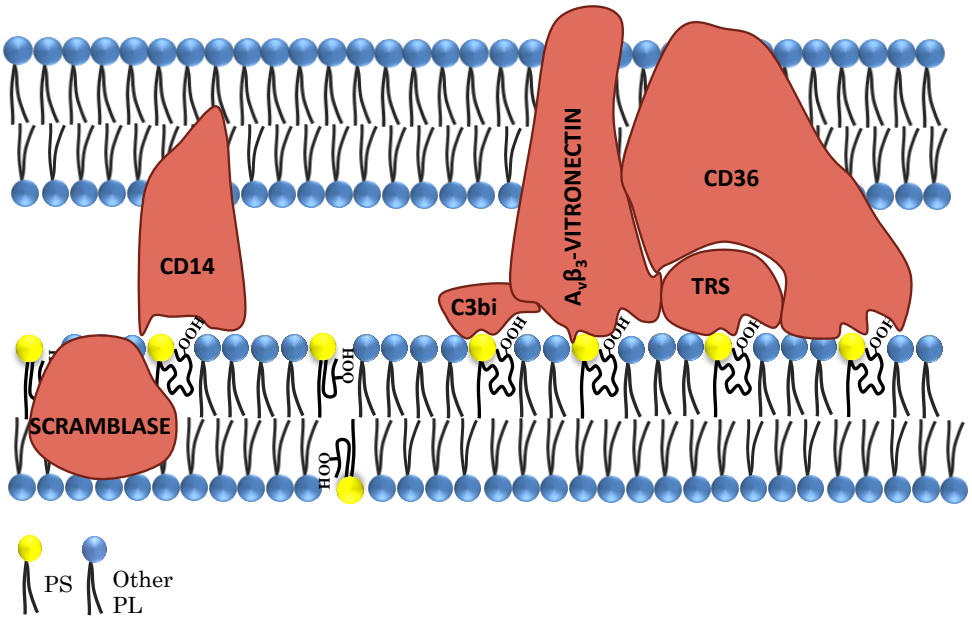

Figure 5: Proposed model by Tyurina *et al.* for participation of oxidized PS in the engulfment of apoptotic cells. Extracted from [103].

More recently, Greenberg et al. [104] demonstrated macrophage recognition of apoptotic cells via CD36 (scavenger receptor in the recognition of apoptotic cells). CD36 receptors are activated by oxPS, particularly the short chain oxidation products of PS and, to a lesser extent, oxidized PC, but not non-oxidized PS molecular species.

Apoptosis or programmed cell death is a physiological process for orderly removal of dead cells in a controlled process where apoptotic cells are rapidly recognized and engulfed by phagocytes (e.g. macrophages), resulting in inhibiting inflammatory response and being an important step in the resolution of inflammation [105,106]. Phagocytic clearance of apoptotic cells is characterized by the active production of anti-inflammatory cytokines, such as transforming growth factor β (TGF-β) and interleukin 10 (IL-10), and down-modulation of the pro-inflammatory cytokines tumor necrosis factor α (TNF-α) and IL-12 that promote an immunosuppressive environment in tissues which is very important for the resolution of inflammation [105,106,107]. Several studies showed that PS suppresses the formation and release of pro-inflammatory mediators and induces production and release of anti-inflammatory cytokines ((TGF-β) and IL-10) from macrophages [84,85,106]. Activated phagocytes also regulate inflammation by generating reactive nitrogen and oxygen such as NO and superoxide. Studies demonstrated that PS

liposomes strongly reduced the LPS-induced release of NO in microglial cultures from neonatal rat brain [108,109] and in apoptotic PC12 cells [110].

Initially, externalization of non-modified PS has been considered the "eat me" signal for apoptotic cell, while nowadays both non modified PS and oxPS are considered active players in this process, in spite of the increasing recognition of the importance of oxPS in this signaling event. The recognition of externalized PS has occurs, most probably through Annexin V due to capacity of PS to bid to protein membranes [111]. The annexins have the biological property of binding to PLs in Ca^{2+}-dependent way [111]. It is a natural ligand for PS, since annexin V preferentially binds to negative charged PLs. This enables the detection of phosphatidylserine exposure on the membrane by flow cytometry analysis using the binding of fluorescein isothiocyanatelabeled annexin V [112]. The interaction between annexin V and PS only occurs when PS is in the leaflet of the membrane [113]. OxPS preserves the negative charge of the polar head, maintaining the availability to bind annexin V. Thus Annexin V does not allow to differentiate oxPS from the native PS. Consequently, more efforts are needed to develop specific methods that allows the distinction among PS and oxPS in cell surface and their specific biological roles.

1.5 Modifications in phosphatidylserine structure

As referred, all PLs, including PS, can be modified under oxidative conditions. This process can lead to important modifications of their structure and thus, in their properties, preventing or modified their role in cells. In addition, modification of PS can impair asymmetry of lipid membrane, which can induce the collapse of the lipid membrane. The modifications of PS via oxidation are possible due to the presence of the unsaturated fatty acyl chain. In these conditions, oxPS, as well as other PLs, can acquire novel biological activities, which are distinct from the non-oxidized PLs. These can include the participation in several important biological processes such as the immune response, inflammation, apoptosis and age-related diseases [114]. Still little is known about the relationship between specific oxidation products and distinct biological effects, because most of them are formed in low abundance and, in consequence, difficult to isolate and identify. Nevertheless, recently, new approaches to this problem using mass spectrometry (MS) allowed to obtain new knowledge on the oxidation of PLs, mainly in the oxidation of

PC, PE and cardiolipins [115,116,117]. MS has been also used to identify oxPS both *in vitro* and *in vivo* [118] .

PS is an amino PL and the presence of a free amino group in PS polar head allows this PL of being a target of modifications such as glycation and to form adducts with small aldehydes (e.g. hexanoylation). The possible mechanism of modifications that can occur in PS structure will be addressed bellow.

1.5.1 PS oxidation: chemistry and biological effects

PS is enriched in unsaturated fatty acids, particularly in in brain where the major abundant PS molecular species have polyunsaturated fatty acids FA 20:4 and FA 22.6. This make PS very prone to be modified under oxidative conditions. There are several published works that have studied the PS oxidation and identified new molecular species formed during PS oxidation. In these studies, different oxidation processes have been used to induce the oxidative stress both *in vivo* and *in vitro*, such as 2,2-azobis(2-amidinopropane) dihydrochloride (AAPH) an azo-initiator [96,119], ɣ-irradiation [120,121,122,123] or myeloperoxidase [104]. Depending of the oxidative conditions, different types of modifications may occur, so it is important clarify the influence of oxidant systems in the PS oxidation process. Oxidation of PLs and also of PS is usually mediated by ROS. These species are highly potent oxidants and can cause several oxidation reactions associated with disruptions in normal cellular signaling, genetic degradation and physiological dysfunction, which can lead to cell death and progressive aging in the organism [124]. In biological systems, these disruptions may occur through radical reactions involving non-enzymatic (HOO•, HO•, Fe^{2+}, Cu^{+}, radiation) or enzymatic systems such as lipoxygenases and myeloperoxidase.

The hydroxyl radical (HO•) is the most reactive oxygen species generated in living systems, being responsible for the oxidation of the generality of biomolecules, including PLs. Hydroxyl radicals may be formed by the reaction of hydrogen peroxide and ferrous ion (Fe^{2+}) (Fenton reaction) or by other metal catalyzed reactions, from peroxynitrite [125], or by high energy irradiation [126].

The lipid oxidation induced by the hydroxyl radical is initiated by the abstraction of one hydrogen atom from a reactive methyl group (C-H), producing alkyl radicals (R). This alteration will promote the reorganization of the adjacent double bonds producing other

alkyl radicals. In the presence of oxygen, the alkyl radicals will react to form peroxyl radicals (ROO) that in turn, by acquiring one hydrogen atom, will produce a lipid hydroperoxide (ROOH). The resulting lipid hydroperoxide may decompose in the presence of metal ions, yielding alcoxil (RO) or epoxyperoxyl (OROO) radicals. These species can abstract hydrogen atoms from lipids, with formation of hydroxyl and hudroxyperoxyl derivatives and the propagation of the lipid peroxidation reaction. This oxidation products have higher molecular weight than the non-modified lipid are named long-chain oxidation products. But the alkoxyl radicals formed during the oxidative reaction may undergo beta cleavage of the fatty acyl chain with formation of oxidation products with shortened fatty acyl chain, and with aldehydic or carboxylic terminal function. These products have lower molecular weight and are called short-chain PL products (Scheme 1) or truncated species. Polyunsaturated fatty acids have bis-allylic hydrogens, which is very reactive in oxidative conditions [20,127,128].

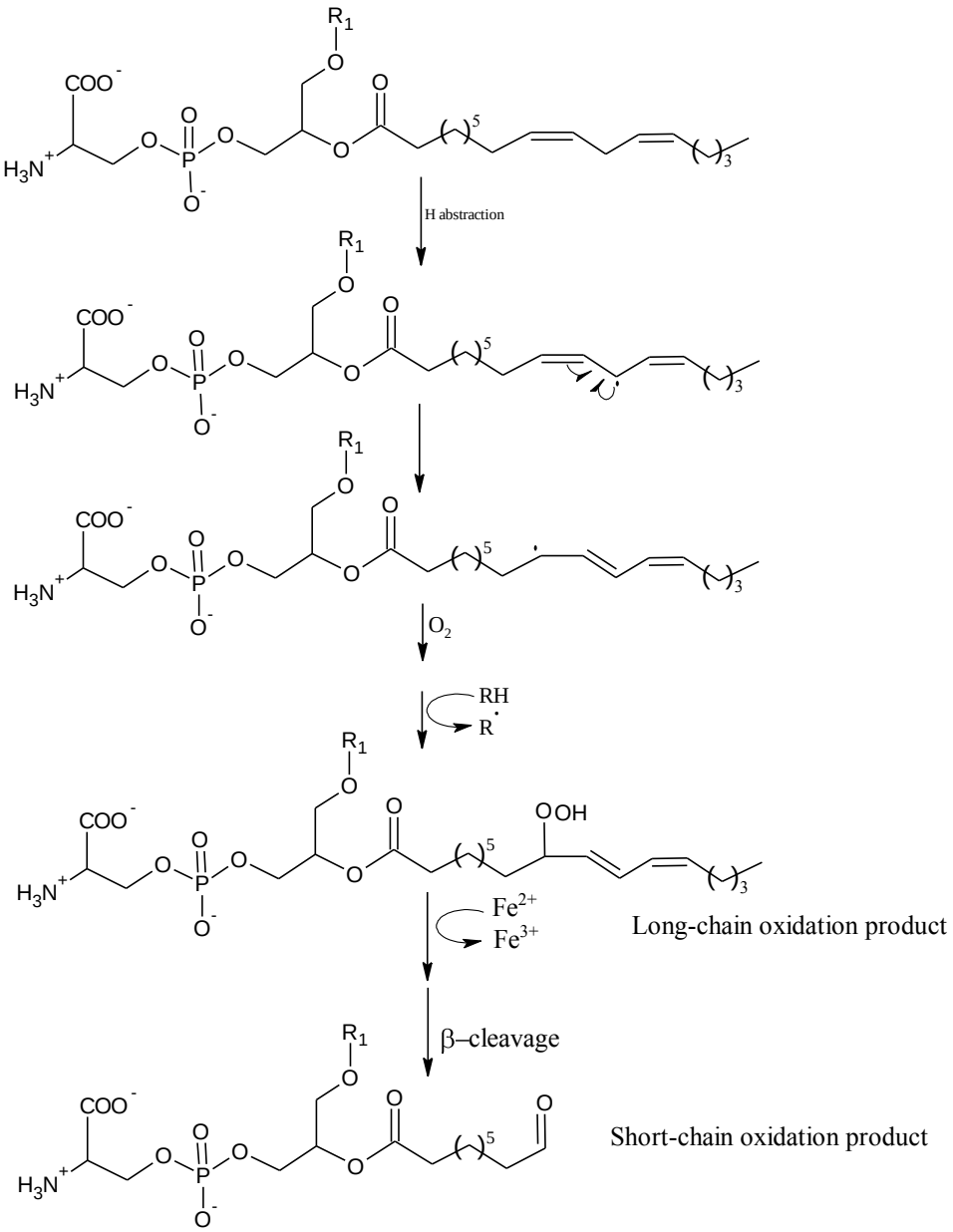

Scheme 1: Generation of the oxidation products from 1-palmitoyl-2-linoleoyl-phosphatidylserine by radical oxidation. Formation of long chain products (hydroperoxides) and short chain products (aldehyde terminal function)

OxPS molecular species, with oxidative modification in the unsaturated fatty acyl chains and with modified polar head were observed in model systems both *in vitro* and *in vivo* [118,129]. PS hydroperoxy and hydroxy are the most abundant species formed during oxidation process, and they have also been detected in several pathological conditions. Monitoring by electrospray (ESI)-MS the oxidation of PS induced by AAPH allowed the identification of the presence of mono and di-hydroperoxide derivatives of PS in liposomes

[96,119]. Richard A. Maki *et al*. [130] observed through fluorescence high-performance liquid chromatography (HPLC) and ESI-MS that phosphatidylserine hydroperoxides (PS-OOH) were elevated in human Alzheimer disease (AD) brains as compared with non-demented controls. The PS hydroperoxide and hydroxide have also been identified by MS in others pathological conditions, such as in intestinal and lung injury induced by γ-irradiation [120,121,122,123], in traumatic brain injury after controlled cortical impact [131], during apoptosis induced by staurosporine [132] and in cells and tissues after pro-apoptotic and pro-inflammatory stimuli [133]. The Kagan's group showed that the pattern of PL oxidation during apoptosis is non-random and that PS is one of the preferred peroxidation substrates [96]. Greenberg *et al.* [104], when studying the role of oxPS in macrophages, have performed an extensive characterization of PS derived oxidation products from synthetic precursor and from apoptotic cell membranes. These studies were performed using multiple mass spectrometric approaches and resulted in the identification of oxidation products with truncated fatty acyl chain containing carboxylic or aldehyde function.

Several works addressed also the oxidative modification of PS mediated by myeloperoxidase (MPO). The MPO is a heme protein secreted by activated phagocytes, such as neutrophils, and is the most abundant protein in polymorphonuclear leukocytes. MPO reacts with hydrogen peroxide in the presence of chloride and bromide to give hypochlorous acid (HOCl) and hypobromous acid (HOBr), which are strong oxidants and can oxidize biological molecules by free radical and non-radical pathways [134,135,136]. The hypochlorite and hypobromide acids promote the formation of oxidized lipids with unique structures, namely as chlorohydrines and bromohydrines, respectively, which can decompose to epoxides. Hypochlorite can react with hydrogen peroxide leading to the formation of singlet oxygen, which can react with lipids with formation of lipid hydroperoxides [137]. MPO mediated oxidation reaction contributes to inactivation and elimination of foreign microorganisms as well as to regulation of inflammatory processes [138,139]. It is known that MPO can bind to the surface of apoptotic cells on PS containing epitopes [140]. Other studies of PS oxidation in the presence of myeloperoxidase (MPO, hydrogen peroxide and chloride (MPO-H_2O_2-Cl^- system), showed the formation of phosphatidylglycoaldehyde and phosphatidylglyconitrile derivatives (Figure 6) [141,142,143]. HOCl converts α-amino acids via chlorinated amine derivatives to aldehyde

and nitrile species. These studies evidenced that in PS not only the fatty acyl chains are able to be modified during oxidation but also the polar head group can undergo structural modifications.

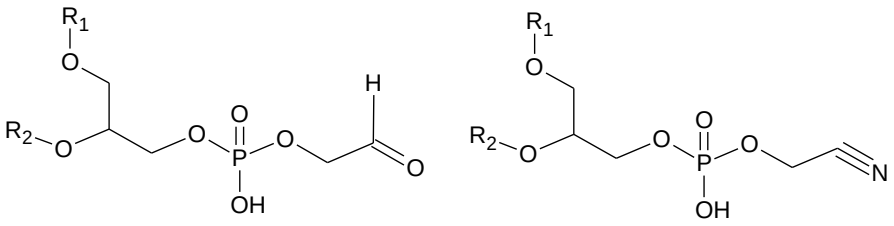

Phosphatidylglycoaldehyde Phosphatidylglyconitrile

Figure 6: HOCl-induced alterations in PS polar head leading to the formation of aldehyde and nitrile species [142].

1.5.2 Modifications on PS amine group

The presence of an amine group in PS, as in PE, polar head make this PL reactive towards lipid peroxidation products such as small molecules bearing carbonyl groups. Recent studies showed that amino groups in the aminophospholipids PE and PS could be modified by linoleic and arachidonic hydroperoxides, accompanied by the formation of hexanoyl moiety at ε-amino group via amide bond [144]. Shinsuke Hisaka and co-workers investigated the *N*-hexanoyl-PS and *N*-hexanoyl-PE formation and found that they can be detected in vivo. Figure 7 shows the *N*-hexanoyl-PS structure [145,146].

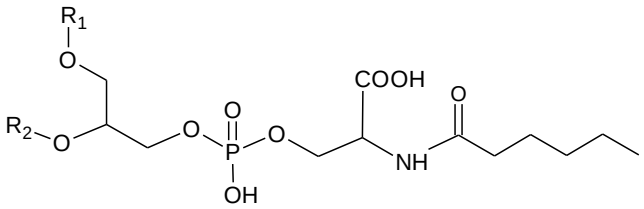

N-hexanoyl-PS

Figure 7: Chemical structure of N-(hexanoyl)phosphatidylserine.

Bucala *et al*. [147] hypothesized that the free amino groups of aminophospholipids are also targets for glycation, which expanded the concept of the Maillard reaction into biological systems. Glucose can react with the amino group of phosphatidylserine to form an unstable Schiff base, which undergoes an Amadori rearrangement to yield the stable deoxy-D-fructosyl PS, namely Amadori-PS (Scheme 2).

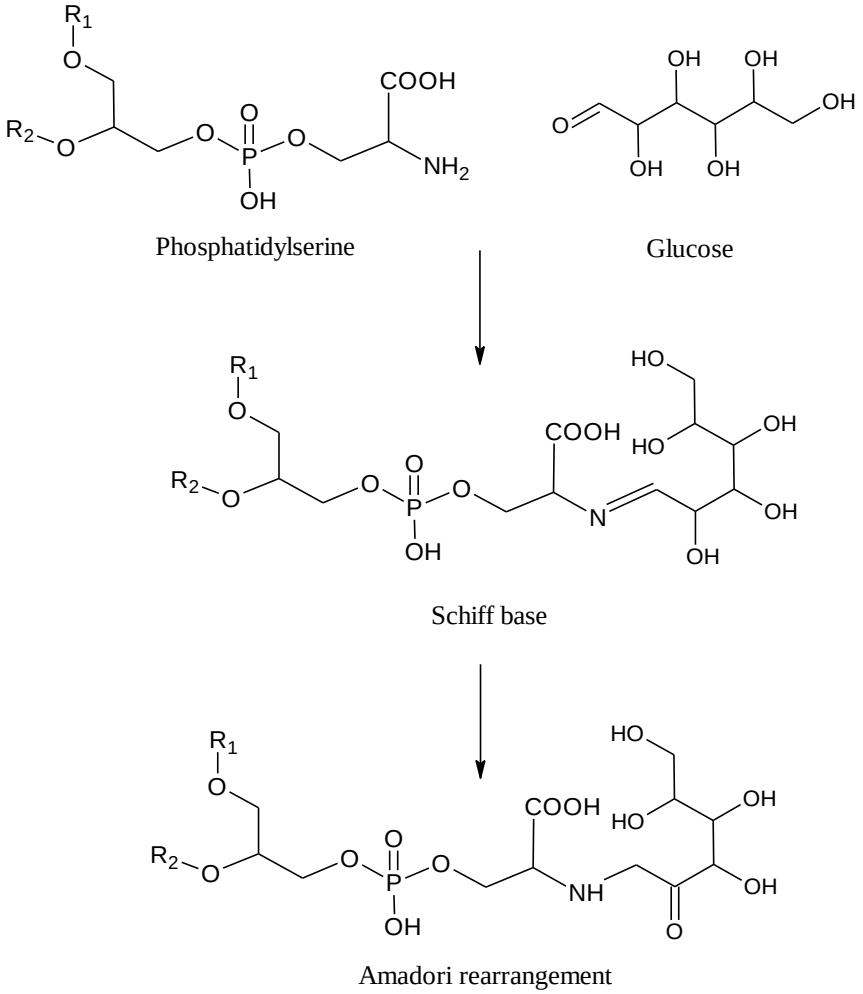

Scheme 2: Scheme for the glycation of phosphatidylserine (PS). Glucose reacts with amino group of PS to form a Schiff base, which undergoes an Amadori rearrangement.

Ravandi *et al.* also studied the glycation of aminophospholipids, but this in this study only glycated PE, but not glycated PS, was detect in human plasma and red blood cell membranes [27]. Glycated PE was also detected in LDL (low-density lipoproteins) and atheroma [28], and in the human plasma and erythrocytes in diabetic patients

[24,25,26,29]. Glycated PS, in contrast, has not been detected in biological samples, but was produced *in vitro* by direct reaction of PS and glucose [148].

Glycation is associated with oxidative stress, mainly due to the formation of oxidation intermediaries like advanced glycated end products (AGEs) [27,149]. Some studies provide evidence that glycated PE promote lipid peroxidation, partly through the generation of ROS, which can be related to inflammation and other diabetes complications [150,151]. Glycated PEs are more prone to undergo oxidation than non-glycated PE. In fact, a recent study from our lab showed that, besides the oxidation of the fatty acyl chain, glycated PE also undertake oxidative modification in the glucose moiety, which makes glycated PE more prone to oxidation [152]. However, no studies on the glycation and glycoxidation of PS and their biological roles have been published.

Although the effort that has been made, and the analytical advances that MS provided in the analysis of oxidized PS, there is still insufficient knowledge on the mechanisms of oxidation, on the nature of the oxidized species formed and in the biological roles of each specific oxidation products, and clearly, further studies are need in this field.

1.6 Aim of this work

As mentioned, the oxidation of PS may generate numerous oxidation products and the nature of these species may depend of the local and degree of unsaturation, so it is important to define exactly which oxidative species are being created, since different oxidation products may potentially exert distinct biologic effects. Despite the importance of oxidized PS has been recognized, only the primary oxidation products have been identified. In addition, no research has been found that surveyed the glycation and glycoxidation of PS, and their biological roles. This is still an unexplored field.

This work will focus on the identification oxidized and glycoxidized PS, contributing for the understanding of the biological role of oxidation products of PS as well as of glycated PS, in immune and inflammatory responses. To fulfill our goals, the work developed in this PhD thesis embraced three main objectives:

- Characterization of the oxidation products of PS and glycated PS formed under oxidative stress by LC-MS and LC-MS/MS.
- Detection of oxidation products of PS in complex biological environments.
- Evaluation of the biological effects of oxidized PS on the immune response.

Chapter II

Overview on analytical strategies

The global strategy used in this work for the structural characterization of oxidation products of PS (oxPS) and glycated PS (oxgluPS), and to detected these species in cell extracts was based on the application of mass spectrometric approaches that were either available or were developed in the course of this thesis.

The oxidation products were analyzed directly by electrospray mass spectrometry (ESI-MS) or/and by high performance liquid chromatography (HPLC) coupled on line to MS (LC-MS) or by off line thin layer chromatography- MS (TLC-MS). TLC and HPLC are key techniques used for the separation of different types of oxidation products within one PL class, allowing also the separation of PLs classes in extracts obtained from biological samples. The developed methodologies allowed the identification of the structural features of oxPS and oxgluPS, to identify specific fragmentation pathways of each product and to propose targeted lipidomic approaches to detect these products in biological environments. The evaluation of anti/pro-inflammatory activities of PS and oxidized PS also was also performed through the analysis of NO production by macrophages and macrophages stimulated by lipopolysaccharide (LPS).

The global strategy used in this work for the structural characterization of oxidation products of PS and glycated PS, comprised an initial step of glycation of PS, followed by the *in vitro* oxidation of the PSs and the identification of the oxidation products and determination of their activity is illustrated in Scheme 3. The developed methodologies allowed the detection of oxPS in cell extracts.

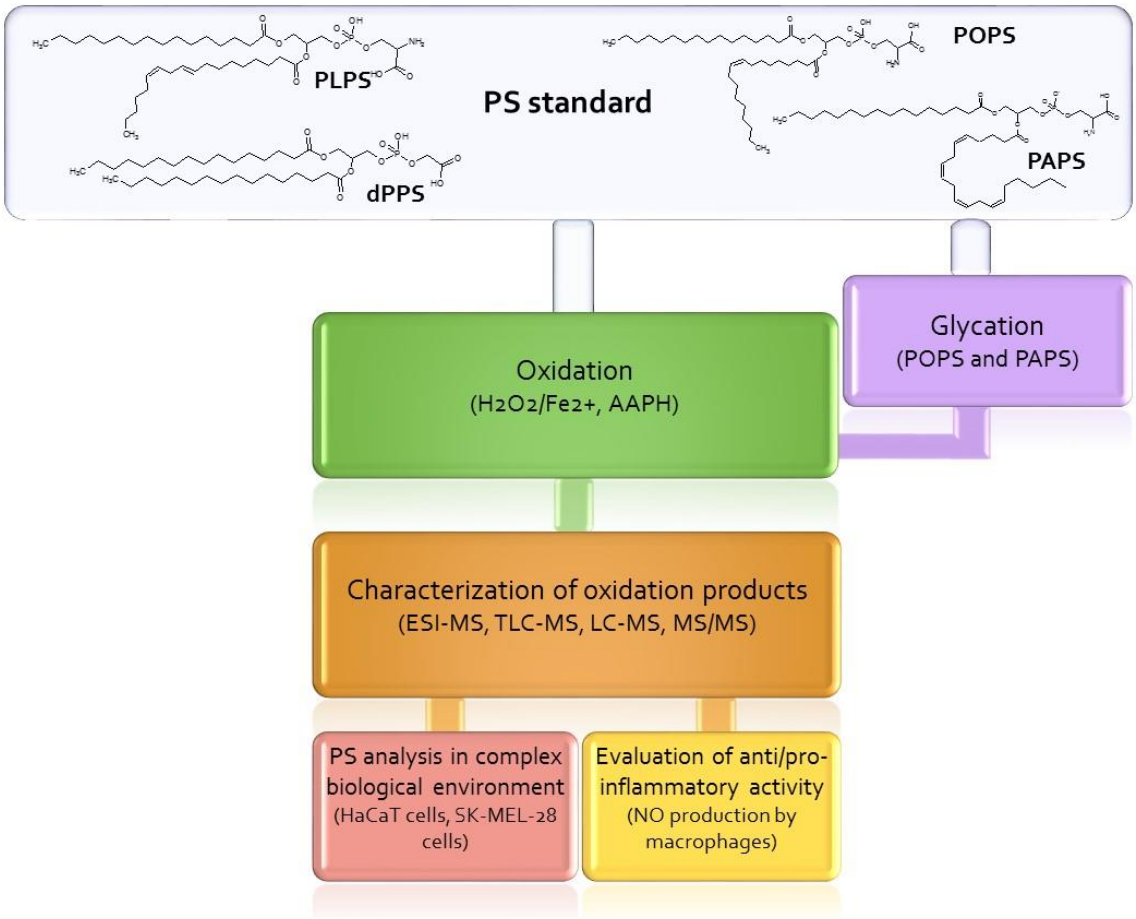

Scheme 3: The flowchart representing analytical approach of this work. The PS standard used in this work were: 1-Palmitoyl-2-linoleoyl-sn-glycero-3-phospho-L-serine (PLPS), 1-palmitoyl-2-oleoyl-sn-glycero-3-phospho-L-serine (POPS), 1,2-dipalmitoyl-sn-glycero-3-phospho-L-serine (DPPS) and 1-palmitoyl-2-arachidonoyl-sn-glycero-3phospho-L-serine (PAPS).

2.1. Synthesis of glycated phosphatidylserine

As referred previously, at the present there are no reports on the glycation of PS *in vivo*, although its formation is hypothesized [147]. In the present study, different solutions were tested in order to obtained high yield of glycated PS. Best results were obtained when PS was solubilized in methanol, and in the absence of water. The glucose and PLs were dissolved in absolute methanol in a proportion of 4:1 (glucose (20mM): phospholipid (5mM)) [25,148]. The final solution was left to react in boiling water during 15 min.

In this conditions, glucose reacts with the amino group of phosphatidylserine to form an unstable Schiff base, which undergoes an Amadori rearrangement to yield the stable deoxy-D-fructosyl PS, namely Amadori-PS as was showed in Scheme 3 (section 1.6.2).

2.2. Oxidation of PS and glycated PS

Oxidation of PS and glycated PS can be induced by different oxidant systems, either enzymatic or non-enzymatic. The study of the fragmentation pattern of non-glycated PS and glycated PS oxidation products is most useful for the identification of mass spectrometry characteristic fragmentation pathways that can be used targeted identification of PS glycoxidation products in complex samples.

One the most important *in vivo* oxidant agent is the hydroxyl radical, usually generated by the Fenton reaction, where iron ions (Fe^{2+}) react with hydrogen peroxide (H_2O_2) [153] (Scheme 4).

In this study, oxidation of different species of PS and glycated PS was performed using the hydroxyl radical generated by the Fenton reaction, by incubating PS and gluPS at 37 ºC with H_2O_2 (10 mM) and $FeCl_2$ (40 μM).

$$Fe^{2+} + H_2O_2 \rightarrow Fe^{3+} + \cdot OH + OH^-$$

Scheme 4: Formation of hydroxyl radical by Fenton reaction.

AAPH is a water-soluble azo-initiator which generates peroxyl radicals (Scheme 5) at a constant rate and at a given temperature by thermal decomposition [154] which is independent of the cellular metabolism. The AAPH peroxyl radical intermediate is the reactive oxygen species responsible for the oxidation of biomolecules such as lipids, peptides and proteins. Azo compounds have been used successfully as radical initiators and it is suitable for studying oxidation in aqueous solutions [155]. Thus, AAPH is a water-soluble azo-initiator is frequently used for oxidation studies in *in vitro* model systems [156].

In this work this oxidative system was used to induce oxidation in POPS standard and in the immortal human keratinocyte line HaCaT. Two different concentration of AAPH were used (30 mM and 50 mM).

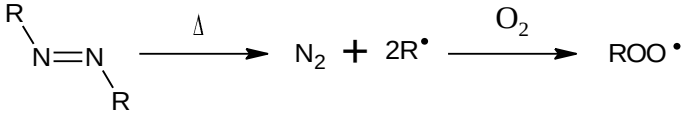

Scheme 5: Decomposition of AAPH produces molecular nitrogen and two carbon centered radicals. The carbon radicals may react with molecular oxygen to give peroxyl radicals.

UVA radiation (320-400 nm) is the most prominent component of terrestrial UV radiation-contributing in 90-95%. The exposure to UVA radiation causes toxic effects in cells, DNA lesions, mutagenesis and carcinogenesis, representing a known factor for the development of malignant melanoma and leading to aging of the skin [157,158]. The exposure to UVA can also lead to the formation of reactive radical oxygen species that further can trigger damage to biomolecules including lipids [159]. Among the ROS, UVA preferentially yield singlet oxygen ($^1O_2$), that is well-known as a strong oxidant, highly reactive towards electron-rich organic molecules, such as PUFA. UVA can also trigger the formation of hydroxyl radical, already reported as an oxidant agent, able to modify lipids. Overall, UVA may induce photooxidation of molecules via two distinct reactions: type I reactions, which involve the formation of free radicals, and type II reactions, which involve energy transfer and singlet oxygen generation (Scheme 6).

The UVA exposure biological effects and impact on photo-carcinogenesis and tumor progression has been receiving increasing attention [160,161,162]. In this work the PL response was evaluate in UVA-irradiated SK-MEL-28 cells (malignant melanoma cell line). The PLs and fatty acids were analyzed immediately after irradiation (total light dose 60 J/cm^2) and after 2 h and 24 h of irradiation (the cells after irradiation were re-incubated at 37 ºC during 2 h and 24 h).

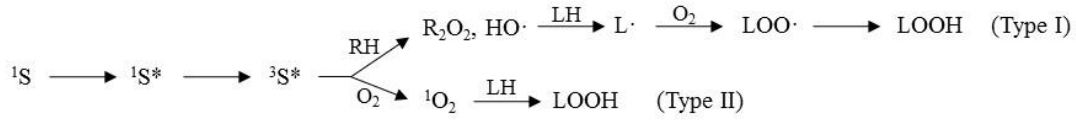

Scheme 6: Mechanisms of UVA-induced photooxidation. Photochemical reactions begin with photosensitizer (^1S) and its activation to a singlet excited state ($^1S^*$) rapidly converted to excited triplet state ($^3S^*$), which can follow two distinct pathways: type I – Charge transfer to oxygen ($^3O_2$) produces superoxide radical anions ($O_2^{\bullet-}$), which could produce hydrogen peroxide (H_2O_2) through

dismutation and, finally, hydroxyl radicals (HO•). Type II – A photosensitizer in an excited triplet state could suffer energy transfer to oxygen, producing singlet oxygen ($^1O_2$) [163].

2.3 Analytical approaches used in this work

PS and oxPS are biomolecules of huge interest due to its role in the regulation of macrophage-dependent clearance of apoptotic cells. In particular, the recent findings that oxidized PS is key player in these processes, revealed that it is needed a more deep understanding of the chemistry of oxPS and also to develop sensitive methods that allows the identification and quantification of oxPS in biological samples.

MS is the method usually used in the analysis of lipids in biological sample, due to its high sensitivity and is also becoming increasingly important in PL oxidation research [118]. MS has been used with success for the identification of oxidation products of PC [20,127,164,165], and in small extent to PE [152,166], PS [132,133,142] and CL [115,116,132,133,167]. Previous works in our laboratory showed that tandem mass spectrometry (MS/MS) alone or coupled with liquid chromatography (LC-MS/MS) allows the identification of huge number of oxidation products of PC, PE, glycated PE and CL. This research is the basis for their sensitive identification in biological samples using a lipidomic approach [20,115,152,164,166,168]. Accordingly, MS was the main method used for the analysis and monitoring of the PS oxidation although, so far, the published work regarding this issue is limited.

The lipidomic approach for the study of lipids from biological samples, usually involve several steps, beginning with the extraction of lipids from biofluids, tissues or cells, additional analyses of the lipid profile through MS with or without chromatographic separation (Figure 8). This methodology is also applied in the analysis of lipid oxidation products that are generated in *in vivo* conditions.

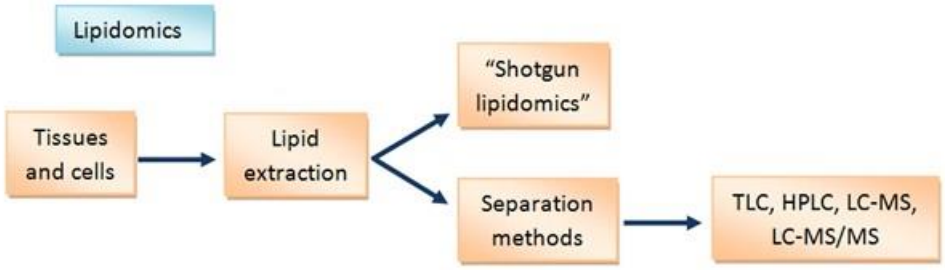

Figure 8: The lipidomic approach comprise a few experimental steps: first lipids are extract from tissues or cells and then are analyzed through MS with or without previous separation.

2.3.1 Lipid extraction

The general procedures for lipid extraction either from liposomes or cells, tissues or biofluids used organic solvents, and the most used methods differ on the type of organic solvents, the number and proportion of the different organic solvents used. Traditionally chloroform – methanol – water mixture is the most common used approach. There are two main extraction protocols using this solvent mixture: one described by Folch *et al* in 1957 [169] and other described by Blight and Dyer in 1959 [170]. The difference between these two methods is the proportion between chloroform and methanol: the Folch method uses $CHCl_3/CH_3OH$ (2:1) while Blight and Dyer method use $CHCl_3/CH_3OH$ (1:2). The basic principle of these two methods is that initially a mixture of chloroform and methanol is added in the sample creating a mono-phase system that extracts the lipids from the sample matrix. Then an amount of water is added to produce a biphasic system: the chloroform layer that contains lipids and methanol –water layer with the non-lipid components. Chloroform dissolves fat, methanol allows to breaks down the lipid protein bonds and inactivates the lipases, while water washes the non-lipid compounds.

After lipid extraction, two different approaches can be used: separation of lipid extracts in different classes by thin layer chromatography or high performed liquid chromatography before their analysis by MS; or direct analysis of the total lipid extract by MS through a direct infusion (shotgun lipidomics).

2.3.2 Lipid separation

The separation of separation of lipid extracts using chromatographic techniques have been extensively used and provide huge advantages in the lipid analysis. The most commonly used in lipid analysis are the gas chromatographic (GC), TLC and LC. Nowadays, the GC is frequently used in fatty acid analysis. The TLC and LC techniques are commonly used to separate different lipid classes before their analysis. Some researchers combine both techniques when analyzing PL: first, TLC is used to separate the different PL classes; and then each class is analyzed by LC-MS. This method is often used to assess phospholipid hydroperoxides [121,133].

Gas chromatography

GC has been used as a method for analyzing lipids and is usually coupled to MS (GC-MS) or with flame-ionization detection (GC-FID). To analyze and quantify the fatty acids by GC they need to be modified in order to be volatile. Thus, chemical derivatization is required. Evaluation of the PLs fatty acyl profile is usually performed by transmethylation in the presence of alkaline or acid catalyst, with further analysis of the fatty acids methyl esters (FAME) [171]. BF_3, HCl and H_2SO_4 are the most common used acid catalysts to perform acid-catalyzed transesterification, usually in methanol to generate FAME of FA esterified to triacylglycerol's and PLs. The most common base used as a catalyst is CH_3NaO, but it does not allow the esterification of free fatty acids [172]. Transmethylation of esterified fatty acids can be easily performed at room temperature using methanolic KOH 2M, and, due to its simplicity, is one of the most used methods for FAME analysis, and was used during our lipidomic studies [171,173,174]. In this work, GC-MS of FAME obtained from the lipid extracts of melanoma cell lines after UVA exposure. The FAMEs were separated based on their polarities and molecular weights.

Thin layer chromatography

TLC is the oldest technique used for lipid separation and fractionation and is still widely used nowadays [175]. The mainly advantages of the TLC are the ability to obtain a rapid screening of the samples and it does not required a sophisticate equipment to separate lipids with different polarities. The major disadvantages are the low resolution and

sensitivity of the technique [175,176]. Several research groups have used TLC (one and two-dimensional) and MS in lipidomics, as reviewed in [177]. This technique also has been applied in PS oxidation studies by Tyurin *et al.,* who used two-dimensional TLC in the identification of PS hydroperoxy- and hydroxy- derivatives [121,122,123,132,133].

Lipids are usually separated by TLC using silica as the stationary phase (designed normal phase TLC). When using adequate mixture of solvents it is possible to separate and subsequently quantify the different lipid classes [175,176,177]. For example, it is possible to separate the nonpolar lipids (triglycerides, free fatty acids, cholesterol and diacylglycerols) from the more complex lipids, like PLs, with an elution system containing ethyl ether and hexane [176]. For the separation of PL classes it is necessary a different elution system, such as, for example, a mixture of chloroform, ethanol, water and triethylamine [176]. In this, case the separation of PL classes reflects the differences in polarity of the polar head of PLs.

In this work, TLC was used to separate phospholipid classes from cell extracts and to fractionate the oxidation products of PS and glycated PS. Separation of oxPS can be achieved, particularly if oxidative modifications occur in serine polar head, changing substantially the polarity of molecule. For that, we used silica gel 60 plates from Merck, with a concentrating zone of 2.5×20 cm, as the stationary phase. The polar groups of PS and resulting from oxidation interact strongly with the surface of the gel particle. For silica gel chromatography, the mobile phase we used was a mixture of organic solvents: chloroform/ethanol/water/triethylamine (30:35:7:35, vol/vol/vol/vol).

The visualization of PLs in a TLC plate requires the use of visualization reagents, such as primule, a non-destructive dye specific for lipid visualization. The analysis of PLs can be performed on the TLC plate by observation of the intensity of the spots after UV irradiation, and is based on the fluorescent properties of primuline. Other revelation methods can be used including iodine vapor, ninhydrin and water. Ninhydrin is normally used to detect ammonia or primary and secondary amines. After visualization of the spots, the identification is based on the comparison with migration of lipid standards applied to the same TLC plate, and /or by the identification using MS analysis of the lipids. The relative quantification of PL classes can be achieved by the quantification of phosphate present in each spot, by measuring the phosphorous amount in each spot.

High-performance liquid chromatography

Several HPLC methods have been developed for the separation and quantitation of PLs. These methods have shown to be sensitive and to provide reliable measurements of tissue PLs [178,179]. HPLC analysis of PLs can be performed either using normal phase or reverse phase columns [180,181]. Normal phase chromatography effectively separates different PLs class [182,183], whereas reverse phase effectively separates PL on the basis of fatty acid residues [184]. Oxidized PL species can be separated from the non-oxidized congeners by reversed-phase chromatography, due to the distinct polarity caused by the position and number of oxygen atoms in the molecule of PL oxidation products [165,166,185]. Hydrophilic Interaction Chromatography (HILIC) is also used to separate PL classes. The HILIC chromatography uses hydrophilic stationary phases with reverse-phase eluents. This is an advantage comparing with normal phase, since it is possible separate PL classes very well similar normal phase chromatography, but using more appropriate solvents for MS analysis [186], such as methanol and acetonitrile. The HILIC methods also demonstrated excellent reproducibility [186]. Nowadays, HPLC is usually coupled with MS (HPLC-MS) as detection and identification method. This instrumental combination opened up completely new analytical perspectives in lipid research by combining the separation power of HPLC with selectivity and sensitivity of MS.

In this work, we have used reversed-phase HPLC, coupled to the MS, for the identification and characterization of the oxidation products from PAPS, glycated PAPS, POPS, glycated POPS and PLPS. Different elution systems were used: one to separate and identify oxidation products from PAPS and glycated PAPS (more details chapter IV.I) and another to separate and identify oxidation products from POPS and glycated POPS (more details chapter IV.II). HILIC-MS and MS/MS were the methods used to analyze the variation of phospholipid profile from melanoma cell lines when exposed to UVA (more details chapter VI).

2.3.3 Mass spectrometry

MS is the method usually used for the analysis of the lipid profile in biological sample and in the study of PL oxidation research, due to its high sensitivity and capability of identifying compounds [118]. MS-based methods measure the mass of electrically charged

molecules. In the analysis of the PLs and PL oxidation products, ESI is the most commonly used ionization source [118]. Phospholipids can form positive and/or negatively charged molecular ions depending on the structure of the polar head group. Usually PC, SM, PE and PS ionize by the uptake of a proton, and thus being identified as $[M+H]^+$ ions, while PE, PS, PI, PG and CL ionize preferentially with formation of negative ions $[M-H]^-$. Although PS can be protonated, it is usually analyzed in the negative ion mode, by the identification of deprotonated ion $[M-H]^-$ [187]. To obtain more information about the molecular structure it is necessary to proceed to the study of fragmentation of selected molecular ions, in a methodology called tandem mass spectrometry (MS/MS). Information gathered from MS/MS data and the identified typical fragmentation pathways allows to draw several conclusions about the structure of the analyzed phospholipids, including the identification of the polar head group, the identification of the fatty acyl chains and their location at *sn*-1 versus *sn*-2 positions [7].

Product ion scanning tandem mass spectrometry is one of the MS/MS approach's and is based in the isolation of a specific ion with a selected *m/z* value, which is induced to dissociate, usually by collision with an inert gas, to produce products ions with lower mass. Typically MS/MS involves multisteps, initiated with the isolation of the selected ion, performed by a first analyzer, followed by fragmentation in the collision cell and then the fragmented ions, called product ions, are separated based on their *m/z* value by the last analyzer (Figure 9). However some instruments (e.g. linear ion trap) with just one analyzer are able to perform multiple stage tandem mass spectrometry (MS^n). A multi analyzer mass spectrometer, such as a triple quadrupole (QqQ) and a Qtrap can also perform other MS/MS scanning modes, such as precursor ion scanning (PIS) and neutral loss scanning (NLS). The tandem mass spectrometry has been widely used in the structural characterization of molecules, including PLs and also of oxidation products of PLs [7,10,188,189,190,191,192]. In the present work, several mass spectrometers coupled to electrospray ionization sources were used, namely an electrospray Q-TOF, a linear ion trap and a Q-trap.

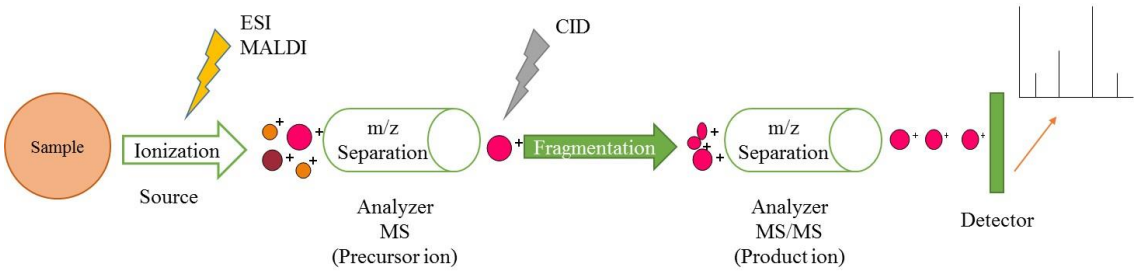

Figure 9: Scheme of tandem mass spectrometry (MS/MS). The sample injected into the mass spectrometer is ionized by electrospray (ESI) or matrix assisted laser desorption ionization (MALDI) and analyzed (MS), then a selected ion is fragmented by collision induced dissociation (CID) and analyzed in a second analyzer (MS/MS) the fragment ions are collected in a detector and the result is a spectrum of the fragment ions.

The presence of specific fragmentation patterns characteristic of each PL class, has turned PIS and NLS on powerful techniques for the identification and quantification of PL. The PIS and NLS modes allow targeted detection of PL polar head groups and the identification of PLs containing hydroperoxides in complex mixtures, as well as the detection of some individual oxidation products by their specific fragmentation patterns [193]. The analysis by PIS is based on a specific fragment ion exclusive to a particular class of PL. For example, PIS for ions at *m/z* 184 specifically detects PC, LysoPC and SM, while PIS for ions at *m/z* 241 allows detecting PI and LysoPI [193]. The NLS is based on identification of a neutral loss which is exclusive to a particular class of PL. For example the analysis of PS in negative ion mode can be screened by NLS of the specific neutral loss of 87 Da (loss of aziridine-2-carboxylic acid) [192,193,194]. PIS and NLS can be performed by direct infusion of the sample in the ESI source without prior separation or coupled with HPLC. The advantage of the former approach, usually called shotgun lipidomics, is the rapid processing of the samples with reproducibility and accuracy. However, this approach has the disadvantage of occurring ion suppression, a process that can be avoid using LC-MS [175]. Multiple reaction monitoring (MRM) approach, usually performed in triple quadruple spectrometers, is a target MS analysis that screen a specific parent ion/fragment ion pairs. This MS/MS mode is commonly used to quantify compounds, usually using the addition of an internal standard per PL class.

Tandem mass spectrometry has been widely used in the structural characterization of molecules including PLs and also of oxidation products of PLs

[7,10,188,189,190,191,192]. In the present work, several mass spectrometers coupled to electrospray ionization sources were used, namely an electrospray Q-TOF, a linear ion trap and a Q-trap. The linear ion trap coupled to HPLC, was widely used throughout this work, to monitor PS oxidation, and to identify specific fragmentation pathways of each oxidation and glycation products. The Q-TOF spectrometer and matrix-assisted laser desorption ionization (MALDI)-TOF-TOF were used to perform exact mass measurements of the new products identified. Targeted lipidomics was performed in this work using a QTrap spectrometer. NLS (of 58 Da) and PIS (for ions at *m/z* 137) specific of fragmentation patterns of newly identified PS oxidation products allowed to detect these type oxidation products in total lipid extracts from keratinocytes treated with AAPH to induce oxidative stress.

2.4. Evaluation of the anti/pro-inflammatory activity of PS and oxPS

Few published works reported the evaluation of the anti-inflammatory activity of PS and the information regarding oxPS is scarce, despite the increasing reports about oxPS exposure on surface of apoptotic cells and their possible role in the resolution of inflammation. Thus it is important to determine whether the exposure on the surface of apoptotic cells of oxidized PS and/or non-oxidized PS differentially modulates the functional responses in macrophages and if these events have anti or pro inflammatory effects. So, in an attempted to discover if PS and oxPS differently modulate a response in macrophages, we have evaluated the effect of these species in macrophage and LPS-induced macrophage activation response and the possible activation of intracellular signaling pathways. The pro inflammatory activity of PS and oxPS was evaluated by measuring the nitric oxide (NO) production by raw 264.7 macrophages incubated with PLPS and oxPLPS. To evaluate the anti-inflammatory properties of oxPS and PS, the macrophages were activated by LPS and co incubated with PS and oxPS. iNOS expression was also evaluated in the same conditions, as well as IL-1β by Real-time reverse transcription polymerase chain reaction (RT-PCR) analysis. In an attempt to elucidate the mechanism of the inhibition, MAPKs and NF-kB activation/inhibition were studied using Western blot analysis (Scheme 7).

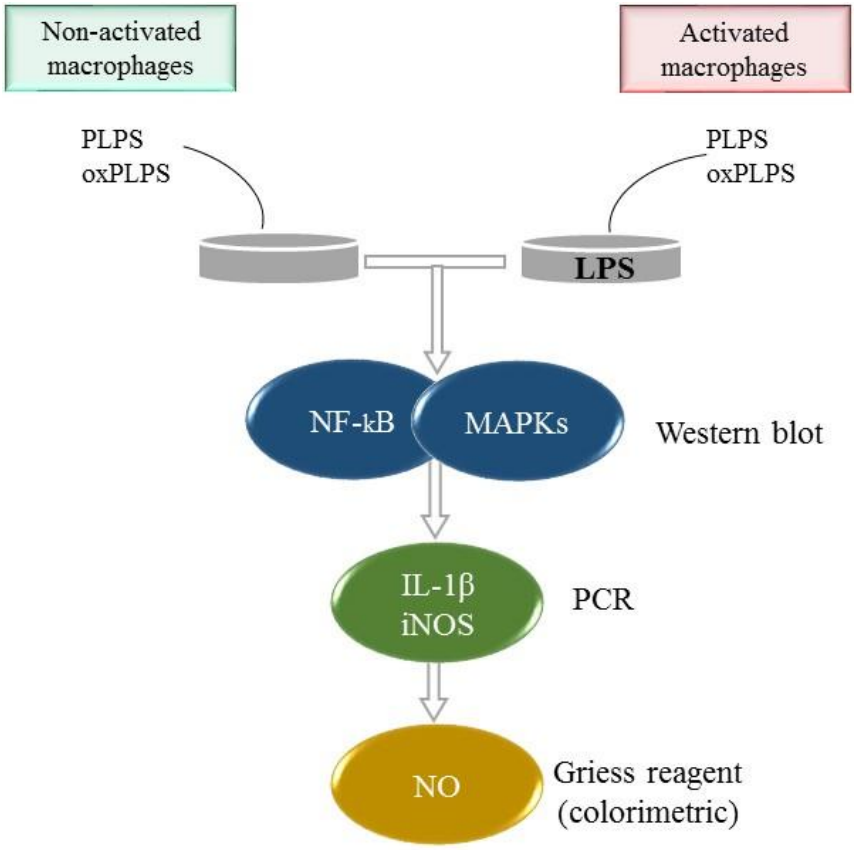

Scheme 7: Experimental design used to evaluate the pro- and anti- inflammatory properties of PLPS and oxPLPS through NO production. The pro-inflammatory properties were evaluated in non-activated macrophages and the anti-inflammatory in activated macrophages by LPS

The production of NO was measured by the accumulation of nitrite in the culture supernatants, using colorimetric reaction with Griess reagent [195] in macrophages and in lipopolysaccharide (LPS)-stimulated macrophages cell lines. LPS is in this context an endotoxin, which stimulates the production of pro-inflammatory mediators such as NO that is associated with the expression iNOS expression. A reduction in NO production indicate the potential of the PLPS and oxPLPS to attenuate an inflammatory response (the experimental details will be described in Chapter VIII)

Chapter III

Structural characterization of oxidized glycerophosphatidylserine: evidence of polar head oxidation

The results presented in this chapter were integrally published as follow:

E. Maciel, R.N. da Silva, C. Simoes, P. Domingues, M.R.M. Domingues, Structural Characterization of Oxidized Glycerophosphatidylserine: Evidence of Polar Head Oxidation, J. Am. Soc. Mass Spectrom., 22 (2011) 1804-1814.

Part of the results described in this chapter were presented in the following international congress

Lipid Maps annual meeting 2011" Lipidomics Impact on Cell Biology, Cancer, and Metabolic Diseases", 2 - 3 May 2011, La Jolla, CA.E. "Identification of oxidative modifications in phosphatidylserine polar head using lipidómica approach" (poster presentation by Elisabete Maciel)

3.1 Abstract

Non-oxidized phosphatidylserine (PS) is known to play a key role in apoptosis but there is considerable research evidence suggesting that oxidized PS also plays a role in this event leading to the increasing interest in studying PS oxidative modifications. In this work, different PS (1-palmitoyl-2-linoleoyl-sn-glycero-3-phospho-L-serine (PLPS), 1-palmitoyl-2-oleoyl-sn-glycero-3-phospho-L-serine (POPS), and 1,2-dipalmitoyl-sn-glycero-3-phospho-L-serine (DPPS) were oxidized in vitro by hydroxyl radical, generated under Fenton reaction conditions, and the reactions were monitored by ESI-MS in negative mode. Oxidation products were then fractionated by thin layer chromatography (TLC) and characterized by tandem mass spectrometry (MS/MS). This approach allowed the identification of hydroxyl, peroxy, and keto derivatives due to oxidation of unsaturated fatty acyl chains. Oxidation products due to oxidation of serine polar head were also identified. These products, with lower molecular weight than the non-modified PS, were identified as $[M-29-H]^-$ (terminal acetic acid), $[M-30-H]^-$ (terminal acetamide), $[M -13-H]^-$ (terminal hydroperoxyacetaldehyde), and $[M-13-H]^-$ (terminal hydroxyacetaldehyde plus hydroxy fatty acyl chain). Phosphatidic acid was also formed in these conditions. These findings confirm the oxidation of the serine polar head induced by the hydroxyl radical. The identification of these modifications may be a valuable tool to evaluate phosphatidylserine alteration under physiopathologic conditions and also to help understand the biological role of phosphatidylserine oxidation in the apoptotic process and other biological functions.

Keywords: Phosphatidylserine, Oxidation, Hydroxyl radical, Electrospray, Mass spectrometry

3.2. Introduction

Phospholipids are prone to oxidative modifications, generating a variety of oxidized products, mainly due to the modification of unsaturated fatty acyl chains [196]. Depending on the predominating oxidative process, different PLs oxidation products can be observed [197]. It is thought that oxidized PLs may have new biological properties, participating in various biological processes such as the immune response, inflammation, apoptosis, and age-related diseases [197]. However, little is known about the relationship between specific oxidation products and their biological effects.

Hydroxy and hydroperoxy phospholipid species were identified in several pathological conditions [121,131,132,133,198]. Kagan and co-workers showed that the pattern of phospholipid oxidation during apoptosis is non-random and that PS is one of the preferred peroxidation substrates [96]. The mass spectrometry has been used in the identification these PS oxidation products [118,192,194,199,200].

Although several studied the role of PS oxidation products in inflammation and apoptosis, there is still insufficient data on the mechanisms of oxidation and on the nature of the oxidized species formed. The objective of this research is to evaluate the molecular changes induced in phosphatidylserines due to oxidation induced by hydroxyl radical, focusing on the oxidation products resulting from oxidation of the polar head. The serine head group of this phospholipid resembles in its structure an α-amino acid, that are known to be prone to oxidation. Studies with myeloperoxidase (MPO), that produce hypoclorous acid (HOCl) in the presence of hydrogen peroxide and chloride, shows the formation of phosphatidylglycoaldehyde as product of reaction of the MPO-H_2O_2-Cl^- system with PS [141,142,143] and phosphatidylglyconitrile [141,142]. HOCl converts α-amino acids via chlorinated amine derivatives to aldehyde and nitrile species.

In order to know if oxidative modification can occur in the serine polar head, different PS species were subjected to oxidation induced by the hydroxyl radical generated under Fenton reaction (H_2O_2/Fe^{2+}) conditions and the oxidation products were subsequently separated by thin layer chromatography (TLC) and analyzed by electrospray (ESI), mass spectrometry (MS), and tandem mass spectrometry (MS/MS).

3.3. Experimental

Materials

1-Palmitoyl-2-linoleoyl-sn-glycero-3-phospho-L-serine (PLPS), 1-palmitoyl-2-oleoyl-sn-glycero-3-phospho-L-serine (POPS), 1,2-dipalmitoyl-sn-glycero-3-phospho-L-serine (DPPS), and phosphatidic acid were obtained from Avanti Polar Lipids, Inc. (Alabaster, AI, USA) and used without further purification. $FeCl_2$, EDTA and H_2O_2 (30%, w/w) were acquired fromMerck (Darmstadt, Germany). Triethylamine (Acros Organics, Geel, Belgium), chloroform (HPLC grade), methanol (HPLC grade) and ethanol absolute (Panreac) were used without further purification. TLC silica gel 60 plates with concentrating zone (2.5×20 cm) were purchased from Merck.

Oxidation of Phosphatidylserine by Fenton Reaction

Ammonium hydrogen carbonate buffer (5 mM, pH 7.4) was added to 1 mg of phospholipid was vortex-mixed and sonicated for the formation of vesicles. Oxidative treatments using Fe (II) and H_2O_2 were carried out by adding 40 μM $FeCl_2$/EDTA (1:1) and 10 mM of H_2O_2 to total a volume of 500 μL of solution. The mixture was left to react at 37 °C in the dark for several days with agitation. Controls were performed by replacing H_2O_2 with water and without H_2O_2 and Fe^{2+}.

ESI-MS Conditions (Linear Ion Trap)

The extent of oxidation was monitored by electrospray mass spectrometry in a linear ion trap mass spectrometer LXQ (ThermoFinnigan, San Jose, CA, USA). The LXQ linear ion trap mass spectrometer was operated in negative mode. ESI conditions were as follows: electrospray voltage was 4.7 kV; capillary temperature was 275 °C, and the sheath gas flow was 25 U. An isolation width of 0.5 Da was used with a 30 ms activation time for MS/MS experiments. Full scan MS spectra and MS/MS spectra were acquired with a 50 ms and 200 ms maximum ionization time, respectively. For MS/MS experiments, normalized collision energy (CE) was applied in the range of 17 to 20 (arbitrary units) for MS/MS. Data acquisition was carried out on an Xcalibur data system (ver. 2.0).

Exact Mass Measurement and Elemental Composition

Identification of the oxidation product ions corresponding to the oxidation in the polar head group was confirmed by exact mass measurement and elemental composition determination in a MALDI-TOF/TOF mass spectrometer. Elemental composition of the ion at *m/z* 721.5 (observed for DPPS) was confirmed by exact mass measurement and elemental composition determination using a ESI-Q-TOF2 mass spectrometer due to the presence of a contaminate with the same *m/z* value in the MALDI-MS spectrum.

MALDI-MS Conditions

MALDI mass spectra were acquired using a MALDI-TOF/TOF Applied Biosystems 4800 Proteomics Analyzer (Applied Biosystems, Framingham, MA, USA) instrument equipped with a nitrogen laser emitting at 337 nm and operating in a reflectron mode. Full scan mass spectra ranging from *m/z* 650 to 4000 were acquired in the negative mode. All spectra were acquired with 2,5-dihydroxybenzoic acid (DHB) matrix. The matrix solution was prepared by dissolving 10 mg of DHB in a 1 mL mixture of methanol: aqueous (1:1, vol/vol). For the accurate mass measurements, the lock mass in each mass spectrum was the calculated monoisotopic mass/charge of the non-modified phosphatidylserine and 1-palmitoyl-2-oleoyl-phosphatidylethanolamine as internal standard.

ESI-MS Conditions (ESI-Q-TOF2)

For the analysis in the ESI-QTOF2 instrument (Micromass, Manchester, UK), the flow rate was 10 μL min–1, the needle voltage was set at 3 kV, the cone voltage at 30 V, the ion source set at 80 °C, and the desolvation temperature at 150 °C. Mass spectra were averaged for 1 min. For the accurate mass measurements, the lock mass in each mass spectrum was the calculated monoisotopic mass/charge of the native phospholipid (non-modified phospholipid).

Separation of Oxidation Products of PS by Thin Layer Chromatography

The oxidation products were separated by thin layer chromatography (TLC) using silica gel 60 plates with concentrating zone 2.5×20 cm (Merck KGaA). Prior to separation, plates were treated with boric acid 2.3% in ethanol. The plates were developed with solvent mixture chloroform/ethanol/water/triethylamine (30:35:7:35, vol/vol/ vol/vol).

Lipid spots on TLC plates were observed by exposure to primuline. The TLC spots identified as oxidized PS were scraped from the plates and extracted using chloroform/methanol (2:1, vol/vol). The oxidation products separated by thin layer chromatography (TLC) were analyzed by electrospray (ESI), mass spectrometry (MS), and tandem mass spectrometry (MS/MS).

3.4. Results and Discussion

This work focuses on the ESI-MS analysis of PS that was submitted to oxidation induced by the hydroxyl radical generated under Fenton reaction (H_2O_2/Fe^{2+}). Selected PS were dipalmitoyl-phosphatidylserine (DPPS; C16:0/C16:0; *m/z* $[M–H]^–$=734), 1-palmitoyl-2-oleoyl-phosphatidylserine (POPS; C16:0/C18:1; *m/z* $[M–H]^–$ =758), and the 1-palmitoyl-2-linoleoyl phosphatidylserine (PLPS; C16:0/ C18:2; *m/z* $[M–H]^–$ =756) (Figure 10). Since DPPS contains saturated acyl chains, it is considered as a model for studying oxidation of the phospholipid polar head [196].

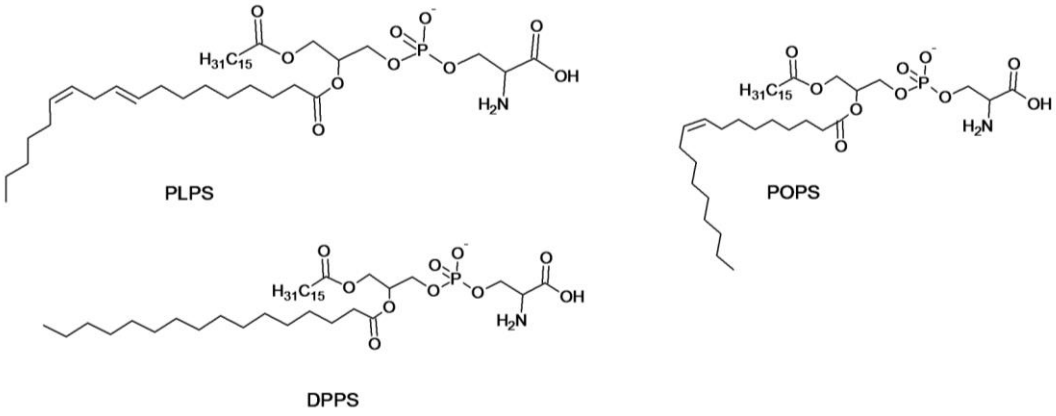

Figure 10: Molecular structures of PLPS, POPS and DPPS

Comparing the ESI-MS spectra of the three PS obtained before and after oxidation (Figure 11), new ions can be observed. These ions correspond to the $[M–H]^–$ molecular ions of oxidation products. The ESI-MS spectra of PLPS (Figure 11a), acquired after exposure to oxidative conditions, show a larger number of new molecular ions. This is due to the presence in this molecule of two double bonds in the sn-2 fatty acyl chain, increasing the number of possible oxidation sites. Lower number of ions were observed for POPS (Figure 11c) and even lower for DPPS (Figure 11e). In the spectra of oxPLPS and oxPOPS, some oxidation products can be observed at higher *m/z* values than the non-

modified PS, corresponding to the oxidation products with insertion of oxygen atoms as hydroperoxides ([M–H+2O]⁻), hydroxide ([M–H+O]⁻), and keto ([M–H+O–2 Da]⁻) derivatives. These oxidation products will be briefly discussed in this work since they have already been described and fully characterized [87,132,201].

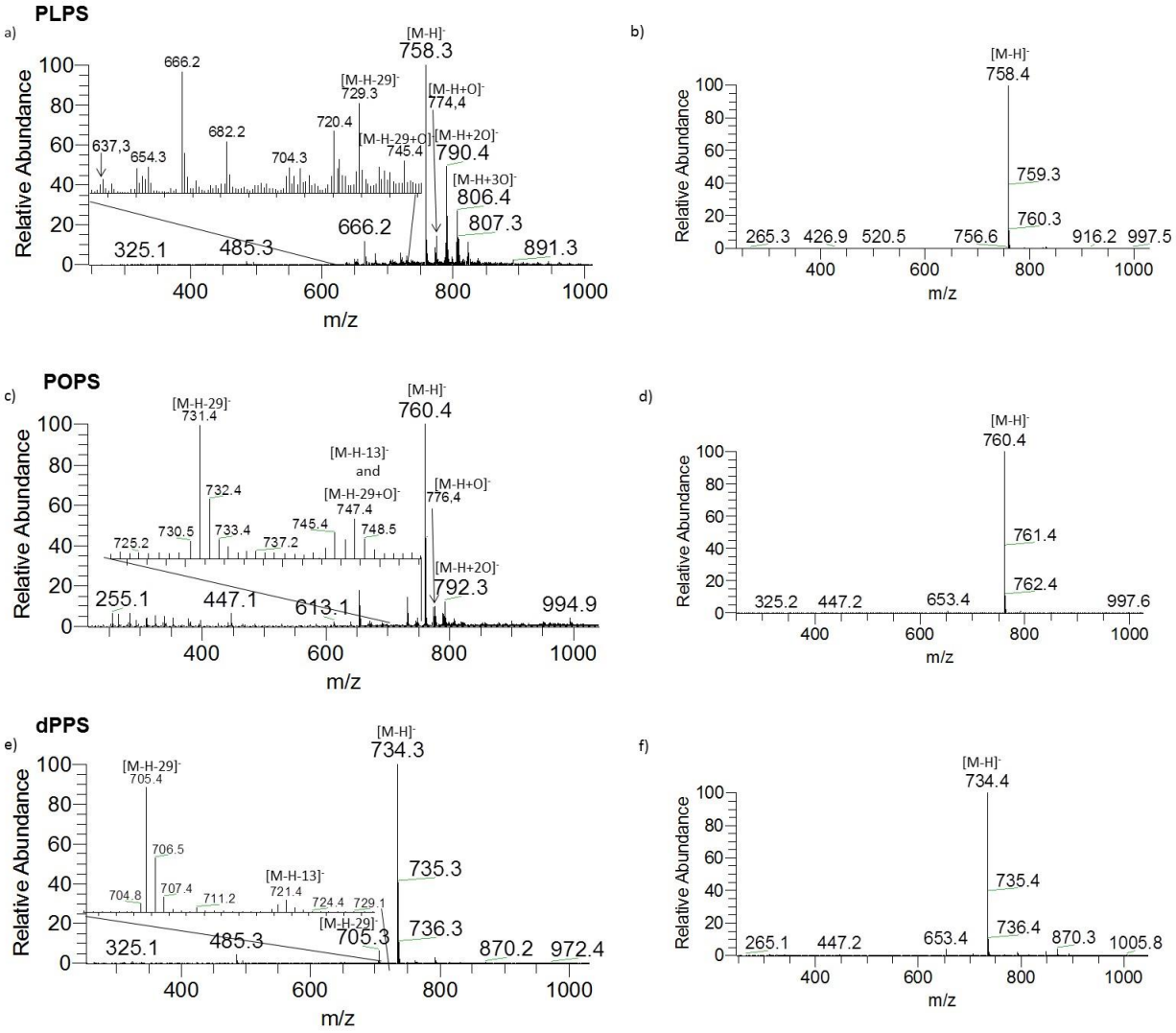

Figure 11: ESI-MS spectra of PLPS (a), (b), POPS (c), (d) and DPPS (e), (f). Spectra a, c, and e were acquired after exposing samples to oxidative stress. Spectra b, d, and f were acquired from control samples

In the spectrum obtained after oxidation of the PLPS (Figure 11a) we can observe new ions at *m/z* 666 and 682 (666 Da+16 Da), with lower *m/z* than the non-modified PLPS. These ions correspond to oxidation products with shortened acyl chain at C9 and a carboxylic acid terminal. Short chain oxidation products originated from cleavage of fatty acyl chains have been described for PS [201] and have been studied in phosphatidylcholine, phosphatidylserine, and cardiolipin phospholipids [116,127,166]. The

shortened oxidation products are generated after abstraction of the bis-allylic hydrogen atoms by the hydroxyl radical, which through a β- scission mechanism, break down to short-chain phospholipid products with terminal aldehydic or carboxylic acid functions. As reviewed elsewhere, these are well known products of lipid peroxidation [165,202]. No short chain oxidation products were formed during POPS oxidation, similar to previously observed POPC oxidation, using the same oxidative conditions [165].

There are other ions observed at lower *m/z* than the non-modified PS in MS spectra of oxidized PLPS, POPS, and DPPS (Figure 11a, c, and e), which were not assigned as short chain compounds. These oxidation products, with less 29, 30, and 13 Da compared with the native PS, occur due to oxidative modification in PS polar head, as confirmed by separation using thin layer chromatography (TLC) (Figure 12), and analysis by tandem mass spectrometry will be described latter. Elemental composition determination for the ions with less 29 Da (for DPPS: $C_{37}H_{70}O_{10}P$, error 18.7 ppm; for POPS $C_{39}H_{72}O_{10}P$, error 27.8 ppm, for PLPS $C_{39}H_{70}O_{10}P$, error −15.4 ppm), with less 30 Da (for DPPS, $C_{37}H_{71}NO_9P$ error 10.3 ppm; for POPS $C_{39}H_{73}NO_9P$, error −1.3 ppm; for PLPS $C_{39}H_{71}NO_9P$ error −32.1 ppm), and with less 13 Da (for DPPS $C_{37}H_{70}O_{11}P$ error −9.9 ppm; for POPS $C_{39}H_{72}O_{11}P$ error 20.9 ppm) confirmed the modification of serine polar head.

Mass spectrometry analysis, in positive mode, of these oxidized PS, showed molecular ions that correspond to the same oxidation products, but observed as low abundant $[M+H]^+$, $[M+Na]^+$, and $[M–H+2Na]^+$ ions (data not shown). However, the oxidation product resulting from loss of 29 Da was not observed. We propose that this oxidation product contains a carboxylic acid group polar head, as will be described latter, forming, preferentially, negative ions. To better characterize these new oxidation products, they were further analyzed by TLC, MS, and MS/MS in negative mode.

Phosphatidylserine Oxidation in Fatty Acyl Chains – Analysis by ESI-MS/MS

Hydroperoxide and hydroxide derivatives are primary oxidation products of lipids and phospholipids, and occur during PLPS and POPS oxidation. DPPS does not yield these oxidation products because it has two saturated fatty acyl chains that do not oxidize [196]. ESI-MS/MS spectra of PLPS and POPS oxidation products show formation of hydroxy $[M–H+O]^–$, keto $[M–H+O–2\ Da]^–$, peroxy $[M–H+2O]^–$, and hydroxy peroxy $[M–H+3O]^–$ derivatives, as summarized in Table 1. In all these MS/MS spectra, we can observe a major

product ion formed by loss of 87 Da, due to loss of phospholipid polar head. This is an abundant loss, typical of PS [194]. MS/MS analysis (Table 1) shows that insertion of oxygen atoms occur in the linoleic (for PLPS) or oleic acids (for POPS), as confirmed by the observation of the carboxylate anions of modified fatty acyl chains $R'COO^-$, in agreement with previous published work [115,116,133,165,166].

Table 1: Product Ions Observed in ESI-MS/MS Spectra of Oxidized PLPS and POPS, which were determined by Tandem Mass Spectrometry to Contain Modified Fatty Acyl Chains

	Modifications		$[M-H]^-$	$R_2'COO^-$	$[M-R_1COOH-87-H]^-$
PLPS	+1 O	-OH	774	295	431
		-=O	772	293	429
	+2 O		790	311	447
	+3 O		806	327	463
	Short (C9)*		666	187	323
	Short (C9)+O		682	203	339
POPS	+1 O		776	297	433
			774	295	431
	+2 O		792	313	449
DPPS	-		-	-	-

*Short chain oxidation product in C9 with carboxylic acid terminal.

Phosphatidylserine Oxidation with Modification of in Polar Head—Analysis by TLC and ESI-MS/MS

Oxidative modifications in the PS polar head should change significantly the polarity of these species. Consequently, their separation may be possible through simple techniques such as TLC, which is widely used for separation of different classes of phospholipids. Thus, oxidative mixtures of the three PS under study were fractioned by TLC, as is illustrated in Figure 12.

In the TLC of the oxidized PS, five new spots were resolved using the same conditions used to separate phospholipid classes, demonstrating that significant changes of polarity have occurred, presumably with formation of new compounds with different polar head structures. The new spots were scraped from the plate, the oxPL extracted, and further analyzed by ESI-MS and MS/MS. Table 2 summarizes are all molecular ions observed in MS spectra for each spot of TLC and the proposed structure.

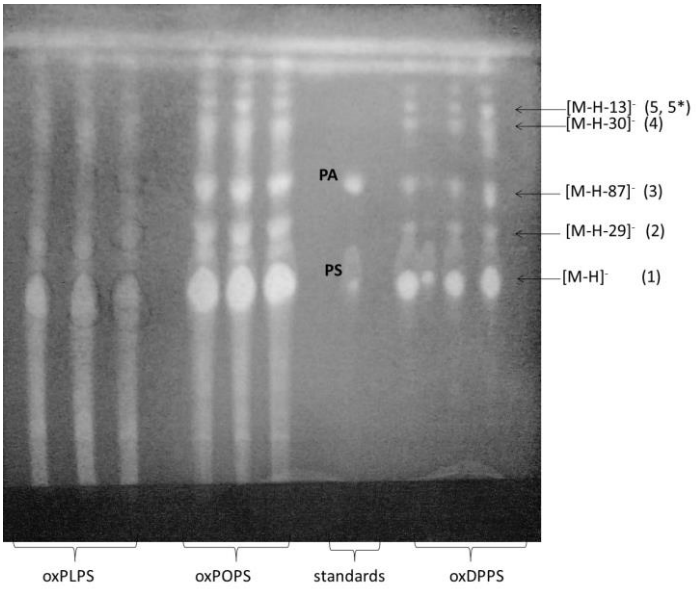

Figure 12: TLC of oxidation products of phosphatidylserines with modifications in the polar head (oxPLPS (lines 1, 2, and 3), oxPOPS (lines 4, 5, and 6), and oxDPPS (lines 8, 9, and 10). PS and PA standards were applied in line 7

Table 2: Molecular ions observed in the ESI-MS spectra from the different spots identified in the TLC plate for each PS. The Table shows the *m/z* value of the $[M–H]^–$ ions, their most probable identification, including the modified polar head group, and the typical neutral loss observed in the MS/MS spectra

Spots #	Modification	[M-H]⁻			Polar Head	Neutral Loss
		PLPS	POPS	DPPS		
1	-	758	760	734	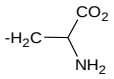	87
	+14	772	774	-		
	+16	774	776	-		
	+30	788	790	-		
	+32	790	792	-		
	+46	804	-	-		
	+48	806	-	-		
2	-29	729	731	705		58
	-29+14	743	745	-		
	-29+16	745	747	-		
	-29+30	759	761	-		
	-29+32	761	763	-		
3	-87	671	673	647	absent	-
	-87+14	685	687	-		
	-87+16	687	689	-		
	-87+30	701	703	-		
	-87+32	703	705	-		
4	-30	728	730	704	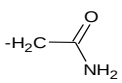	57
	-30+14	742	744	-		
	-30+16	744	746	-		
	-30+30	758	760	-		
	-30+32	760	762	-		
5	-13	-	747	721		74
	-13+16	-	763	-		
5*	-13		747			58

In spots #1 (Figure 12, Table 2) we have identified the non-modified PS together with the hydroperoxides, keto, and hydroxides oxidation products (Table 1), in agreement with previous results [133]. In the spots #2 (Figure 12, Table 2) we identified, for all PS, oxidation products with polar head modifications $[M–H–29]^-$. Spots #3 (Figure 12, Table 2) shows a Rf similar to the phosphatidic acid (PA) standard. The MS spectra acquired from samples of these spots show $[M–H–87]^-$ ions, thus indicating that PA is generated during PS oxidation, with complete loss of polar head. PA was also observed during cardiolipin oxidation by γ- irradiation [203,204]. The oxidation products from spots #4 (Figure 12, Table 2) contained a head modification, with a mass difference of less 30 Da. It is also possible to observe spots #5 (Figure 12, Table 2) in the DPPS and POPS. Analysis of the MS spectrum of these samples shows the presence of ions at *m/z* 747 and 763 for POPS, and an ion at *m/z* 721 for DPPS. These ions have a difference of 13 Da compared with the non-modified PS. In the case of PLPS, these oxidation products were not observed, probably because they might decompose to fatty acyl short chain derivatives, which are not observed in TLC plate. The MS spectra of POPS samples from spots #5 show ions at the same *m/z* of ions found in spots #2. These are necessarily different compounds, since they have different Rf. The nature of these ions was determined by MS/MS analysis and will be discussed in another section of this manuscript. In each spot of PLPS and POPS oxidized samples, additional ions with plus 14 Da (+O-2 Da), 16 Da (+O), 30 Da (+2O-2 Da), 32 Da (+2O) 46 Da (+3O-2 Da), and 48 Da (+3O) were observed. These ions resulted from additional oxidation in unsaturated fatty acyl chain, as is shown in Table 2.

In order to confirm the structure of the oxidation products found in spots #2 to #5, MS/MS of all the identified molecular ions (Table 2) were obtained and analyzed. These spots corresponded to oxidation products resulting from modification of PS polar head.

The oxidation products with less 29 Da than the non-oxidized PS, found in spots #2, show a neutral loss of 58 Da, instead of the typical 87 Da of PS (Figure 13). The MS/MS of these ions $[M–H–29]^-$ show the non-modified carboxylate anions $RCOO^-$, thus confirming that the structural changes occurred at the polar head and not at the fatty acyl chains. This main fragmentation pathway (loss of 58 Da) is also observed for the oxidation products with additional oxidation (+nO) in the unsaturated fatty acyl chains observed for PLPS and POPS. Tandem mass spectra of these ions also showed the modified $RCOO^-$.

Oxidation products with less 29 Da were observed during the oxidation of amino acids and were identified as the result of oxidative reactions that lead to loss of an amine group and CO_2, with formation of a terminal carboxylic acid group [205]. We propose that oxidation products observed in spots #2 are glycerophosphoaceticacid derivatives (GPAA) (Scheme 8).

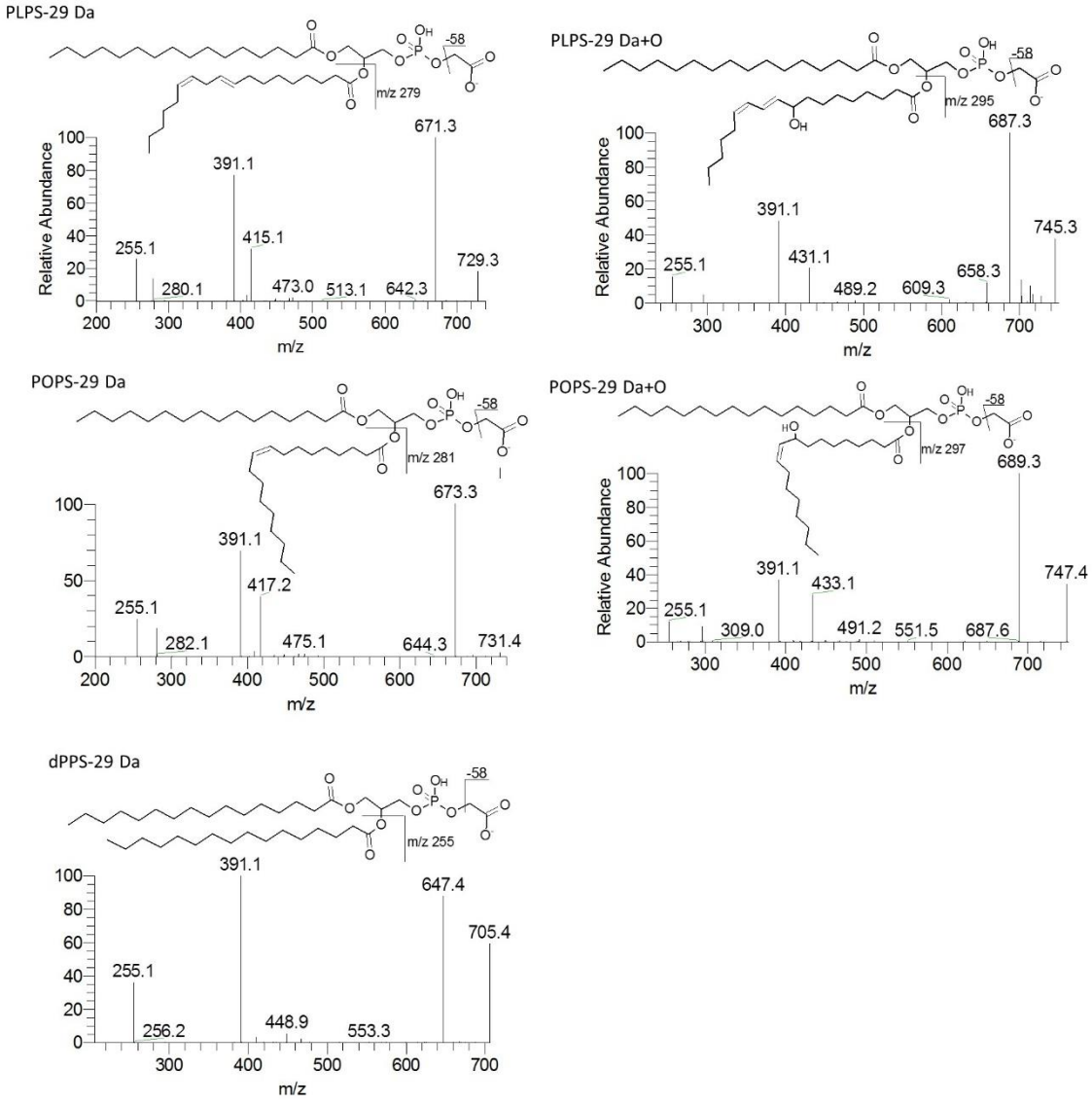

Figure 13: ESI-M/MS spectra of $[M–H–29]^-$ molecular ions that resulted from oxidation of PLPS (*m/z* 729 and 745), POPS (*m/z* 731 and 747), and DPPS (*m/z* 705), found in spots #2. The proposed structures of each molecular ion are also shown. The structures of the oxidation products PLPS–29 Da+O and POPS –29 Da+O illustrate one possible location of the hydroxyl group in the unsaturated fatty acyl chains

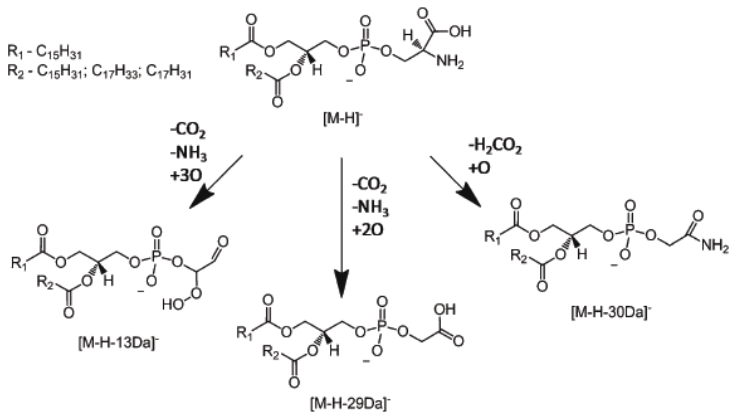

Scheme 8: Oxidation products of PS formed by Fenton reaction with observed modifications on the polar head group: terminal hydroperoxyacetaldehyde (−13 Da), terminal acetic acid (−29 Da), and terminal acetamide (−30 Da)

The new oxidation products identified in spots #3 are due to oxidation in polar head group of the PS. These oxidative modifications are not observable when a neutral loss scan of aziridine-2-carboxylic acid (neutral loss of 87 Da) is performed to detect oxidized PS from in vivo samples [201].

The MS/MS spectra of molecular ions $[M–H–30]^–$ found in spots #4 of the three PS show loss of the head group as loss of 57 Da, but typical loss of 87 Da is not observed. We propose that these oxidation products resulted from decarboxylation and generation of a keto moiety, as observed during amino acid and peptides oxidation (Scheme 8) [205]. In these species, loss of modified polar head group (−57 Da) is not the base peak of the spectra, in contrast with the typical behavior of PS and the other identified PS oxidation products. A minor loss of polar head group resembles the behavior observed in negative mode tandem mass spectra of PE. Also, as observed in PE tandem mass spectra, $R_1COO^–$ ions were found to be more abundant than $R_2COO^–$ ions. This is in contrast with the typical behavior of PS and other oxidation products with a terminal carboxylic acid function, which show in their MS/MS spectra that RA of $R_2COO^–$>$R_1COO^–$ [7]. These findings also contributed to proposing the presence of a free amine moiety in these oxidation products (M-30 Da). We propose that oxidation products observed in spots #3 are glycerophosphoacetamide derivatives (Scheme 8) (Figure 14).

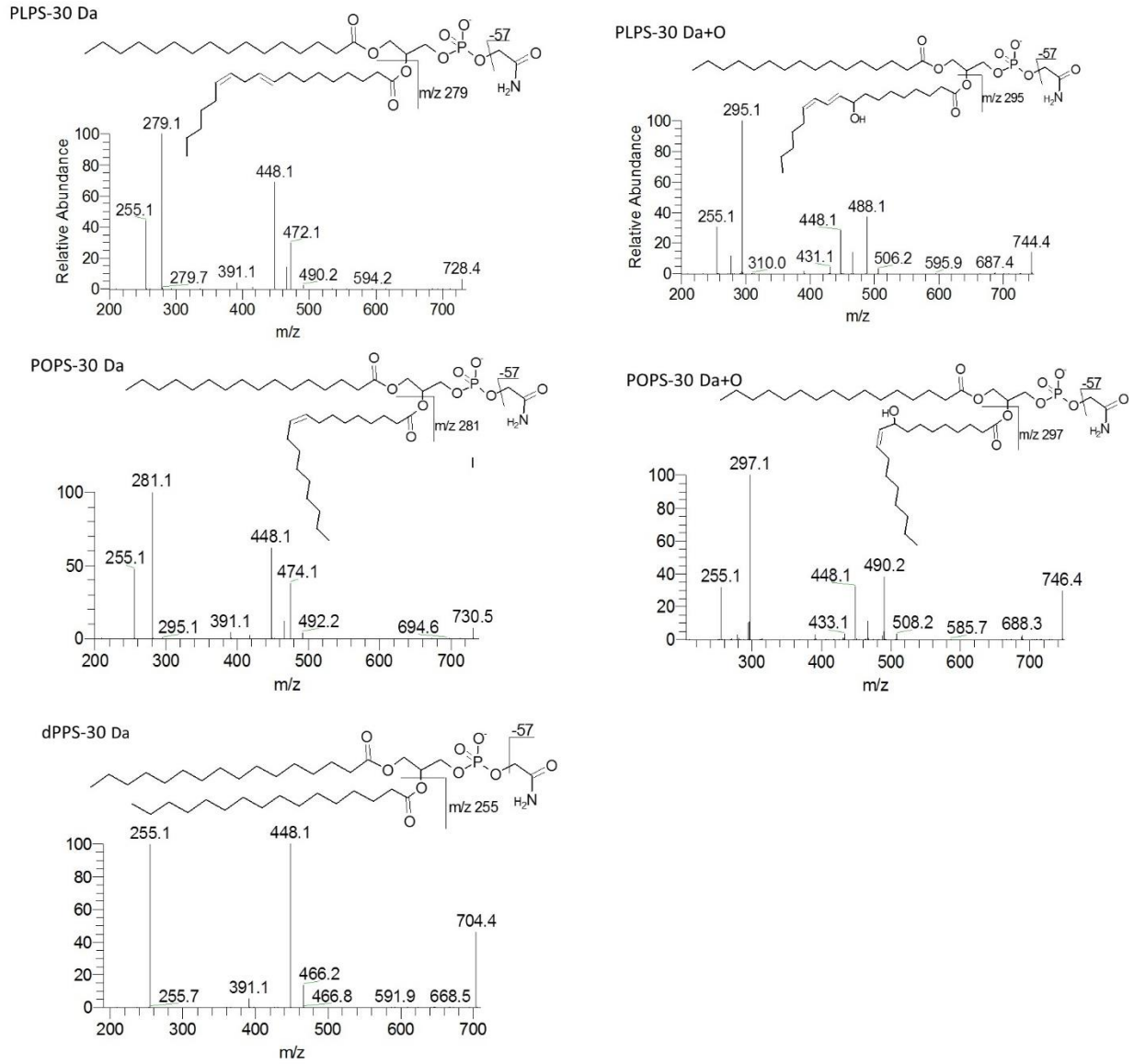

Figure 14: ESI–MS/MS spectra of $[M–H–30]^-$ ions that resulted from oxidation of PLPS, POPS and DPPS, found in spots #4. The proposed structures of each molecular ion are also shown

The MS/MS spectra of $[M–H–13\ Da]^-$ molecular ions that resulted from oxidation of DPPS and POPS (Figure 15) and were found in spots #5 (Table 2), are very similar. In these spectra, we observe a major fragment ion formed by loss of 32 Da ($-O_2$), indicating the presence of a hydroperoxides [116,206]. Due to the fact that DPPS does not oxidize in the fatty acyl chain, the hydroperoxide moiety should be located in polar head group. We propose that these oxidation products resulted from oxidation in the polar head group, with formation of terminal hydroperoxydeacetaldehyde, as shown in Table 2. The presence of a modified polar head group is also evidenced by the presence of carboxylate anions of the

non-modified fatty acyl chains in the MS/MS spectra and the observation of a neutral loss of 74 Da (hydroperoxydeacetaldehyde). The MS/MS spectra of POPS (*m/z* 747) found in spots #5* also shows oleoyl carboxylate anion +16 Da (*m/z* 297) and loss of 58 Da (CH2(OH)HC=O). This suggests the presence of an isobar originated by oxidation of the polar head group, with formation of a species containing a terminal hydroxyacetaldehyde, and a hydroxylated acyl chain (Figure 15a). The ion at *m/z* 763, observed in POPS spots #5, corresponds to a species with a hydroperoxydeacetaldehyde polar and a hydroxylated acyl chain, as suggested by the fragment ion at *m/z* 297 $[RCOO+O]^-$ and a neutral loss 74 Da (Figure 15 b).

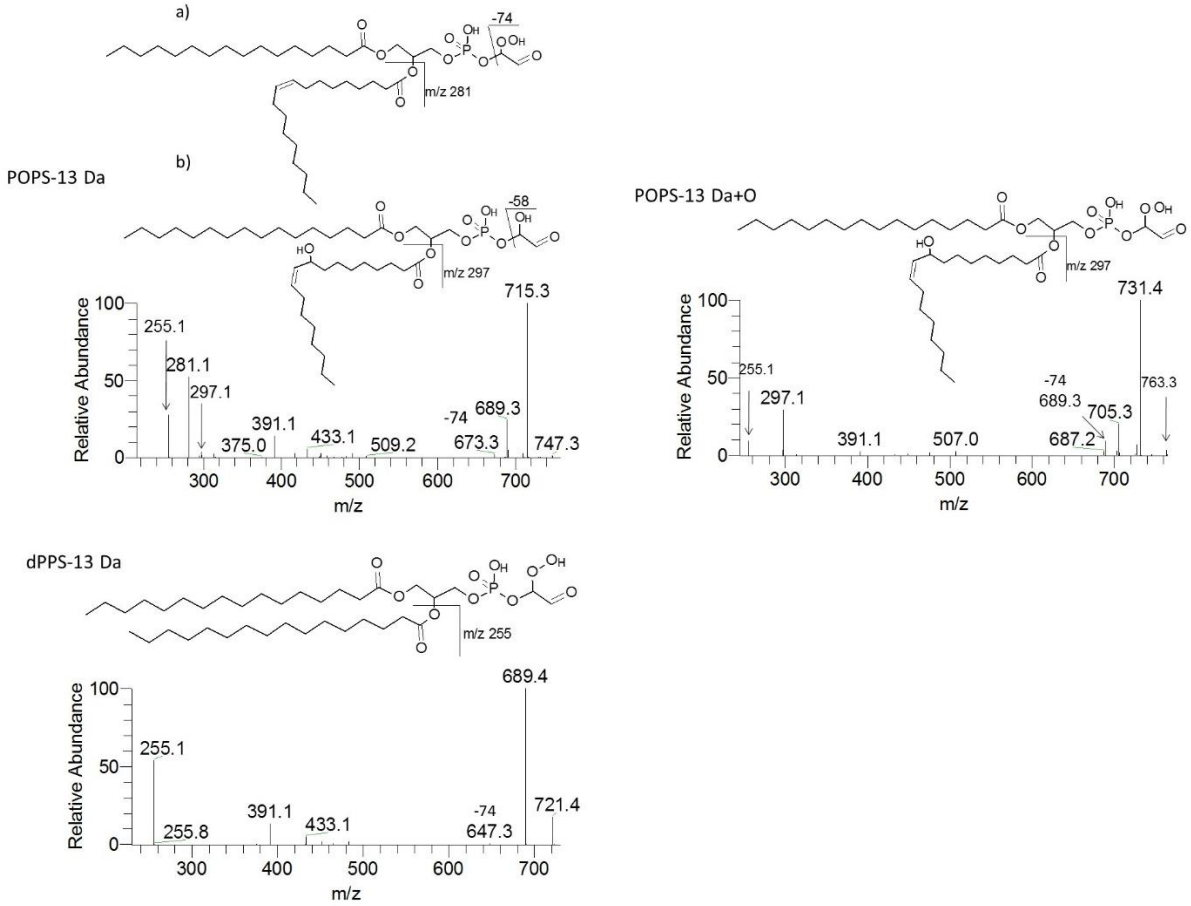

Figure 15: ESI-M/MS spectra of the [M – H – 13]– ions that resulted from oxidation of POPS (*m/z* 747 and 763) and DPPS (*m/z* 721), found in spots #5. The proposed structures of each molecular ion are also shown

Phosphatidylserine polar head group has a serine amino acid moiety linked to the phosphate group It is well known that amino acids are prone to oxidation, not only in the

side chains but also in the alpha carbon [205,207,208]. Oxidative modification of the PS polar head group has been reported to occur during oxidation induced by HClO and catalyzed by myeloperoxidase [141,142], confirming the reactivity of serine under oxidative conditions. The oxidation products reported to be formed in those conditions were not the same as the ones reported in this work. In those works, the authors reported the formation of 1,2-dipalmitoyl-sn-glycero-3-phosphoacetaldehyde and 1,2dipalmitoyl-sn-glycerol-3-phosphonitrile derivatives.

The changes of the serine polar head group induced by the hydroxyl radical resemble the oxidative modifications of the amino acid structure, such as the oxidative decarboxylation with formation of an additional keto group (oxidation products with −30 Da). Decarboxylation of amino acids is a well-known reaction occurring during amino acid and peptide oxidation. Loss of CO_2 from the C terminal is due to β-scission of an alkoxyl radical at the C terminal alpha carbon. This reaction is proposed to be initiated from the abstraction of hydrogen linked to an alpha carbon, generating a tertiary radical that is stabilized by the amine nitrogen and carbonyl group [207,209].

The modification in the PS polar head group leading to the formation of the oxidation products with less 29 Da should occur by decarboxylation plus deamination with formation of a terminal carboxylic acid moiety (oxidation products with −29 Da). Loss of amine and CO_2 resembles typical modification already observed during amino acid oxidation, as reviewed elsewhere [205,208].

3.5. Conclusions

Oxidative modifications induced to phosphatidylserine were identified and characterized by thin layer chromatography combined with tandem mass spectrometry. Oxidation products were fractionated by TLC and further characterized by MS/MS. This approach allowed the identification of hydroxyl, peroxy, and keto derivatives due to oxidation of unsaturated fatty acyl chains. Additionally, we have identified for the first time five families of oxidation products, with lower molecular weight than the non-modified PS, which resulted from oxidative modifications on the serine polar head group. They were identified as $[M–29–H]^-$ (terminal acetic acid), $[M–30–H]^-$ (terminal acetamide), $[M–13–H]^-$ (terminal hydroperoxideacetaldehyde), and $[M–29–H]^-$ (terminal hydroxyacetaldehyde). Phosphatidic acid derivatives were also formed as result of PE

oxidation. Hydroxy, keto, peroxy, and short chain acyl derivatives of these new molecules were also identified for PS phospholipids with unsaturated fatty acyl chains. The results presented here allowed the identification, for the first time, of modification of PS polar head group induced by the hydroxyl radical mediated oxidation in vitro conditions. The identification of oxidation products of PS is far from being completely explored, although it is essential to understanding the relation between the PS oxidation products formed and the specific biological activity that they mediate.

Chapter IV

Oxidation of PS and glycated PS analysis by LC-MS and LC-MS/MS

Chapter IV.I

Evaluation of oxidation and glycoxidation of 1-palmitoyl-2- arachidonoyl-phosphatidylserine by LC-MS/MS

Chapter IV.II

Liquid chromatography-tandem mass spectrometry of phosphatidylserine advanced glycated end products

Chapter IV.I

Evaluation of oxidation and glycoxidation of 1-palmitoyl-2- arachidonoyl-phosphatidylserine by LC-MS/MS

The results presented in this chapter were integrally published as follow:

E. Maciel, R. Faria, D. Santinha, M.R.M. Domingues, P. Domingues, Evaluation of oxidation and glyco-oxidation of 1-palmitoyl-2-arachidonoyl-phosphatidylserine by LC–MS/MS, J. Chromatogr. B, 929 (2013) 76-83.

4.1.1 Abstract

Phosphatidylserine (PS) is an aminophospholipid found mainly in the plasma membranes of all mammalians cells, playing important roles in biological processes such as apoptosis and cell signaling. Due to the presence of a free amine group, under hyperglycemic conditions, PS can undergo glycation reaction, which may increase the susceptibility to oxidation. However, far too little attention has been paid to glycation and oxidation of PS. In this work we studied the oxidation, glycation and glyco-oxidation of 1-palmitoyl-2-arachidonoyl-sn-glycero-3-phospho-l-serine (PAPS). PAPS and glycated PAPS were oxidized through a Fenton reaction and the oxidation products were monitored by ESI-MS in negative mode. Also, we developed a new sensitive liquid chromatography method coupled with tandem mass spectrometry (LC–MS/MS) to provide a complete profile of oxidized and glyco-oxidized PS. We were able to separate and identify several oxidation products of PAPS and glycated PAPS with modifications in unsaturated fatty acyl chain as long chain oxidation product (hydroxy and mono to tetra-hydroperoxy derivatives), and short chain products with a shortened fatty acyl chain with C5 and C8 length and aldehyde or carboxylic terminal. We have also observed oxidation products arising from structural changes in the serine polar head, which lead to oxidation products with an acetic acid terminal (glycerophosphoacetic acid derivatives) and lysoPS species. Oxidation of glycated PAPS gave rise to several products involving oxidative cleavages of the glucose moiety, mainly between C1 and C2 of the sugar unit. These oxidation products with different polar head groups have shown distinct neutral loss fragmentation patterns. Simultaneous oxidative modifications of the polar head and the fatty acyl chains were also observed. The findings from this study contribute to an ongoing effort to detect PS oxidation and glycoxidation products in biological systems.

Keywords: Phosphatidylserine; Aminophospholipid; Oxidative stress; Glycation; Mass spectrometry

4.1.2 Introduction

Phosphatidylserine (PS) is an acidic natural occurring phospholipid, found in the cellular membrane of a great variety of organisms [38,210]. PS is present in higher proportions in brain and the central nervous system, comprising about 15% of the total phospholipid pool [39]. Changes in PS composition have been correlated with brain diseases, such as depression and neurodegenerative diseases [211]. In fact, there is increasing evidence that neurodegenerative diseases are associated with oxidative stress [212] and lipid peroxidation [213]. Hydroxyl and hydroperoxy derivatives of oxidized PS, arising from oxidation in fatty acyl chains were detected in pro-inflammatory conditions by Kagan and co-workers [133]. Maki et al. [130] observed that peroxidation products of phosphatidylserine (PS-OOH) and phosphatidylinositol (PI-OOH) were elevated in human brains of patients with Alzheimer's disease (AD). Hyperglycemic conditions are usually associated with glycation of biomolecules, such as nucleotides, proteins and aminophospholipids. Consequences of glycation damage include increased oxidative stress, DNA mutations and compromised lipid membrane integrity [214]. Recently, it has been recognized that hyperglycemia due to Type 2 diabetes mellitus (T2DM) is a risk factor for cognitive dysfunction or dementia, especially related to Alzheimer's disease (AD) [215]. However, the research to date has tended to focus on protein glycation rather than phospholipid glycation. Nevertheless, glycated phosphatidylethanolamine (PE) has been implicated in the in vivo rise of ROS production [24,25,26,27,28,29]. Also, early evidence suggested that glycated PE promote lipid peroxidation, partly through the generation of ROS [28,216]. Glycation is associated with oxidative stress, mainly due to the formation of oxidation intermediaries like Schiff bases, Amadori rearrangement products, and advanced glycation end products (AGEs) [27,149]. This dual relation between glycation and oxidation may play a key role in inflammation and other diabetes complications [150,151].

A detection method for analyzing oxidized phospholipids in biological systems should be able to detect modified phospholipids, including the modified polar head groups. In fact, modified serine head groups, arising from PS oxidation, have been identified in mitochondria of brain of rats subjected to oxidize stress induced by tacrine [217]. It has been described that the brain is more vulnerable to oxidative stress oxidative stress than other organs, due to the high content in polyunsaturated fatty acyl chains, including

arachidonic acid [218,219]. In this work we developed a new sensitive liquid chromatography method coupled with tandem mass spectrometry to provide a complete profile of oxidized and glycoxidized PS. We have tested this method studying oxidative modifications induced by the hydroxyl radical in 1-palmitoyl-2 arachidonoyl-PS (PAPS) and glycated PAPS (gluPAPS).

The generation of phospholipid oxidation products in model systems using pure phospholipids and glycated phospholipids standards allows the mass spectrometric characterization of these products. This knowledge is essential to design diagnostic assays, which can be used as methodology in analyzing complex biological matrices. However, since PSs are minor phospholipids (~10% of the total PL content), it is expected that such methodologies should require targeted analysis using multiple resonance monitoring (MRM) [220,221]. This work provides information of fragmentation pattern of the different oxidation products, providing information needed for targeted analysis.

4.1.3 Material and methods

Materials

1-Palmitoyl-2-arachidonoyl-phosphatidylserine was purchased from Avanti and was used without further purification. Ferrous chloride and hydrogen peroxide (30%, w/v) (Merck, Darmstadt, Germany) were used for oxidation reactions. Triethylamine (Acros organics), chloroform (Analytical reagent grade), methanol (HPLC grade, Fisher Chemical), ethanol absolute (Panreac) and TLC silica gel 60 with concentrating zone (2.5 cm × 20 cm) (Merck Darmstad, Germany) were used for the separation of oxidized and glyco-oxidized samples.

Phosphatidylserine glycation

Glycated PS samples were synthetized by adding 1 mg of phospholipid to 1,2 mg of glucose, dissolved in 300 μL of methanol. The solution was mixed and the reaction tube was immersed in the boiling water during 15 min, as previously described for the glycation of aminophospholipids [24,25]. The glycation reaction was monitored by electrospray mass spectrometry (ESI-MS).

Oxidation of phosphatidylserine and glycated phosphatidylserine by Fenton reaction

Vesicles of phospholipids and glycated phospholipids were prepared in ammonium bicarbonate buffer 5 mM (pH 7.4). In a typical experiment, 1 mg of phospholipid in chloroform was evaporated to dryness, 446 μL of buffer was added, and the mixture was shaken mechanically on a vortex mixer for 10 min and then sonicated for 1 min. The sample was kept under nitrogen atmosphere at all times [222]. The oxidation was induced by hydroxyl radical generated under Fenton reaction conditions (Fe^{2+}/H_2O_2). Hydroxyl radical is highly reactive oxygen species, involved in lipid peroxidation in vivo [223]. The oxidation was performed by adding to the solution 4 μL of $FeCl_2$ (5 mM stock solution) and 50 μL of H_2O_2 (500 mM stock solution) in order to obtain a final concentration of 40 μM of $FeCl_2$ and 50 mM of H_2O_2 in a total volume of 500 μL. The mixture was incubated at 37 °C in the dark for 2 days. Controls were performed by replacing hydrogen peroxide with water. The oxidation was monitored by ESI-MS.

LC–ESI-MS conditions

HPLC–MS and HPLC–MSn experiments were performed on a Waters Alliance (Milford, USA) Model 2690 chromatographic system equipped with a pre-column split (Accurate, LC Packings, USA) and a Supelco Bio Wide Pore C5 column (15 cm × 0.5 mm, 5 μm) kept at room temperature (22 °C). The reaction mixture was diluted 50 fold before injection and a volume of 10 μL was introduced into the column, using a flow rate of 20 μL min−1. The phospholipid oxidation products were separated using water–methanol (90:10, v/v, eluent A) and methanol (100%, eluent B) programmed as follows: isocratic mode for 5 min with 20% B and a linear increase from 20% B to 80% B in 35 min and a further increase to 100% B in 5 min. The mobile phase was brought back to the initial conditions in 10 min and allowed to equilibrate for 15 min until the next injection.

The LXQ linear ion trap mass spectrometer (ThermoFinnigan, San Jose, CA) was operated in negative mode. ESI conditions were as follows: electrospray voltage was 4.7 kV; capillary temperature was 275 °C and the sheath gas flow was 25 units. An isolation width of 0.5 Da was used with a 30 ms activation time for MS/MS experiments. Full scan MS spectra and MS/MS spectra were acquired with a 50 ms and 200 ms maximum ion injection time, respectively. Normalized collision energy™ (CE) was varied between 15 and 20 (arbitrary units) for MS/MS. To obtain the product-ion spectra of the major

components during LC experiments, cycles consisting of one full scan mass spectrum and four data-dependent MS/MS scans were repeated continuously throughout the experiments with the following dynamic exclusion settings: repeat count, 3; repeat duration, 15 s; and exclusion duration, 45 s. Data acquisition was carried out on an Xcalibur data system (V2.0).

Thin layer chromatography

The oxidation products were separated by thin layer chromatography (TLC) using silica gel 60 plates with concentrating zone 2.5 cm × 20 cm (Merck KGaA). Prior to separation, plates were treated with 2.3% boric acid in ethanol. The mobile phase was chloroform/ethanol/water/triethylamine (30:35:7:35, vol/vol/vol/vol) [224]. The lipid spots on TLC plates were observed by exposure to primuline. The TLC spots identified as oxidized PS were scraped from the plates and extracted using chloroform/methanol (2:1, vol/vol). The oxidation products separated by thin layer chromatography (TLC) were further analyzed by ESI-MS.

4.1.4 Results

PAPS and gluPAPS were oxidized under Fenton reaction conditions (H_2O_2/Fe^{2+}). Oxidative reactions were monitored by ESI-MS in the negative mode (Figure 16). The oxidation products of PAPS (oxPAPS) and of gluPAPS (oxgluPAPS) were identified and structurally characterized by LC–MS and MS/MS as resumed in Table 3 and Table 4. The ions identified as oxidation products of PAPS and gluPAPS were detected both at higher *m/z* values and at lower *m/z* values when compared with the non-oxidized PL species (PAPS and gluPAPS). The oxidation products with higher molecular weight were assigned as hydroxy and hydroperoxy derivatives. These typical oxidative modifications occur mainly in fatty acyl chains (PL+nO) and are named long chain oxidation products [20,118,133]. Scheme 9 shows the proposed structure of the observed oxidation products resulting from oxidation of PAPS and gluPAPS.

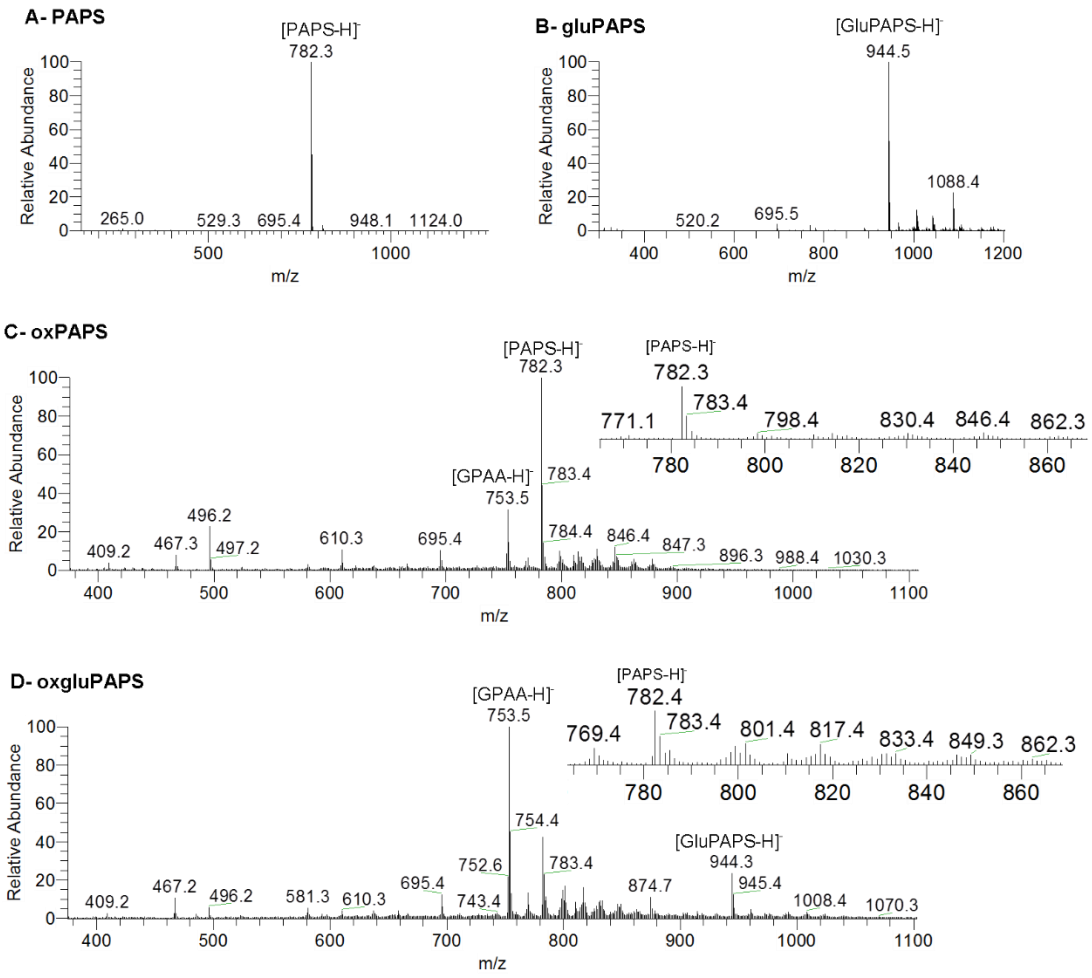

Figure 16: ESI-MS spectra, acquired in the negative mode of: (A) PAPS, (B) glycated PAPS, (C) oxidized PAPS, and (D) oxidized glycated PAPS.

Oxidative cleavages involving the fatty acyl chains gave rise to oxidation products with lower *m/z* values, named short chain oxidation products. These short chain oxidation products are oxidation products with shorter fatty acyl chain (C5 or C8) and carboxylic or aldehyde terminals. LysoPS were also observed, arising from oxidative elimination of one fatty acyl chain (loss of $R_2C=O$). These modifications have also been observed in the oxidation induced by the hydroxyl radical in phosphatidylcholine (PC) and phosphatidylethanolamine (PE) [20,118,127,165,166].

Glycerophosphoacetic acid derivatives (GPAA) were also observed. These lower molecular weight PS oxidation products arise from polar head oxidation and cleavage of the serine group, originating oxidation products with a mass shift of −29 Da (Scheme 9). Combined cleavage of polar head group and fatty acyl chain (short chain products) was

also observed as result of PAPS oxidation. The cleavage in the serine moiety has been described in when studying the oxidation of serine amino acid but also in peptides [205,225]. This cleavage involves the loss of the amine group and CO_2, with formation of terminal carboxylic acid group. However, oxidative modification of phospholipids polar head groups is not commonly observed. These polar head modifications have been identified in the oxidation glycated PE but not in non-glycated PE [152]. In Figure 16 we can see that the ions corresponding to the GPAA have a higher relative abundance in the gluPAPS spectrum. These GPAA derivatives can be separated by thin layer chromatography (TLC) (Figure 17), as reported in a previous work [168].

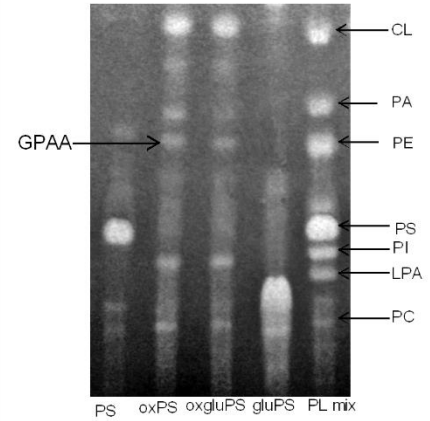

Figure 17: Mobility rate along a TLC plate of phosphatidylserine, oxidized phosphatidylserine, oxidized glycated phosphatidylserine and glycated with other phospholipid classes (phosphatidylcholine (PC), lysophosphatidic acid (LPA), phosphatidylinositol (PI), phosphatidic acid (PA), phosphatidylethanolamine (PE) and cardiolipin (CL))

In gluPAPS, we have also detected oxidation products arising from oxidative modifications in the glucose moiety. During oxidation of gluPAPS, cleavages in the C1 single bond C2 bonds of glucose moiety can occur, leading to the formation of new oxidation products. In this study we identified oxidation products with formamide terminal in polar head group, arising from cleavage of C1 in the glucose moiety.

4.1.4.1 Analysis of oxidation products of PAPS by LC–MS and LC–MS/MS

After using MS for an initial characterization of the oxPAPS and oxgluPAPS samples, we further characterized the oxidation products of PAPS using LC–MSn. Table 3 shows the main oxidation products that were identified in the LC–MS spectra of oxPAPS, along

with the corresponding retention times (RT). In this table, the observed oxidation products were grouped accordingly to the location and nature of the modifications. GPAA oxidation products were found to have a lower retention time than the non-modified PAPS (Figure 18) and the corresponding oxidation products with the serine polar head. The short chain products, as expected, had the shorter RT.

Table 3: Identification of the main oxidation products observed in the LC-MS spectrum of oxPAPS, grouped accordingly to the location and nature of the modifications. The table also shows the *m/z* values of the $[M-H]^-$ ions and the retention time (RT).

Oxidation products of PAPS	Intact serine polar head (NL=87) *m/z* (RT)	Glycerophosphoacetic acid derivatives (NL=58) *m/z* (RT)
Long chain oxidation products		
($C_{16:0}$)($C_{20:4}$)	782.4 (42.5 min)	753.3 (37.0 min)
($C_{16:0}$)($C_{20:4+O}$)	798.4 (36.0 min)	769.4 (34.7 min)
($C_{16:0}$)($C_{20:4+2O}$)	814.4 (35.9 min)	785.4 (32.3 min)
($C_{16:0}$)($C_{20:4+3O}$)	830.4 (35.9 min)	801.4 (32.1 min)
($C_{16:0}$)($C_{20:4+4O}$)	846.4 (35.9 min)	817.4 (32.3 min)
($C_{16:0}$)($C_{20:4+5O}$)	862.4 (35.4 min)	833.4 (32.3 min)
($C_{16:0}$)($C_{20:4+6O}$)	878.4 (35.4 min)	849.4 (31.5 min)
($C_{16:0}$)($C_{20:4+7O}$)	894.4 (35.4 min)	865.4 (31.4 min)
($C_{16:0}$)($C_{20:4+8O}$)	910.4 (35.4 min)	881.4 (31.3 min)
Short chain oxidation products at the Sn-2 position		
($C_{16:0}$)(C_4COOH)	610.3 (13.9 min)	581.2 (10.6 min)
($C_{16:0}$)(C_4CHO)	594.2 (29.9 min)	565.2 (17.6 min)
($C_{16:0}$)(C_5(O)C_7COOH)	666.3 (12.5 min)	637.2 (10.6 min)
($C_{16:0}$)(C_5(O)C_7CHO)	666.3 (29.0min)	637.2 (16.4 min)
($C_{16:0}$)	496.2 (26.1 min)	467.2 (13.2 min)

NL – neutral loss.

The long chain oxidation products (hydroperoxy and hydroxy derivatives) eluted between 35 and 37 min (Figure 18). These products were observed at *m/z* 798.4 (782 + 16 Da), 814.4 (782 + 32 Da), 830.4 (782 + 48 Da), 846.4 (782 + 64 Da), 862.4 (782 + 80 Da), 878.4 (782 + 96 Da), 894.4 (782 + 112 Da) and 910.4 (782 + 128 Da) (Table 3). The long chain oxidation products of the GPAA derivatives, arising from the addition of 1–8 oxygen atoms to the arachidonoyl chain, eluted between 31 and 35 min. These species were observed as deprotonated molecular ions at *m/z* 769.4, 785.4, 8014, 817.4, 833.4, 849.4, 865.4 and 881.4 (Table 3). Tandem mass spectra, obtained using data dependent acquisition, were used to identify the structures of these oxidation products. The LC–MS/MS spectra of these ions showed the neutral loss of 58 Da, instead of the characteristic

loss observed in the spectra of PS molecular ions (−87 Da) [189]. As an example, we show in Figure 19 the LC–MS/MS spectra of the molecular ions at *m/z* 846 (PS-(C16:0)(C20:4+4O)) and 769 (GPAA-(C16:0)(C20:4+O)).

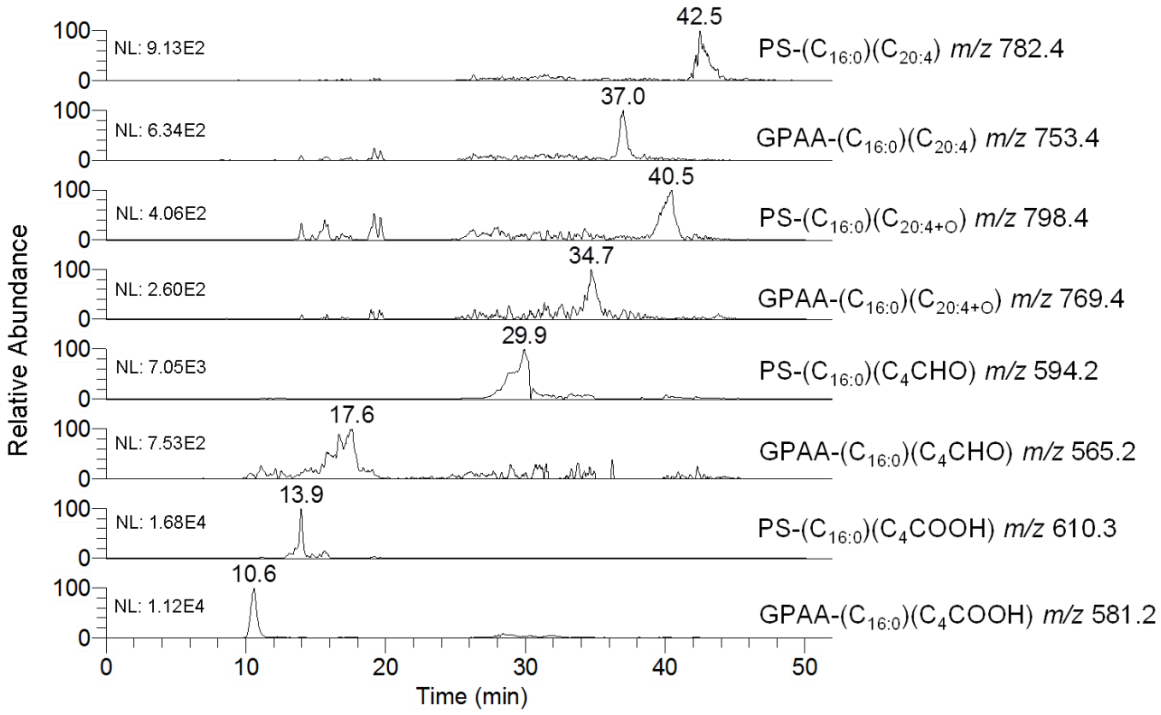

Figure 18: LC–MS recorded ion chromatogram (RIC) of the deprotonated molecular ions $[M-H]^-$ of the oxidation products of PAPS (NL = absolute intensity).

The short chain oxidation products, arising from cleavage of unsaturated sn-2 acyl chain, eluted between 12.5 and 13.9 min when a carboxyl group was present and between 29.0 and 29.9 min when an aldehyde group was present (Table 3). The most abundant short chain oxidation product was observed at *m/z* 610, corresponding to the oxidation product with a carboxyl group at C-5 (R'_2C_4COOH, RT=13.9 min). The deprotonated molecular ion at *m/z* 594.4, eluting at RT 29.9 min, corresponds to the short chain oxidation product with a C5 aldehyde group (R'_2C_4CHO).

The GPAA with fatty acyl chain shortened at C5 and C8 eluted between 10 and 11 min (carboxyl group) and between 16 and 17 min (aldehyde group) (Table 3). In Figure. 19C we can see the LC–MS/MS spectra and the proposed structures of the deprotonated molecular ion $[M-H]^-$ at *m/z* 610, identified as oxPS with a short fatty acyl chain and a C5 terminal carboxylic acid. The LC–MS/MS spectra of the product ion at *m/z* 581, identified

as a GPAA oxidation product with a short fatty acyl chain with C5 carboxyl group are shown in Figure 19D. In both spectra we can see the fragment ion at *m/z* 523, arising from the neutral loss of polar head (87 Da for the ion at *m/z* 610 and 58 Da for the ion at *m/z* 581). The fragment ions at *m/z* 496 (Figure 19C) and 467 (Figure 19D) arise from the neutral loss of the C5 fatty acyl chain with a carboxylic acid group (R′2COOH), while the fragment ion at *m/z* 267 arises from the neutral loss of palmitoyl (R_1COOH) from the ion at *m/z* 523 ([PA′-H]$^-$).

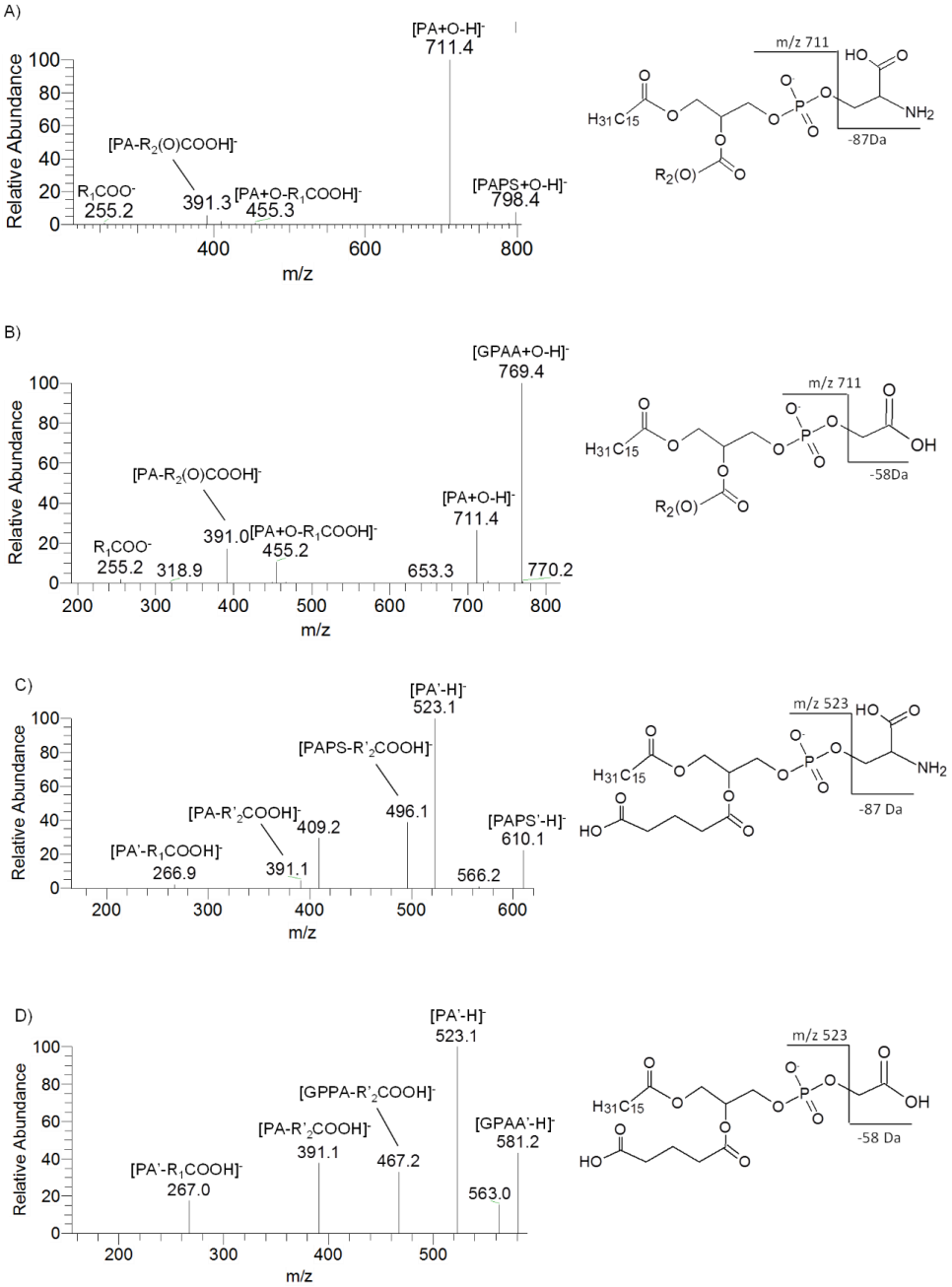

Figure 19: LC–MS/MS spectrum of the ion at *m/z* 798, identified as PS-(OH) (A). LC–MS/MS spectrum of the ion at *m/z* 769 identified as GPAA-OH (B). LC–MS/MS spectrum of the molecular

ion at *m/z* 610, identified as PS-(C_4CHO) (C). LC–MS/MS spectrum of the ion at *m/z* 581 identified as PS-(C_4CHO) (D). All spectra were recorded in the negative mode.

In this work, we have also observed the formation of lysoPAPS ([PAPS-R_2C=O]−) as PS and gluPS oxidation products. The lysoPAPS with no modification in the polar head group was observed in the LC–MS spectrum at *m/z* 496 (RT 26.1 min) and the lyso oxidation product with a glycerophosphoacetic acid polar head group was observed at *m/z* 467 (RT 13.2 min) (Figure 20). These lysoPS with modifications in polar head group were observed for the first time in this work.

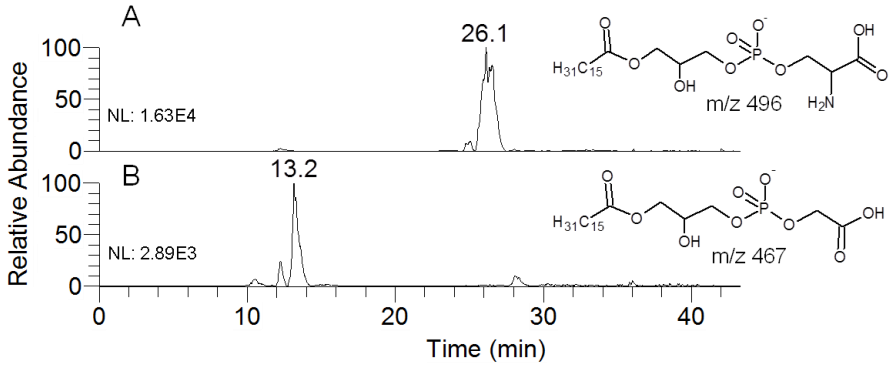

Figure 20: LC–MS recorded ion chromatogram (RIC) of the ions: at *m/z* 496 (RT 26.6 min) identified as lysoPS without modifications in polar head group (A) and at *m/z* 467 (RT 13.5 min) identified as lysoPS with modification in polar head group (acetic acid as polar head group) (B) (NL = absolute intensity).

Isobaric compounds were also separated and further identified by LC–MS/MS. As it is shown in Figure 21, the isobaric ions observed at *m/z* 666.3 (RT 12.5 and 29 min) were identified as the oxidation product with a hydroxylated C8 carboxylic group chain ($R'_2C_5(O)C_7COOH$) and the oxidation product with an hydroperoxylated C8 aldehyde group ($R'_2C_5(OO)C_7C=O$), respectively. The characterization of these structures was only possible due to their different retention times: In the LC–MS/MS spectrum acquired at 12.5 min, we can observe de neutral the loss of 44 Da due to the loss of CO_2 from the carboxylic acid group, indicating that this was an oxidation product with a carboxylic group in the fatty acyl chain (Figure 21). The neutral loss of 44 Da was not observed in the LC–MS/MS spectrum acquired at 29 min.

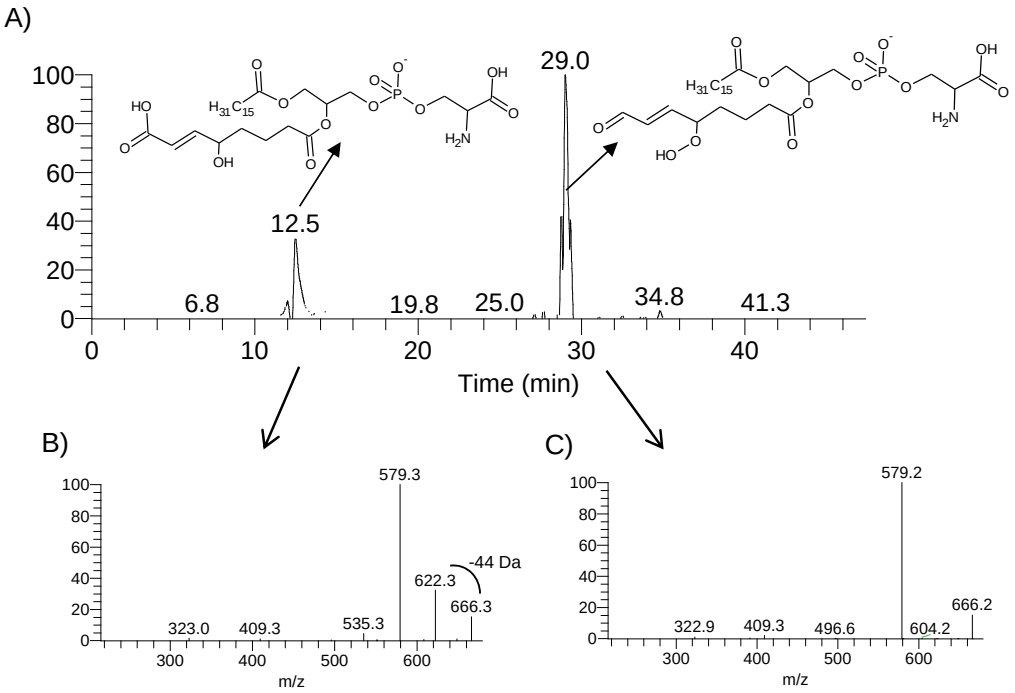

Figure 21: LC–MS recorded ion chromatogram (RIC) (A) and LC–MS/MS spectra of isobaric compounds observed at *m/z* 666.3, observed at a retention time of 12.5 min (B) and29 min (C) and proposed structures.

4.1.4.2 Analysis of oxidation products of gluPAPS by LC–MS and LC–MS/MS

The free amino groups of aminophospholipids (PE and PS) are targets for glycation. This corresponds, as described for peptides and proteins, to an extension of the concept of the Maillard reaction into biological systems [147]. Glycated phosphatidylethanolamines (gluPE) were characterized by tandem mass spectrometry, showing a predominant neutral loss of the glucose moiety (−162 Da) [152]. However, the fragmentation pattern of glycated PS has not been described before. In this work, we have studied the fragmentation pattern of gluPAPS in the negative ion mode. The MS/MS spectrum of the deprotonated molecular ions $[M\text{-}H]^-$ of gluPAPS is shown in Figure 22. The most abundant product ions were observed at *m/z* 782.3 and 695.3, arising respectively from the loss of the glucose moiety (−162 Da) and from the combined loss of aziridine-2-carboxylic acid and the glucose moiety (87 Da+ 162 Da) (Figure 22). Other minor fragment ions were also observed in the MS/MS spectra: product ions arising from glucose fragmentation with the loss of 90 Da ($-C_3H_6O_3$); product ions arising from loss of the fatty acyl chain; and the product ion at *m/z* 303.1, identified as the fatty acid anion (R_2COO^-).

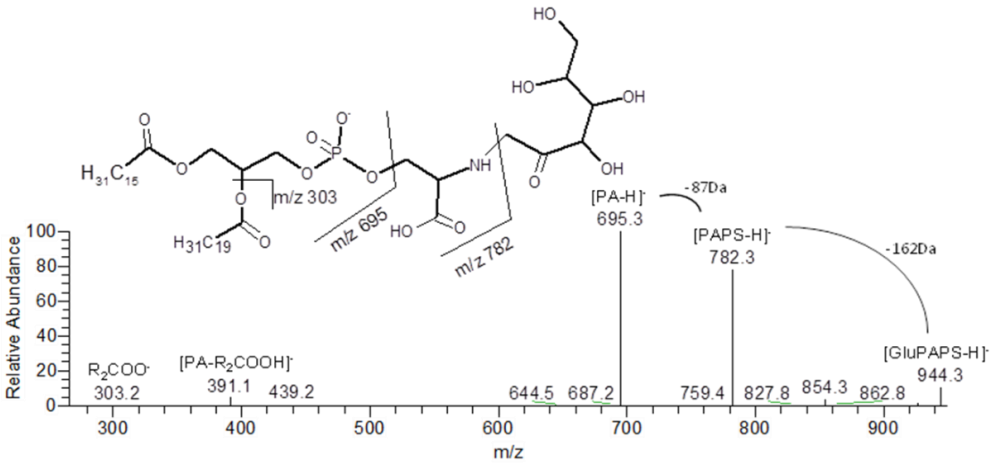

Figure 22: LC–MS/MS spectrum, recorded in the negative mode, of the deprotonated molecular ion of glycated PAPS observed at *m/z* 944.

Subsequently, the glycated PAPS was oxidized by Fenton reaction and analyzed by LC–MS and LC–MS/MS, as described in Section 4.1.3. The oxidation of gluPAPS leaded to modifications in unsaturated fatty acyl chain and formation of glycerophosphoacetic acid derivatives (Scheme 9) and lysoPS. Table 4 shows the main oxidation products that were identified in the LC–MS spectra of oxgluPAPS. Oxidation products identified as formamide (R-NHCHO) derivatives arising from oxidative cleavage of glucose were also identified in oxgluPAPS, but not in oxPAPS.

Table 4: Identification of the main oxidation products observed in the LC–MS spectrum of oxgluPAPS, grouped accordingly to the location and nature of the modifications. The table also shows the *m/z* values of the [M-H]− ions and the retention time (RT).

Oxidation products of GluPAPS	Glucose moiety in the serine polar head (NL=87+162) *m/z* (RT)	Formamide derivatives *m/z*(RT)	Glycerophospho acetic acid derivatives (NL=58) *m/z*(RT)	Phosphatidic Acid (PA) *m/z*(RT)
Long chain oxidation products				
($C_{16:0}$)($C_{20:4}$)	944.3 (41.7 min)	810.3 (31.6min)	753.5 (37.0 min)	
($C_{16:0}$)($C_{20:4+O}$)	960.3 (39.6 min)		769.4 (34.7 min)	
($C_{16:0}$)($C_{20:4+2O}$)	976.4 (32.3 min)		785.4 (32.3min)	727.4 (35.7 min)
($C_{16:0}$)($C_{20:4+3O}$)	992.4 (32.3 min)		801.4 (32.1 min)	743.4 (35.6 min)
($C_{16:0}$)($C_{20:4+4O}$)	1008.4 (31.3 min)		817.4 (32.3 min)	
($C_{16:0}$)($C_{20:4+5O}$)	1024.4 (31.2 min)		833.4 (32.3 min)	
($C_{16:0}$)($C_{20:4+6O}$)	1040.4 (31.5 min)		849.4 (31.5 min)	
Short chain oxidation products at the Sn-2 position				
($C_{16:0}$)(C_4COOH)	772.3 (11.8 min)	638.3 (9.1 min)	581.3 (10.6 min)	523.2 (15.6 min)
($C_{16:0}$)(C_4CHO)	756.3 (27.9 min)		565.3 (17.6 min)	507.2 (29.5 min)
($C_{16:0}$)(C_5(O)C_7COOH)	828.3 (10.8 min)		637.3 (10.1 min)	579.2 (15.6 min)
($C_{16:0}$)(C_5(O)C_7CHO)	828.3 (27.5 min)		637.3 (16.6 min)	579.2 (28.8 min)
($C_{16:0}$)	658.3 (25.6min)		467.2 (13.2 min)	409.2 (26.5 min)

The oxidation products of glycated PS with additional 2–6 oxygen atoms in the unsaturated fatty acyl chain (*m/z* 976, 992, 1008, 1024 and 1040) eluted between 30 and 33 min, while the hydroxyl derivative (gluPAPS + O), observed at *m/z* 960.4, eluted at 39.6 min (Figure 23). The oxidation products with additional oxygen atoms are more polar compounds, eluting with a shorter retention time when compared to gluPAPS (RT = 42 min).

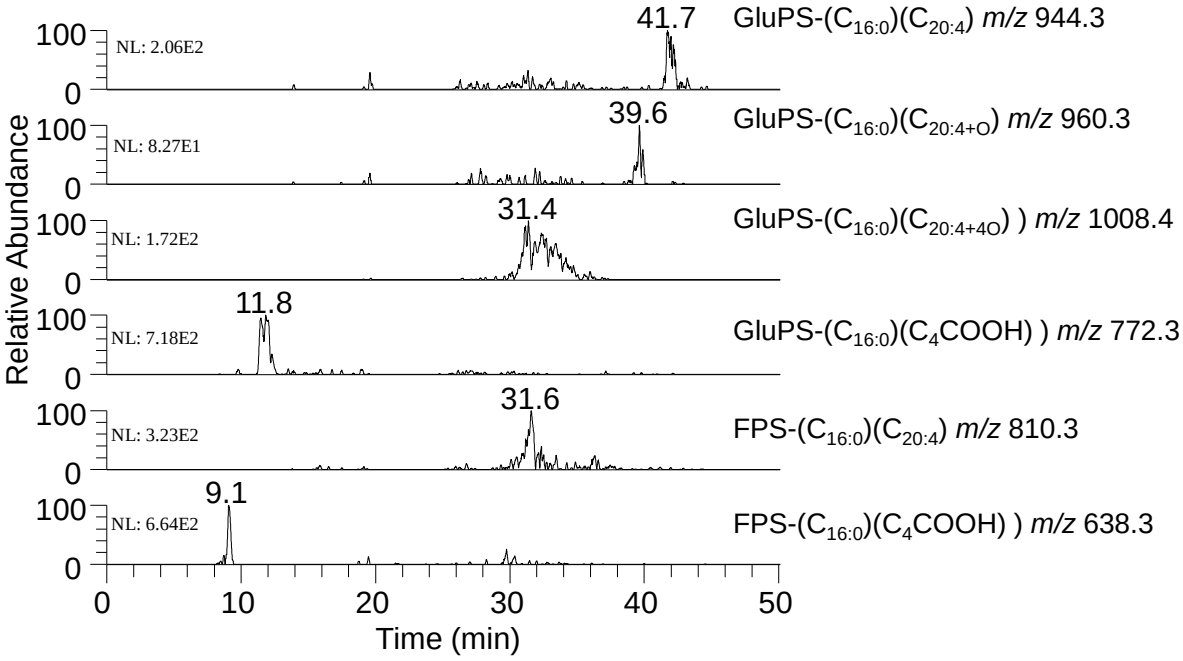

Figure 23: LC–MS recorded ion chromatogram (RIC) of the deprotonated molecular ion $[M-H]^-$ of the oxidation products of glycated PAPS. (NL = absolute intensity).

Oxidation products of gluPS, with shortened fatty acyl chains and carboxylic or aldehyde groups were also observed. The oxidation products with carboxylic groups, identified at *m/z* 772 (R'_2C_5OOH) and *m/z* 828 ($R'_2C_5(O)C_7COOH$), eluted between 11.8 and 10.8 min, respectively. Short chain oxidation products with an aldehyde group, identified at *m/z* 756 ($R'_2C_5{=}O$) and 828 ($R'_2C_5(OO)C_7C{=}O$), eluted at 27.9 and 27.5 min, respectively. The lysogluPAPS oxidation product ($[gluPAPS\text{-}R_2{=}C{=}O]^-$) was detected at *m/z* 658 (RT 25.6 min) (Table 4).

Other oxidation products, arising from oxidative cleavages in glucose moiety, were observed in the LC–MS spectrum of oxgluPAPS (Scheme 9). These oxidation products

arise from cleavage of the C1-C2 bond of the glucose moiety, leading to the formation of an aldehyde group (-NHCHO derivative) and were identified at *m/z* 810.3 (with unmodified fatty acyl chain, RT = 31.6 min) and 638.3 (with carboxylic C5 acyl group, RT = 9.1 min). Figure 24 shows the LC–MS/MS spectrum and the proposed structure for the ion at *m/z* 638. In this spectrum we can see the fragment ion at *m/z* 594, arising from loss of CO_2, and the fragment ion at *m/z* 523, arising from neutral loss of 115 Da ($CH_2CH(COOH)NHCHO$). These type of oxidative cleavages in glycated species were also observed in the oxidation of glycated PE [152].

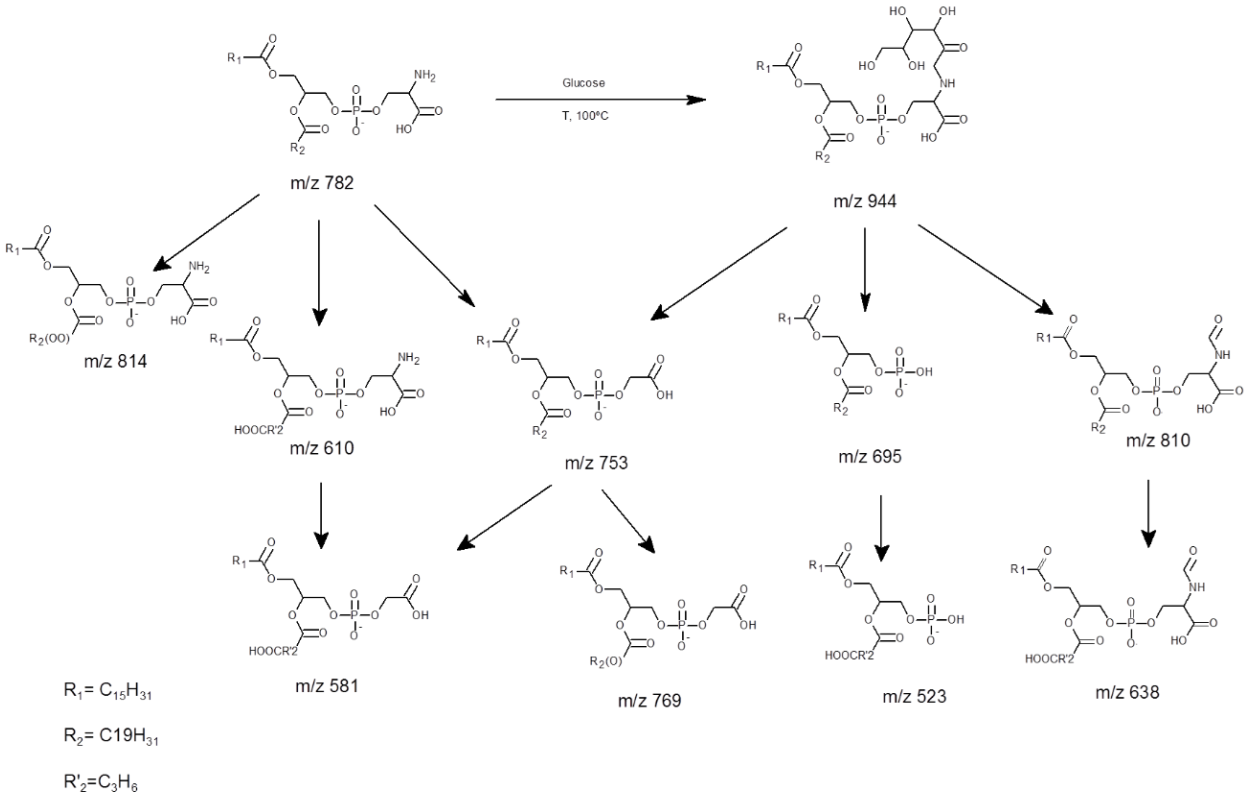

Scheme 9: Proposed structures for the main oxidation products of PAPS and gluPAPS observed in this work

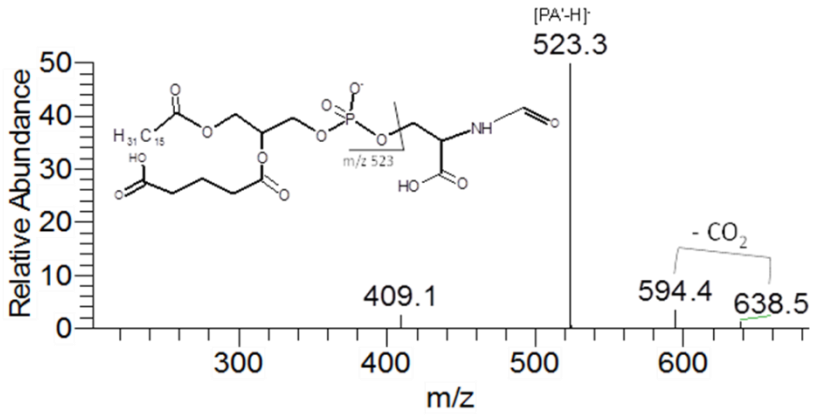

Figure 24: LC–MS/MS spectrum, recorded in the negative mode, of the ion at *m/z* 638.5. The proposed structure is also shown.

4.1.5 Conclusion

In this work, we have characterized by negative mode LC–MS and –MS/MS the oxidation products resulting of oxidation of PAPS and glycated PAPS using Fenton reaction. Therefore, we developed a new sensitive liquid chromatography method coupled with tandem mass spectrometry to provide a complete profile of oxidized and glyco-oxidized PS. This LC–MS/MS study of oxidation of PAPS and gluPAPS has identified new oxidation products. In oxPAPS samples, we identified long chain oxidation products as hydroxy and peroxy derivatives, short chain products with aldehyde and carboxyl moieties at C5 and C8, lysoPS and glycerophosphoacetic acid derivatives. In oxgluPAPS samples, we identified long chain oxidation products, short chain oxidation products and lyso products of gluPAPS and GPAA derivatives, long chain oxidation products and short chain oxidation products of PAPS. Some oxidation products were only observed as oxidation products of gluPAPS: phosphatidic acid derivatives (PA), lysophospahtidic acid (lysoPA) and formamide derivatives. With the exception of short-chain oxidation products, the main oxidation products that were observed were lysoPAPS at *m/z* 496 ([PAPS-R_2=C=O]$^-$), lyso gluPAPS at *m/z* 658 ([gluPAPS- R_2=C=O]$^-$ and lysoPAPS with modified polar head (at *m/z* 467). It is worth noting that lysoPS phospholipids have been detected in many biological fluids, and are known as signaling phospholipids in mast cells, enhancing histamine release and eicosanoid production [226,227,228]. Also, it has been suggested that in skeletal muscle and adipose tissue, lysoPS species are involved in the regulation of

glucose homeostasis [229]. When assessing the influence of glycation on PS oxidation we can conclude that glycated PS species are more susceptible to the formation of oxidation products with modified polar head (acetic acid terminal) than the non glycated PS. They are also more susceptible of forming phosphatidic acid derivatives. Both modifications were observed to occur simultaneously with the oxidation in polyunsaturated fatty acyl chain. The glycerophosphoacetic acid derivatives were previously observed in oxidized glycated phosphatidylethanolamines. This oxidation product was detected in vivo although its biological significance is not known. The differences in the oxidative modifications observed between glycated and non glycated PS can be important, as it appears that glycation enhances the oxidative damage in PS.

This work has performed a detailed molecular characterization of different oxidation products of phosphatidylserine and glycated phosphatidylserine. We have determined the fragmentation pattern of the different oxidation products, providing information about the characteristic neutral loss accordingly with the nature of the oxidative modification. This information is essential for targeted analysis methods to be developed, as for example the use of multiple reaction monitoring (MRM) mass spectrometry. Also, we have developed a chromatographic method that allows the separation of these oxidation products. The results of this study can be an important contribution for the identification of oxidative and glycated modifications of phosphatidylserines in biological systems.

Chapter IV.II

Liquid chromatography-tandem mass spectrometry of phosphatidylserine advanced glycated end products

The results presented in this chapter were integrally published as follow:

E. Maciel, R.N. da Silva, C. Simões, T. Melo, R. Ferreira, P. Domingues, M.R.M. Domingues, Liquid chromatography–tandem mass spectrometry of phosphatidylserine advanced glycated end products, Chem. Phys. Lipids, 174 (2013) 1-7.

4.2.1 Abstract

Phosphatidylserine (PS) is an aminophospholipid that is prone to glycation. In oxidative conditions, glycated PS may lead to the formation of Amadori compounds and advanced glycated end products (AGEs), which are known to accumulate in diabetic patients. Nevertheless, there have been no studies that identified products from the oxidative reaction of glycated PS. In this study, glycated 1-palmitoyl-2-oleoyl-PS was synthesized and further oxidized by Fenton reagent. The AGES formed were structurally characterized by liquid chromatography coupled to tandem mass spectrometry (LC–MS/MS) in negative mode. The oxidation products from glycated PS that we have found include products arising from the oxidation of the fatty acyl chains (hydroperoxides, hydroxides and keto derivatives), and arising from oxidative cleavage of serine polar head and lyso-glycated PS. Oxidation in C6 of glucose lead to the formation of glucuronyl-PS. In addition, new products arising from oxidative cleavage of glucose moiety (between C1single bond C2, C2single bondC3 and C3single bondC4 bonds) were identified as PS-AGES. The current findings add substantially to the best of our knowledge of PS glycoxidation products, opening new perspectives for the detection of these products in complex biological matrices.

Keywords

Phospholipid; Glycation; Oxidation; Hydroxyl radical; HPLC–MS/MS; AGES

4.2.2 Introduction

Protein glycation has recently attracted increased attention in proteomics research because of its association with oxidation and oxidative stress pathologies. In fact, considering the negative impact in cell homeostasis of non-enzymatic glycation, this reaction has been thoroughly investigated (reviewed in [230]). The aminophospholipids phosphatidylserine (PS) and phosphatidylethanolamine (PE) also have a free amino group that is prone to non-enzymatic glycation. Although not well studied, in vivo lipid glycation has also been described to occur, for example in blood plasma and red blood cells [25,27,147,231]. This reaction is more likely to occur among persons with diabetes mellitus, as a consequence of the increased levels of glucose and other saccharides derivatives in the plasma. Also, lipid glycation can be involved in the pathogenesis of several diseases, including atherosclerosis, retinopathy and nephropathy, and its complications. The mechanisms underlying these complications are not completely understood, but are related to increased oxidative stress, DNA damage and compromised lipid membrane integrity. These processes can be promoted by glycation products [214] such as Schiff bases, Amadori rearrangement products, and advanced glycation end products (AGEs) [27,149].

As referred previously, so far, there has been little discussion about glycation of aminophospholipids. Nevertheless, Ravandi et al. [27] identified glycated PE in in vitro systems and also in human plasma and red blood cell membranes. In this study, in vitro glycated PS were also studied, but these species were not detected in vivo. In other studies, glycated PE was also detected in isolated LDL (low-density lipoproteins), in atheroma [28], and in the human plasma and erythrocytes of diabetic patients [24,25,26,29]. However, until now glycated PS (gluPS) was only characterized in in vitro systems with phospholipid standards [148]. Nevertheless, it seems reasonable to suppose that glycated PS can as well be formed in vivo.

A recent study from our group showed that, besides the oxidation in the fatty acyl chain, gluPE also oxidizes in the glucose moiety. In fact, gluPE species were found to be more prone to oxidation and consequently to degradation [152], which may difficult the detection of these species. In addition, oxidation of glycated aminophospholipids and particularly glycated PS may generate AGEs, as observed in protein glycoxidation [232,233]. However, these oxidation products have not been detected in the oxidation of

gluPS. To overcome the difficulties of detecting PS glycation products in complex biological matrices, it is necessary to previously characterize these phospholipid oxidation products in model systems. It is expected that this approach allows detecting and quantifying PS-AGEs under oxidation and glycoxidation conditions.

In this work, we have characterized the oxidation products of glycated 1-palmitoyl-2-oleoyl-phosphatidylserine (POPS) by electrospray tandem mass spectrometry. POPS was selected because it has been previously detected in many cells and tissue, such as keratinocytes [234], intestinal [121] and lung tissues [122]. For this purpose, glycated POPS (gluPOPS) was synthesized and MS/MS fragmentation patterns were studied in the negative mode. In this study, we have identified, using HPLC–MS/MS, glycoxidized POPS (oxgluPOPS) products formed under the Fenton.

4.2.3 Experimental

Materials

1-Palmitoyl-2-oleoyl-sn-glycero-3-phospho-L-serine (POPS) was purchased to Avanti polar lipids, Inc. and used without further purification. d-glucose was purchased from Merck (Darmstadt, Germany). $FeCl_2$, EDTA and H_2O_2 (30%, w/w), used for the oxidation reaction, were acquired from Merck (Darmstadt, Germany). Chloroform, methanol and acetonitrile HPLC grade were acquired from Fisher Scientific.

Phosphatidylserine glycation

Glycated POPS was synthetized in methanol, as previously proposed for the glycation of aminophospholipids [25,235]. Briefly, 1.2 mg of glucose dissolved in methanol (300 μL) and 1 mg of phospholipid were mixed and the reaction tube was immersed in boiling water during 15 min. Phospholipids were extracted from the reaction mixture following the modified Folch method [169]. The glycation reaction was monitored by electrospray mass spectrometry (ESI-MS).

Oxidation of glycated phosphatidylserine by Fenton reaction

Vesicles of glycated phospholipid were prepared in ammonium bicarbonate buffer 5 mM (pH 7.4). In a typical experiment, 1 mg of glycated phospholipid in methanol was evaporated to dryness, 446 μL of buffer was added, and the mixture was mechanically

stirred on a vortex for 2 min and then sonicated for 1 min. The sample was kept under nitrogen atmosphere at all times [222]. The oxidation was initiated with the Fenton oxidant (Fe^{2+}/H_2O_2) by adding to the solution 4 μL of $FeCl_2$ and 50 μL of H_2O_2 in order to obtain a final concentration of 40 μM of $FeCl_2$ and 50 mM of H_2O_2 in a total volume of 500 μL. The mixture was incubated at 37 °C in the dark for two days. Controls were performed by replacing hydrogen peroxide with water. The oxidation was monitored by ESI-MS, after diluting the oxidative mixture in methanol (1:100, v/v).

ESI-MS conditions (linear ion trap)

The extent of glycation and oxidation reactions was monitored by electrospray mass spectrometry in a linear ion trap mass spectrometer LXQ (ThermoFinnigan, San Jose, CA, USA). The LXQ linear ion trap mass spectrometer was operated in negative mode. ESI conditions were as follows: electrospray voltage was 4.7 kV; capillary temperature was 275 °C and the sheath gas flow was 25 U. An isolation width of 0.5 Da was used with a 30 ms activation time for MS/MS experiments. Full scan MS spectra and MS/MS spectra were acquired with a 50 ms and 200 ms maximum ion injection time, respectively. For MS/MS experiments, normalized collision energy™ (CE) was applied in the range of 17–20 (arbitrary units). Data acquisition was carried out on an Xcalibur data system (V2.0).

HPLC–MS and HPLC–MS/MS conditions

The glyco-oxidized mixture was separated by HPLC performed on a HPLC system (Waters Alliance 2690) coupled to a linear ion trap mass spectrometer LXQ (ThermoFinnigan, San Jose, CA, USA). 5 μL of glyco-oxidized mixture, diluted in water with 20% of methanol, were introduced into a Supelco Bio Wide Pore C5 column (15 cm × 0.5 mm, 5 μm). The mobile phase A consisted of 95% water and 5% acetonitrile. The mobile phase B consisted of 100% of acetonitrile. The mobile phase gradient was programmed as follows: the initial conditions were 40% of B for 5 min; 5–30 min linear gradient to 60% of B; 30–65 min linear gradient to 80% of B. To obtain the product-ion spectra of the major components during LC experiments, cycles consisting of one full scan mass spectrum and four data-dependent MS/MS scans were repeated continuously throughout the experiments with the following dynamic exclusion settings: repeat count 3;

repeat duration 15 s; exclusion duration 45 s. Data acquisition was carried out on an Xcalibur data system (V2.0).

4.2.4 Results and discussion

In this work, glycated POPS (gluPOPS) was used as a model for evaluating the oxidative modification of glycated PS. POPS was chosen as model due to its prevalence in biological systems and the potential outcomes of its structural alterations. The fatty acid composition of POPS, i.e., saturated chain in the sn-1 position and mono-unsaturated chain in sn-2 position, makes it less susceptible to oxidation in comparison with polyunsaturated fatty acids (PUFA). This property facilitates the evaluation of the oxidative changes that can occur in glycated polar head group and the identification of potential advanced glycated end products.

Glycation of POPS was monitored by electrospray tandem mass spectrometry (ESI-MS/MS) in negative mode (Figure 25) and the representative fragmentation pathways were identified. In the ESI-MS/MS spectrum of the [M−H]− ion of gluPS the most abundant product ions were observed at *m/z* 760.3 and 673.3, arising respectively from the loss of the glucose moiety (−162 Da) and from the combined loss of aziridine-2-carboxylic acid plus glucose moiety (loss of 87 Da + 162 Da) (Figure 25B). Neutral loss of 87 Da is a well-known PS fragmentation pathway, observed when performing ESI-MS/MS in negative mode. Other minor product ions were also observed, which can be attributed to glucose cleavages with loss of 90 Da (C3H6O3) (*m/z* 832.3), loss of the fatty acyl chains (*m/z* 391.2 and 417.2) and, the oleoyl carboxylate anion (R2COO−) (*m/z* 281.2).

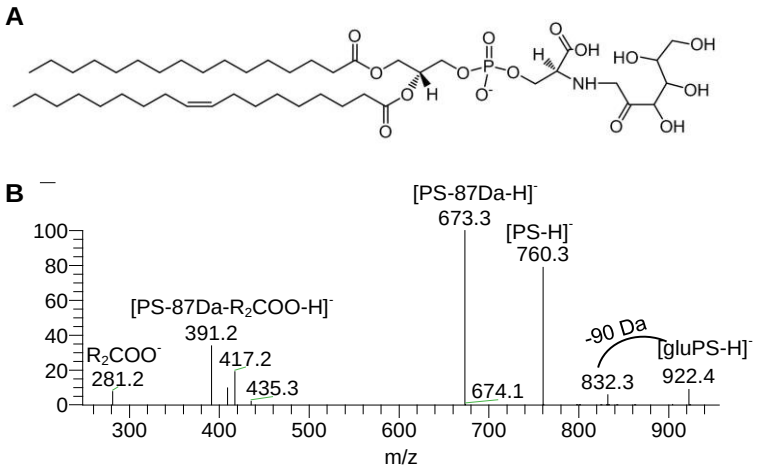

Figure 25: Tandem Mass spectrometric analysis of glycated POPS in negative mode: ESI-MS/MS spectrum of the ions at *m/z* 992.4 ($[M-H]^-$) correspondent to the glycated POPS

Oxidation of glycated POPS was induced using Fenton oxidant (H_2O_2/Fe^{2+}), as described in the experimental section, and the formation of oxidation products were monitored by ESI-MS and LC-ESI-MS in negative mode. Analysis of the ESI-MS spectra of the solutions after (Figure 26B) and before the oxidative reaction (Figure 26A) revealed the presence of new $[M-H]^-$ ions, assigned as oxidation products. Also, in these spectra, we can observe the ions at *m/z* 760.3 correspondent to native POPS, and the ions at *m/z* 922.4 correspond to gluPOPS. In Figure 26B we have assigned some of the ions that were attributed to the oxidation products of POPS (*m/z* 774.4, 776.4, 792.3) and gluPOPS (*m/z* 936.3, 938.3, 954.3, 984.2), as keto (+14 Da), hydroxyl (+16 Da) and hydroperoxy (+32 Da) derivatives. An oxidation product resultant from the oxidative cleavage of serine moiety in glycated polar head with lower molecular weight than POPS was also identified as $[PS-29\ Da-H]^-$. This oxidation product was assigned as $[M-H]^-$ ion at *m/z* 731.4 and presents a terminal acetic acid linked to the phosphate group, as shown in Scheme 10. A similar cleavage in the serine moiety was previously identified in PS oxidation, and presumably results from a radical attack to the alpha carbon of serine in polar head group [168]. In Figure 26B, other oxidation products can be observed in the mass range between *m/z* 760.5 (POPS) and 922.5 (gluPOPS). This suggests the presence of oxidative species resulting from the oxidative cleavage of the glycated moiety in gluPOPS (Scheme 10). In order to identify the gluPOPS oxidation species and to unveil possible isomeric structures, we have further analyzed the oxidative mixture using LC–MS and LC–MS/MS.

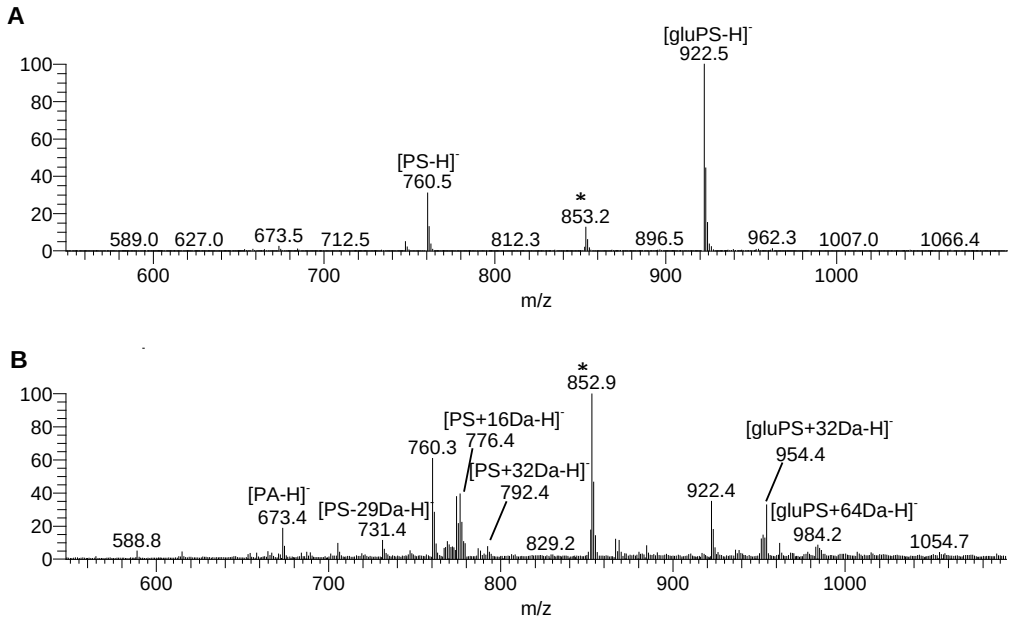

Figure 26: Mass spectrometric analysis of oxidized glycatedPOPS: ESI-MS spectra obtained in negative ion mode of the glycated POPS under non-oxidized (A) and oxidation (B) conditions. * Impurities of solvents.

5.4.1 Oxidation products of glycated POPS analyzed by LC–MS and LC–MS/MS

The oxidation products of glycated POPS observed at *m/z* 954.3 and 938.3 in MS spectra of the oxidative mixture (Figure 26B) were identified as hydroperoxy (*m/z* 954.3) and hydroxy (*m/z* 938.3) derivatives of gluPOPS. In the LC–MS run, both these species eluted in one major peak at 18.9 min and 20.8 min, respectively (Figure 27A), indicating the absence of isomeric species. The LC–MS/MS spectrum of the hydroxyl gluPOPS, [gluPS+16 Da−H]$^-$ at *m/z* 938.4 (Figure 27A) showed the product ions arising from the loss of glucose (−162 Da) at *m/z* 776.4, loss of glycated polar head (−(162 Da + 87 Da)) at *m/z* 689.4 and the carboxylate anion of the hydroxyl-oleic acid at *m/z* 297.1 ([R_2COO+16 Da]$^-$). Altogether, this data shows the presence of the hydroxyl group in the unsaturated fatty acyl chain. The LC–MS/MS spectrum of the hydroperoxy derivative ([gluPS+32 Da−H]−) at *m/z* 954.4, showed the most abundant product ions arising from the loss of glucose at *m/z* 792.4.4, and loss of glycated polar head at *m/z* 705.4, also confirming the presence of hydroperoxyl group in the unsaturated fatty acyl chain (Figure 27B).

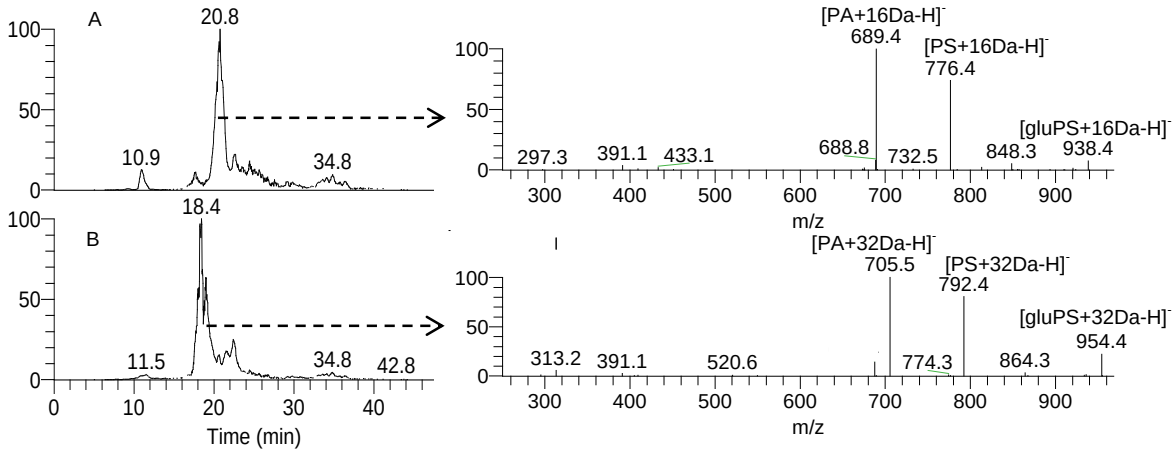

Figure 27: LC-MS and MS/MS analysis of hydroxy and hydroperoxy derivatives of glycated POPS: Reconstructed ion chromatogram and the LC-MS/MS spectrum of the ions at *m/z* 938.4 ($[M-H]^-$) correspondent to the hydroxide derivative of gluPOPS (gluPOPS+16 Da) (A). Reconstructed ion chromatogram and the LC-MS/MS spectrum of the ions at *m/z* 954.4 ($[M-H]^-$) correspondent to the hydroperoxide derivative of gluPOPS (gluPOPS+32 Da) (B).

Other oxidation products of glycated POPS like keto derivatives (*m/z* 936.4 (922.4 + 14 Da)) eluted in two major peaks, one at 11.0 min and the other at 19.7 min (Figure 29A). This suggests the presence of two isomeric structures, confirmed by the LC–MS/MS spectra obtained in each retention time. The LC–MS/MS spectrum of the $[M-H]^-$ at *m/z* 936.3 obtained at RT 11.0 (Figure 28B) showed product ions at *m/z* 760.4 identified as $[POPS-H]^-$, arising from loss of a neutral with (162+14) Da, at *m/z* 673.3, arising from the neutral loss of (162+87+14) Da and the product ions at *m/z* 281.2, assigned as the non-modified carboxylate anion (oleic acid anion). Altogether, these product ions indicate that the presence of the keto group in the glucose moiety of this oxidation product. The product ions at *m/z* 832.5 (Figure 28B) further suggests that the keto group is at C6 of the glucose residue, corresponding not to a keto derivative but to the formation of a glucuronic acid. The LC–MS/MS spectrum of the $[M-H]^-$ ion at *m/z* 936.3 obtained at RT 19.7 min (Figure 29D), showed product ions at 774.3 (−162 Da, $[PS+14\ Da-H]^-$), *m/z* 687.4 (−162 Da−87 Da, $[PA+14\ Da-H]^-$), and 295.1 ($[R_2COO+14\ Da]^-$), confirming the presence of the keto group in the unsaturated fatty acyl chain (Figure 28E).

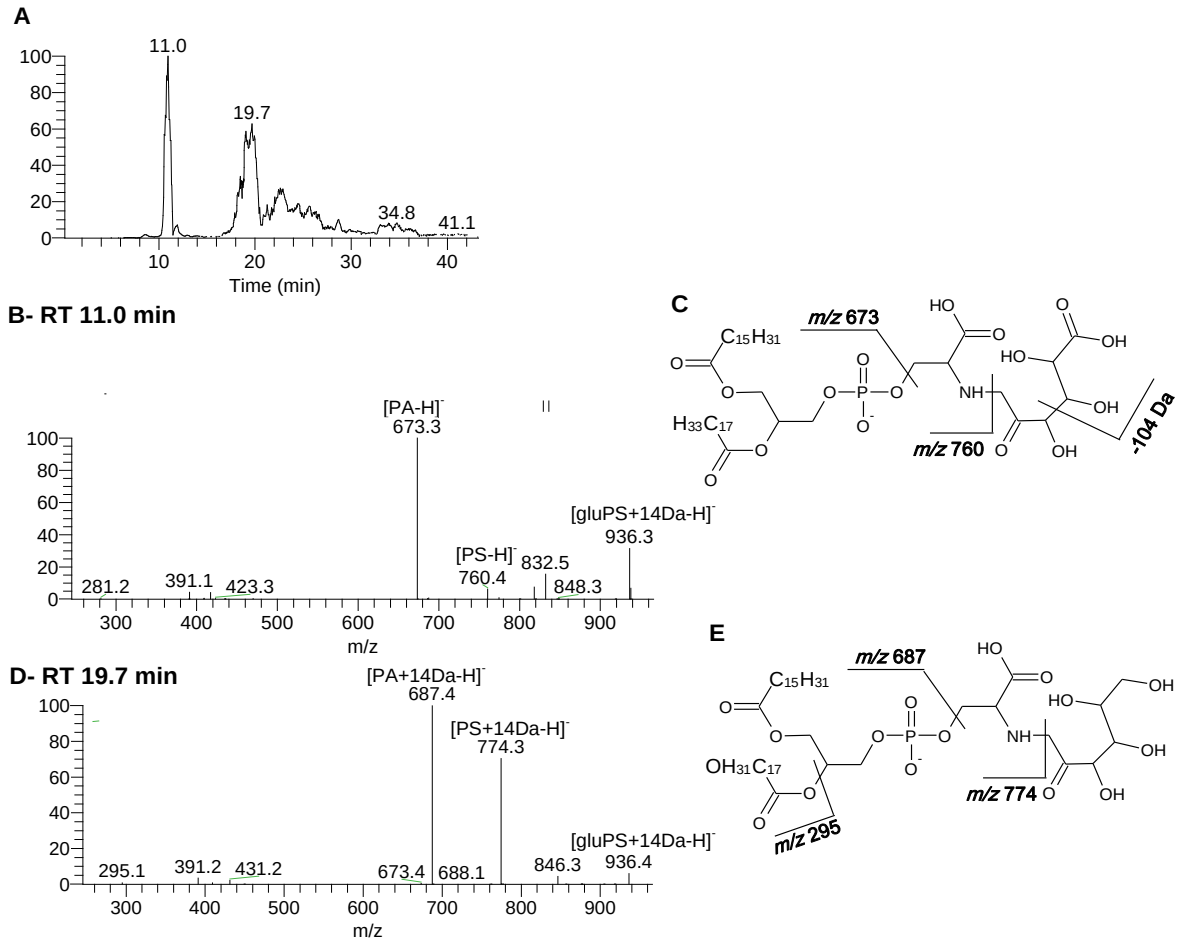

Figure 28: Differentiation of isomers of glycated POPS+O - 2Da by LC-MS and MS/MS analysis: Reconstructed ion chromatogram of the ions at *m/z* 936 ($[M-H]^-$) correspondent to glu-PS +14 Da) (A). LC-MS/MS spectrum of the ions at *m/z* 936 ($[M-H]^-$) , RT= 11.0 minutes (B) and the proposed structure (C). LC-MS/MS spectrum of the ions at *m/z* 936 ($[M-H]^-$) RT= 19.7 minutes (D) and proposed structure (E).

The glycated lysoPS (*m/z* 658.3) formed due to loss of the oleoyl fatty acyl chain was observed with a retention time of 7.2 min (Figure 29A). The LC–MS/MS spectrum shows a fragment ions arising from loss of 162 Da (*m/z* 496.1) loss of the glycated polar head (loss of 162 Da + 87 Da) (*m/z* 409.2). Also, we have observed the formation of a lyso the oxidation product at *m/z* 467.2 (RT 6.6 min, Figure 29B), arising from the modification of the polar head with the acetic terminal linked to the phosphate (lysoPS−29 Da).

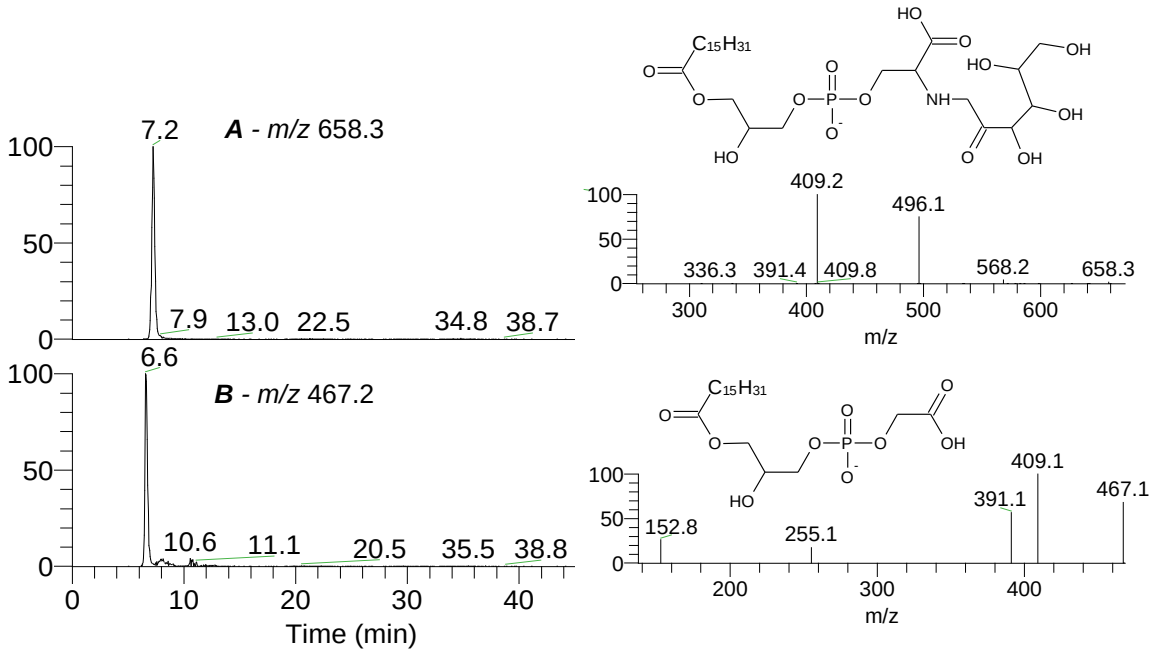

Figure 29: LC-MS/MS analysis of lyso- derivatives formed during glycated POPS oxidation. Reconstructed ion chromatograms, LC-MS/MS spectra of the ions at *m/z* 658.3 ($[M-H]^-$), and the proposed structure (A). Reconstructed ion chromatograms, LC-MS/MS spectra the ions at *m/z* 467.2 ($[M-H]^-$) and the proposed structure (B).

Radical induced oxidation also observed in the glucose located at the glycated polar head. This oxidative pathway generated several products observed at lower *m/z* than the glu POPS. The occurrence of oxidative cleavage of the glucose moiety between C1-C2, C2-C3 and C3-C4 bonds was assigned after LC–MS/MS analysis and identification of typical neutral losses arising from the modified polar head, as represented in Scheme 10. These oxidation products were observed in the LC–MS chromatogram at *m/z* 788.4 (gluPOPS−134 Da), *m/z* 818.4 (gluPOPS−104 Da) and *m/z* 832.4 (gluPOPS−90 Da). The retention times of these oxidation products were lower than the retention of non-modified gluPOPS (Figure 30).

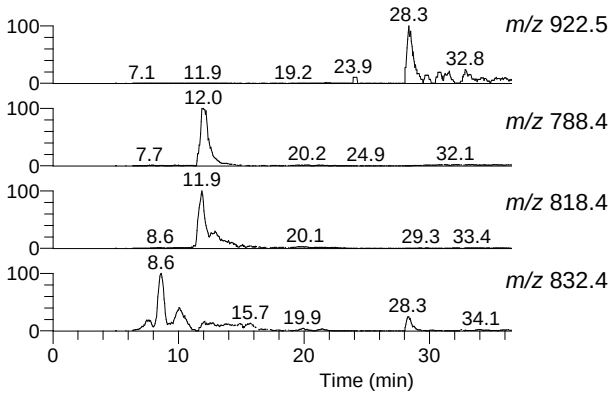

Figure 30: LC-MS of POPS advanced glycated end products. Reconstructed Ion Chromatograms (RIC) of the ions *m/z* 922.5 ($[M-H]^-$) [of glycated POPS (and of their oxidation products formed due to cleavages in the glucose moiety at *m/z* 788.2 (cleavage in C1-C2 bond), *m/z* 818.4 (cleavage in C2-C3 bond) and *m/z* 838.4 (cleavage in C2-C3 bond with oxidation in fatty acyl chain and cleavage in C3-C4 bond).

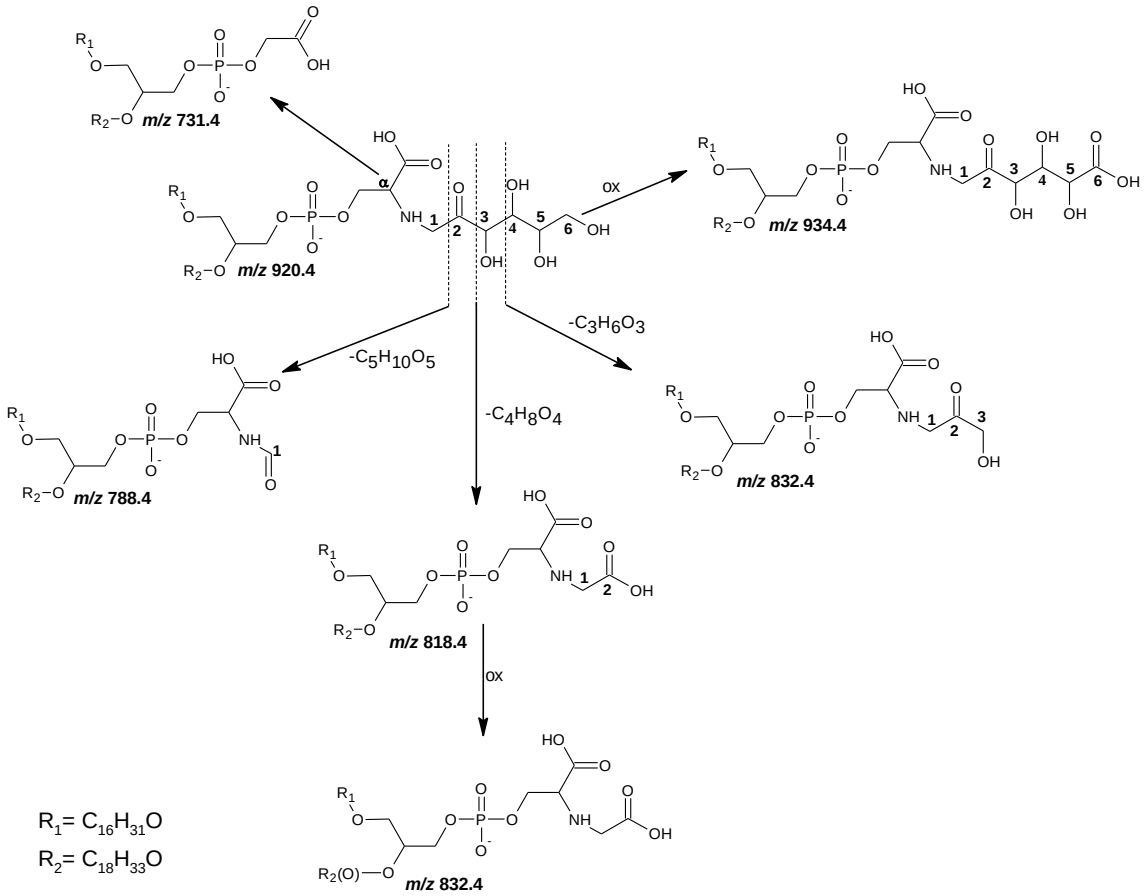

Scheme 10: POPS advanced glycated end products arising from hydroxyl radical oxidation. Oxidation in glycated serine polar head induced by the hydroxyl radical (Fenton reagent) generated different glycated end products due to cleavage in glucose moiety.

The oxidation product arising from cleavage of the glucose moiety between C1-C2 bond (*m/z* 788.4) eluted in one peak at 12.0 min. The LC–MS/MS spectrum showed a fragment ion arising from loss of 115 Da, suggesting that the formation of formamide terminal (-$CH_2CH(COOH)NHCHO$) had occurred (Figure 31A). The presence of product ions at *m/z* 673.3 ($[PA-H]^-$), arising from the loss of the modified polar head, indicates that the oxidation in the fatty acyl chains has not occurred. The fragment ions observed in the MS/MS spectra of this oxidation product were similar to the fragment ions previously observed in the oxidation product of gluPAPS [236].

The oxidation product at *m/z* 818.4, arising from cleavage of the glucose moiety between C2-C3 bond, eluted at 11.9 min. In the LC–MS/MS spectrum (Figure 31B) we can see product ions at *m/z* 760.6, arising from the neutral loss of 58 Da. This suggests the presence of acetic acid attached to the amine group of phosphatidylserine ($NHCH_2COOH$). The absence of evidences of oxidation in oleic acid was reinforced by the presence of the product ions at *m/z* 673.3 ($[PA-H]^-$) and 281.1 ($R2COO^-$) in the MS/MS spectrum. Glucose oxidative cleavages in C2-C3 and C1-C2 were previously identified during glycated PE oxidation induced by the hydroxyl radical and by photoxidation [152,235].

The oxidation product of gluPOPS observed at *m/z* 832.4 eluted at several different retention times, with two peaks at RT 8.6 min and 28.3 min (Figure 30). The LC–MS/MS spectrum obtained at 8.6 min (Figure 31C) showed the product ions at *m/z* 774.4 ($[PS+14\ Da-H]^-$) arising from the loss of 58 Da. This data supports the presence of an oxidation product with a keto derivative in oleoyl fatty acyl chain, and a polar head with a terminal $NHCH_2COOH$ (formed by C2-C3 glucose cleavage). The location of the keto group in the oleoyl acid, was confirmed by the product ions at *m/z* 687.3 ([PA+14 Da−H]−), arising from the loss of the modified polar head group. The analysis the LC–MS/MS spectrum of the precursor ions at *m/z* 832.4 obtained at 28.3 min suggests the presence of an isomer. This spectra shows the product ions at *m/z* 760.4 ($[PS-H]^-$), 673.3 ($[PA-H]^-$) and 281.1 (R_2COO^-). The presence of these product ions confirmed both that the fatty acyl chains were not oxidized, and that the cleavage in the C3-C4 bond, with the formation of $NHCHOHCH_2CO$ (hydroxypropanone) terminal in the polar head, had occurred. Oxidation products resulting from the cleavage of the glucose moiety are well known in glycated peptides [237,238]. These products have been also described for glycated PE when subject to oxidation [152,235]. Nevertheless, there are few studies reporting the presence of

glycated PE oxidation products, usually called AGEs, in diabetic patients [239,240]. It is believed that AGE-PE accumulates more in diabetic patients with severe complications, as a consequence of the oxidative stress underlying hyperglycemic conditions [240]. Due to their similar nature, the same effect is expected to occur with PS and the search for in vivo oxidized glycated PS species that were identified in this study may help to define the molecular mechanisms underlying some pathogenic conditions. It is expectable that the structural alterations associated with glycation in PS, an important phospholipid in brain, and accumulation of PS-AGES can contribute to the increased risk of neurodegenerative diseases associated with diabetes. Moreover, considering the involvement of PS in cellular processes as apoptosis, the knowledge of PS structural alterations in response to oxidative stress and hyperglycemia might also help to understand the pathogenic pathways underlying some pathophysiological processes like diabetes mellitus and diabetic complications.

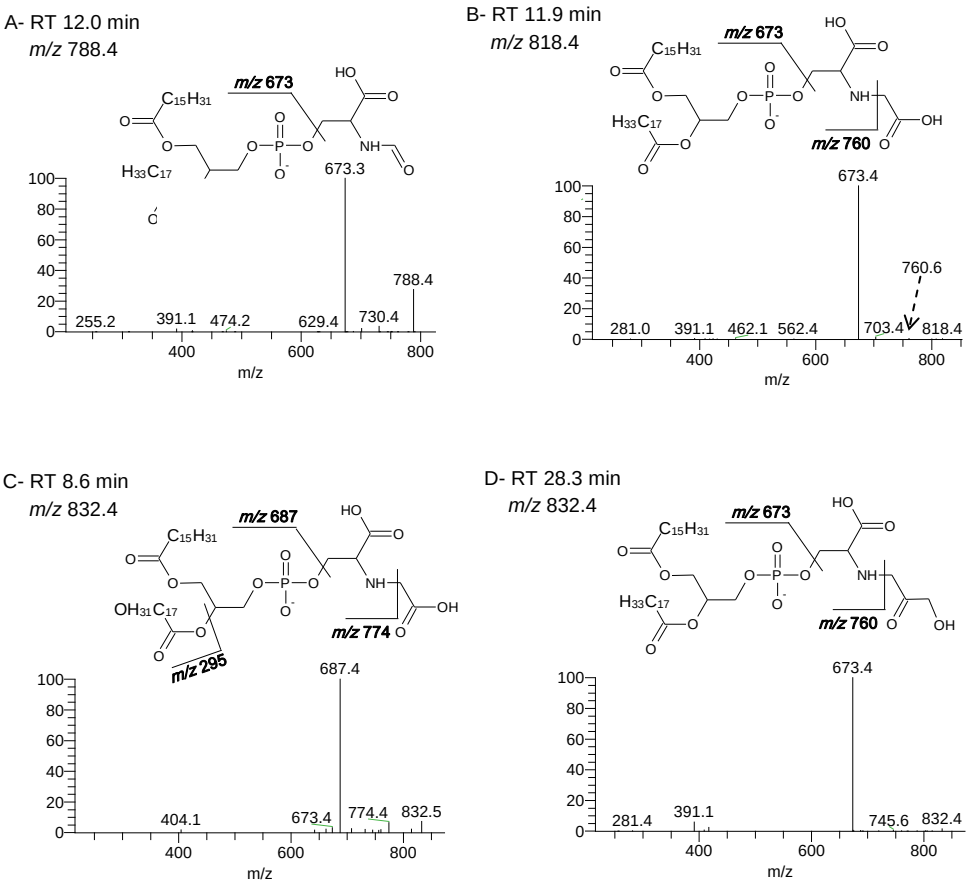

Figure 31: Tandem mass spectrometry analysis of POPS advanced glycated end products: LC-MS/MS spectra and proposed structures for the oxidations products that result from cleavages of carbon bonds in the glucose moiety. LC-MS/MS spectrum and structure of the ions at m/z 788.4 ($[M-H]^-$) (cleavage in C1-C2 bond) (A). LC-MS/MS spectrum and structure of the ions at m/z 818.4 ($[M-H]^-$) (cleavage in C2-C3 bond) (B). LC-MS/MS spectrum and structure of the ions at m/z 832 ($[M-H]^-$) (cleavage in C2-C3 bond and with keto/epoxy group in fatty acyl chain) (C). LC-MS/MS spectrum and structure of the ions at m/z 832.4 ($[M-H]^-$) (cleavage in C3-C4 bond) (D).

4.2.5 Conclusion

In the present work, we have synthesized glycated PS and characterized this adduct by ESI-MS/MS. The glycated product was further oxidized using the Fenton reagent and the glyco-oxidation products were separated and analyzed by LC–MS and LC–MS/MS. We have found oxidation products arising both from oxidation of the fatty acyl chains and the glycated phospholipid head. The oxidation products, arising from the oxidation of the fatty acyl chains that we have found and characterized include hydroperoxides, hydroxides and keto derivatives. Also, we have found evidence for the presence of positional and functional isomers, both from the retention time and the MS/MS spectra. Oxidation products resulting from the cleavage of the glucose moiety were also found, including products arising from cleavage of the glucose moiety between C1-C2 bond with formation of formamide terminal; between the C2-C3 bond with acetic acid attached to amine group and between the C3-C4 bond with formation of hydroxypropanone terminal in polar head group.

In overall, the in-depth structural characterization of glycated and glycoxidated PS shown in this study provides a basis for the future understanding of PS susceptibility to glycation and oxidation in vivo and its relevance in specific pathophysiological conditions.

Chapter V

Detection of phosphatidylserine with a modified polar head group in human keratinocytes exposed to the radical generator AAPH

The results presented in this chapter were integrally published as follow:

E. Maciel, B.M. Neves, D. Santinha, A. Reis, P. Domingues, M. Teresa Cruz, A.R. Pitt, C.M. Spickett, M.R.M. Domingues, Detection of phosphatidylserine with a modified polar head group in human keratinocytes exposed to the radical generator AAPH, Arch. Biochem. Biophys., 548 (2014) 38-45.

5.1 Abstract

Phosphatidylserine (PS) is preferentially located in the inner leaflet of the cell membrane, and translocation of PS oxidized in fatty acyl chains to the outside of membrane has been reported as signaling to macrophage receptors to clear apoptotic cells. It was recently shown that PS can be oxidized in serine moiety of polar head-group. In the present work, a targeted lipidomic approach was applied to detecting oxPS modified at the polar head-group in keratinocytes that were exposed to the radical generator AAPH. Glycerophosphoacetic acid derivatives (GPAA) were found to be the major oxidation products of oxPS modified at the polar head-group during oxidation induced by AAPH-generated radicals, similarly to previous observations for the oxidation induced by OHradical dot radical. The neutral loss scan of 58 Da and a novel precursor ion scan of *m/z* 137.1 ($HOPO_3CH_2COOH$) allowed the recognition of GPAA derivatives in the total lipid extracts obtained from HaCaT cells treated with AAPH. The positive identification of serine head group oxidation products in cells under controlled oxidative conditions opens new perspectives and justifies further studies in other cellular environments in order to understand fully the role of PS polar head-group oxidation in cell homeostasis and disease.

Keywords: Phosphatidylserine; Keratinocytes; AAPH; Oxidative stress; Mass spectrometry; Shotgun lipidomic

5.2 Introduction

Phosphatidylserine (PS) is a phospholipid that has been identified to be a preferential target of *in vivo* oxidation. PS is located preferentially in the inner leaflet of cell membranes, but PS oxidation products are translocated to the outside of membrane. These products are considered to be markers of the early stages of apoptosis. It is known that one of the first steps of cellular apoptosis involves PS oxidization in the fatty acyl chains that are recognized by macrophages receptors for the clearance of apoptotic cells [98,102,241]. Several studies showed that oxidized PS is preferentially recognized by macrophage scavenger receptors over non-oxidized PS [96,100,103,104]. The oxidation products of PS identified in vivo consisted of oxidative modifications in the fatty acyl chains, such as PS hydroxide and hydroperoxide derivatives and truncated sn-2 fatty acyl species [104,132,133]. These types of oxidation products retained an intact PS head-group and are usually identified by the typical fragmentation pathways under MS/MS conditions, which involved the loss of the serine group [133,168,194]. However, in a recent study of oxidation of PS standards using the Fenton reagent, it was observed that the PS head-group can also undergo oxidative modifications leading to the formation of modified polar head-groups [168,242]. Among these oxidation products, the derivatives with a polar head-group containing an acetic acid linked to the phosphate group, called glycerophosphoacetic acid (GPAA), were found to be the most abundant [168]. These products showed a distinct fragmentation and neutral loss under MS/MS conditions and the typical loss of the serine group is absent. This behavior explains why this type of PS oxidation product has been overlooked. As yet, PS modified in the serine polar head-group has only been found in mitochondria from brain of rats treated with tacrine, which is associated with neurotoxicity and oxidative stress conditions [217]. Evaluation of pro-inflammatory activities of PS oxidation products with modifications in serine polar head-group was tested through cytokine production, and it was found that GPAA had no pro-inflammatory activity [242]. Until now, no other efforts have been made to detect these species with oxidative modifications on the polar head-group of PS. Nevertheless, it is likely that they can occur in vivo, in cells exposed to oxidative conditions.

To give new insight into this subject, the present work aimed to evaluate the formation of GPAA species in keratinocytes (HaCaT cells) after exposure to a radical generator. Keratinocytes were selected as a cell model since externalized PS and oxidation of fatty

acyl chains in PS were identified in human keratinocytes during oxidative stress [55,243]. These cells are frequently used in oxidation studies, because they are susceptible to modifications under oxidative stress conditions, such as UV, organic peroxides, or radical generators such as AAPH [124,156,244,245]. The immortal human keratinocyte line HaCaT is frequently employed for studies of skin keratinocytes in vitro, since they retain their differentiation capacity [246]. Keratinocytes were incubated with the water-soluble azo-initiator (AAPH), which is frequently used in vitro for oxidation studies. The GPAA derivatives were detected in total lipid extracts using a targetted lipidomic approach involving neutral loss and precursor ion scanning modes, following optimization of this strategy with commercial 1-palmitoyl-2-oleoyl-phosphatidylserine (POPS) as a model system.

5.3 Materials and methods

Materials

2,2′-azobis(2-amidinopropane) dihydrochloride (AAPH) was from Sigma Aldrich. Trypsin and Dulbecco's Modified Eagle Medium (DMEM) were obtained from Sigma Chemical Co. (St. Louis, MO, USA). Fetal calf serum, streptomycin and penicillin were purchased from Invitrogen (Paisley, UK). 1-Palmitoyl-2-oleoyl-phosphatidylserine (POPS) was purchased from Avanti Polar Lipids, Inc. (Alabaster, AI, USA). Chloroform (Analytical reagent grade), and methanol (HPLC grade) were from Fisher (UK).

Oxidation of phosphatidylserine with AAPH

Vesicles of POPS were prepared in ammonium bicarbonate buffer 5 mM (pH 7.4). In a typical experiment, 250 μg of phospholipid dissolved in chloroform was evaporated to dryness, the buffer was added and the mixture was vortexed for 2 min and then sonicated for 1 min in a sonicating water bath. The oxidation was performed by addition of 15 μL of AAPH to a final concentration of 30 mM and 50 mM in a volume of 250 μL. The mixture was incubated at 37 °C in the dark for 24 h. The phospholipid oxidation products were extracted using a modification of the Folch method [169] with chloroform–methanol (2:1, v/v).

Cell culture

The human keratinocyte cell line HaCaT was obtained from DKFZ (Heidelberg, Germany). HaCaT is a spontaneously transformed immortalized human epithelial cell line from adult skin that maintains full epidermal differentiation capacity [247]. The cells were used after reaching 70–80% confluence, which occurs approximately every 3 days after initial plating. Cells beyond passage 45 were discarded. The cells were cultured in Dulbecco's Modified Eagle Medium (high glucose) supplemented with 4 mM glutamine, 10% heat inactivated fetal bovine serum, 100 U/mL penicillin, and 100 µg/mL streptomycin at 37 °C in a humidified atmosphere of 95% air and 5% CO2.

Chemical treatment

HaCaT cells (15 × 106) were cultured in 150-cm^2 flasks and subjected to AAPH exposure for 24 h, at 37 °C. The AAPH was dissolved in culture medium to obtain a final concentration of 30 mM and 50 mM. Control experiments consisted of untreated cells.

Cell viability/metabolic activity assay

The effects of AAPH exposure on cell viability/metabolic activity were evaluated by the resazurin assay [248]. Briefly, cells were plated in triplicate in a 96 well plate at a density of 0.4 × 106 cells/mL, in a final volume of 0.2 mL/well and exposed to 30 mM or 50 mM AAPH. After 20 h, the cells were washed with PBS and fresh culture medium containing 50 µM of resazurin was added to each well. After 4 h (in a total of 24 h AAPH treatment) absorbance was read at 570 and 600 nm with a standard spectrophotometer (Multiskan GO, Thermo Scientific). Viable and therefore metabolic active cells are able to reduce resazurin (a blue dye) into resorufin (pink colored) and, hence, their number correlates with the magnitude of dye reduction.

Assessment of cell PS externalization/apoptosis

PS externalization following AAPH-cell treatment was analyzed by fluorescent microscopy using the FITC-Annexin V apoptosis detection kit with 7-AAD from Biolegend (San Diego, CA, USA). Briefly, 0.4 × 106 cells were plated in each well of a µ-Slide 8 well plate (IBIDI GmbH, Germany), in a final culture medium volume of 0.2 mL. The cells were then treated with 30 mM or 50 mM AAPH for 24 h, or with 1 µM

Staurosporine for 4 h (as a positive control for induction of apoptosis). Cells were washed twice with sterile PBS and incubated for 20 min in fresh culture medium containing 2 μg/ml Hoescht 33258 (Molecular Probes, Invitrogen, Paisley, UK). After this, medium was removed and the wells washed twice with PBS, following by 15 min incubation in the dark with FITC-Annexin V/7-AAD staining solution. After three washing steps, slides were analyzed with a fluorescent microscope (Nikon Corporation, Japan) at 630× magnification. Images were captured with a DS-Fi2 High-definition digital camera and analyzed in NIS-Elements Imaging Software (Nikon Corporation, Japan).

Lipid extraction

For lipid extraction, untreated cells and AAPH-treated cells (after 24 h stimulation) were washed twice with ice-cold phosphate-buffered saline (PBS), scraped into 5 mL of ice-cold PBS and the cells pelleted by centrifugation at 200g for 4 min. The pellet was resuspended in 1 mL of milli-Q ddH2O. Thereafter, total lipids were extracted using the Bligh and Dyer [170]. Lipid extracts were evaporated to dryness under nitrogen and resuspended in 500 μL of chloroform.

ESI-MS conditions

Oxidation products of phosphatidylserine standards and HaCaT total lipid extracts were diluted in methanol (1:10, v/v) and detected using a 5500 QTrap mass spectrometer (ABSciex, Warrington, UK) operating in negative ion detection mode with direct infusion at a flow rate of 5 μL min−1. Mass spectra were acquired over a mass range of 400–1000 Da. Turbo spray source temperature was set at 150 °C, spray voltage was set at −4.5 kV, declustering potential was set at −50 eV and nominal curtain gas flow was set at 20. Enhanced mass spectra were acquired at 10,000 Da/s in dynamic fill. Targeted detection of GPAA was performed by neutral loss scans (NLS) for 58 Da at a scan speed of 10,000 Da/s, with collision energy set at −45 eV, Q1 set to low resolution and Q3 set to unit resolution. Targeted detection of GPAA by precursor ion scanning (PIS) at *m/z* 137.1 were collected at 1000 Da/s scan speed with step size of 0.5 Da, collision energy at −45 eV and with Q1 and Q3 set to unit resolution. Enhanced product ion (EPI) spectra were acquired for the ion of interest with collision energy varying between 40 and 50 eV. Dynamic fill time was used with a maximum fill time of 250 ms and all other parameters optimized to

give maximum signal. There was a small error in the calibration of the instrument, resulting in masses slightly higher than the theoretical mass of the lipids by 0.1–0.2 Da, especially in targetted scan modes.

5.4 Results and discussion

To observe whether PS polar head-group oxidation occurred in HaCaT cells after AAPH incubation, as observed after radical oxidation of PS by hydroxyl radical [168,236], cells were subjected to oxidation with AAPH (30 and 50 mM). The oxidative stimuli used were the same as reported in a previous study that mimicked oxidative stress injury in keratinocytes as a model of inflammation [156]. AAPH was chosen as it is a water-soluble azo-initiator frequently used for oxidation studies, using in in vitro, model systems. AAPH after activation lead to alkylperoxyl radicals and akylperoxides that are capable of initiating radical lipid peroxidation in liposomes and cells [156].

As can be observed in Figure 32A and B, the concentrations of AAPH used effectively induce apoptosis in keratinocytes, as demonstrated by PS externalization and a marked decrease in cell metabolic activity. Moreover, apoptosis induction was clearly dependent on AAPH concentration, as keratinocytes treated with 50 mM were uniformly in the late stage of apoptosis, characterized by massive externalization of cell membrane PS (in green) and nuclear binding of the 7-AAD probe (in red). These findings support the AAPH-treated HaCaT cell model as a suitable one to investigate the oxidation of PS in apoptosis.

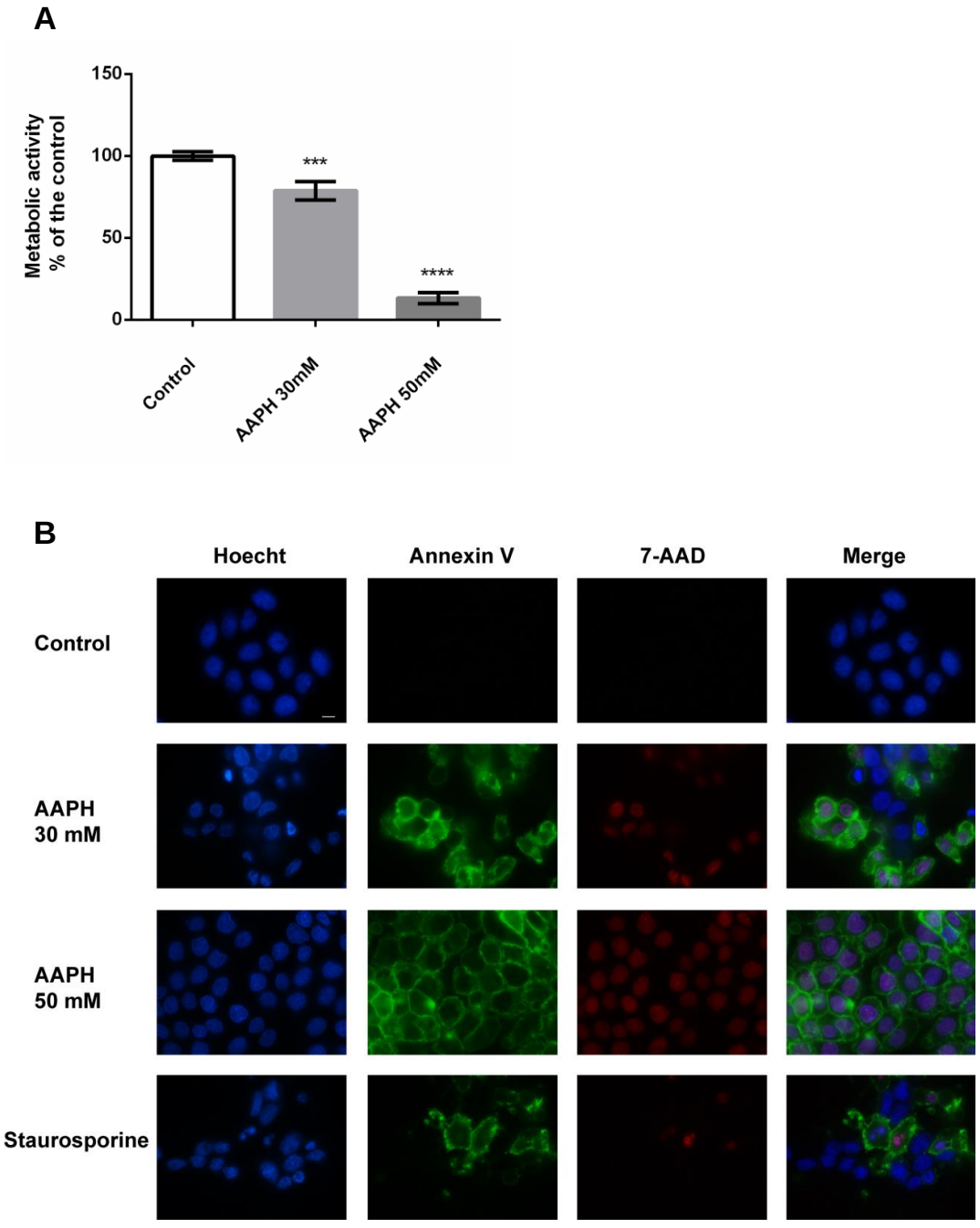

Figure 32: Effect of AAPH on cell metabolic activity and PS externalization. A) Cells were treated with 30 mM or 50 mM AAPH during 24h and the viability was assessed by resazurin assay. In this assay metabolic conversion of resazurin into resorufin will be proportional to cell viability. B) Keratinocytes were treated with 30 mM or 50 mM AAPH during 24h, and the apoptosis stage was analyzed by fluorescent microscopy using Annexin V, 7-AAD and Hoescht 33258 probes. Intact cells appear with just blue nuclei, early apoptotic cells present blue nuclei and green membranes (PS externalization) and finally late apoptotic cells present marked green fluorescence and red nuclei. Images representative of different fields were acquired with a DS-Fi2 High-definition digital camera coupled to a Nikon fluorescent microscope (magnification 630x) and analyzed in NIS-Elements Imaging Software (Nikon Corporation, Japan). Bar scale : 10 µm

The analysis of the lipid extracts obtained from keratinocytes was first undertaken using ESI-MS in negative mode (Figure 33). PS species were observed as $[M-H]^-$ in low abundance since they are minor PL in total extracts, and thus oxidation products were not detectable. In order to achieve the sensitivity required to identify PS oxidation species, either in the fatty acyl chain or the polar head-group, a targeted shotgun lipidomic approach involving neutral loss scanning of 87 Da was performed on control and oxidized cell extracts (Figure 34). Loss of 87 Da is a well-known and typical fragmentation of phosphatidylserine under MS/MS conditions. The most abundant phosphatidylserine species observed were at *m/z* 788.7, identified as PS-(18:0/18:1), and at *m/z* 760.7, identified as PS-(16:0/18:1). It should be noted that the observed masses of the phospholipids were slightly above their theoretical masses (e.g. 788.54 for PS-(18:0/18:1), owing to small deviations in the calibration of the instrument. The composition of non-modified PS species was confirmed by MS/MS. The full list of PS species observed are summarized in Table 5; many of these species have been identified previously in keratinocytes and cell cultures [234].

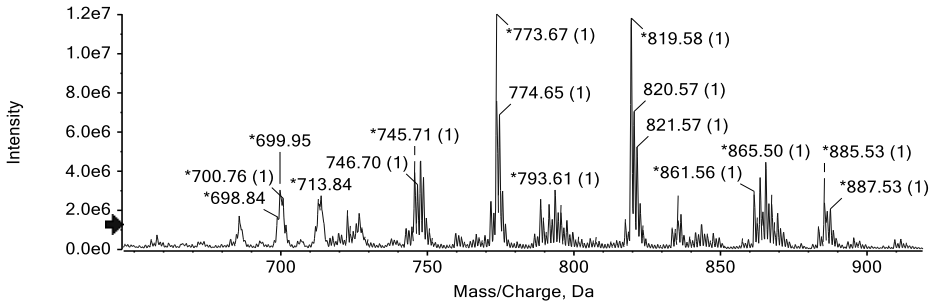

Figure 33: The lipid profile of control HaCaT cells. MS spectrum obtained in negative ion mode from total lipid extract of HaCaT cells.

Table 5: Identification of major PS species identified by NLS of 87 Da in the HaCaT cells lipid extract, with the indication of the *m/z* values of the [M-H] ions observed.

PS species (fatty acyl composition)	**NLS of 87Da $[M-H]^-$ *m/z***
16:0/18:1	760.7
18:0/18:2	786.7
18:0/18:1 **16:1/20:0**	788.7
18:0/18:0	790.7
18:0/20:2	814.7
18:0/22:6	834.7
18:0/22:5	836.7

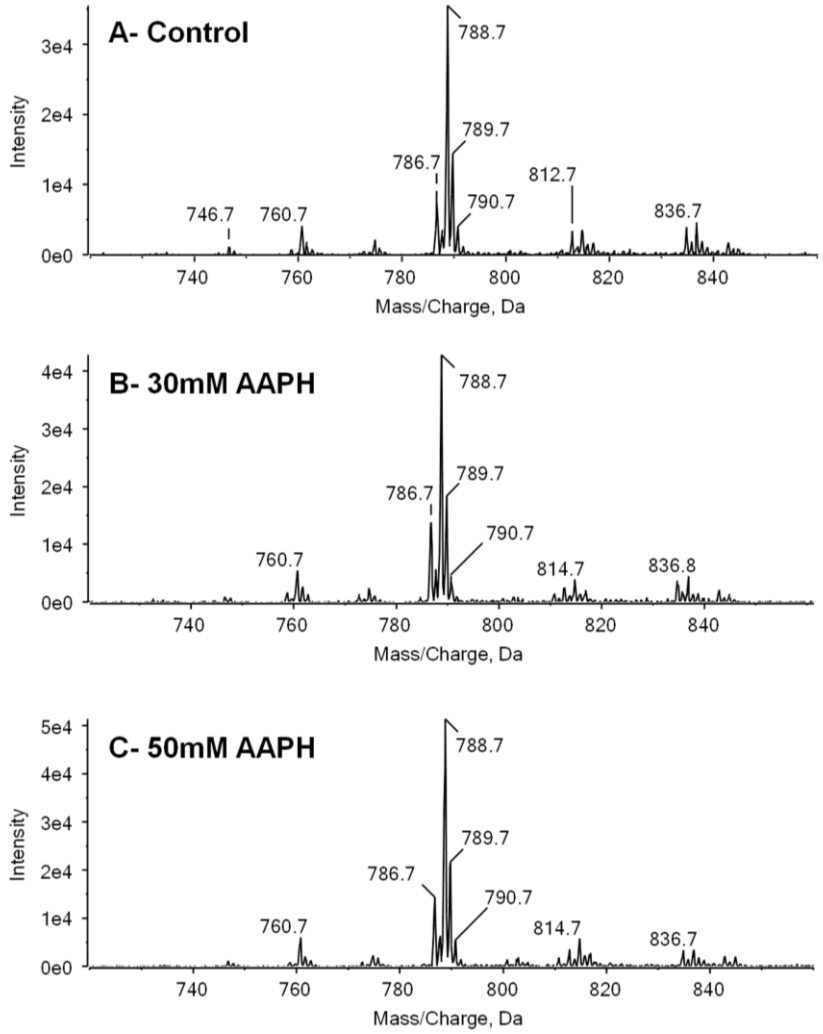

Figure 34: The lipid profile of control and cells exposed to AAPH. Spectra of neutral loss of 87 Da scanning of lipid extracts of HaCaT cells. (A) Control lipid extracts. (B) Lipid extracts obtained from HaCaT cells incubated with 30 mM AAPH. (C) Lipid extracts obtained from HaCaT cells incubated with 50 mM AAPH

Comparing the spectra obtained by NLS of 87 Da from the total lipid extract of HaCaT cells treated with AAPH (30 mM and 50 mM) with control HaCat cells, no differences between spectra were observed, suggesting that PS modified exclusively in fatty acyl chains are not formed or were formed at very low abundance and not detected under the experimental conditions used. However, we used direct infusion of a total lipid extract and it is possible that ion suppression of oxidized PS with oxygenated acyl chains occurred. For complete confidence in the absence of these oxidation products, an LC–MS analysis would be required. In contrast, using NLS of 58 Da, which is selective for GPAA as a polar head-group, clear evidence for the oxidation of the PS head-group in cells treated

with 50 mM AAPH was obtained (Figure 35). The neutral loss of 58 Da is a characteristic fragmentation of GPAA, which contains an acetic acid functional group as a polar head-group (Scheme 11), as described previously [168,236,249]. In GPAA fragmentation the neutral loss of 87 Da does not occur. In Figure 35, ions at *m/z* 731.6, 757.5, 759.5 and 807.7 were observed and identified as GPAA derivatives, and their identity was confirmed by further MS/MS studies. The MS/MS spectrum of the most abundant ion at *m/z* 759.5 is shown as an example in Figure 36. This precursor ion is 29 Da smaller than an un-modified PS at *m/z* 788.6, and fragments to yield product ions at *m/z* 281.3 and 283.3, corresponding to the deprotonated oleic acid and stearic acid, respectively, and an ion at *m/z* 419.3 corresponding to lyso-phosphatidic acid, LPA-(18:0). The ion at *m/z* 253.3 also indicates the presence of a GPAA-(16:1/20:0) species. This enabled the identification of *m/z* 759.5 as the product of PS-(18:0/18:1) oxidation in the serine polar head-group.

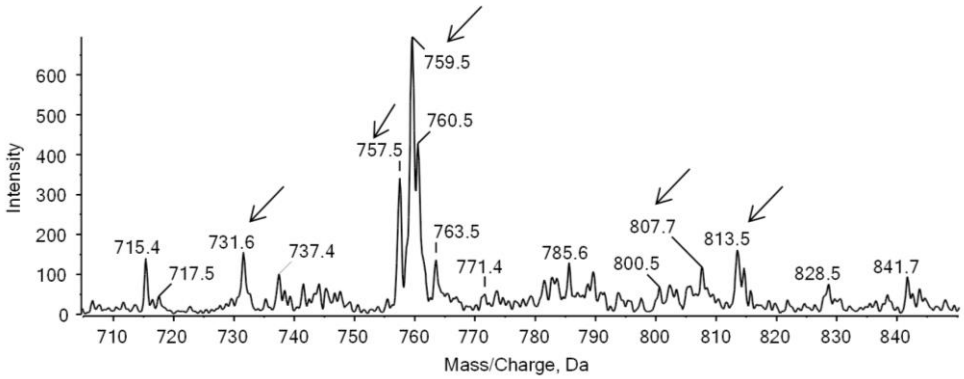

Figure 35: PS oxidized in the serine headgroup was observed in HaCaT cells after oxidative stress. Spectrum of neutral loss scan of 58 Da obtained from HaCaT cells incubated with 50 mM AAPH.

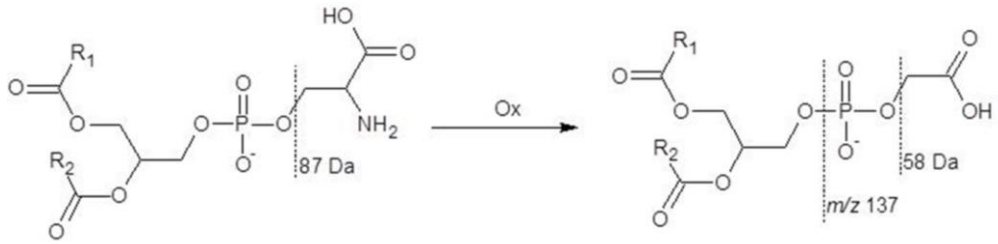

Scheme 11: Phosphatidylserine and glycerophosphoacetic acid (GPAA) structures. Specific neutral loss of 87 Da from non-modified PS and neutral loss of 58 Da from GPAA. Formation of an ion at *m/z* 137 observed during GPAA fragmentation.

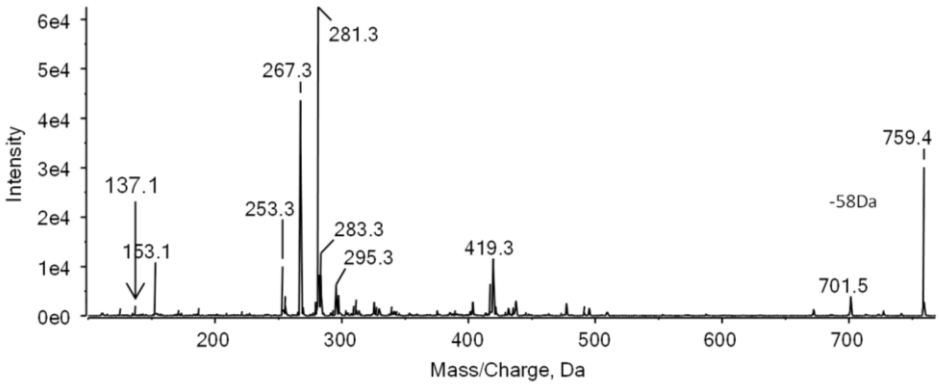

Figure 36: Tandem mass spectrometric analysis of GPAA species. MS/MS spectrum of the ion [MH] at *m/z* 759.5 corresponding to the GPAA species formed by PS head group oxidation.

Interestingly, in all the MS/MS spectra of GPAA derivatives (Figure 36) it was possible to observe a product ion at *m/z* 137.1, which was assigned as $HOPO_3CH_2COO^-$ following fragmentation studies. This product ion is absent in the MS/MS spectra of un-modified PS and it was not observed in our previous work that identified GPAA derivatives for the first time, because those experiments were conducted in a linear ion trap mass spectrometer; these instruments have a cut off of 30% of the *m/z* value of the precursor ion, so the ion at *m/z* 137 could not be detected. This demonstrates the advantages of a Q-trap for the identification of novel diagnostic ions for lipid oxidation products. To test the value of this diagnostic marker, PIS at *m/z* 137.1 was used to confirm the occurrence of GPAA modifications in cells exposed to AAPH (Figure 37), and lipids containing GPAA were clearly observed in samples treated with 30 and 50 mM AAPH. These novel results show that PIS for this diagnostic ion is more sensitive than NLS for 58 Da, which only allows detection of GPAA under the higher stress conditions, but its selectivity is not as good, as several ions that did not correspond to the GPAA derivatives were also observed, such as ions at *m/z* 746.9 and 818.8/818.9. The combined information from NLS of 58 Da and precursor ion scan (PIS) 137.1 allowed confirmation of the presence of species that correspond to the GPAA derivatives in HACT cells. Table 6 summarizes the ions corresponding to GPAA that were observed in the NLS of 58 and PIS *m/z* 137 spectra obtained from total lipid extract of HaCaT cells incubated with 30 mM and 50 mM of AAPH.

Table 6: The major GPAA species observed in HaCaT cells incubated with 30 mM and 50 mM AAPH and the *m/z* values of the [MH] ions observed in the 58 Da of HaCaT cells incubated with 50 mM AAPH, and in the PIS at *m/z* 137.1 for HaCaT cells incubated with 30 mM and 50 mM AAPH.

	NLS of 58 Da		**PIS *m/z* 137**	
GPAA species	30mM	50mM	30mM	50mM
16:0/18:1	-	731.6	-	731.7
18:0/18:2	-	757.5	757.7	757.7
18:0/18:1 **16:1/20:0**	-	759.6	759.7	759.7
18:0/18:0	-	-	-	761.6
18:0/22:5	-	807.6	-	807.7

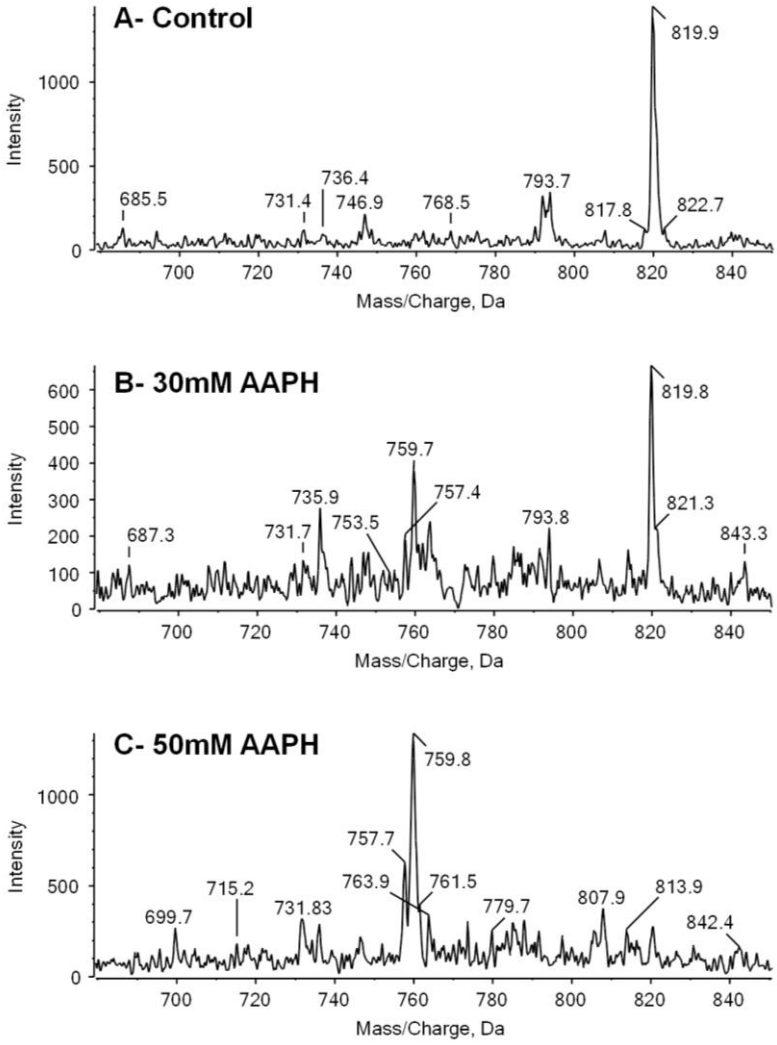

Figure 37: Use of the diagnostic marker at *m/z* 137.1 to detect oxidized PS in cells exposed to AAPH. (A) Spectrum of precursor ion scanning of the ion at *m/z* 137.1 obtained from control

HaCaT cells. (B) Spectrum of precursor ion scanning of the ion at *m/z* 137.1 obtained from HaCaT cells incubated with 30 mM AAPH during 24 h. (C) Spectrum of precursor ion scanning of the ion at *m/z* 137.1 obtained from HaCaT cells after incubation with 50 mM AAPH during 24 h.

To confirm and corroborate our results from HaCaT cells, further characterization of oxidation and fragmentation pathways following AAPH-induced oxidation of a PS standard, 1-palmitoyl-2-oleoylphosphatidylserine (POPS (16:0/18:1), was performed. The reaction was monitored by ESI-MS and MS/MS in negative ion. POPS was selected since PS (18:0/18:1) and PS-(16:0/18:1) are known to be the most abundant species of PS in HaCaT cells [234]. Analysis of the ESI-MS spectrum obtained for POPS after treatment with AAPH (Figure 38A) allows several deprotonated molecular ions ($[M-H]^-$) to be identified, corresponding to the PS oxidation products. The ions at higher *m/z* than the native POPS (*m/z* 760.6) were found to be oxidation products of the unsaturated fatty acyl chain (*m/z* 776.6, PS+16 Da (hydroxy), 792.6, PS+32 Da (hydroperoxy), *m/z* 774.6, PS+14 Da (keto/epoxy derivatives). These are typical oxidation products of PS observed previously both in vitro and in vivo [121,122,123,133,168]. Other ions at *m/z* values smaller than the non-modified PS were also detected and were identified as oxidation products with modifications in the serine polar head-group. These products were identified as PS with a glycerophosphoacetic acid linked to the phosphate group (GPAA), (*m/z* 731.6), confirming that the PS modified at the polar head-group can be formed during AAPH-induced radical attack, as previously reported during the oxidation of PS induced by hydroxyl radical [168]. Oxidation products at the serine polar head-group and the fatty acyl chain (*m/z* 745.6 (GPAA+14 Da), 747.6 (GPAA+16 Da) and 763.6 (GPAA+32 Da) were also identified (Figure 38). Tandem mass spectrometry (MS/MS) was used to confirm the previous assignments. In the ESI-MS/MS spectra of GPAA in negative ion mode a neutral loss of 58 Da was observed, corresponding to the loss of CH_3COOH (acetic acid). These PS oxidation products are easily differentiated from the native PS and PS oxidized at the fatty acyl chains, as the latter show a typical neutral loss of 87 Da (loss of aziridine-2-carboxylic acid). Also, comparing the ESI-MS/MS spectra of non-modified POPS and GPAA, it can be seen that the product ion at *m/z* 137.1 (assigned as $HOPO_3CH_2COO^-$) is only present in the GPAA MS/MS spectrum. Figure 38B and C shows that by using neutral loss scanning (NL of 87 Da and NL of 58 Da) precursor ion scan (PIS) at *m/z* 137.1 based on these distinct fragmentation profiles of PS oxidation products, it was possible to identify

GPAA derivatives in the total lipid extracted obtained from HaCaT cells incubated with AAPH.

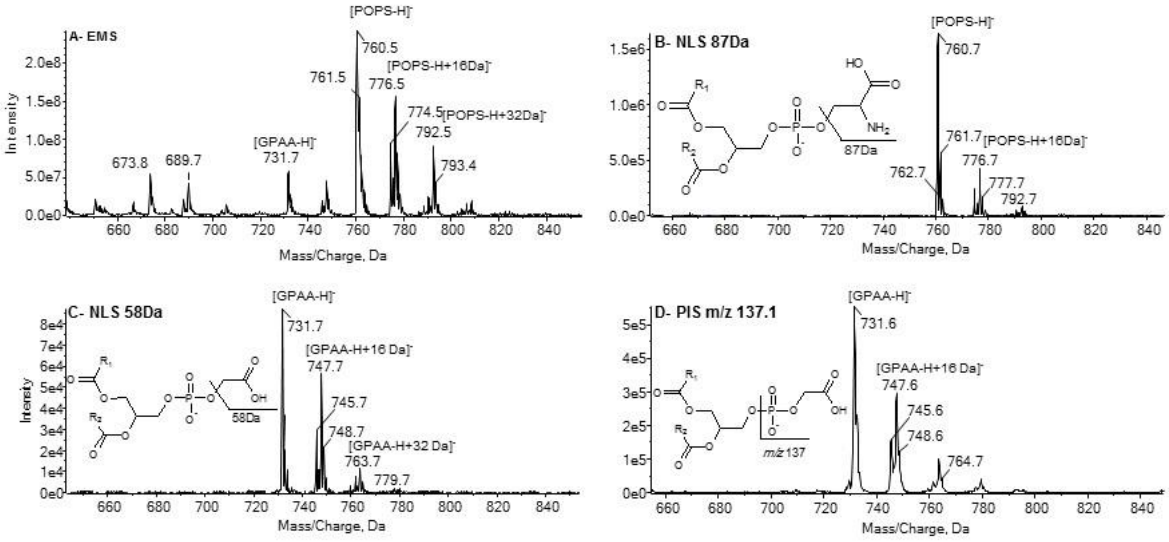

Figure 38: Mass spectrometric analysis of oxidized POPS by different scanning routines. (A) MS spectrum obtained in negative ion mode of an oxidized mixture of POPS showing the [MH] ions. Oxidation of POPS was induced after incubation with 30 mM AAPH. (B) Spectrum of neutral loss scanning of 87 Da obtained from an oxidized mixture of POPS. (C) Spectrum of neutral loss scanning of 58 Da obtained from an oxidized mixture of POPS. (D) Spectrum of precursor ion scanning of the ion at *m/z* 137.1 obtained from an oxidized mixture of POPS. Mass spectra were acquired using a 5500 QTrap mass spectrometer.

AAPH is a water-soluble azo-initiator which generates peroxyl radicals (Scheme 12, equation 1) at a constant rate and at a given temperature by thermal decomposition [154] and is independent of the cellular metabolism. The AAPH peroxyl radical intermediate is the reactive oxygen species responsible for the oxidation of biomolecules such as lipids and peptides and proteins. The formation of the GPAA derivatives occurs due to the AAPH-induced oxidation at the serine polar head-group, similar to the mechanism that occurs in amino acids and peptides [250]. This reaction is proposed to be initiated by the AAPH peroxyl radical, which causes the abstraction of the hydrogen linked to the α-carbon, generating a tertiary radical that is stabilized by the amine nitrogen and carbonyl group [154]. This carbon-centered radical reacts with an oxygen molecule and decomposes further leading to other oxidation products. Oxidative decarboxylation with formation of an additional keto group is usually observed during amino acid oxidation [208]. This occurs due to the loss of CO_2 from C terminal via β-scission of an alkoxyl radical at the C terminal α-carbon (Scheme 12 equations 2 and 3) [209].

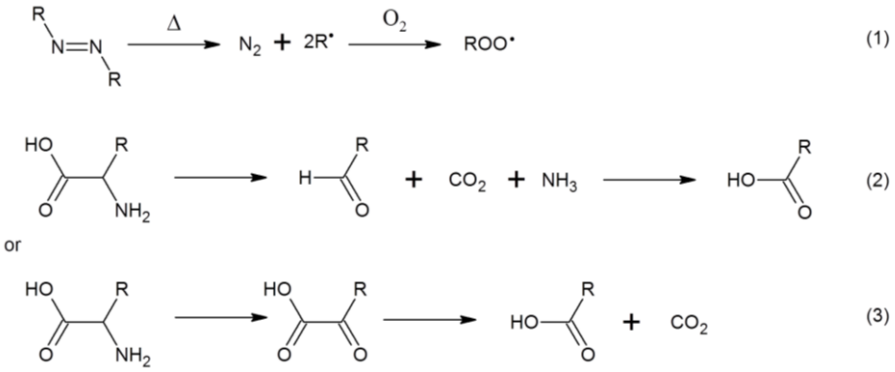

Scheme 12: Reaction pathways that occurred during PS polar head oxidation by AAPH radical generator: Decomposition of AAPH produces molecular nitrogen and two carbon centered radicals. The carbon radicals may react with molecular oxygen to give peroxyl radicals (1). There are two possible pathways for the formation of GPAA derivatives from PS oxidation. PS polar head group may be deaminated and carboxylated to yield an aldehyde one carbon shorter than the original and the aldehyde may be oxidized to a carboxylic acid (2). Alternatively PS polar head group may be transaminated, resulting in the formation of an a-keto acid which can be oxidatively decarboxylated to yield a carboxylic acid one carbon shorter than the original PS polar head (3).

In spite of the important role of PS oxidation, there is limited knowledge of the modifications that can be generated in this phospholipid under oxidative stress, particularly in the serine polar head-group. The possibility of formation of several oxidation products makes it important to define exactly which are being formed during stress, so that biological effects can be correctly linked to the precise products. PS is normally maintained in the inner leaflet membrane by the action of aminophospholipid translocase; it seems probable that GPAA derivatives in membranes, like PS oxidized at the fatty acyl chains, would not be recognized by this enzyme, thus promoting the presence of PS modified in polar head-group in outer leaflet membrane and contributing to the recognition of apoptotic cells. Interestingly, a recent study evaluated the capacity of GPAA to stimulate monocytes and dendritic cells to produce pro-inflammatory cytokines and the results showed that GPAA has no pro-inflammatory activity [242]. Nevertheless, the specific role of these species in remains to be elucidated and more studies are needed. PS oxidized at the polar head-group may also have a significant role in these processes and should be explored further in the future.

5.5 Conclusions

This study highlights that oxidation of the serine polar head group, as well as fatty acyl chains, in phosphatidylserines in keratinocytes can occur after radical attack by the azo-initiator AAPH, and is likely to be missed by conventional techniques for identifying PS oxidation that depend on detection of the PS head-group. The GPAA derivatives formed due to serine head-group modification can be identified using an improved targetted lipidomic approach, based on the observation that GPAA oxidative products have a specific fragmentation pathway producing a product ion at *m/z* 137 ($HOPO_3CH_2COOH$) and a neutral loss of 58 Da. Further studies are needed to investigate the possible formation of these species in other cell and tissues.

Chapter VI

UVA exposure induces changes in the lipid profile of human melanoma cells

The results presented in this chapter were integrally submitted as follow:

E. Maciel, J. Felgueiras, E.M.P Silva., A.S.P Moreira, M. Fardilha, P. Domingues, M.R.M. Domingues, UVA exposure induces changes in the lipid profile of human melanoma cells, submitted to Free Radical Biology & Medicine.

6.1 Abstract

Extensive exposure to UVA is thought to increase the risk, malignancy and progression of human melanoma, the most serious type of skin cancer. Furthermore, it is well known that alterations in lipid metabolism represent an early event in carcinogenesis. Thus, in this study we aimed to investigate if UVA exposure exerted changes in lipid composition in melanoma cell lines. After UV irradiation, the lipid extracts from SK-MEL-28 cells were analyzed at 0, 2 and 24 hours. The fatty acids analysis were performed by GC-MS and the analysis of phospholipids were performed by LC-MS and MS/MS. The results showed an increase of mono-unsaturated fatty acid (MUFA), as well as, an increase of stearic acid (FA18:0). In contrast, a decrease of palmitic acid (FA16:0) was observed. The most significant changes in phospholipids content occurred in phosphatidylcholines (PC) and phosphatidylinositol (PI) classes. The results revealed a decrease of PC and an increase of PI content in human melanoma cells after UV irradiation. Moreover, LC-MS data showed a specific response at the molecular level within each class, with increase of MUFA with time, similar with a variation of FA profile. Overall, these data indicate membrane lipid changes associated with lipogenesis after UVA exposure which, in turn, is usually determinant for cell survival. The absence of cleaved caspase-3 after 2 h and 24 h of re-incubation correlates with impairment of apoptosis. The observed alterations in the lipid metabolism may be correlated with malignant transformations associated with cancer development and progression. Thus, lipids might constitute challenging therapeutic targets for the treatment of highly resistant-melanoma.

Keywords: UVA, Phospholipids, fatty acids, melanoma, LC-MS, apoptosis

6.2 Introduction

Solar radiation is considered the most relevant environmental carcinogen causing melanoma, a cutaneous cancer with increasing incidence in white populations [251]. The toxic effects resultant from sun exposure are primarily mediated by UV radiation, which is known to cause mutations in melanocytes and initiate melanoma. Nonetheless, information is still lacking regarding the role of UV radiation on melanoma progression and outcome. It is generally accepted that UVB is the most aggressive amongst radiations' wavelengths and is capable of initiating melanoma [252]. Both UVB and UVA exposures for long periods have deleterious effects and contribute to the onset of the disease, although the impact of UVA is less extensive (as reviewed in [253]). The molecular mechanisms that underlie UVA toxicity are not fully elucidated. Among the candidates are the formation of free radicals and DNA damage, which render cells prone to aging, mutagenesis, and carcinogenesis [157,158]. Since UVA is the most prominent component of terrestrial UV radiation, contributing in 90-95% in total, its biological effects and impact on photo-carcinogenesis and tumor progression has been receiving increasing attention [160,161,162].

Activation of lipid metabolism is an early event in carcinogenesis and a hallmark of many types of cancers [254,255]. Therefore, the study of lipidomics is one of the main current focus in cancer research. Lipids are key components of cell membranes, providing structural support, conditioning fluidity, and regulating permeability and stability of biological membranes, as well as, acting as important players in signal transduction [254,256,257]. Alterations in the lipid profile have been correlated with cell differentiation and malignancy [258]. For instance, phosphoinositides and ceramides are precursors for second messengers in signaling pathways that regulate cell growth and proliferation [254,259,260,261]. *De novo* lipid synthesis, particularly of fatty acids (FA), is required for carcinogenesis and tumor cell survival, as reported in prostate and breast cancers [255,262]. The enhanced metabolism of choline and the increase in the lysophosphatidic acid (LPA) content are also observed in many types of cancer [263,264,265,266,267]. Moreover, some acidic glycosphingolipids have been reported to be highly expressed in melanoma and to promote malignant properties by activating cell growth and adhesion

signals [268,269,270]. The surface exposure of phosphatidylserine (PS) has also been described in melanoma cells, which seems paradoxical since PS acts as an apoptotic recognition signal for macrophages and tumor cells are able to evade apoptosis [66,271]. These and other significant findings have culminated in the identification of lipid composition as an additional valuable source of information on disease progression, being a potential biomarker for the diagnosis and prognosis of cancer [254]. The analysis of lipid profiles have been, nevertheless, difficult due to the presence of the several thousand of molecular species that characterize the human lipidome and their structural diversities [254]. The emerging mass spectrometry-based lipidomics strategies allow the measurement of many lipid species from a complex biological mixture and, thus, have been applied in the study of several malignancies [272,273].

In this study, our primary goal was to obtain a deeper insight into the impact of UVA exposure in the dynamics of lipids, and therefore complement the already existing and largely explored knowledge on DNA and protein damage [274,275]. Lipidomics-based approaches were used to characterize phospholipids and FA profiles of human melanoma cells' membranes. These data were further correlated with cell death.

6.3 Material and Methods

Material

Dulbecco's Modified Eagle Medium (DMEM), fetal bovine serum (FBS), 100 U/mL penicillin and 100 µg/mL streptomycin solution (Pen/Strep), and 0.25% trypsin/1 mM EDTA were purchased from Gibco (Invitrogen, Spain). Phosphate buffered saline (PBS) were purchased from Thermo Scientific (Thermo Fisher Scientific, Germany). Caspase-3 antibody was acquired from GeneTex (Tebu-bio, Portugal). Cleaved caspase-3 was purchased from Millipore (Merck Millipore, Germany). Infrared IRDye-labeled anti-rabbit antibody specific to Li-Cor's Odyssey Infrared was acquired from LI-COR Biosciences (LI-COR Biosciences, Germany).

Phospholipid internal standards (1,2-dimyristoyl-*sn*-glycero-3-phosphocholine (dMPC), 1,2-dimyristoyl-*sn*-glycero-3-phosphoethanolamine (dMPE), 1,2-dimyristoyl-*sn*-glycero-3-phospho-(1′ -rac-glycerol) (dMPG) and 1,2-dimyristoyl-*sn*-glycero-3-phospho-L-serine (dMPS) were purchased from Avanti Polar Lipids, Inc. (Alabaster, AL, USA).

Acetonitrile, chloroform, methanol and hexane from Fisher scientific (Leicestershire, UK); all were of HPLC grade and were used without further purification. All the other reagents and chemicals used were of the highest grade of purity commercially available. The water was of MilliQ purity filtered through a 0.22-mm filter (Millipore, USA).

Cell culture and exposure to UVA

SK-MEL-28, a human malignant melanoma cell line, was kindly given by Dr. Ricardo Pérez-Tomás (University of Barcelona, Barcelona, Spain). Cells were cultured in DMEM, supplemented with 10% FBS and 1% Pen/Strep, and maintained overnight at 37°C in a 5% CO_2 humidified incubator. Subsequently, medium was removed and cells underwent a 20 min period of irradiation, the time needed to deliver a total light dose of 60 J/cm^2 with a fluence rate of 50 mW/cm^2 measured with a radiometer Li-COR Model LI-250. The UVA source, an Exo Terra Sun Glo A 40W H2104 lamp with a spectrum of emission in the UVA range (320–400 nm), was fitted 15 cm above the cells. After irradiation, cells were either collected, using trypsin followed by centrifugation (1000 rpm, 3 min) or returned to the CO_2 incubator for 2 h or 24 h, after which the same method of collection was applied. Collected cells were immediately frozen.

Lipid extraction

Lipids were extracted from SK-MEL-28 cells through the Bligh and Dyer method [276]. In brief, 3.75 mL of chloroform–methanol 1:2 (v/v) were added to each sample, vortexed, and incubated on ice for 30 min. After the incubation period, 1.25 mL of chloroform plus 1.25 mL of doubly distillated water were added, and the samples were vortexed and centrifuged at 153x*g* for 5 min at 22 ºC to obtain a two-phase system (aqueous top phase and organic bottom phase) [234,277]. The lipid extracts, recovered from the bottom phase, were dried using a nitrogen flow and stored at −20 °C until used.

Characterization of phospholipids profile

The characterization of individual molecular species of phosphatidylcholine (PC), lysophosphatidylcholine (LPC), phosphatidylethanolamine (PE), phosphatidylserine (PS), phosphatidylinositol (PI), phosphatidylglycerol (PG) and sphingomyelin (SM) classes was

achieved by mass spectrometry (MS), using a linear ion trap (LXQ; Thermo Finnigan, San Jose, CA, USA) mass spectrometer after separation by liquid chromatography (LC). HPLC system (Waters Alliance 2690) was used with a Ascentis®Si column (15 cm × 1 mm, 3 μm) and a precolumn split (Acurate, LC Packings, USA) in order to obtain a flow rate of 60 μL min^{-1}. The solvent system consisted of two mobile phases as follows: mobile phase A (acetonitrile:methanol:water; 50:25:25 (v/v/v) with 1 mM ammonium acetate) and mobile phase B (acetonitrile:methanol 60:40 (v/v) with 1 mM ammonium acetate). Initially, 0% of mobile phase A was held isocratically for 8 min followed by linear increase to 60% of A within 7 min and maintained for 22 min. The LXQ was operated in the negative mode (electrospray voltage −4.7 kV), the capillary temperature was 275 C and the sheath gas flow was 8 U. Normalized collision energy™ (CE) ranged between 20 and 27 (arbitrary units) for MS/MS experiments. Data acquisition was carried out on an Xcalibur data system (V2.0) [278]. Relative quantitation of individual phospholipid species was determined by the ratio between the area of reconstructed ion chromatogram of a given *m/z* value against the area of the reconstructed ion chromatogram of the respective class [279].

Fatty acid analysis

The FA content of the total lipid extracts was assessed by measuring the fatty acid methyl esters through gas chromatography (GC), according to a previously described method [280]. Briefly, a methanolic solution of potassium hydroxide (2 M) and a saturated solution of NaCl were added to lipid extracts (20 μg). The solution was then vortexed and centrifuged for 5 min at 613x*g* to obtain a two-phase system. The FA methyl esters recovered from the bottom phase were dried using a nitrogen flow and resuspended in hexane. Methyl esters of FA were analyzed by GC-MS on an Agilent Technologies 6890N Network (Santa Clara, CA) equipped with a DB-FFAP column with 30 m of length, 0.32 mm of internal diameter, and 0.25 μm of film thickness (J&W Scientific, Folsom, CA). The GC was connected to an Agilent 5973 Network Mass Selective Detector, operating with an electron impact source at 70 eV and the scanning range was *m/z* 40-500 in a 1 s cycle in a full scan mode acquisition. The oven temperature was programmed from an initial temperature of 80 ºC, standing at this temperature for 3 min, a linear increase to 160 ºC at 25 ºC/min, followed by linear increase at 2 ºC/min to 210 ºC, and then at 30 ºC/min to 250 ºC remaining at this temperature during 10 min. The injector and detector

temperatures were 220 and 280 °C, respectively. Helium was used as carrier gas at a flow rate of 1.7 mL/min.

Immunoblot assay

Total proteins were extracted from cells with boiling 1% sodium dodecyl sulfate. The protein content in each sample was determined using the bicinchoninic acid assay [281]. Equal amounts of protein (50 μg of protein) were separated on 12% SDS-PAGE and transferred onto nitrocellulose membranes. Membranes were then blocked with 5% non-fat milk in 1×Tris buffered saline with 0.1% Tween-20 (TBST) for 1 hour at room temperature, washed with 1×TBST three times, and incubated with the appropriate primary antibody. After being washed three times with 1×TBST, cells were incubated with a proper secondary antibody. All antibodies were previously diluted in 3% non-fat milk in 1xTBST. Detection of the secondary antibodies was achieved using the Li-Cor's Odyssey Infrared Imaging System (LI-COR Biosciences, Bad Homburg, Germany). Quantitative analysis was performed using Quantity One 1-D Analysis Software 4.6.5 (Bio-Rad, Amadora, Portugal).

Statistical analysis

The results were expressed as means and standard error means (mean±SD) for each experimental group. To obtain the correlations and similarities between groups a 2-way ANOVA independent-measures test followed by the Bonferroni post hoc test where differences were considered significant at $p < 0.05$. Graph pad (version 6.0) was used for all comparisons.

6.4 Results

In order to assess the effects of UVA exposure on membrane lipids, total lipids were extracted from SK-MEL-28 cells at three time points: immediately after UVA exposure (0 h) and 2 h and 24 h after. Non-irradiated SK-MEL-28 cells were used as control. The profiles of FA and phospholipids were determined and apoptosis was analyzed for each sample. All experiments were performed in triplicates.

6.4.1 GC-MS analysis of FA profile from SK-MEL-28 cells exposed to UVA

FA are known to influence cell proliferation both *in vitro* and *in vivo*. In this study, the variation of FA profile in melanoma cells exposed to UVA was determined by GC-MS. The relative content of each FA was calculated immediately after UVA exposure (0 h) and after 2 h and 24 h, as presented in Table 1. The most abundant FA have 16 and 18 carbons length and none or one unsaturation (16:0, 16:1, 18:0, 18:1), followed by FA ranging from 14:0 to 22:6 (Figure 39, Table 7). Interestingly, distinct variations in the relative content of FA were observed in response to UVA exposure: immediately after irradiation we observed a decrease of FA18:1, FA20:4 and FA22:6 and an increase of the relative content of FA16:0 and FA16:1; after the re-incubation period of 2 h, the relative content of FA16:0 decreased, whereas the relative content of FA18:0 and FA18:1 increased. We also observed an increase of the FA16:1 abundance after 24 h. The FA 20:4 levels 2 h and 24 h after UV exposure are similar with the control. The levels of FA 22:6 remain lower than the control, R.A.<1,38, throughout the experiment. Additionally, there was also variations on the content of saturated (SFAs) (Figure 39A), MUFAs (Figure 39B), and polyunsaturated FA (PUFA) (Figure 39C), when comparing control cells *versus* cells exposed to UVA. It was observed that SFA increased immediately after exposure to UVA, while PUFA decreased and MUFA registered only a slight increase. However, these tendencies revert when analyzing FA after 2 h and 24 h, since SFA and PUFA returned to levels similar to the control, and MUFA increased after 24 h incubation.

Table 7: The effect of UVA in SK-MEL-28 cell line's fatty acid content. Relative abundance of fatty acids observed in GC-MS chromatogram for lipid extracts from melanoma cells control, melanoma cells immediately after irradiation (0 h) and after 2 h and after 24 h of exposition.

	Control	0 h	2 h	24 h
C14:0	2.82±0.42	3.48±0.12*	2.60±0.12	1.56±0.31****
C16:0	26.03±1.41	28.11±0.21****	23.89±0.55****	23.94±0.65****
C16:1	9.71±0.26	11.57±0.30****	10.25±0.11	11.36±0.64****
C18:0	11.06±0.19	11.85±0.08**	12.91±0.21****	13.32±0.47****
C18:1n9c	26.20±0.54	25.09±0.13***	27.08±0.39**	28.20±0.31****
C18:1n9t	13.10±0.18	13.36±0.23	13.41±0.09	11.81±0.48****

C18:2n9c	1.84±0.07	1.59±0.07	2.16±0.06	2.32±0.28
C20:0	0.13±0.05	0.31±0.05	0.32±0.06	0.45±0.09
C20:1n9	0.59±0.31	0.33±0.08	0.50±0.11	0.48±0.05
C20:3n3	0.54±0.26	0.21±0.07	0.54±0.12	0.45±0.02
C20:4n6	3.02±0.56	1.54±0.18****	2.90±0.31	2.77±0.18
C20:5n3	0.35±0.22	0.07±0.03	0.27±0.09	0.17±0.06
C22:5	0.91±0.20	0.24±0.01*	0.60±0.13	0.65±0.09
C22:6	2.63±0.05	0.97±0.05****	1.38±0.19****	1.17±0.17****

Values are mean ± standard deviation of mean for 3 replicates of each assay. Comparisons were performed using two-way ANOVA, with Bonferroni as a posttest for control versus 0 h, 2 h and 24 h. **** $P < 0.0001$, *** $P < 0.001$, ** $P < 0.01$ and * $P < 0.05$.

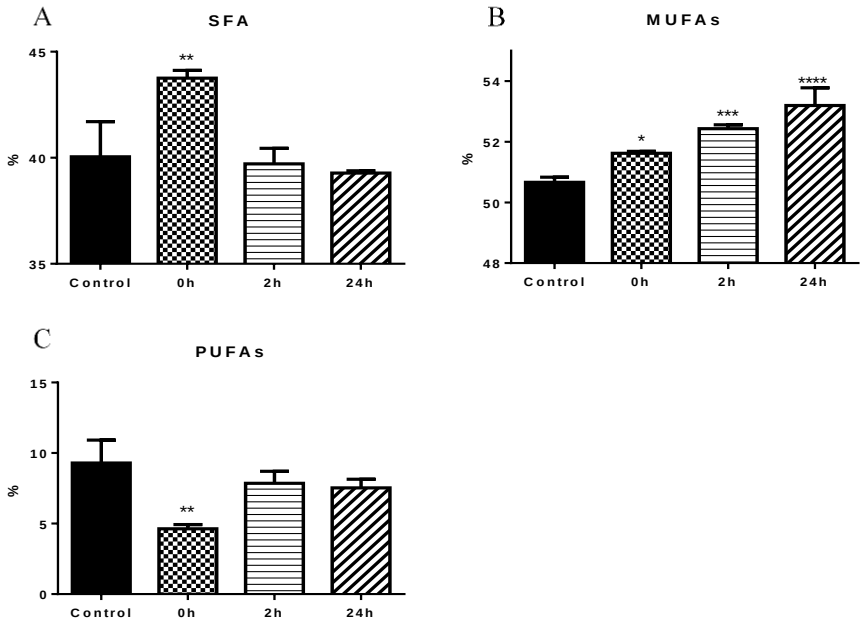

Figure 39: Effect of UVA on fatty acid composition of SK-MEL-28 cell line. Effect on saturated fatty acids (SFAs) (A), mono-unsaturated fatty acids (MUFAs) (B) and polyunsaturated fatty acids (PUFAs) (C) from control cells, cells immediately after UVA exposure, after 2 h and 24 h of exposition.

6.4.2 LC-MS and MS/MS analysis of phospholipid profile from SK-MEL-28 cells expose to UVA

The HILIC-LC-MS approach allowed the determination of the phospholipid profile at molecular level of melanoma cells prior and following irradiation. As an example, the obtained LC-MS chromatograms of the total lipid extract before irradiation and 24h of the incubation after the irradiation are presented in Figure 40A. After 24 h of UVA exposure, differences were observed in the relative abundance (RA) of phospholipid classes (Figure 40B), particularly in PI and PC since the PI content increased while the PC content decreased.

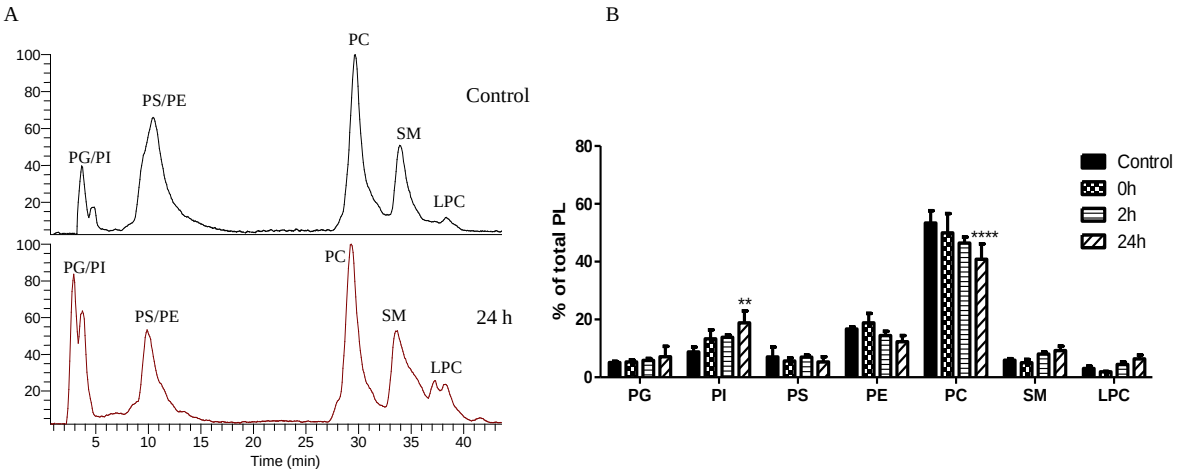

Figure 40: LC-MS chromatogram for total lipid extracts from SK-MEL-28 cell line, both control cells and cells 24 h after UVA exposure (A). Relative abundance of phospholipid classes observed in LC-MS chromatogram for lipid extracts from control cells, cells collected immediately after irradiation (0 h) and after 2 h and 24 h of exposition (B). Values are expressed as mean ± standard deviation of 3 replicates for each assay. Comparisons were performed using two-way ANOVA, with Bonferroni as a posttest for control versus 0 h, 2 h and 24 h. ****$P < 0.0001$, **$P < 0.01$

Individual phospholipid molecular species were further analyzed and MS data is presented by means of RA per phospholipid class. All species were observed in the mass spectra obtained in the negative ion mode as $[M-H]^-$ ions, in the case of PE, PS and PI, or $[M+OAc]^-$ ions, in the case of LPC, PC and SM. LC-MS/MS was performed for each ion to identify and confirm the respective structures, according to the typical fragmentation pathways [7]. Differences in the RA of the molecular species, within classes, were observed in the analysis of the cells collected immediately after exposure and after re-

incubation (2 h and 24 h), in comparison to the control. SM did not evidenced significant differences in any moment of the experiment and, thus, were not reported herein.

Generally, the PC is the most abundant phospholipid class in cell membranes, which was also verified for the SK-MEL-28 cell line (Figure 40B). The PC content significantly decreased upon UVA exposure (Figure 40B), particularly 24 h after irradiation. The molecular analysis of PC class by LC-MS and MS/MS at the distinct time points identified the same PC $[M+OAc]^-$ ions, but variations in their RA were detected (Figure 41A). The PC (16:0/18:1) is the most abundant molecular species in all LC-MS spectra and was observed at *m/z* 818.4, as shown in Figure 41A. Comparison between PC molecular species before and after UVA exposure revealed alterations in their RA, with significant differences for almost all PC molecular species identified, especially at 24h. The RA of PC (16:1/18:1) (*m/z* 816.4), PC (18:1/18:1) (*m/z* 844.4), PC (18:0/18:1) (*m/z* 846.4), PC (18:1/20:4) (*m/z* 866.4) and PC (18:1/22:5) (*m/z* 892.4) molecular species increased 2 h and 24 h after UVA exposure. The levels of the ether linked PC, with mono-saturated fatty acid PC (O-16:0/16:1) (*m/z* 776.4) increased, while saturated PC (O-16:0/16:0) (*m/z* 776.4) decreased. The RA of other molecular species bearing saturated FA, such as PC (14:0/16:0) (*m/z* 764.4) and PC (16:0/16:0) (*m/z* 792.4) decreased, in accordance to FA analysis by GC-MS.

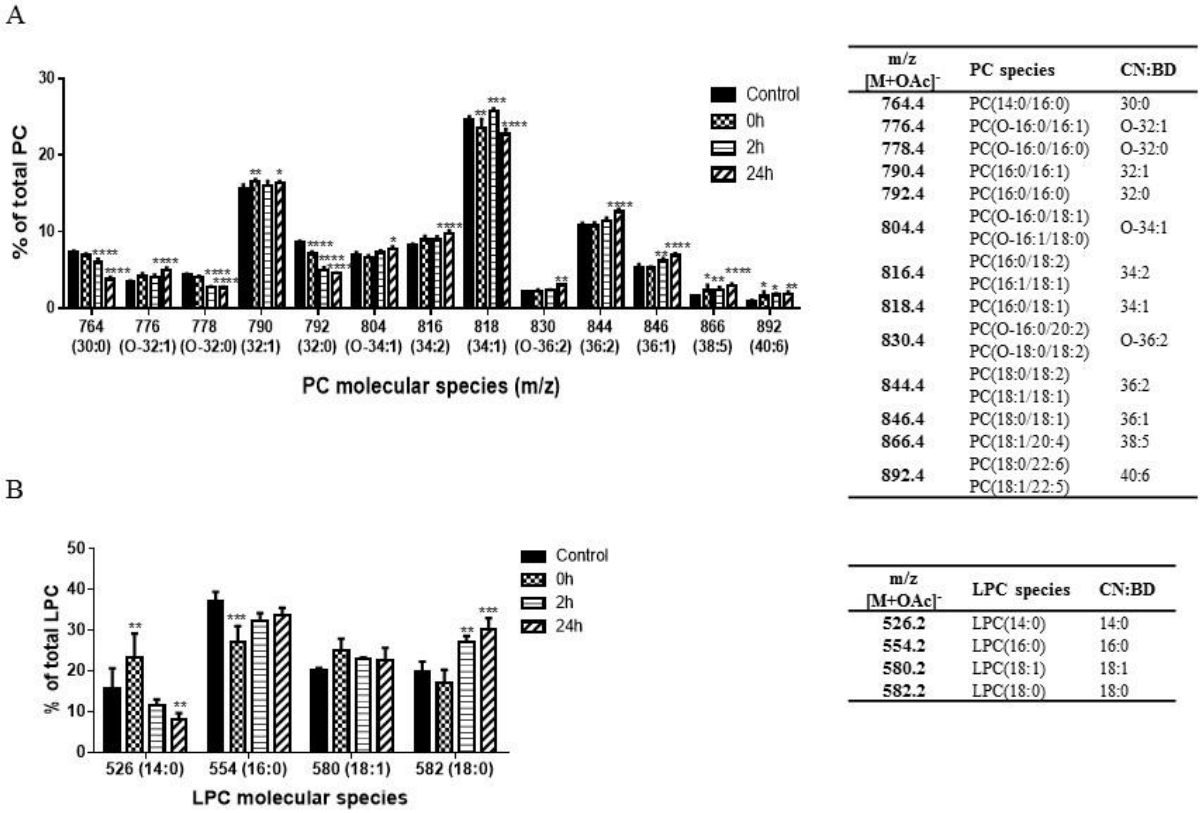

m/z [M+OAc]⁻	PC species	CN:BD
764.4	PC(14:0/16:0)	30:0
776.4	PC(O-16:0/16:1)	O-32:1
778.4	PC(O-16:0/16:0)	O-32:0
790.4	PC(16:0/16:1)	32:1
792.4	PC(16:0/16:0)	32:0
804.4	PC(O-16:0/18:1) PC(O-16:1/18:0)	O-34:1
816.4	PC(16:0/18:2) PC(16:1/18:1)	34:2
818.4	PC(16:0/18:1)	34:1
830.4	PC(O-16:0/20:2) PC(O-18:0/18:2)	O-36:2
844.4	PC(18:0/18:2) PC(18:1/18:1)	36:2
846.4	PC(18:0/18:1)	36:1
866.4	PC(18:1/20:4)	38:5
892.4	PC(18:0/22:6) PC(18:1/22:5)	40:6

m/z [M+OAc]⁻	LPC species	CN:BD
526.2	LPC(14:0)	14:0
554.2	LPC(16:0)	16:0
580.2	LPC(18:1)	18:1
582.2	LPC(18:0)	18:0

Figure 41: Relative abundance of $[M+OAc]^-$ ions of PC molecular species (A) and LPC molecular species (B) observed in the LC-ESI-MS spectra for lipid extracts from SK-MEL-28 cell line (control cells, cells collected immediately after irradiation (0 h) and after 2 h and 24 h of exposition). Values are expressed as mean ± standard deviation of 3 replicates for each assay. In inset, the PC and LPC molecular species corresponding to each $[M+OAc]^-$ ion are presented. Comparisons were performed using two-way ANOVA, with Bonferroni as a posttest for control versus 0 h, 2 h and 24 h. ***$P < 0.0001$, ***$P < 0.001$, **$P < 0.01$, *$P < 0.05$

Additionally, the LPC molecular species were also affected by UVA exposure (Figure 41B). LPC were also identified as $[M+OAc]^-$ ions. An increase of LPC (14:0) molecular species at *m/z* 526.2 and a decrease of LPC (16:0) molecular species at *m/z* 554.2 can be observed immediately after exposure to UVA. However, upon re-incubation the levels of the LPC (14:0) molecular species decreased, while the LPC (18:0) at *m/z* 582.2 increased. Similarly to what was observed in PC and FA, the RA of the species with shorter carbon chain length decreased whereas the RA of species with FA 18:0 increased after exposure to UVA.

The LC-MS analysis of the PE classes showed the same molecular species of PE in all spectra, but in contrast with PC, the RA of PE molecular species with longer and more

unsaturated chains (PE (18:1/18:1)/PE (18:0/18:2), PE (18:1/20:4), PE (18:0/20:4)/PE (18:1/20:3), PE (18:0/22:6)/PE (18:1/22:5)) decreased during re-incubation, whereas the RA of the molecular specie PE (O-16:1/18:1) at *m/z* 700.5 increased significantly after 24 h of re-incubation (Figure 42).

In the case of PS, the most abundant molecular species is PS (18:0/18:1) at *m/z* 788.4, which was also the only molecular species level exhibiting a significant RA decrease immediately after UVA exposure. The RA levels returned to near the control levels after 24 h re-incubation (Figure 43).

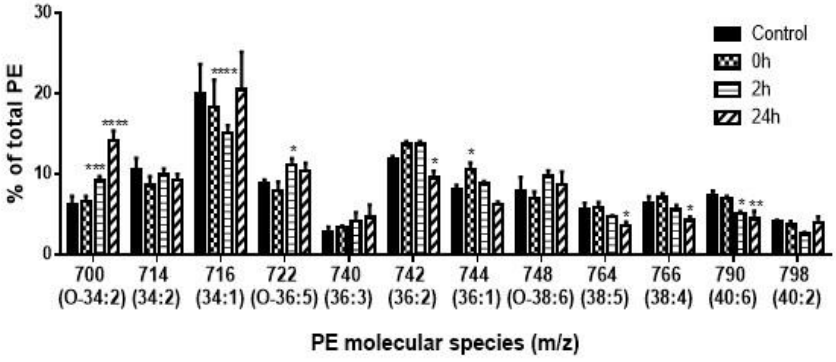

m/z [M-H]⁻	PE species	CN:BN
700.5	PE(O-16:1/18:1) PE(O-16:0/18:2)	O-34:2
714.4	PE(16:1/18:1) PE(16:0/18:2)	34:2
716.4	PE(16:1/18:0) PE(16:0/18:1)	34:1
722.5	PE(O-16:1/20:4)	O-36:5
740.5	PE(18:1/18:2) PE(16:0/20:3)	36:3
742.5	PE(16:1/20:2) PE(18:1/18:1) PE(18:0/18:2)	36:2
744.5	PE(18:0/18:1)	36:1
748.5	PE(O-16:1/22:5)	O-38:6
764.5	PE(18:1/20:4)	38:5
766.5	PE(18:0/20:4) PE(18:1/20:3)	38:4
790.5	PE(18:0/22:6) PE(18:1/22:5)	40:6
798.5	PE(18:0/22:2)	40:2

Figure 42: Relative abundance of $[M-H]^-$ ions of PE molecular species observed in the LC-ESI-MS spectra for lipid extracts from SK-MEL-28 cell line (control cells, cells collected immediately after irradiation (0 h) and after 2 h and 24 h of exposition). Values are expressed as mean ± standard deviation of 3 replicates for each assay. In inset, the PE molecular species corresponding to each $[M-H]^-$ ion are presented. Comparisons were performed using two-way ANOVA, with Bonferroni as a posttest for control versus 0 h, 2 h and 24 h. ***P < 0.0001, ***P < 0.001, **P < 0.01, *P < 0.05

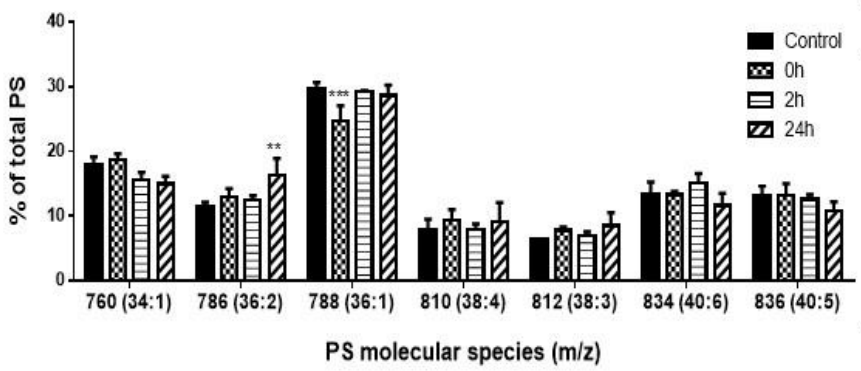

m/z [M-H]⁻	PS species	CN:BN
760.4	PS(16:1/18:0) PS(16:0/18:1)	34:1
786.4	PS(18:0/18:2) PS(18:1/18:1)	36:2
788.4	PS(18:0/18:1)	36:1
810.4	PS(18:0/20:4) PS(18:1/20:3)	38:4
812.4	PS(18:0/20:3)	38:3
834.4	PS(18:0/22:6) PS(18:1/22:5)	40:6
836.4	PS(18:0/22:5)	40:5

Figure 43: Relative abundance of $[M-H]^-$ ions of PS molecular species observed in the LC-ESI-MS spectra for lipid extracts from SK-MEL-28 cell line (control cells, cells collected immediately after irradiation (0 h) and after 2 h and 24 h of exposition). Values are expressed as mean ± standard deviation of 3 replicates for each assay. In inset, the PS molecular species corresponding to each $[M-H]^-$ ion are presented. Comparisons were performed using two-way ANOVA, with Bonferroni as a posttest for control versus 0 h, 2 h and 24 h. ***P < 0.0001, ***P < 0.001, **P < 0.01, *P < 0.05

The most abundant PG molecular species in SK-MEL-28 cell line are PG (18:1/22:6) (*m/z* 819.4), PG (16:0/18:1) (*m/z* 747.4) and PG (18:1/18.1) (*m/z* 773.4) (Figure 44). Immediately after irradiation no significant changes occurred in the PG molecular profile. However, after 2 h and particularly after 24 h of UVA exposure, significant changes were detected particularly in the RA of molecular species PG (16:0/18:2) and PG (16:1/18:1) at *m/z* 745.4. It was observed an increase of the RA of these two molecular species and there was also a significant decrease of the RA of PG (18:1/22:6) (*m/z* 819.4) molecular species.

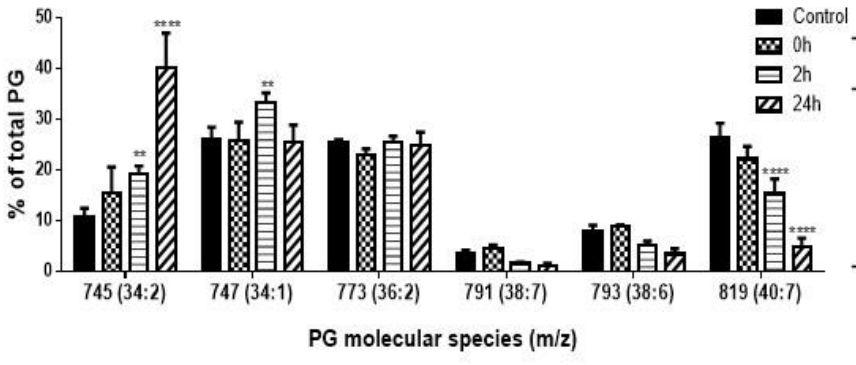

m/z [M-H]⁻	PG species	CN:BN
745.4	PG(16:1/18:1) PG(16:0/18:2)	34:2
747.4	PG(16:0/18:1)	34:1
773.4	PG(18:1/18:1)	36:2
791.4	PG(16:1/22:6)	38:7
793.4	PG(16:0/22:6)	38:6
819.4	PG(18:1/22:6)	40:7

Figure 44: Relative abundance of $[M-H]^-$ ions of PG molecular species observed in the LC-ESI-MS spectra for lipid extracts from SK-MEL-28 cell line (control cells, cells collected immediately after irradiation (0 h) and after 2 h and 24 h of exposition). Values are expressed as mean ± standard deviation of 3 replicates for each assay. In inset, the PG molecular species corresponding to each

$[M-H]^-$ ion are presented. Comparisons were performed using two-way ANOVA, with Bonferroni as a posttest for control versus 0 h, 2 h and 24 h. ***P < 0.0001, ***P < 0.001, **P < 0.01, *P < 0.05

The content of PI class increased 24h after re-incubation, comparing to other phospholipids (Figure 40B). A detailed analysis of the molecular species of PI class (Figure 45) showed that the RA of PI (18:1/18:1) (*m/z* 861.5), PI (18:0/18:1) (*m/z* 863.5) and PI (18:0/20:4)/PI (18:1/20:3) (*m/z* 885.5) increased after UVA exposure.

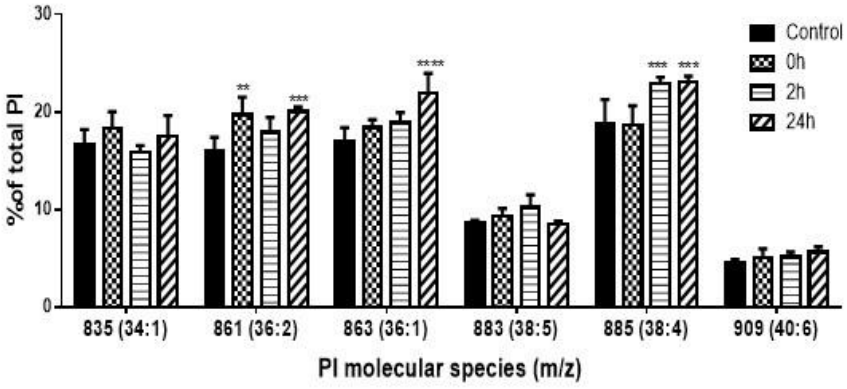

m/z $[M-H]^-$	PI species	CN:BN
835.5	PI(16:0/18:1)	34:1
861.5	PI(18:1/18:1) PI(18:0/18:2)	36:2
863.5	PI(18:0/18:1)	36:1
883.5	PI(18:0/20:4) PI(18:2/20:3)	38:5
885.5	PI(18:0/20:4) PI(18:1/20:3)	38:4
909.5	PI(18:0/22:6) PI(18:1/22:5)	40:6

Figure 45: Relative abundance of $[M-H]^-$ ions of PI molecular species observed in the LC-ESI-MS spectra for lipid extracts from SK-MEL-28 cell line (control cells, cells collected immediately after irradiation (0 h) and after 2 h and 24 h of exposition). Values are expressed as mean ± standard deviation of 3 replicates for each assay. In inset, the PI molecular species corresponding to each $[M-H]^-$ ion are presented. Comparisons were performed using two-way ANOVA, with Bonferroni as a posttest for control versus 0 h, 2 h and 24 h. ***P < 0.0001, ***P < 0.001, **P < 0.01, *P < 0.05

Assessment of apoptosis in SK-MEL-28 extracts

The impact of UVA exposure in the programed death of SK-MEL-28 cells was also investigated by analyses of the activation of caspase-3, resultant from the cleavage of procaspase-3 (Figure 46A). Anti-procaspase-3 and anti-caspase-3 antibodies were used to determine the expression levels of procaspase-3 and caspase-3, respectively. Ponceau staining was used as loading control [282]. As depicted in Figure 46B, the expression levels of procaspase-3 decreased after UV exposure (2 h and 24 h), but cleaved caspase-3, which exhibits only residual levels in control cells, was not detected 2 h and 24h after irradiation

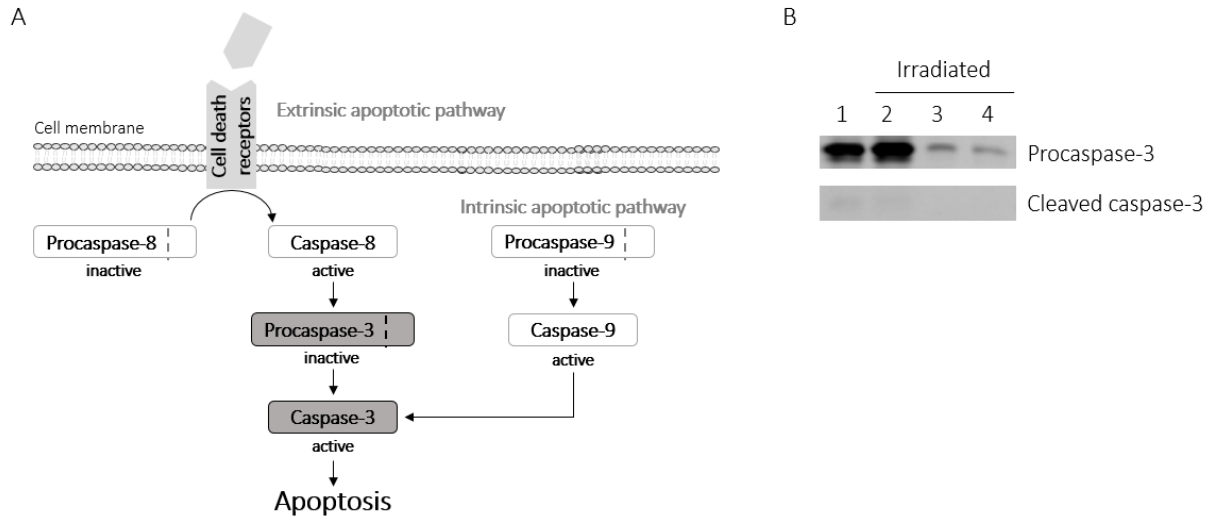

Figure 46: Consequences of UVA exposure in apoptosis. A) Apoptosis was assessed through the analysis of the expression levels of procaspase-3 and caspase-3 (the active cleaved form), a central player in the apoptosis signaling pathway. B) SK-MEL-28 cells were irradiated with UVA for 20 minutes total light dose of 60 J/cm^2 with a fluence rate of 50 mW/cm^2. Cells were immediately collected (2), or left to collect for 2 h (3) or 24 h (4). Non-irradiated cells (1) were used as control. Ponceau staining was used as loading control.

6.5 Discussion

In the present study, the effect of UVA exposure on the lipid content of SK-MEL-28 cell line was investigated in an attempt to correlate changes in the phospholipid bilayer of human melanoma cell membranes with the progression of the disease. The content of phospholipids and fatty acids was therefore determined after acute exposure to UVA (0 h) and after a recovery time (2 h and 24 h after irradiation). Several alterations in the lipid metabolism were identified, which may be associated with malignant transformations.

FA are important contributors to proliferation and survival of the cancer cells and, accordingly, several recent studies have reported *de novo* synthesis of FA in these cells (reviewed in [283]). Thus, in this study the effect of UVA exposure on SFAs, MUFA, and PUFA was accessed. These classes of FA differ in their susceptibility to peroxidation and other structural and physicochemical properties [284]. As depicted in Figure 39, acute UVA exposure led to significant decrease of PUFA—the most toxic FA for melanoma cells in general [285]—and increase of SFA and MUFA. UVA is known to generate high amounts of reactive oxygen species (ROS) that might be responsible for the degradation of PUFAs, which are the most susceptible to lipid peroxidation [23,284]. In mouse melanoma

cells, PUFAs were shown to mediate the growth inhibitory effect of transforming growth factor β1 [286]. Therefore, the UVA-induced reduction in PUFAs' content found here and the reduced sensitity to their toxic effects, described by L.N. Andrade *et al.* [285], may partially explain the resistant phenotype intrinsic to SK-MEL-28 cells.

Interestingly, the re-incubation of cells after UVA exposure changed SFAs and PUFAs trend, which returned to near control levels, but not MUFAs tendency, which was still increasing in a time-dependent way (Figure 39). This behavior favors the formation of mono-unsaturated acyl chains and FA elongation, mainly C18, suggesting preponderant modifications in lipid metabolism in response to UVA exposure. The increase of C18 and the decrease of C16 during the re-incubation period (Table 1) are in agreement with the proposed elongation of FAs from palmitic acid (FA 16:0), the only FA described as toxic for SK-MEL-28 cells [285], to stearic acid (FA 18:0) via elongation of very long chain fatty acids protein 6 ($ELOVL_6$)[287,288]. Furthermore, *de novo* synthesis of SFAs and MUFAs seems to be particularly enriching for the cell membrane of mammalian cells and specially for cancer cells, which are able to synthesize up to 95% of SFAs and MUFAs *de novo* due to the enhanced lipogenesis [283]. This is not only crucial for tumor cell survival but may also contribute to the resistance of cancer cells to therapy [284]. Overall, the UVA-induced alterations in the FA profile of SK-MEL-28 cells may contribute to a more resistant phenotype, since MUFAs are less prone to lipid peroxidation and, therefore, prevent cells from ROS attack and increase cancer cell survival [284].

The increase of the species FA 18:0 and MUFA has been observed in phospholipid molecular species and is being associated with tumor lipogenesis as a metabolic response to cell survival and proliferation of tumor cells [283]. Remodeling of the phospholipid content of the cell membrane has important biological impacts. The detailed analysis of phospholipid classes described in this work showed that different classes of phospholipids have distinct responses to UVA exposure. Moreover, within each class, there are molecular specie-specific responses. PC is a major constituent of eukaryotic cell membranes and, not surprisingly, it is the most abundant class of phospholipids in SK-MEL-28 cells. Overall, PC decreased in response to UVA exposure, in a time-dependent manner (Figure 40). This observation is largely attributed to a decrease of saturated species, whereas the RA of mono- and poly-unsaturated species increased.

When comparing with other phospholipids, the PC content significantly decreased after 24 h of irradiation, and although not as significant, the LPC content showed a tendency to increase. Balogh *et al* suggested in their work with B16-F10 mouse melanoma cells, the action of PLA_2 enzyme to explain the reduction of PC species with rise of the correspondent LPC species after the treatment with heat and benzoyl alcohol [289]. The same study also showed a decrease of PI content as a consequence of the decrease of unsaturated species. In contrast, in our study, PUFA decreased immediately after UVA exposure returning to the control levels after 24 h. At 24h it was also observed the decrease of PC and an increase of PI content. In addition, after 24 h of UVA exposure, we observed a rise of the LPC (18:0) molecular species, as well as the elevation of PC and PI molecular species with long chains, reinforcing the idea that FA elongases action may occurred. Another study explored the metabolic response to Hsp90 inhibition in human melanoma cells. The authors associated Hsp90 inhibition with an increase of PC content, showing the importance of metabolic changes as potentially biomarkers of anti-cancer with Hsp90 drugs in malignant melanoma [290]. In this study, the authors came to the conclusion that the UVA exposure lead to augment of melanoma progression (Figure 47). The decrease of PC abundance and an increase of PI abundance can be perhaps an important signal of this progression, as well as a signal of FA remodelation in order to promote tumor cell survival. Higher levels of PI and alterations in its profile have been observed by different authors in breast cancer cells [273,291,292]. In fact, PI is an important structural phospholipid that is regulated by reversible phosphorylation. The phosphorylated derivatives of PI, called phosphoinositides, are mediators of carcinogenesis: they bind signaling proteins, thus regulating numerous cellular responses (e.g. cell growth and proliferation) [257], and they are critical second messenger molecules of signaling pathways involved in the control of cytoskeletal re-organization and membrane trafficking [293]. Alterations in the remaining phospholipid classes were less evident. PE, which exhibited a slight time-dependent decrease after irradiation, was shown to have anti-tumor effects on mice melanoma cells, both by inducing apoptosis and inhibiting cell proliferation [294]. Thus, a decrease of PE could also be an adaptive response of tumor cell survival.

The alterations in the lipid metabolism observed in this study pointed to the increased ability of SK-MEL-28 cells to evade apoptosis and sustain survival after UVA exposure. To further investigate this hypothesis we analyzed the expression of procaspase-3 and its

cleaved active form (caspase-3), a central player in both extrinsic and intrinsic pathways of apoptosis (Figure 46A). Caspase-3 is endogenously expressed as an inactive proenzyme (procaspase-3) which has to be cleaved into two active fragments (17 and 12 kDa) that, in turn, are capable of regulate downstream targets essential to induce cell death. With this experiment we have showed that UVA exposure clearly downregulated procaspase-3; however, this event did not result its an enhanced concentration of the active form (Figure 46B). Actually, active caspase-3 was undetectable after UVA exposure, in spite of the already scarce levels in control cells (Figure 46B). Downregulation of procaspase-3 was previously demonstrated in poorly differentiated tumors in head and neck squamous cell carcinoma [295], and correlated with poor prognosis in resected nonsmall-cell lung cancer [296] and increased resistance to methotrexate- and doxorubicin-induced apoptosis in osteosarcoma cells [297]. Caspase-3 activation could be prevented via interaction between procaspase-3 and p21, a cell cycle regulator whose expression was shown to be induced by UV radiation [298]. On the other hand, active caspase-3 could be inactivated by IAP family members. Interestingly, melanoma inhibitor of apoptosis protein (ML-IAP) is highly expressed in melanoma and is particularly effective in inhibiting caspase-3 [299].

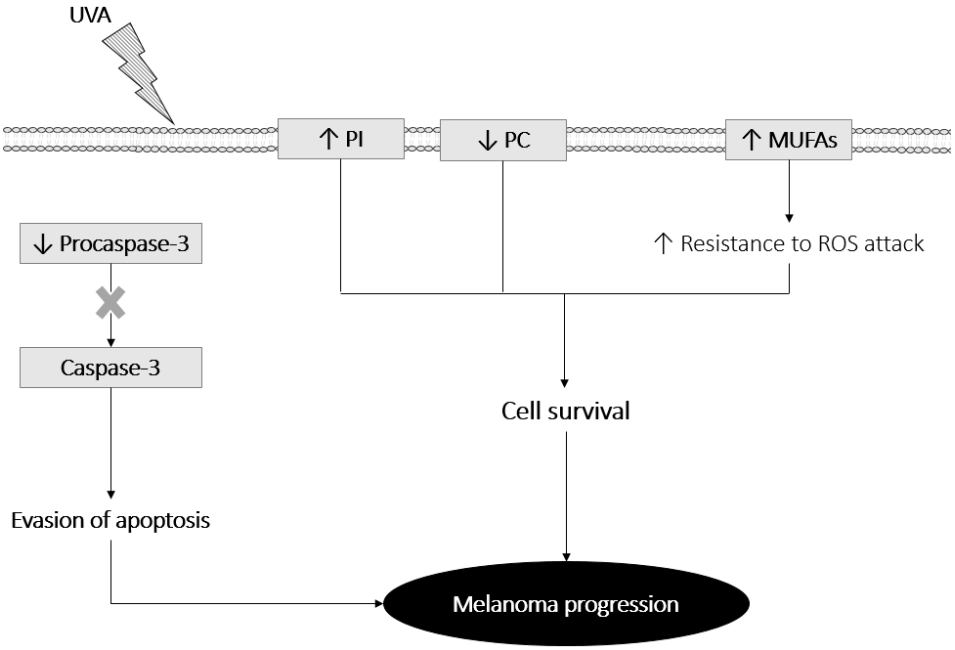

Figure 47: Scheme of the major findings the study of UVA-induced lipid membrane alterations in SK-MEL-28 cell line in order to prevent cell death

6.6 Conclusion

The data obtained from human melanoma cells after UVA exposure evidenced membrane lipid changes associated with lipogenesis and, consequently, cell survival. The UVA exposure resulted in increased PI and reduced PC content in human melanoma cells. These results together with an increase of MUFA and FA18:0 in opposition to the decrease of FA16:0 after 24 h of the UVA exposure indicate *de novo* synthesis of MUFA and SFA. The absence of cleaved caspase-3 after to 2 h and 24 h of UVA exposure, supports the hypothesis that UVA alters the phospholipidome in human melanoma cell line in order to prevent cell death. These results gave further insights on the harmful effect of the UVA, and the consequent adaptations of lipid metabolism, that must underlie cell survival and proliferation, associated with carcinogenesis, tumor development and malignancy.

Chapter VII

Anti-inflammatory effect of oxidized 1-palmitoyl-2-linoleoyl phosphatidylserine in activated macrophages

7.1 Abstract

Recent evidence suggests that phosphatidylserine (PS) and its oxidized species drive the clearance of apoptotic and necrotic cells by macrophages with putative inflammatory and immune response modulation. However, currently it is not clear whether PS and oxidized PS differentially modulate the functional responses of macrophages. The purpose of this paper is to deeply explore this question by evaluating the influence of PS oxidation products on the macrophages inflammatory status. Thus, we determined the effects of oxidized 1-palmitoyl-2-linoleoyl-phosphatidylserine (oxPLPS) and PLPS on the production of the pro-inflammatory mediator nitric oxide (NO) and the inducible NO synthase (*iNos*) and *IL1β* mRNA transcription levels, in RAW 264.7 macrophages, cultured in the absence or in the presence of the *Toll-like* 4 receptor agonist lipopolysaccharide (LPS). Additionally, a range of inflammation-associated signaling pathways, such as nuclear factor (NF)-κB and mitogen-activated protein kinases (MAPKs) were also disclosed.

The results obtained showed that both PLPS and oxPLPS species are deprived of intrinsic pro-inflammatory activity. Exquisitely, only oxidized PLPS were found to significantly inhibit NO production and *iNos* and *IL1β* genes transcription induced by LPS. At a molecular level, these effects were partially due to attenuation of LPS-induced c-Jun-N-terminal kinase (JNK) phosphorylation and p65 NF-κB nuclear translocation. Overall our data suggest that oxPLPS, but not native PLPS, mitigates pro-inflammatory signaling in macrophages, contributing to containment of inflammation during apoptotic cell engulfment.

Keywords: phospholipids, oxidation, inflammation, macrophages

7.2 Introduction

Clearance of apoptotic cells by phagocytes is a crucial homeostatic function in several cellular processes such as embryonic development, tissue remodeling and resolution of inflammation [300,301]. The removal of dying cells prior to the loss of plasma membrane integrity prevents the release of toxic or immunogenic intracellular contents, limiting the establishment of a deleterious inflammatory cascade and autoimmune responses.

The role of macrophages as the main cells involved in apoptotic cell removal is well-established. However, the nature of the "eat-me" signals and receptors that lead to cell recognition and engulfment are still in debate. Several receptors on the surface of macrophages such as CD14 [302], CD91 [303] and scavenge receptors [304] have been implicated in the recognition of apoptotic cells. The constitutive expression of the scavenge receptor CD36 on macrophages and dendritic cells was shown to be crucial for their capacity to recognize and engulf dying cells. Furthermore, ectopic expression of the receptor on non-professional phagocytes such as fibroblasts and melanoma cells confers them phagocytic activity over cells undergoing apoptosis [305,306].

Regarding *eat-me* signals, the translocation of phosphatidylserine (PS) to the outer leaf of cytoplasmic membrane is the central phagocytosis-associated event occurring in apoptotic cells [87,88,100,103]. In fact, masking PS exposure in dying cells was shown to inhibit their engulfment *in vitro* and *in vivo* [307,308]. However, the exact nature of the PS species that drive this strong *eat-me* signal is not totally disclosed. Greenberg and co-workers in an elegant study about macrophage recognition of apoptotic cells via CD36 have shown that recognition occurs via membrane associated oxidized PS (oxPS) and, to a lesser extent, oxidized phosphatidylcholine (oxPC), but not by non-oxidized phospholipid species [104]. It is well known that PS is susceptible to alterations under oxidative stress conditions and that these modifications occur before their externalization. During apoptosis, the asymmetric transbilayer distribution of PS is lost, bringing PS to the surface. The appearance of PS in outer monolayer of the plasma membrane could be related to its oxidation in membrane of apoptotic cells, and that oxidized PS may fail to be recognized by aminophospholipid translocases (APT), preventing the translocation to the inner leaflet of plasma membrane [95,96]. Oxidized PS has already been detected in apoptotic cells [98,241]. Besides this role in tagging apoptotic cells for engulfment, it is plausible that

oxPS may also contribute to modulate intracellular signaling pathways in phagocytes in order to limit their activation. However, the role of oxidized phospholipids (oxPLs) in inflammatory response is unclear, and it is reported that oxPLs can present anti- or pro-inflammatory properties [309]. The research to date has tended to focus on the effect of oxPC in the inflammatory response rather than oxPS. Regarding oxPS role in inflammation, it was demonstrated that it has pro-inflammatory properties in several cases including endothelial cells [114,310] and species of oxPLs were identified in some cases of chronic inflammation as in the case of atherosclerosis [311]. However, other studies suggest that some phospholipids exert anti-inflammatory actions and that this ability is improved upon their oxidation [312]. Accordingly, it was reported that PS is able to suppress the formation and release of pro-inflammatory mediators while inducing the production and release of anti-inflammatory cytokines (transforming growth factor β (TGFβ) and interleukin 10 (IL-10)) in activated macrophages [84,85,106,313]. Moreover, PS liposomes were shown to reduce the LPS-induced release of NO in microglial cultures from neonatal rat brain [108,109] and in apoptotic PC12 cells [110]. Similarly, it was reported that PS inhibited the production of the inflammatory mediators IL-6, IL-8, vascular endothelial growth factor and prostaglandin E2 in IL-1β-stimulated fibroblast-like synoviocytes from rheumatoid arthritis patients via modulation of NF-κB and JNK/p38 MAPK signaling pathways [314]. Despite these evidences for PS involvement in the modulation of inflammatory responses, knowledge regarding the influence of PS oxidation products is scarce.

Therefore, in the present study, we have evaluated the influence of PS oxidation products in the modulation of pro-inflammatory events in macrophages. We have compared the effects of 1-palmitoyl-2-linoleoyl-sn-glycero-3-phospho-L-serine (PLPS) and oxidized PLPS (oxPLPS) on LPS-stimulated RAW 264.7 macrophages. We found that both PLPS and oxPLPS are deprived of intrinsic pro-inflammatory activity, but that oxPLPS may contribute to restrain inflammatory events in macrophages during apoptotic cell recognition and engulfment.

7.3 Material and methods

Material

PLPS was obtained from Avanti polar lipids, Inc. and used without further purification. $FeCl_2$, EDTA and H_2O_2 (30%, w/w) were acquired from Merck. Triethylamine (Acros organics), chloroform (HPLC grade), methanol (HPLC grade) and ethanol absolute (Panreac) were used without further purification. TLC silica gel 60 plates with concentrating zone (2.5x20cm) were purchased from Merck. Dulbecco's Modified Eagle Medium (DMEM), penicillin, streptomycin, resazurin and LPS from Escherichia coli (serotype 026:B6) were obtained from Sigma–Aldrich Química (St Louis, MO, USA). Fetal calf serum and trypsin were purchased from Invitrogen (Paisley, UK). The protease and phosphatase inhibitor cocktails, cOmplete Mini Protease Inhibitor and PhosSTOP respectively, were obtained from Roche (Mannheim, Germany). Antibodies against phospho-p44/p42 MAPK (ERK1/ERK2), phospho-p38 MAPK, phospho-SAPK/JNK, and anti-NF-kB p65 were from Cell Signaling Technologies (Danvers, MA, USA). Antibodies anti-actin and anti-lamin were from Millipore (Bedford, MA, USA) and Calbiochem (Darmstadt, Germany), respectively. The alkaline phosphatase-linked secondary antibodies and the enhanced chemifluorescence (ECF) reagent were obtained from GE Healthcare (Chalfont St. Giles, UK), and the polyvinylidene difluoride (PVDF) membranes were from Millipore Corporation (Bedford, MA). TRIzol® reagent was purchased from Invitrogen (Barcelona, Spain). The iScript Select cDNA Synthesis Kit and SYBR green were obtained from BioRad (Hercules, CA, USA). Primers were from MWG Biotech (Ebersberg, Germany). Unless otherwise stated, all other reagents were from Sigma Chemical Co. (St. Louis, MO, USA) or from Merck (Darmstadt, Germany).

Oxidation of phosphatidylserine by Fenton reaction

Ammonium hydrogen carbonate buffer (5 mM, pH 7.4) was added to 1 mg of phospholipid and the solution was vortex-mixed and sonicated for the formation of vesicles. Oxidative treatments using Fe (II) and H_2O_2, were carried out by adding 40 μM $FeCl_2$ and 10 mM of H_2O_2 to total a volume of 500 μL of solution. The mixture was left to react at 37°C in the dark for several hours with agitation [168,236,249].

Cell culture

Raw 264.7, a mouse leukaemic monocyte macrophage cell line from American Type Culture Collection (ATCC number: TIB-71), was cultured in DMEM supplemented with 10% non-inactivated fetal bovine serum, 100 U/ml penicillin, and 100 µg/ml streptomycin at 37 ºC in a humidified atmosphere of 95% air and 5% CO2. Along the experiments, cells were monitored by microscope observation in order to detect any morphological change.

Determination of cell viability by resazurin assay

Assessment of metabolically active cells was performed using 7-hydroxy-3H-phenoxazin-3-one-10-oxide sodium salt (resazurin) colorimetric assay as previously reported [248]. Briefly, Raw 264.7 cells (60×10^5 cells/well) were plated and allowed to stabilize for 12h in 200 µl medium in 96 well plates. Following this period, cells were either maintained in culture medium (control) or incubated with 5 different concentrations of the lipids to be tested. After 20h, a resazurin stock solution (500µM in phosphate buffered saline) was added to a final concentration of 50 µM and cells further incubated at 37 ºC for 4h, in a humidified atmosphere of 95% air and 5% CO_2. The bioreduction of the dye was quantified by absorbance measurement at 570 nm, with a reference wavelength of 620 nm in an automated plate reader (Multiskan 60, Thermo Scientific).

Measurement of nitrite production by the Griess reagent

The production of nitric oxide (NO) was measured by the accumulation of nitrite in the culture supernatants, using a colorimetric reaction with the Griess reagent [195]. Briefly, 170 µl of culture supernatants were diluted with equal volumes of the Griess reagent [0.1% (w/v) N-(1-naphthyl)-ethylenediamine dihydrochloride and 1% (w/v) sulphanilamide containing 5% (w/v) H_3PO_4] and maintained during 30 min, in the dark. Culture medium was used as blank and nitrite concentration was determined from a regression analysis using serial dilutions of sodium nitrite as standard. The absorbance at 550 nm was measured in an automated plate reader (Multiskan 60, Thermo Scientific).

RNA extraction

Raw cells were plated at $2x10^6$ cells/well in 6-well microplates in a final volume of 2 ml and treated during 24 h with PLPS (30 µg/mL) or oxPLPS (30 µg/mL). When testing

the effect of lipids over LPS stimulation, the cells were exposed to the lipid during 1h prior to the addition of 1µg/ml of LPS. Total RNA was isolated from cells with the TRIzol® reagent according to the manufacturer's instructions. Briefly, cells were washed with ice-cold PBS harvested and homogenized in 1 ml of Trizol by pipetting vigorously. After addition of 200 µl of chloroform the samples were vortexed, incubated for 2 min at room temperature and centrifuged at 12,000×g, for 15 min, at 4ºC. The aqueous phase containing RNA was transferred to a new tube and RNA precipitated with 500 µl of isopropanol for at least 10 min at room temperature. Following a 10 min centrifugation at 12,000g, the pellet was washed with 1 ml 75% ethanol and resuspended in 100 µl 60 ºC heated RNA Storage Solution (Ambion, Foster City, CA, USA) . The RNA concentration was determined by OD260 measurement using a Nanodrop spectrophotometer (Wilmington, DE, USA) and quality was inspected for absence of degradation or genomic DNA contamination, using the Experion RNA StdSens Chips in the Experion™ automated microfluidic electrophoresis system (BioRad Hercules, CA, USA). RNA was stored at -80ºC until use.

Real-time RT-PCR

One microgram of total RNA was reverse transcribed using the iScript Select cDNA Synthesis Kit. Briefly, 2 µl of random primers and the necessary volume of RNase-free water to complete 15 µl, were added to each RNA sample. The samples were heated at 65 ºC, for 5 mim, and snap-chilled on ice for 1 min. After this, 5µl of a Master Mix containing 1 µl of iScript reverse transcriptase and 4 µl of 5x Reaction Buffer were added to each sample. A protocol for cDNA synthesis was run on all samples (5 min at 25 ºC, 30 min at 42 ºC, 5 min at 85ºC and then put on hold at 4 ºC). After the cDNA synthesis, the samples were diluted with RNase-free water up to a volume of 100 µl. Real-time PCR was performed in a 20 µl volume containing 5 µl cDNA (50 ng), 10 µl 2x Syber Green Supermix, 2 µl of each primer (250 nM) and 1 µl H_2O PCR grade. Samples were denatured at 95ºC during 3 min. Subsequently, 40 cycles were run for 10 sec at 95 ºC for denaturation, 30 sec at the appropriate annealing temperature and 30 sec at 72 ºC for elongation. Real-time RT-PCR reactions were run in duplicate for each sample on a Bio-Rad My Cycler iQ5. Primers were designed using Beacon Designer® Software v7.2, from Premier Biosoft International and thoroughly tested. Primer sequences are given in Table 8.

Table 8: Oligonucleotide primer pairs used for real-time RT- PCR.

PRIMER	5'-3' SEQUENCE F: FORWARD; R; REVERSE	REFSEQ ID
HPRT1	F: GTTGAAGATATAATTGACACTG R: GGCATATCCAACAACAAAC	NM_013556
IL-1 B	F: ACCTGTCCTGTGTAATGAAAG R: GCTTGTGCTCTGCTTGTG	NM_008361
INOS	F: GCTGTTAGAGACACTTCTGAG R: CACTTTGGTAGGATTTGACTTTG	NM_010927

Amplification reactions were monitored using a SYBR-Green assay. Gene expression changes were analyzed using the built-in iQ5 Optical system software v2. The software enables analyzing the results with the Pfaffl method [304], a variation of ΔΔCT method corrected for gene-specific efficiencies, and to report gene expression changes as relative fold changes compared to control samples. The results were normalized using a reference gene, *HPRT-1*, determined with Genex® software (MultiD Analyses AB) as the most stable for the treatment conditions used.

Western Blot

Total cell lysates were prepared using the RIPA buffer [50 mM Tris‑HCl (pH 8.0), 1% Nonidet P-40, 150 mM NaCl, 0.5% sodium deoxycholate, 0.1% SDS and 2 mM EDTA] freshly supplemented with 1 mM DTT, protease and phosphatase inhibitor cocktails. Cytoplasmic and nuclear extracts were obtained by a commercial nuclear extract kit (Active Motif, Rixensart, Belgium), according to the manufactor instructions. Protein concentration of cell lysates was determined by the bicinchoninic acid protein assay. Cell lysates were denaturated at 95 ºC, for 10 min, in sample buffer [0.125 mM Tris (pH 6.8), 2% (w/v) SDS, 100 mM DTT, 10% glycerol and bromophenol blue].

Cell lysates were subjected to SDS-polyacrylamide gel electrophoresis transferred to polyvinylidene fluoride membranes and specific antibodies against phospho- or total forms of ERK1/2, JNK, p38 MAPKs and against NF-$_k$B p65 were used. The immune complexes were detected using the enhanced chemifluorescence reagent on the Typhoon FLA 9000 (GE Healthcare, Chalfont St. Giles, UK) and analyzed with the software ImageQuant TL® (GE Healthcare, Chalfont St. Giles, UK). To demonstrate equivalent protein loading, membranes were stripped and reprobed with antibodies against actin or lamin.

Statistical analysis

The results were expressed as means and standard error means (mean±SD) for each experimental group. To obtain the correlations and similarities between groups a 1-way ANOVA independent-measures test followed by the Dunnett's test was used and differences were considered significant at $p < 0.05$. Graph pad (version 6.0) was used for all comparisons.

7.4 Results

7.4.1 PLPS and oxPLPS do not modulate the inflammatory status of macrophages

Production of NO by RAW 264.7 macrophages incubated with PLPS and oxPLPS was evaluated and no significant differences were observed between samples and control (unstimulated cells) (Figure 48A). NO is produced under inflammatory conditions by inducible NO synthase (*Nos2 or iNos*) in activated inflammatory cells, including macrophages. Therefore, we analyzed the effects of PLPS and oxPLPS on the expression levels of *iNos.* The results show that oxPLPS did not significantly affected ($p>0.05$) the expression of *iNos.* In contrast, PLPS slightly induced transcription of this gene ($p<0.05$) (Figure 48B) which, however, is not reflected in a significant variation in NO production (Figure 48A). Overall oxPLPS and PLPS did not show significant pro inflammatory properties in macrophages, in the conditions tested in this study.

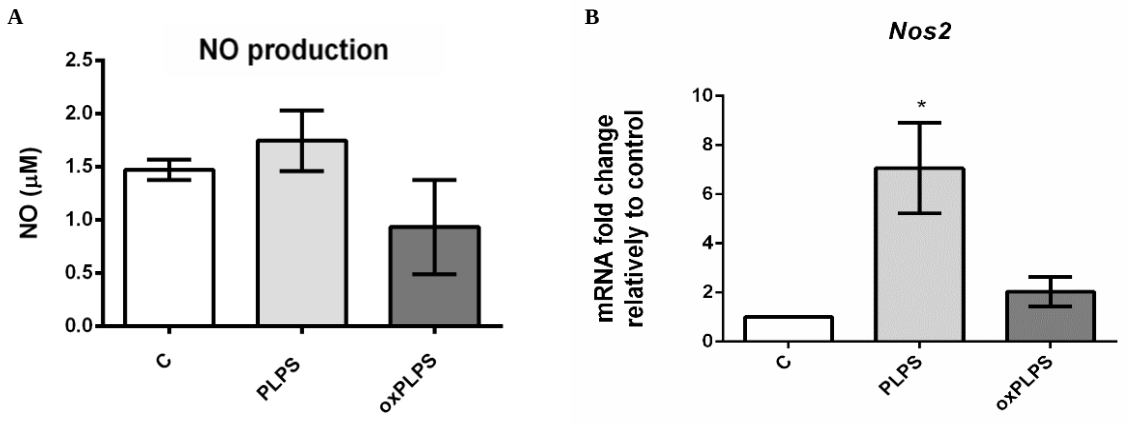

Figure 48: Effect of PLPS and oxPLPS on NO production and *iNos* gene expression in macrophages. RAW 264.7 macrophages were maintained in culture medium (control) or treated either with non- and oxidized PLPS (30 µg/mL) for 24h. (A) Nitrite levels in the culture supernatants were evaluated by the Griess reaction as described in material and methods. Nitrite

concentration was determined from a sodium nitrite standard curve and the results are expressed as concentration (μM) of nitrite in culture medium. Each value represents the mean±SD from at least 3 experiments. (B) The total RNA was extracted and retro-transcribed as described in the material and methods. The mRNA levels of *iNos* gene are depicted as normalized fold expression relatively to control. The relative expression of *iNos* gene was normalized using *HPRT1* as reference gene. Each value represents the mean±SD from at least 3 experiments. (* $P<0.05$).

7.4.2 OxPLPS, but not PLPS, showed anti-inflammatory properties in LPS-triggered activation of macrophages

Macrophages were incubated with PLPS and oxPLPS in the presence of the TLR4 agonist and pro-inflammatory agent LPS in order to evaluate their anti-inflammatory properties. First, the variation in NO production induced by LPS was assessed and the results obtained in this assay showed that the non-oxidized PLPS had no inhibitory effect on the LPS-evoked NO production ($p>0.05$) (Figure 49A). In contrast, oxPLPS inhibits NO production triggered by LPS in a dose-dependent way ($p<0.01$ for 15 μg/mL and $p<0.0001$ for 30, 45 and 60 μg/mL of oxPLPS) (Figure 49A and 49B). In a second approach we analyzed the effects of PLPS and oxPLPS on the expression of *iNos* gene (Figure 49C) induced by LPS. Data showed a decrease in *iNos* expression in macrophages treated with oxPLPS (30 μg/mL) ($p<0.05$), which corroborates the results previously obtained for NO quantification (Figure 49A). Interestingly, Arg-1, which participates in the regulation of *iNos* activity by competing for the common substrate L-arginine, is overexpressed in macrophages treated with oxPLPS ($p<0.05$) but not in macrophages treated with PLPS ($p>0.05$) (Figure 49D).

Additionally the analysis of the *IL1β* gene expression was also performed and no significant changes were induced by either PLPS or oxPLPS (Figure 49E) in the absence of LPS ($p>0.05$), confirming the lack of intrinsic pro-inflammatory activity of these lipids. LPS strongly induces the expression of *IL1β* and, when cells were simultaneously exposed to LPS and oxPLPS, LPS-induced expression of *IL1β* was significantly decreased ($p<0.05$) while no significant alterations were observed when PLPS was used ($p>0.05$) (Figure 49F). These results confirm the anti-inflammatory properties of oxPLPS, previously revealed by the reduction of LPS-induced NO production (Figure 49A and 49B).

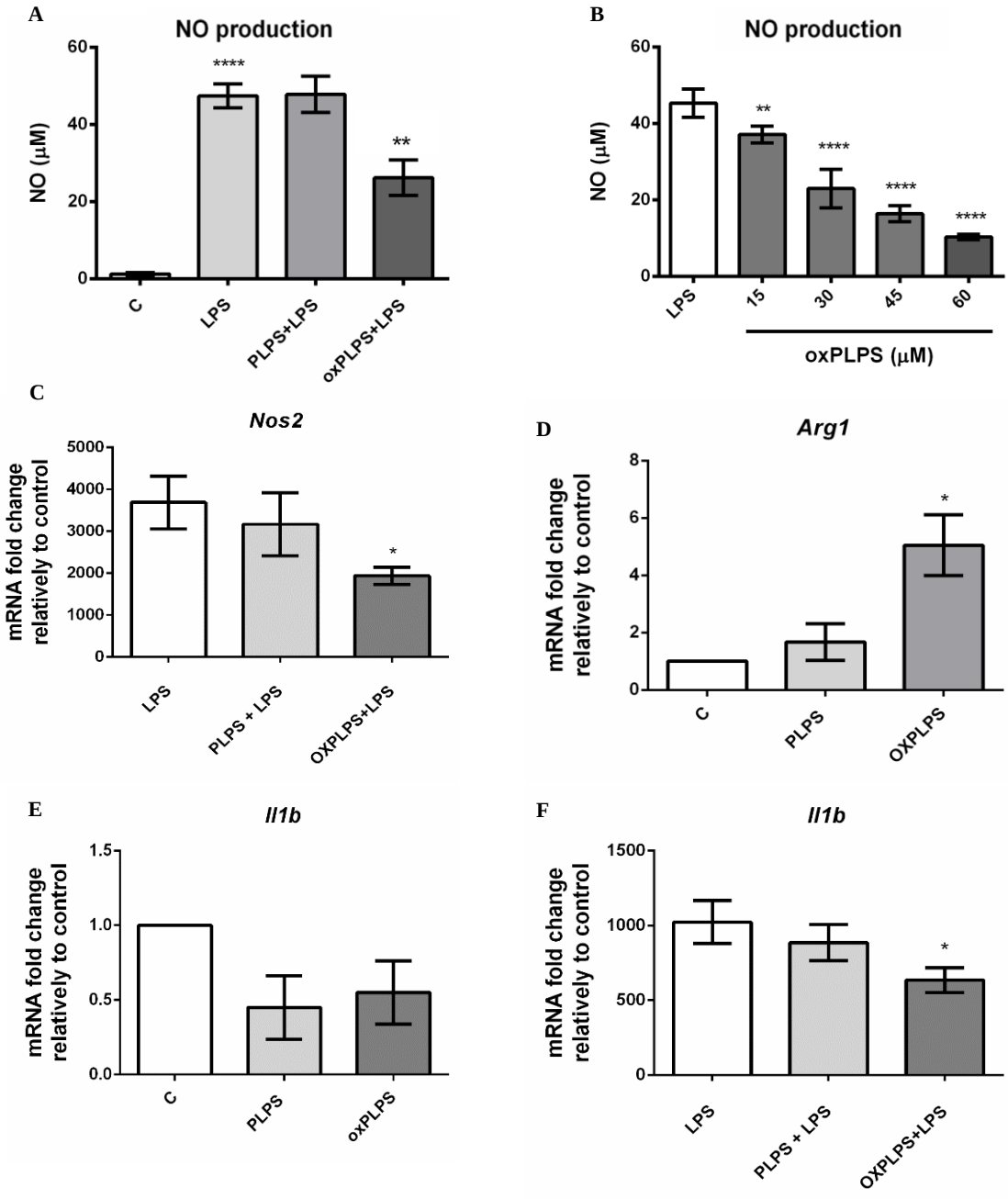

Figure 49: Influence of PLPS and oxPLPS on LPS-induced macrophage pro-inflammatory status. Raw 264.7 cells were incubated with culture medium alone (Control; C), with LPS (1µg/mL) and with non-oxidized (PLPS) or oxidized PLPS (oxPLPS; 30µg/mL except in (B) where concentrations are indicated) for 24h (A and B). Nitrite levels in the culture supernatants were evaluated by the Griess reaction as described in material and methods. Nitrite concentration was determined from a sodium nitrite standard curve and the results are expressed as concentration (µM) of nitrite in culture medium. The total RNA was extracted and retro-transcribed as described in the material and methods. The mRNA levels of *iNos* (C) *Arg1* (D) and *IL1β* (E, F) genes are

depicted as normalized fold expression relatively to control. The relative expression of the indicated genes was normalized using *HPRT1* as reference gene. Each value represents the mean±SD from at least 3 experiments. (* $P<0.05$, ** $P<0.01$, *** $P<0.001$, **** $P<0.0001$)

7.4.3 OxPLPS but not PLPS inhibited JNK phosphorylation triggered by LPS in macrophages

The expression of pro-inflammatory molecules is tightly regulated by several transcription factors and signaling pathways. Among these pathways, mitogen- activated proteins kinases (MAPKs) and the transcription factor NF-κB are signaling molecules that play critical roles in the regulation of cell survival/apoptosis and cellular response to cytokines and stress. To elucidate the mechanisms underlying inhibition of LPS-induced macrophages activation upon oxPLPS stimulation, the effect on the activation of the pro-inflammatory signaling pathways MAPKs and NF-κB were examined. Three groups of MAPKs were studied: extracellular signal-regulated kinases (ERK), c-Jun NH_2-terminal kinase (JNK) and p38 MAPK.

In macrophages stimulated with oxPLPS and PLPS in the absence of LPS no activation (evaluated by protein phosphorylation) was detected for ERK1/2, JNK and p38 MAPK relatively to control cells ($p>0.05$) (Figure 50). Interestingly, oxPLPS partially inhibited JNK p46 and JNK p54 ($p<0.01$) activation triggered by LPS, but no inhibition was detected for ERK1/2 or p38 MAPKs ($p>0.05$). No significant effect was observed in PLPS-treated cells ($p>0.05$) (Figure 51).

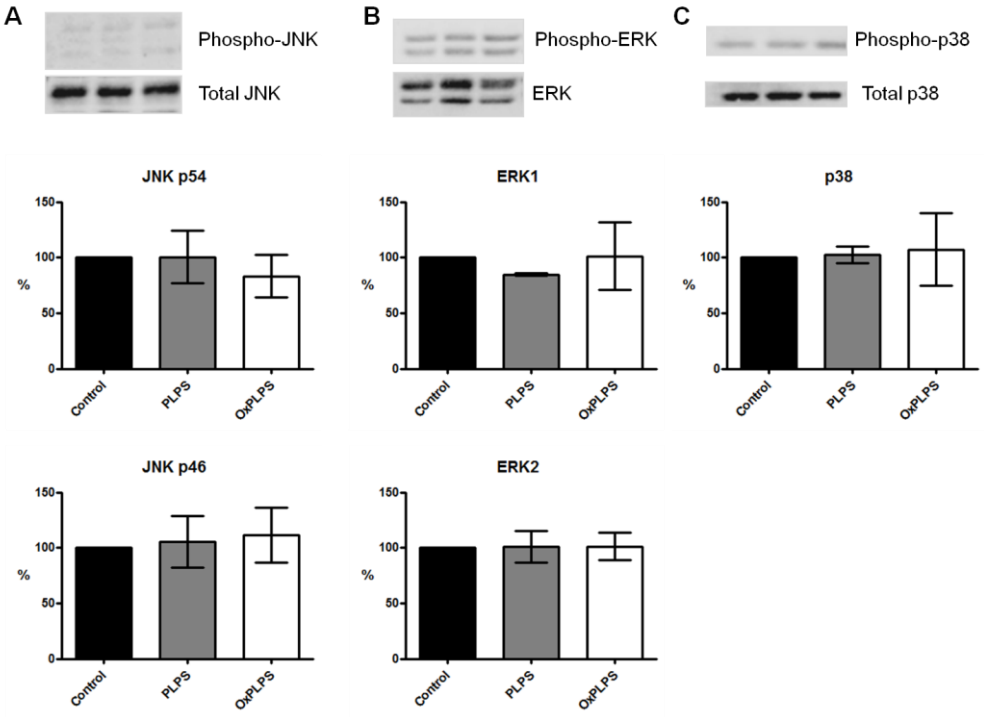

Figure 50: Influence of PLPS and oxPLPS on MAPKs activation in macrophages. Total cell extracts were analyzed by Western blot using antibodies against (A) phospho-JNK p54/p46, (B) phospho-ERK 1/2 and (C) p38MAPK. The results are expressed as percentage of immunoreactivity in control cells and protein loading was controlled using antibodies against total (A) JNK, (B) ERK and (C) p38 MAPKs. A representative blot and the mean±SD from at least 3 experiments are shown.

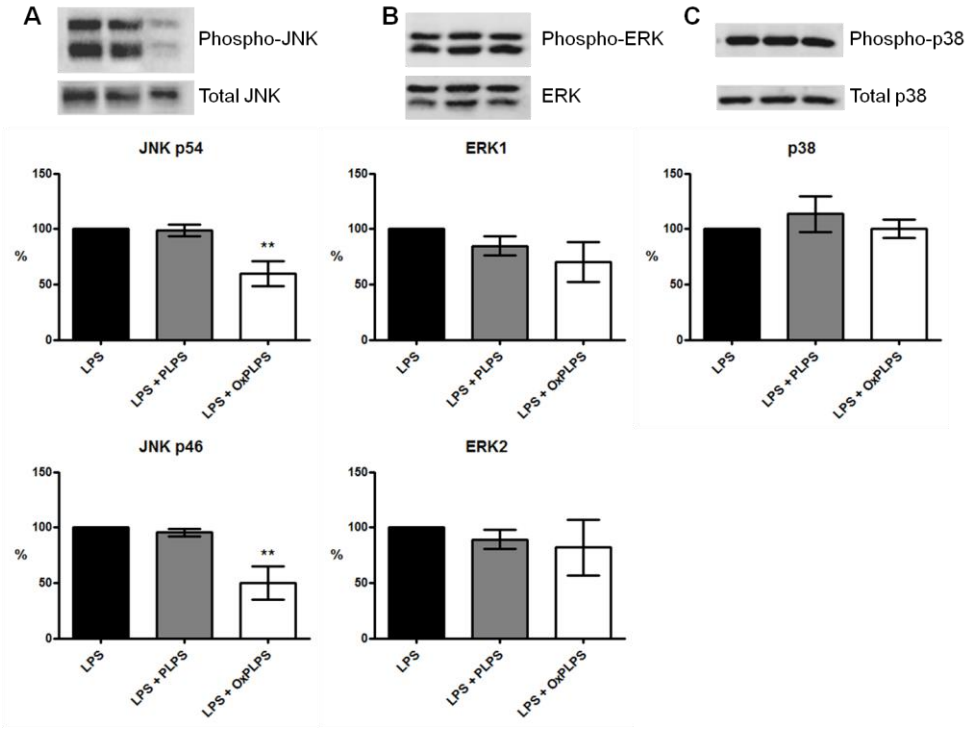

Figure 51: Influence of PLPS and oxPLPS on MAPKs activation triggered by LPS in macrophages. Total cell extracts were analyzed by Western blot using antibodies against (A) phospho-JNK p54/p46, (B) phospho-ERK 1/2 and (C) p38MAPK. The results are expressed as percentage of immunoreactivity in LPS-treated cells and protein loading was controlled using antibodies against total (A) JNK, (B) ERK and (C) p38 MAPKs. A representative blot and the mean±SD from at least 3 experiments are shown. $^{**}P<0.01$

7.4.4 Inhibition of p65 nuclear translocation by oxPLPS on LPS-stimulated macrophages

The NF-κB transcription factor regulates the expression of many genes involved in immune and inflammatory responses, including *iNos*. To elucidate whether oxPLPS and PLPS modulate the nuclear translocation of NF-κB p65 in macrophages treated in the absence or in the presence of LPS Western blot analysis was performed to quantify the cytosolic and nuclear p65. In macrophages stimulated with oxPLPS and PLPS in the absence of LPS no effect was observed in the protein levels of both cytosolic and nuclear p65 relatively to control ($p>0.05$) (Figure 52A). In contrast, oxPLPS increases the levels of cytosolic p65 in macrophages treated concomitantly with LPS ($p<0.05$) (Figure 52A). As opposed, no effect was observed in cytosolic p65 after macrophages treatment with PLPS ($p>0.05$). Concerning nuclear p65, no significant effect was observed in both PLPS- and OxPLPS treated cells ($p>0.05$), although in the presence of oxPLPS nuclear levels of p65 are slightly decreased relatively to LPS-stimulated cells. Taken together these data suggest that oxPLPS selectively decreases the nuclear translocation of p65 NF-κB.

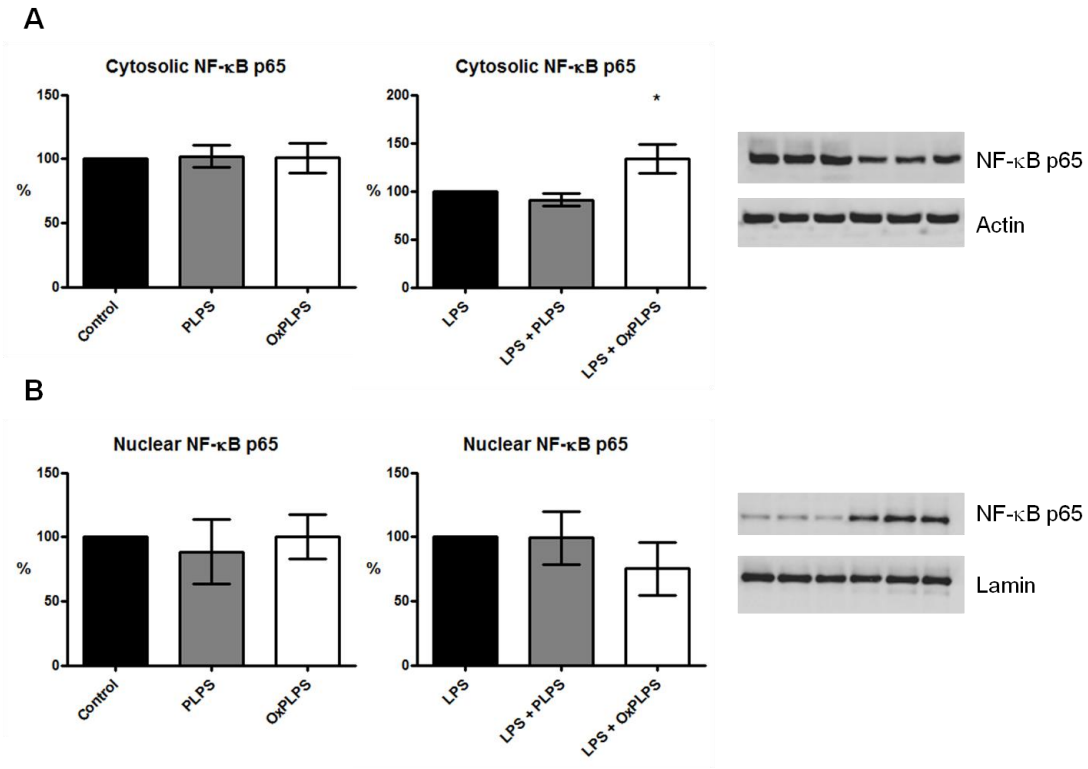

Figure 52: Effect of PLPS and oxPLPS on cytosolic (A) and nuclear (B) p65 protein levels of macrophages cultured in the absence (left) or in the presence (right) of LPS. The migration of NF-κB p65 to the nucleus was analyzed using an antibody against NF-κB p65 in cytoplasmic (A) and nuclear (B) protein extracts. Equal protein loading was controlled using antibodies against actin and lamin in cytosolic and nuclear extracts respectively. A representative blot and the mean±SD from at least 3 experiments are shown. * $P<0.05$.

7.5 Discussion

Cellular apoptosis and subsequent 'silent' removal represents an important check-point for the resolution of inflammation. Failure in apoptotic cells clearance resulting in secondary necrosis-driven tissue damage has been implicated in conditions of chronic inflammation and autoimmunity. Apoptotic cells undergo profound biophysical changes, such as PS externalization, that warrant their efficient recognition and uptake by macrophages before fading to secondary necrosis. However, the nature of the “eat-me” signals and receptors that lead to cell recognition, engulfment and concomitantly silence a pro-inflammatory pathological condition are still under discussion. In this study, we evaluated the influence of PS oxidation products in the modulation of pro-inflammatory events in macrophages. Therefore, we have compared the effects of PLPS and oxPLPS on LPS-stimulated RAW 264.7 macrophages. We found that both PLPS and oxPLPS are

deprived of intrinsic pro-inflammatory activity. Exquisitely, oxPLPS may contribute to restrain inflammatory events in macrophages during apoptotic cell recognition and engulfment. More specifically oxPLPS, in contrast to PLPS, inhibits NO production and *iNos* expression in LPS-stimulated macrophages (Figure 49A, B and C). The results obtained from *IL1β* analysis also confirm the absence of activated (M1) macrophages, (Figure 49F) thus highlighting a putative role of oxPLPS in tempering inflammation. Corroborating these results, we also disclosed that oxPLPS, but not native PLPS, mitigate pro-inflammatory signaling in macrophages, thus reinforcing the contribution of oxPLPS to containment of inflammation during apoptosis. The results obtained in this work for non-oxidized PLPS are somewhat in disagreement with previous published work that ascribed to PS an inhibitory role on LPS-induced NO production [315,316,317]. However, Greenberg *et a*l also reported that oxPS, but not non-oxidized PS, participates in macrophages recognition of apoptotic cells via CD36 [104]. These contradictory results may be partially explained by different experimental conditions used, namely the concentrations of PS utilized as well as its oxidation levels are certainly important. The dissimilar performance of non-oxidized versus oxPLs species has also been observed for PC species. Friedl and co-workers, demonstrated that oxPC, but not native PC, inhibits iNOS expression in macrophages [318].

It is well-known that oxidation of phospholipids can generate a plethora of oxidation products with different structural features and also different properties [22,114]. PS, upon oxidation, can also generate not only distinct products with oxygenated fatty acyl chain, but also products resulting from PS polar head oxidation [168]. Recently, it was reported that several isolated oxidation products of 1-palmitoyl-2-oleoyl-PS did not induce cytokine production in monocytes, while PS oxidation products with a terminal hydroperoxyacetaldehyde in the polar head showed pro-inflammatory properties, promoting an increase in pro-inflammatory cytokines (IL-1β, IL-6, IL-8, MIP-1β and TNF-α) production [242]. Bochkov and colleagues showed the crucial role of oxidized phospholipids as biological active compounds (as reviewed in [114]). Seyerl *et al* have also verified that oxidized phospholipids, including PS, but not their native forms, are specific regulators of T cell activation [319]. Furthermore, it was also demonstrated that the polar groups of oxidized phospholipids affected the dysfunction of endothelial cells induced by LPS *in vitro* and *in vivo*, leading to attenuated RHO GTPases activation [320]. Further

studies taking into account the oxidation of the polar group are highly needed and will be of outmost importance to clarify their role in the inflammatory response modulation evoked during apoptotic cell recognition and engulfment.

The modulation of intracellular signaling pathways by PLPS and oxPLPS was also examined. The inhibitory effect of oxPLPS in NO production can be partially associated with NF-κB and MAPKs modulation since activation of macrophages by LPS involves the simultaneous activation of all classes of MAPK (JNK, ERK and p38) and NF-κB. These findings suggest that down-regulation of *iNos* and *IL1β* genes results from an inhibitory effect of oxPLPS on NF-κB signaling pathway, through an impairment of p65 translocation into the nucleus (Figure 52). Additionally, JNK also assumes a protagonist role in the anti-inflammatory potential of oxPLPS (Figure 51). Indeed, it is well known that iNOS expression is controlled by several signaling pathways, among them NF-kB and MAPK [321,322].

In conclusion, and in addition to their role in the promotion of phagocytosis of apoptotic cells by macrophages, oxPLPS appears to exert signalling characteristics important for tempering inflammation. Given that "silent" clearance of apoptotic cells is critical for restoration of tissue function, we hypothesize that oxPLPS play a key role in promoting timely resolution of inflammation. However, the biological relevance of these findings needs to be deeply explored and validated in *in vivo* models.

Chapter VIII

General Conclusions

Phospholipids are structural components in cell membranes and lipoproteins and have been recognized as important signalling molecules, crucial for homeostasis and also associated with the development of diseases. Among phospholipids, phosphatidylserines, which are ubiquitously distributed in all cells, although in minor abundance, participate in important signalling events, including in blood clotting, apoptosis and in tumours. Some evidences show that oxidized PS molecular species are more active than non-oxidized PS species, as the case of apoptosis [104].

The present work was conducted to address the problem of the identification of the products generated during oxidation PS using different oxidation systems, namely the hydroxyl radical and a radical generator, the AAPH. It is known from studies of other phospholipid classes, that different oxidation systems can generate different oxidation products, that can have distinct biological significance and that possess different identification problems. In this work, we have studied several model PS species bearing different combinations of fatty acyl chains, namely with palmitic acid in *sn*-1 and *sn*-2 (DPPS) and with palmitic acid linked to *sn*-1 and unsaturated fatty acids, oleic acid, linoleic acid and arachidonic acid linked to *sn*-2 designated respectively as POPS, PLPS and PAPS. The different PS model compounds were used to evaluate the influence of fatty acid composition in the oxidation process at the molecular level. New PS oxidation products were identified during oxidation of each PS molecular species and these species were characterized by off-line TLC-MS and on-line LC-MS and MS/MS. The identified PS oxidation products included long chain products, which preserved the phospholipid skeleton (hydroxy, peroxy, and keto derivatives). These species were identified during oxidation of POPS, PLPS and PAPS. Short chain products, formed by cleavage of the unsaturated fatty acyl chains, giving rise to shortened fatty acyl chain with a terminal aldehyde or carboxylic groups, were only identified during oxidation of PLPS and PAPS. Products with cleavage in the polar head group were also identified during oxidation of DPPS, POPS, PLPS and PAPS. The glycerophosphoacetic acid derivatives (GPAA) products, resulting from oxidative cleavage of the serine polar head group, were identified for the first time in the present work, as well as other products with polar head groups, assigned as acetamide and hydroperoxyacetaldehyde terminal, observed in the DPPS and POPS. The results of our work allowed identifying for the first time new oxidation products of PS, due to oxidative cleaved of serine moiety.

The hydroxyl radical was used also to induce the oxidation of glycated POPS and PAPS, mimicking the oxidation in hyperglycemia conditions. The results obtained revealed that glycated PS oxidized earlier than non glycated PS, leading to more abundant oxidation products. The glycoxidation products observed, when glycated PAPS was used as a model compound, included products from oxidation in fatty acyl chain and products with a terminal formamide in polar head group formed from a cleavage in the glucose moiety (cleavage in C1-C2 bond). Interestingly, in these studies it was also possible to identify molecular species arising from oxidative cleavage in glycated polar head and also new products arising from oxidative cleavage of the glucose moiety between C1-C2 bond with formation of formamide terminal. Products arising from oxidative cleavage of the glucose moiety between the C2-C3 bond with acetic acid attached to amine group and between the C3-C4 bond with formation of hydroxypropanone terminal in polar head group were also identified. The identification of these PS-AGES arising from glycated POPS oxidation gave new insights on the glycation PS mechanisms, opening new perspectives for the detection of these products in complex biological matrices. PS is an amino phospholipid, similarly to PE, and thus most probably with similar propensity to be glycated: However, although glycated PE has been identified and quantified in plasma of diabetic patients [24], glycated PS was only reported to be formed *in vitro*, but it has never been identified *in vivo* [27]. This fact may be to the result of the *in vivo* low abundance of these species or due to their easy degradation under oxidative conditions. Glycation of biomolecules is a well-known reaction that occurs *in vivo*, particularly in hyperglycemia. Glycation of proteins has been extensively studied and is recognized as an important event that occurs in diabetes mellitus patients [230]. It is also recognized that glycated biomolecules and their degradation products trigger an increase of oxidative stress and an inflammatory response, which is responsible for different diabetic complications, such as micro and macrovascular complications, atherosclerosis and others. In spite of the recognition of the importance of protein glycation as important biomarkers of uncontrolled hyperglycemia, glycation of other biomolecules, including phosphatidylserines, is still an unexplored field. Since diabetes is associated with an increase of the oxidative stress status, the modifications occurring in glycated PS species were assessed in this work by LC-MS and MS/MS, but further work is needed to understand the biological effects of combined glycation and oxidative induced PS modifications.

PS is present in biological matrices in low amounts comparing with other phospholipid classes such as PC and PE. In oxidative stress conditions, only a small percentage of PS is oxidized and several products are generated during this oxidative process, difficulting their identification. Most of the PS oxidation products already identified in complex samples were hydroperoxide (PS-OOH) or hydroxide (PS-OH) derivatives, since they are the primary and the most abundant products formed. However, more sensitive approaches are required to overcome the challenge of the detection and quantification of PS oxidation products in biological systems, suggesting that targeted analytical approaches, based on mass spectrometry, are needed. The fragmentation pathways identified in this work, which are specific of the PS oxidation products with modified in serine polar head (the GPAA derivatives), were used to develop a target lipidomic strategies to screen the formation of these species in cells after an oxidative stimuli. The approach that we have developed involved the neutral loss and precursor ion scanning modes, which was optimized previously with oxidized POPS. Keratinocytes were selected as a cell model, since externalized PS and oxidation of fatty acyl chains in PS were previously identified in these cells during oxidative stress [55, 243]. Using this targeted lipidomic approach, GPAA derivatives were successfully detected from total lipid extracts. The positive identification of serine head oxidation products in cells under controlled oxidative conditions opens new perspectives and justifies further studies in other cellular systems in order to understand fully the role of PS polar head group oxidation in cell homeostasis and disease.

The extracellular exposure of PS has been associated with several physiopathological situations, including apoptosis and in tumor cells. The biological significance of the PS externalization in tumor cells has not been fully elucidated, since tumor cells are not recognized by macrophages receptors. Thus, this process of externalization does not seem to promote any signaling event, at least in order to facilitate the elimination of these cells. Several reports have shown the increased exposure of PS on the outer leaflet of the plasma membrane in several tumor cell lines such as melanoma and melanoma metastases, gastric carcinoma, leukemia, tumor blood vessels [62, 66-69]. PS externalization seems to be correlated with malignancy, suggesting that PS can be a uniform marker of tumor cells and metastases and a potential target for the further development of cationic antitumor peptide drugs [62, 65, 72]. In this work, human melanoma cells were exposed to UVA radiation in

an attempt to give some insight in a possible correlation of PS, oxidation, apoptosis and tumor malignancy, since UVA exposition has been considered to be associated with the onset and progression of the disease. Interestingly, the results from the lipidomic analysis showed only a few modifications in PS species, like the decrease of PS-18:0/18:1 in the moment of irradiation, and no oxidation product were detected. The results also showed the occurrence of the remodeling of the phospholipid profile, confirmed with fatty acids analysis by GC-MS. The changes were correlated with lipogenesis and *de novo* synthesis of saturated and mono-saturated fatty acids, presumably to promote the cell survival. In fact, the increase of the ratio of mono-unsaturated fatty acid/polyunsaturated fatty acid makes the phospholipid membrane less susceptible to be oxidized. The absence of cleaved caspase-3 after 2h and 24h of re-incubation correlates with the impairment of apoptosis. The observed alterations in the lipid metabolism may be correlated with malignant transformations associated with cancer development and progression. Thus, lipids might constitute challenging therapeutic targets for the treatment of highly resistant-melanoma.

The biological effects of the PLPS and oxPLPS were evaluated in Raw 264.7, a mouse leukaemic monocyte macrophage cell line; the results showed that oxPS but not native PS has anti-inflammatory activity due to its ability to inhibit the LPS-induced NO production and *Nos2* and *il1b* gene transcription. At the molecular level, this was shown to be the result of attenuation of LPS-induced JNK phosphorylation and p65 NF-$_k$B nuclear translocation. These data suggest that oxPLPS, but not native PLPS, mitigates pro-inflammatory signaling in macrophages, contributing to containment of inflammation during apoptotic cell engulfment.

The results described in this work gave new insights on the modifications of PS and showed the importance of oxPS versus non-oxidized PS in response of macrophages to pro-inflammatory stimulus. Nonetheless, for more detailed understanding of the mechanisms that rule the safe removal of apoptotic cells, which might be significant for the design of novel therapeutic strategies, it is important to determine whether the exposure on the surface of apoptotic cells of different oxidation products of PS differentially modulates the functional responses of macrophages. Despite the contribution of this work for the identification of oxidation products of PS, this field of research is far from being

completely explored, although it is essential for the understanding of the relation between the PS oxidation products formed and the specific biological activity.

Chapter IX

References

[1] K. Athenstaedt, G. Daum, Phosphatidic acid, a key intermediate in lipid metabolism, European Journal of Biochemistry 266 (1999) 1-16.
[2] L. Chernomordik, M.M. Kozlov, J. Zimmerberg, Lipids in biological membrane-fusion, Journal of Membrane Biology 146 (1995) 1-14.
[3] C.P. Reynolds, B.J. Maurer, R.N. Kolesnick, Ceramide synthesis and metabolism as a target for cancer therapy, Cancer Letters 206 (2004) 169-180.
[4] W.H. Cho, R.V. Stahelin, Membrane-protein interactions in cell signaling and membrane trafficking, Annual Review of Biophysics and Biomolecular Structure, 2005, pp. 119-151.
[5] M.R. Wenk, The emerging field of lipidomics, Nature Reviews Drug Discovery 4 (2005) 594-610.
[6] A.D. Watson, Lipidomics: a global approach to lipid analysis in biological systems, Journal of Lipid Research 47 (2006) 2101-2111.
[7] M. Pulfer, R.C. Murphy, Electrospray mass spectrometry of phospholipids, Mass Spectrometry Reviews 22 (2003) 332-364.
[8] M. White, Mediators of inflammation and the inflammatory process, Journal of Allergy and Clinical Immunology 103 (1999) S378-S381.
[9] E.M. Hein, L.M. Blank, J. Heyland, J.I. Baumbach, A. Schmid, H. Hayen, Glycerophospholipid profiling by high-performance liquid chromatography/mass spectrometry using exact mass measurements and multi-stage mass spectrometric fragmentation experiments in parallel, Rapid Communications in Mass Spectrometry 23 (2009) 1636-1646.
[10] C.J. DeLong, P.R.S. Baker, M. Samuel, Z. Cui, M.J. Thomas, Molecular species composition of rat liver phospholipids by ESI-MS/MS: the effect of chromatography, Journal of Lipid Research 42 (2001) 1959-1968.
[11] B. Fuchs, J. Schiller, Application of MALDI-TOF mass spectrometry in lipidomics, European Journal of Lipid Science and Technology 111 (2009) 83-98.
[12] U. Loizides-Mangold, On the future of mass-spectrometry-based lipidomics, FEBS Journal 280 (2013) 2817-2829.
[13] M. Ramirez, L. Amate, A. Gil, Absorption and distribution of dietary fatty acids from different sources, Early Human Development 65 (2001) S95-S101.
[14] W.W. Christie, Phosphatidylcholine and related lipids, http://lipidlibrary.aocs.org/Lipids/pc/index.htm, last update 2014.
[15] W.W. Christie, Phosphatidylethanolamine and related lipids, http://lipidlibrary.aocs.org/Lipids/pe/index.htm, last updated 2014.
[16] W.W. Christie, Phosphatidylinositol and related lipids, http://lipidlibrary.aocs.org/Lipids/pi/index.htm, last updated 2014.
[17] W.W. Christie, Cadiolipin http://lipidlibrary.aocs.org/Lipids/dpg/index.htm, last updated 2014.
[18] M. Pennings, I. Meurs, D. Ye, R. Out, M. Hoekstra, T.J.C. Van Berkel, M.V. Eck, Regulation of cholesterol homeostasis in macrophages and consequences for atherosclerotic lesion development, Febs Letters 580 (2006) 5588-5596.
[19] A.D. Postle, Phospholipid lipidomics in health and disease, European Journal of Lipid Science and Technology 111 (2009) 2-13.
[20] A. Reis, P. Domingues, A. J. V. Ferrer-Correia, M.R.M. Domingues, Tandem mass spectrometry of intact oxidation products of diacylphosphatidylcholines: evidence

for the occurrence of the oxidation of the phosphocholine head and differentiation of isomers, Journal of mass spectrometry 39 (2004) 1513-1522.
[21] M. Mapstone, A.K. Cheema, M.S. Fiandaca, X. Zhong, T.R. Mhyre, L.H. Macarthur, W.J. Hall, S.G. Fisher, D.R. Peterson, J.M. Haley, M.D. Nazar, S.A. Rich, D.J. Berlau, C.B. Peltz, M.T. Tan, C.H. Kawas, H.J. Federoff, Plasma phospholipids identify antecedent memory impairment in older adults, Nature Medicine 20 (2014) 415-418.
[22] E. Niki, Lipid peroxidation: Physiological levels and dual biological effects, Free Radical Biology and Medicine 47 (2009) 469-484.
[23] G.O. Fruhwirth, A. Loidl, A. Hermetter, Oxidized phospholipids: From molecular properties to disease, Biochimica et Biophysica Acta (BBA) - Molecular Basis of Disease 1772 (2007) 718-736.
[24] C.M. Breitling-Utzmann, A. Unger, D.A. Friedl, M.O. Lederer, Identification and Quantification of Phosphatidylethanolamine-Derived Glucosylamines and Aminoketoses from Human Erythrocytes—Influence of Glycation Products on Lipid Peroxidation, Archives of Biochemistry and Biophysics 391 (2001) 245-254.
[25] S. Lertsiri, M. Shiraishi, T. Miyazawa, Identification of deoxy-D-fructosyl phosphatidylethanolamine as a non-enzymic glycation product of phosphatidylethanolamine and its occurrence in human blood plasma and red blood cells, Bioscience, biotechnology, and biochemistry 62 (1998) 893-901.
[26] K. Nakagawa, J.H. Oak, O. Higuchi, T. Tsuzuki, S. Oikawa, H. Otani, M. Mune, H. Cai, T. Miyazawa, Ion-trap tandem mass spectrometric analysis of Amadori-glycated phosphatidylethanolamine in human plasma with or without diabetes, Journal of Lipid Research 46 (2005) 2514-2524.
[27] A. Ravandi, A. Kuksis, L. Marai, J.J. Myher, G. Steiner, G. Lewisa, H. Kamido, Isolation and identification of glycated aminophospholipids from red cells and plasma of diabetic blood, Febs Letters 381 (1996) 77-81.
[28] A. Ravandi, A. Kuksis, N.A. Shaikh, Glucosylated Glycerophosphoethanolamines are the Major LDL Glycation Products and Increase LDL Susceptibility to Oxidation, Arteriosclerosis, Thrombosis, and Vascular Biology 20 (2000) 467-477.
[29] P. Sookwong, K. Nakagawa, I. Fujita, N. Shoji, T. Miyazawa, Amadori-Glycated Phosphatidylethanolamine, a Potential Marker for Hyperglycemia, in Streptozotocin-Induced Diabetic Rats, Lipids 46 (2011) 943-952.
[30] K. Suzuki, K. Nakagawa, T. Miyazawa, Augmentation of blood lipid glycation and lipid oxidation in diabetic patients, Clinical Chemistry and Laboratory Medicine 52 (2014) 47-52.
[31] V.E. Kagan, G.G. Borisenko, Y.Y. Tyurina, V.A. Tyurin, J.F. Jiang, A.I. Potapovich, V. Kini, A.A. Amoscato, Y. Fujii, Oxidative lipidomics of apoptosis: Redox catalytic interactions of cytochrome C with cardiolipin and phosphatidylserine, Free Radical Biology and Medicine 37 (2004) 1963-1985.
[32] J. Folch, Brain cephalin, a mixture of phosphatides. Separation from it of phosphatidyl serine, phosphatidyl ethanolamine, and a fraction containing an inositol phosphatide, Journal of Biological Chemistry 146 (1942) 35-44.
[33] J. Folch, The chemical structure of phosphatidylserine, Journal of Biological Chemistry 174 (1948) 439-450.
[34] E. Baer, J. Maurukas, Phosphatidylserine, Journal of Biological Chemistry 212 (1955) 25-38.

[35] R.A. Chaurio, C. Janko, L.E. Munoz, B. Frey, M. Herrmann, U.S. Gaipl, Phospholipids: Key Players in Apoptosis and Immune Regulation, Molecules 14 (2009) 4892-4914.
[36] J.E. Vance, R. Steenbergen, Metabolism and functions of phosphatidylserine, Progress in Lipid Research 44 (2005) 207-234.
[37] Q. Zhou, J. Zhao, J.G. Stout, R.A. Luhm, T. Wiedmer, P.J. Sims, Molecular Cloning of Human Plasma Membrane Phospholipid Scramblase: A protein mediating transbilayer movement of plasma membrane phospholipids, Journal of Biological Chemistry 272 (1997) 18240-18244.
[38] P.A. Leventis, S. Grinstein, The Distribution and Function of Phosphatidylserine in Cellular Membranes, in: D.C.D.K.A.W.J.R. Rees (Ed.), Annual Review of Biophysics, Vol 39, 2010, pp. 407-427.
[39] J. Baumeister, T. Barthel, K.R. Geiss, M. Weiss, Influence of phosphatidylserine on cognitive performance and cortical activity after induced stress, Nutritional Neuroscience 11 (2008) 103-110.
[40] R. Wood, R.D. Harlow, Structural analyses of rat liver phosphoglycerides, Archives of Biochemistry and Biophysics 135 (1969) 272-281.
[41] H.-Y. Kim, B.X. Huang, A.A. Spector, Phosphatidylserine in the brain: Metabolism and function, Progress in Lipid Research 56 (2014) 1-18.
[42] F. Lauretani, S. Bandinelli, B. Benedetta, A. Cherubini, A.D. Iorio, A. Ble, V. Giacomini, A.M. Corsi, J.M. Guralnik, L. Ferrucci, Omega-6 and omega-3 fatty acids predict accelerated decline of peripheral nerve function in older persons, European Journal of Neurology 14 (2007) 801-808.
[43] H.-Y. Kim, Novel metabolism of docosahexaenoic acid in neural cells, Journal of Biological Chemistry 282 (2007) 18661-18665.
[44] J.E. Vance, Thematic review series: Glycerolipids. Phosphatidylserine and phosphatidylethanolamine in mammalian cells: two metabolically related aminophospholipids, Journal of Lipid Research 49 (2008) 1377-1387.
[45] R. Mozzi, S. Buratta, G. Goracci, Metabolism and functions of phosphatidylserine in mammalian brain, Neurochemical Research 28 (2003) 195-214.
[46] O. Kuge, M. Nishijima, Biosynthetic regulation and intracellular transport of phosphatidylserine in mammalian cells, Journal of Biochemistry 133 (2003) 397-403.
[47] A.K. Kimura, H.-Y. Kim, Phosphatidylserine synthase 2: high efficiency for synthesizing phosphatidylserine containing docosahexaenoic acid, Journal of Lipid Research 54 (2013) 214-222.
[48] R.F.A. Zwaal, P. Comfurius, E.M. Bevers, Surface exposure of phosphatidylserine in pathological cells, Cellular and Molecular Life Sciences 62 (2005) 971-988.
[49] T. Improta-Brears, S. Ghosh, R.M. Bell, Mutational analysis of Raf-1 cysteine rich domain: Requirement for a cluster of basic aminoacids for interaction with phosphatidylserine, Molecular and Cellular Biochemistry 198 (1999) 171-178.
[50] S. Tomiuk, M. Zumbansen, W. Stoffel, Characterization and subcellular localization of murine and human magnesium-dependent neutral sphingomyelinase, Journal of Biological Chemistry 275 (2000) 5710-5717.
[51] S. Suzuki, H. Yamatoya, M. Sakai, A. Kataoka, M. Furushiro, S. Kudo, Oral administration of soybean lecithin transphosphatidylated phosphatidylserine improves memory impairment in aged rats, The Journal of nutrition 131 (2001) 2951-2956.

[52] J. Baumeister, T. Barthel, K. Geiss, M. Weiss, Influence of phosphatidylserine on cognitive performance and cortical activity after induced stress, Nutritional neuroscience 11 (2008) 103-110.
[53] V. Krishnan, E.J. Nestler, The molecular neurobiology of depression, Nature 455 (2008) 894-902.
[54] B. Uttara, A.V. Singh, P. Zamboni, R.T. Mahajan, Oxidative Stress and Neurodegenerative Diseases: A Review of Upstream and Downstream Antioxidant Therapeutic Options, Current Neuropharmacology 7 (2009) 65-74.
[55] S. Cho, H.H. Kim, M.J. Lee, S. Lee, C.-S. Park, S.-J. Nam, J.-J. Han, J.-W. Kim, J.H. Chung, Phosphatidylserine prevents UV-induced decrease of type I procollagen and increase of MMP-1 in dermal fibroblasts and human skin in vivo, Journal of Lipid Research 49 (2008) 1235-1245.
[56] S.-H. Lee, J.-H. Yang, Y.-K. Park, J.-J. Han, G.-H. Chung, D.-H. Hahm, H.-D. Choi, Protective effect and mechanism of phosphatidylserine in UVB-induced human dermal fibroblasts, European Journal of Lipid Science and Technology 115 (2013) 783-790.
[57] E.M. Bevers, P. Comfurius, J.L.M.L. Van Rijn, H.C. Hemker, Generation of Prothrombin-Converting Activity and the Exposure of Phosphatidylserine at the Outer Surface of Platelets, European Journal of Biochemistry 122 (1982) 429-436.
[58] F. Lupu, M. Calb, A. Fixman, Alteration of phospholipid asymmetry in the membrane of spontaneously aggregated platelets in diabetes, Thrombosis Research 50 (1988) 605-616.
[59] S.T. Wahid, S.M. Marshall, T.H. Thomas, Increased Platelet and Erythrocyte External Cell Membrane Phosphatidylserine in Type 1 Diabetes and Microalbuminuria, Diabetes Care 24 (2001) 2001-2003.
[60] R.K. Wali, S. Jaffe, D. Kumar, V.K. Kalra, Alterations in organization of phospholipids in erythrocytes as factor in aherence to endothelial-cells in diabetes-mellitus, Diabetes 37 (1988) 104-111.
[61] S. Khandelwal, R.K. Saxena, A role of phosphatidylserine externalization in clearance of erythrocytes exposed to stress but not in eliminating aging populations of erythrocyte in mice, Experimental Gerontology 43 (2008) 764-770.
[62] S. Riedl, B. Rinner, M. Asslaber, H. Schaider, S. Walzer, A. Novak, K. Lohner, D. Zweytick, In search of a novel target — Phosphatidylserine exposed by non-apoptotic tumor cells and metastases of malignancies with poor treatment efficacy, Biochimica et Biophysica Acta (BBA) - Biomembranes 1808 (2011) 2638-2645.
[63] Wang Yingjie , Beck Werner, Deppisch Reinhold, Marshall Sally M., Hoenich Nicholas A., Thompson Michael G., Advanced glycation end products elicit externalization of phosphatidylserine in a subpopulation of platelets via 5-HT2A/2C receptors, American Journal of Physiology - Cell Physiology 293 (2007) C328-C336.
[64] H.P. Dong, A. Holth, L. Kleinberg, M.G. Ruud, M.B. Elstrand, C.G. Tropé, B. Davidson, B. Risberg, Evaluation of Cell Surface Expression of Phosphatidylserine in Ovarian Carcinoma Effusions Using the Annexin-V/7-AAD Assay: Clinical Relevance and Comparison With Other Apoptosis Parameters, American Journal of Clinical Pathology 132 (2009) 756-762.
[65] H. Schröder-Borm, R. Bakalova, J. Andrä, The NK-lysin derived peptide NK-2 preferentially kills cancer cells with increased surface levels of negatively charged phosphatidylserine, Febs Letters 579 (2005) 6128-6134.

[66] T. Utsugi, A.J. Schroit, J. Connor, C.D. Bucana, I.J. Fidler, Elevated Expression of Phosphatidylserine in the Outer Membrane Leaflet of Human Tumor Cells and Recognition by Activated Human Blood Monocytes, Cancer Research 51 (1991) 3062-3066.

[67] S. Riedl, B. Rinner, H. Schaider, K. Lohner, D. Zweytick, Killing of melanoma cells and their metastases by human lactoferricin derivatives requires interaction with the cancer marker phosphatidylserine, BioMetals 27 (2014) 981-997.

[68] H. Woehlecke, A. Pohl, N. Alder-Baerens, H. Lage, A. Herrmann, Enhanced exposure of phosphatidylserine in human gastric carcinoma cells overexpressing the half-size ABC transporter BCRP (ABCG2), Biochemical Journal 376 (2003) 489-495.

[69] S. Ran, A. Downes, P.E. Thorpe, Increased exposure of anionic phospholipids on the surface of tumor blood vessels, Cancer Research 62 (2002) 6132-6140.

[70] M.S. Soengas, P. Capodieci, D. Polsky, J. Mora, M. Esteller, X. Opitz-Araya, R. McCombie, J.G. Herman, W.L. Gerald, Y.A. Lazebnik, C. Cordón-Cardó, S.W. Lowe, Inactivation of the apoptosis effector Apaf-1 in malignant melanoma, Nature 409 (2001) 207-211.

[71] T. Miyashita, J.C. Reed, Bcl-2 oncoprotein blocks chemotherapy-induced apoptosis in a human leukemia cell line, Blood 81 (1993) 151-157.

[72] N. Papo, Y. Shai, Host defense peptides as new weapons in cancer treatment, Cellular and Molecular Life Sciences 62 (2005) 784-790.

[73] P. Williamson, E.M. Bevers, E.F. Smeets, P. Comfurius, R.A. Schlegel, R.F.A. Zwaal, Continuous analysis of the mechanism of activated transbilayer lipid movement in platelets, Biochemistry 34 (1995) 10448-10455.

[74] R. Majumder, M.A. Quinn-Allen, W.H. Kane, B.R. Lentz, A phosphatidylserine binding site in factor V(a)C1 domain regulates both assembly and activity of the prothrombinase complex, Blood 112 (2008) 2795-2802.

[75] C.L. Stace, N.T. Ktistakis, Phosphatidic acid- and phosphatidylserine-binding proteins, Biochimica Et Biophysica Acta-Molecular and Cell Biology of Lipids 1761 (2006) 913-926.

[76] R.F.A. Zwaal, P. Comfurius, E.M. Bevers, Lipid-protein interactions in blood coagulation, Biochimica Et Biophysica Acta-Reviews on Biomembranes 1376 (1998) 433-453.

[77] E.M. Bevers, P. Comfurius, R.F.A. Zwaal, Changes in membrane phospholipid distribution during platelet activation, Biochimica Et Biophysica Acta 736 (1983) 57-66.

[78] P.J. Sims, T. Wiedmer, Unraveling the mysteries of phospholipid scrambling, Thrombosis and Haemostasis 86 (2001) 266-275.

[79] C. Lupu, M. Calb, M. Ionescu, F. Lupu, Enhanced ptothrombin and intrinsic factor-X activation on blood-platelets from diabetic-patients, Thrombosis and Haemostasis 70 (1993) 579-583.

[80] M.K. Callahan, P. Williamson, R.A. Schlegel, Surface expression of phosphatidylserine on macrophages is required for phagocytosis of apoptotic thymocytes, Cell Death and Differentiation 7 (2000) 645-653.

[81] V.A. Fadok, A. de Cathelineau, D.L. Daleke, P.M. Henson, D.L. Bratton, Loss of phospholipid asymmetry and surface exposure of phosphatidylserine is required for phagocytosis of apoptotic cells by macrophages and fibroblasts, Journal of Biological Chemistry 276 (2001) 1071-1077.

[82] V.A. Fadok, D.R. Voelker, P.A. Campbell, J.J. Cohen, D.L. Bratton, P.M. Henson, Exposure of phosphatidylserine on the surface of apoptotic lymphocytes triggers specific recognition and removal by macrophages, Journal of Immunology 148 (1992) 2207-2216.

[83] S.J. Martin, C.P.M. Reutelingsperger, A.J. McGahon, J.A. Rader, R. Vanschie, D.M. Laface, D.R. Green, Early redistribution of plasma-membrane phosphatidylserine is a general feature of apoptosis regardless of the initiating stimulus - inhibition by overexpression of BLC-2 and ABL, Journal of Experimental Medicine 182 (1995) 1545-1556.

[84] G.G. Borisenko, T. Matsura, S.X. Liu, V.A. Tyurin, J.F. Jiang, F.B. Serinkan, V.E. Kagan, Macrophage recognition of externalized phosphatidylserine and phagocytosis of apoptotic Jurkat cells - existence of a threshold, Archives of Biochemistry and Biophysics 413 (2003) 41-52.

[85] G. Brouckaert, M. Kalai, D.V. Krysko, X. Saelens, D. Vercammen, M. Ndlovu, G. Haegeman, K. D'Herde, P. Vandenabeele, Phagocytosis of necrotic cells by macrophages is phosphatidylserine dependent and does not induce inflammatory cytokine production, Molecular Biology of the Cell 15 (2004) 1089-1100.

[86] V.A. Fadok, D.L. Bratton, D.M. Rose, A. Pearson, R.A.B. Ezekewitz, P.M. Henson, A receptor for phosphatidylserine-specific clearance of apoptotic cells, Nature 405 (2000) 85-90.

[87] Y.Y. Tyurina, K. Kawai, V.A. Tyurin, S.X. Liu, V.E. Kagan, J.P. Fabisiak, The plasma membrane is the site of selective phosphatidylserine oxidation during apoptosis: Role of cytochrome c, Antioxidants & Redox Signaling 6 (2004) 209-225.

[88] J.F. Jiang, V. Kini, N. Belikova, B.F. Serinkan, G.G. Borisenko, Y.Y. Tyurina, V.A. Tyurin, V.E. Kagan, Cytochrome c release is required for phosphatidylserine peroxidation during fas-triggered apoptosis in lung epithelial A549 cells, Lipids 39 (2004) 1133-1142.

[89] D.L. Daleke, J.V. Lyles, Identification and purification of aminophospholipid flippases, Biochimica Et Biophysica Acta-Molecular and Cell Biology of Lipids 1486 (2000) 108-127.

[90] J.T. Ding, Z. Wu, B.P. Crider, Y.M. Ma, X.J. Li, C. Slaughter, L.M. Gong, X.S. Xie, Identification and functional expression of four isoforms of ATPase II, the putative aminophospholipid translocase - Effect of isoform variation on the ATPase activity and phospholipid specificity, Journal of Biological Chemistry 275 (2000) 23378-23386.

[91] B. Verhoven, S. Krahling, R.A. Schlegel, P. Williamson, Regulation of phosphatidylserine exposure and phagocytosis of apoptotic T lymphocytes, Cell Death and Differentiation 6 (1999) 262-270.

[92] D.L. Bratton, V.A. Fadok, D.A. Richter, J.M. Kailey, L.A. Guthrie, P.M. Henson, Appearance of phosphatidylserine on apoptotic cells requires calcium-mediated nonspecific flip-flop and is enhanced by loss of the aminophospholipid translocase, Journal of Biological Chemistry 272 (1997) 26159-26165.

[93] M.D. Jacobson, Reactive oxygen species and programmed cell death, Trends in Biochemical Sciences 21 (1996) 83-86.

[94] I. Stoian, A. Oros, E. Moldoveanu, Apoptosis and Free Radicals, Biochemical and Molecular Medicine 59 (1996) 93-97.

[95] V.E. Kagan, G.G. Borisenko, B.F. Serinkan, Y.Y. Tyurina, V.A. Tyurin, J. Jiang, S.X. Liu, A.A. Shvedova, J.P. Fabisiak, W. Uthaisang, B. Fadeel, Appetizing rancidity of apoptotic cells for macrophages: oxidation, externalization, and recognition of phosphatidylserine, American Journal of Physiology-Lung Cellular and Molecular Physiology 285 (2003) L1-L17.

[96] Y.Y. Tyurina, V.A. Tyurin, Q. Zhao, M. Djukic, P.J. Quinn, B.R. Pitt, V.E. Kagan, Oxidation of phosphatidylserine: a mechanism for plasma membrane phospholipid scrambling during apoptosis?, Biochemical and Biophysical Research Communications 324 (2004) 1059-1064.

[97] J.P. Fabisiak, Y.Y. Tyurina, V.A. Tyurin, J.S. Lazo, V.E. Kagan, Random versus selective membrane phospholipid oxidation in apoptosis: Role of phosphatidylserine, Biochemistry 37 (1998) 13781-13790.

[98] V.E. Kagan, B. Gleiss, Y.Y. Tyurina, V.A. Tyurin, C. Elenstrom-Magnusson, S.X. Liu, F.B. Serinkan, A. Arroyo, J. Chandra, S. Orrenius, B. Fadeel, A role for oxidative stress in apoptosis: Oxidation and externalization of phosphatidylserine is required for macrophage clearance of cells undergoing Fas-mediated apoptosis, Journal of Immunology 169 (2002) 487-499.

[99] T. Matsura, M. Kai, K. Yamada, A.A. Shvedova, V.E. Kagan, Fine-tuning phagocytic clearance of apoptotic cells by phosphatidylserine oxidation, Journal of Clinical Biochemistry and Nutrition 34 (2003) 11-24.

[100] Y.Y. Tyurina, A.A. Shvedova, K. Kawai, V.A. Tyurin, C. Kommineni, P.J. Quinn, N.F. Schor, J.P. Fabisiak, V.E. Kagan, Phospholipid signaling in apoptosis: peroxidation and externalization of phosphatidylserine, Toxicology 148 (2000) 93-101.

[101] V.E. Kagan, J.P. Fabisiak, A.A. Shvedova, Y.Y. Tyurina, V.A. Tyurin, N.F. Schor, K. Kawai, Oxidative signaling pathway for externalization of plasma membrane phosphatidylserine during apoptosis, Febs Letters 477 (2000) 1-7.

[102] T. Matsura, A. Togawa, M. Kai, T. Nishida, J. Nakada, Y. Ishibe, S. Kojo, Y. Yamamoto, K. Yamada, The presence of oxidized phosphatidylserine on Fas-mediated apoptotic cell surface, Biochimica Et Biophysica Acta-Molecular and Cell Biology of Lipids 1736 (2005) 181-188.

[103] Y.Y. Tyurina, V.A. Tyurin, S.X. Liu, C.A. Smith, A.A. Shvedova, N.F. Schor, V.E. Kagan, Phosphatidylserine peroxidation during apoptosis. A signaling pathway for phagocyte clearance, Sub-cellular biochemistry 36 (2002) 79-96.

[104] M.E. Greenberg, M. Sun, R. Zhang, M. Febbraio, R. Silverstein, S.L. Hazen, Oxidized phosphatidylserine-CD36 interactions play an essential role in macrophage-dependent phagocytosis of apoptotic cells, Journal of Experimental Medicine 203 (2006) 2613-2625.

[105] E. Solary, L. Dubrez, B. Eymin, The role of apoptosis in the pathogenesis and treatment of diseases, European Respiratory Journal 9 (1996) 1293-1305.

[106] B. Favaloro, N. Allocati, V. Graziano, C. Di Ilio, V. De Laurenzi, Role of Apoptosis in disease, Aging 4 (2012) 330-349.

[107] M.L.N. Huynh, V.A. Fadok, P.M. Henson, Phosphatidylserine-dependent ingestion of apoptotic cells promotes TGF-beta 1 secretion and the resolution of inflammation, Journal of Clinical Investigation 109 (2002) 41-50.

[108] R. De Simone, M. Antonietta-Cat, A. Nicolini, L. Minghetti, Expression of phosphatidylserine receptor and down-regulation of pro-inflammatory molecule

production by its natural ligand in rat microglial cultures, Journal of Neuropathology and Experimental Neurology 61 (2002) 237-244.
[109] R. Matsuno, Y. Aramaki, S. Tsuchiya, Involvement of TGF-beta in inhibitory effects of negatively charged liposomes on nitric oxide production by macrophages stimulated with LPS, Biochemical and Biophysical Research Communications 281 (2001) 614-620.
[110] R. De Simone, M.A. Ajmone-Cat, P. Tirassa, L. Minghetti, Apoptotic PC12 cells exposing phosphatidylserine promote the production of anti-inflammatory and neuroprotective molecules by microglial cells, Journal of Neuropathology and Experimental Neurology 62 (2003) 208-216.
[111] I. Vermes, C. Haanen, H. Steffens-Nakken, C. Reutellingsperger, A novel assay for apoptosis Flow cytometric detection of phosphatidylserine expression on early apoptotic cells using fluorescein labelled Annexin V, Journal of Immunological Methods 184 (1995) 39-51.
[112] G. Koopman, C.P.M. Reutelingsperger, G.A.M. Kuijten, R.M.J. Keehnen, S.T. Pals, M.H.J. Vanoers, Annexin V for flow cytometric detection of phosphatidylserine expression on B cells undergoing apoptosis, Blood 84 (1994) 1415-1420.
[113] T. Liu, W. Zhu, X. Yang, L. Chen, R. Yang, Z. Hua, G. Li, Detection of Apoptosis Based on the Interaction between Annexin V and Phosphatidylserine, Analytical Chemistry 81 (2009) 2410-2413.
[114] V.N. Bochkov, O.V. Oskolkova, K.G. Birukov, A.-L. Levonen, C.J. Binder, J. Stoeckl, Generation and Biological Activities of Oxidized Phospholipids, Antioxidants & Redox Signaling 12 (2010) 1009-1059.
[115] E. Maciel, P. Domingues, M.R.M. Domingues, Liquid chromatography/tandem mass spectrometry analysis of long-chain oxidation products of cardiolipin induced by the hydroxyl radical, Rapid Communications in Mass Spectrometry 25 (2011) 316-326.
[116] E. Maciel, P. Domingues, D. Marques, C. Simoes, A. Reis, M.M. Oliveira, R.A. Videira, F. Peixoto, M.R.M. Domingues, Cardiolipin and oxidative stress: Identification of new short chain oxidation products of cardiolipin in in vitro analysis and in nephrotoxic drug-induced disturbances in rat kidney tissue, International Journal of Mass Spectrometry 301 (2011) 62-73.
[117] Y.Y. Tyurina, R.M. Domingues, V.A. Tyurin, E. Maciel, P. Domingues, A.A. Amoscato, H. Bayir, V.E. Kagan, Characterization of cardiolipins and their oxidation products by LC–MS analysis, Chemistry and Physics of Lipids.
[118] M.R.M. Domingues, A. Reis, P. Domingues, Mass spectrometry analysis of oxidized phospholipids, Chemistry and physics of lipids 156 (2008) 1-12.
[119] A.A. Shvedova, Y.Y. Tyurina, V.A. Tyurin, Y. Kikuchi, V.E. Kagan, P.J. Quinn, Quantitative analysis of phospholipid peroxidation and antioxidant protection in live human epidermal keratinocytes, Bioscience Reports 21 (2001) 33-43.
[120] H. Bayir, B. Fadeel, M.J. Palladino, E. Witasp, I.V. Kurnikov, Y.Y. Tyurina, V.A. Tyurin, A.A. Amoscato, J. Jiang, P.M. Kochanek, S.T. DeKosky, J.S. Greenberger, A.A. Shvedova, V.E. Kagan, Apoptotic interactions of cyctochrome c: Redox flirting with anionic phospholipids within and outside of mitochondria, Biochimica Et Biophysica Acta-Bioenergetics 1757 (2006) 648-659.
[121] Y.Y. Tyurina, V.A. Tyurin, M.W. Epperly, J.S. Greenberger, V.E. Kagan, Oxidative lipidomics of gamma-irradiation-induced intestinal injury, Free Radical Biology and Medicine 44 (2008) 299-314.

[122] Y.Y. Tyurina, V.A. Tyurin, V.I. Kapralova, K. Wasserloos, M. Mosher, M.W. Epperly, J.S. Greenberger, B.R. Pitt, V.E. Kagan, Oxidative Lipidomics of gamma-Radiation-Induced Lung Injury: Mass Spectrometric Characterization of Cardiolipin and Phosphatidylserine Peroxidation, Radiation Research 175 (2011) 610-621.

[123] Y.Y. Tyurina, V.A. Tyurin, A.M. Kaynar, V.I. Kapralova, K. Wasserloos, J. Li, M. Mosher, L. Wright, P. Wipf, S. Watkins, B.R. Pitt, V.E. Kagan, Oxidative lipidomics of hyperoxic acute lung injury: mass spectrometric characterization of cardiolipin and phosphatidylserine peroxidation, American Journal of Physiology-Lung Cellular and Molecular Physiology 299 (2010) L73-L85.

[124] M. Orciani, S. Gorbi, M. Benedetti, G. Di Benedetto, M. Mattioli-Belmonte, F. Regoli, R. Di Primio, Oxidative stress defense in human-skin-derived mesenchymal stem cells versus human keratinocytes: Different mechanisms of protection and cell selection, Free Radical Biology and Medicine 49 (2010) 830-838.

[125] J.S. Beckman, T.W. Beckman, J. Chen, P.A. Marshall, B.A. Freeman, Apparent hydroxyl radical production by peroxynitrite: Implications for endothelial injury from nitric oxide and superoxide, Proceedings of the National Academy of Sciences of the United States of America 87 (1990) 1620-1624.

[126] T. Miyazaki, S. Nagasaka, Y. Kamiya, K. Tanimura, Formation of excited hydroxyl radicals in high-energy-electron-irradiated ice at very low temperature, The Journal of Physical Chemistry 97 (1993) 10715-10719.

[127] A. Reis, P. Domingues, A.J.V. Ferrer-Correia, M.R.M. Domingues, Fragmentation study of short-chain products derived from oxidation of diacylphosphatidylcholines by electrospray tandem mass spectrometry: identification of novel short-chain products, Rapid Communications in Mass Spectrometry 18 (2004) 2849-2858.

[128] G. Spiteller, Peroxyl radicals: Inductors of neurodegenerative and other inflammatory diseases. Their origin and how they transform cholesterol, phospholipids, plasmalogens, polyunsaturated fatty acids, sugars, and proteins into deleterious products, Free Radical Biology and Medicine 41 (2006) 362-387.

[129] Z. Guan, Discovering novel brain lipids by liquid chromatography/tandem mass spectrometry, Journal of Chromatography B-Analytical Technologies in the Biomedical and Life Sciences 877 (2009) 2814-2821.

[130] R.A. Maki, V.A. Tyurin, R.C. Lyon, R.L. Hamilton, S.T. DeKosky, V.E. Kagan, W.F. Reynolds, Aberrant Expression of Myeloperoxidase in Astrocytes Promotes Phospholipid Oxidation and Memory Deficits in a Mouse Model of Alzheimer Disease, Journal of Biological Chemistry 284 (2009) 3158-3169.

[131] H. Bayir, V.A. Tyurin, Y.Y. Tyurina, R. Viner, V. Ritov, A.A. Amoscato, Q. Zhao, X.J.J. Zhang, K.L. Janesko-Feldman, H. Alexander, L.V. Basova, R.S.B. Clark, P.M. Kochanek, V.E. Kagan, Selective early cardiolipin peroxidation after traumatic brain injury: An oxidative lipidomics analysis, Annals of Neurology 62 (2007) 154-169.

[132] V.A. Tyurin, Y.Y. Tyurina, W. Feng, A. Mnuskin, J.F. Jiang, M.K. Tang, X.J. Zhang, Q. Zhao, P.M. Kochanek, R.S.B. Clark, H. Bayir, V.E. Kagan, Mass-spectrometric characterization of phospholipids and their primary peroxidation products in rat cortical neurons during staurosporine-induced apoptosis, Journal of Neurochemistry 107 (2008) 1614-1633.

[133] V.A. Tyurin, Y. Tyurina, M.Y. Jung, M.A. Tungekar, K.J. Wasserloos, H. Bayir, J.S. Greenberger, P.M. Kochanek, A.A. Shvedova, B. Pitt, V.E. Kagan, Mass-

spectrometric analysis of hydroperoxy- and hydroxy-derivatives of cardiolipin and phosphatidylserine in cells and tissues induced by pro-apoptotic and pro-inflammatory stimuli, Journal of Chromatography B-Analytical Technologies in the Biomedical and Life Sciences 877 (2009) 2863-2872.

[134] O.M. Panasenko, T.V. Vakhrusheva, I.I. Vlasova, A.V. Chekanov, Y.V. Baranov, V.I. Sergienko, Role of myeloperoxidase-mediated modification of human blood lipoproteins in atherosclerosis development, Bulletin of Experimental Biology and Medicine 144 (2007) 428-431.

[135] E. Malle, G. Marsche, J. Arnhold, M.J. Davies, Modification of low-density lipoprotein by myeloperoxidase-derived oxidants and reagent hypochlorous acid, Biochimica Et Biophysica Acta-Molecular and Cell Biology of Lipids 1761 (2006) 392-415.

[136] J.W. Heinecke, Pathways for oxidation of low density lipoprotein by myeloperoxidase: tyrosyl radical reactive aldehydes, hypochlorous acid and molecular chlorine, Biofactors 6 (1997) 145-155.

[137] N. Noguchi, A. Nakada, Y. Itoh, A. Watanabe, E. Niki, Formation of active oxygen species and lipid peroxidation induced by hypochlorite, Archives of Biochemistry and Biophysics 397 (2002) 440-447.

[138] M.L. Brennan, A. Gaur, A. Pahuja, A.J. Lusis, W.F. Reynolds, Mice lacking myeloperoxidase are more susceptible to experimental autoimmune encephalomyelitis, Journal of Neuroimmunology 112 (2001) 97-105.

[139] C. Milla, S.X. Yang, D.N. Cornfield, M.L. Brennan, S.L. Hazen, A. Panoskaltsis-Mortari, B.R. Blazar, I.Y. Haddad, Myeloperoxidase deficiency enhances inflammation after allogeneic marrow transplantation, American Journal of Physiology-Lung Cellular and Molecular Physiology 287 (2004) L706-L714.

[140] J. Flemmig, J. Lessig, U. Reibetanz, P. Dautel, J. Arnhold, Non-Vital Polymorphonuclear Leukocytes Express Myeloperoxidase on their Surface, Cellular Physiology and Biochemistry 21 (2008) 287-296.

[141] J. Flemmig, J. Arnhold, Interaction of hypochlorous acid and myeloperoxidase with phosphatidylserine in the presence of ammonium ions, Journal of Inorganic Biochemistry 104 (2010) 759-764.

[142] J. Flemmig, H. Spalteholz, K. Schubert, S. Meier, J. Arnhold, Modification of phosphatidylserine by hypochlorous acid, Chemistry and Physics of Lipids 161 (2009) 44-50.

[143] Y. Kawai, H. Kiyokawa, Y. Kimura, Y. Kato, K. Tsuchiya, J. Terao, Hypochlorous acid-derived modification of phospholipids: Characterization of aminophospholipids as regulatory molecules for lipid peroxidation, Biochemistry 45 (2006) 14201-14211.

[144] Y. Kato, Y. Miyake, K. Yamamoto, Y. Shimomura, H. Ochi, Y. Mori, T. Osawa, Preparation of a Monoclonal Antibody to Nϵ-(Hexanonyl)lysine: Application to the Evaluation of Protective Effects of Flavonoid Supplementation against Exercise-Induced Oxidative Stress in Rat Skeletal Muscle, Biochemical and Biophysical Research Communications 274 (2000) 389-393.

[145] S. Hisaka, T. Osawa, Lipid Hydroperoxide-Derived Adduction to Amino-Phospholipid in Biomembrane, in: Y. Kato (Ed.), Lipid Hydroperoxide-Derived Modification of Biomolecules, Springer Netherlands, 2014, pp. 41-48.

[146] S. Hisaka, N. Yamada, K. Naito, T. Osawa, The immunological and chemical detection of N-(hexanoyl)phosphatidylethanolamine and N-

(hexanoyl)phosphatidylserine in an oxidative model induced by carbon tetrachloride, Biochemical and Biophysical Research Communications 393 (2010) 631-636.
[147] R. Bucala, Z. Makita, T. Koschinsky, A. Cerami, H. Vlassara, Lipid advanced glycosylation - pathway for lipid oxidation in-vivo, Proceedings of the National Academy of Sciences of the United States of America 90 (1993) 6434-6438.
[148] A. Ravandi, A. Kuksis, L. Marai, J.J. Myher, Preparation and characterization of glucosylated aminoglycerophospholipids, Lipids 30 (1995) 885-891.
[149] M. Kalousova, T. Zima, V. Tesar, S. Dusilova-Sulkova, J. Skrha, Advanced glycoxidation end products in chronic diseases-clinical chemistry and genetic background, Mutation Research-Fundamental and Molecular Mechanisms of Mutagenesis 579 (2005) 37-46.
[150] I.A.M. van den Oever, H.G. Raterman, M.T. Nurmohamed, S. Simsek, Endothelial Dysfunction, Inflammation, and Apoptosis in Diabetes Mellitus, Mediators of inflammation (2010).
[151] H. Vlassara, M.R. Palace, Glycoxidation: The menace of diabetes and aging, Mount Sinai Journal of Medicine 70 (2003) 232-241.
[152] C. Simões, V. Simões, A. Reis, P. Domingues, M. Domingues, Oxidation of glycated phosphatidylethanolamines: evidence of oxidation in glycated polar head identified by LC-MS/MS, Analytical and Bioanalytical Chemistry 397 (2010) 2417-2427.
[153] M.G. Repetto, A. Boveris, Transition metals: Bioinorganic and redox reactions in biological systems, Transition Metals: Characteristics, Properties and Uses, 2011, pp. 349-370.
[154] Y. Yoshida, N. Itoh, Y. Saito, M. Hayakawa, E. Niki, Application of water-soluble radical initiator, 2,2 '-azobis- 2-(2-imidazolin-2-yl)propane dihydrochloride, to a study of oxidative stress, Free Radical Research 38 (2004) 375-384.
[155] E. Niki, [3] Free radical initiators as source of water- or lipid-soluble peroxyl radicals, in: A.N.G. Lester Packer (Ed.), Methods in Enzymology, Academic Press, 1990, pp. 100-108.
[156] Y. Cui, D.S. Kim, S.H. Park, J.A. Yoon, S.K. Kim, S.B. Kwon, K.C. Park, Involvement of ERK and p38 MAP kinase in AAPH-induced COX-2 expression in HaCaT cells, Chemistry and Physics of Lipids 129 (2004) 43-52.
[157] Z. Liu, H. Chen, H. Yang, J. Liang, X. Li, Low-dose UVA radiation-induced adaptive response in cultured human dermal fibroblasts, International Journal of Photoenergy 2012 (2012).
[158] T.J. McMillan, E. Leatherman, A. Ridley, J. Shorrocks, S.E. Tobi, J.R. Whiteside, Cellular effects of long wavelength UV light (UVA) in mammalian cells, Journal of Pharmacy and Pharmacology 60 (2008) 969-976.
[159] M.C. DeRosa, R.J. Crutchley, Photosensitized singlet oxygen and its applications, Coordination Chemistry Reviews 233–234 (2002) 351-371.
[160] A.J. Ridley, J.R. Whiteside, T.J. McMillan, S.L. Allinson, Cellular and sub-cellular responses to UVA in relation to carcinogenesis, International Journal of Radiation Biology 85 (2009) 177-185.
[161] A. Choromańska, J. Saczko, J. Kulbacka, N. Skolucka, M. Majkowski, The potential role of photodynamic therapy in the treatment of malignant melanoma - An in vitro study, Advances in Clinical and Experimental Medicine 21 (2012) 179-185.
[162] J. Saczko, J. Kulbacka, A. Chwiłkowska, M. Drag-Zalesińska, T. Wysocka, M. Ługowski, T. Banaś, The influence of photodynamic therapy on apoptosis in

human melanoma cell line, Folia Histochemica et Cytobiologica 43 (2005) 129-132.
[163] S. Miyamoto, P. Di Mascio, Lipid hydroperoxides as a source of singlet molecular oxygen, Sub-cellular biochemistry 77 (2014) 3-20.
[164] A. Reis, M.R.M. Domingues, F.M.L. Amado, A.J. Ferrer-Correia, P. Domingues, Radical peroxidation of palmitoyl-lineloyl-glycerophosphocholine liposomes: Identification of long-chain oxidised products by liquid chromatography-tandem mass spectrometry, Journal of Chromatography B-Analytical Technologies in the Biomedical and Life Sciences 855 (2007) 186-199.
[165] A. Reis, M.R.M. Domingues, F.M.L. Amado, A.J.V. Ferrer-Correia, P. Domingues, Separation of peroxidation products of diacyl-phosphatidylcholines by reversed-phase liquid chromatography-mass spectrometry, Biomedical Chromatography 19 (2005) 129-137.
[166] M.R.M. Domingues, C. Simoes, J.P. da Costa, A. Reis, P. Domingues, Identification of 1-palmitoyl-2-linoleoyl-phosphatidylethanolamine modifications under oxidative stress conditions by LC-MS/MS, Biomedical Chromatography 23 (2009) 588-601.
[167] R. Yurkova, D. Huster, J. Arnhold, Free radical fragmentation of cardiolipin by cytochrome c, Chemistry and Physics of Lipids 158 (2009) 16-21.
[168] E. Maciel, R.N. da Silva, C. Simoes, P. Domingues, M.R.M. Domingues, Structural Characterization of Oxidized Glycerophosphatidylserine: Evidence of Polar Head Oxidation, Journal of the American Society for Mass Spectrometry 22 (2011) 1804-1814.
[169] J. Folch, M. Lees, G.H.S. Stanley, A simple method for the isolation and purification of total lipides from animal tissues, Journal of Biological Chemistry 226 (1957) 497-509.
[170] E.G. Bligh, W.J. Dyer, A rapid method of total lipid extraction and purification, Can J Biochem Physiol 37 (1959) 911-917.
[171] T. Seppänen-Laakso, I. Laakso, R. Hiltunen, Analysis of fatty acids by gas chromatography, and its relevance to research on health and nutrition, Analytica Chimica Acta 465 (2002) 39-62.
[172] K. Eder, Gas chromatographic analysis of fatty acid methyl esters, Journal of Chromatography B: Biomedical Applications 671 (1995) 113-131.
[173] C.D. Bannon, J.D. Craske, A.E. Hilliker, Analysis of fatty acid methyl esters with high accuracy and reliability. IV. Fats with fatty acids containing four or more carbon atoms, Journal of the American Oil Chemists' Society 62 (1985) 1501-1507.
[174] G. Gutnikov, Fatty acid profiles of lipid samples, Journal of Chromatography B: Biomedical Sciences and Applications 671 (1995) 71-89.
[175] A. Carrasco-Pancorbo, N. Navas-Iglesias, L. Cuadros-Rodriguez, From lipid analysis towards lipidomics, a new challenge for the analytical chemistry of the 21st century. Part 1: Modern lipid analysis, Trac-Trends in Analytical Chemistry 28 (2009) 263-278.
[176] G. Subbanagounder, A.D. Watson, J.A. Berliner, Bioactive products of phospholipid oxidation: Isolation, identification, measurement and activities, Free Radical Biology and Medicine 28 (2000) 1751-1761.
[177] B. Fuchs, R. Suess, K. Teuber, M. Eibisch, J. Schiller, Lipid analysis by thin-layer chromatography-A review of the current state, Journal of Chromatography A 1218 (2011) 2754-2774.

[178] G.M. Patton, J.M. Fasulo, S.J. Robins, Separation of phospholipids and individual molecular species of phospholipids by high-performance liquid chromatography, Journal of Lipid Research 23 (1982) 190-196.
[179] W.W. Christie, Rapid separation and quantification of lipid classes by high performance liquid chromatography and mass (light-scattering) detection, Journal of Lipid Research 26 (1985) 507-512.
[180] J.F. Brouwers, Liquid chromatographic–mass spectrometric analysis of phospholipids. Chromatography, ionization and quantification, Biochimica et Biophysica Acta (BBA) - Molecular and Cell Biology of Lipids 1811 (2011) 763-775.
[181] Y.-Q. Xia, M. Jemal, Phospholipids in liquid chromatography/mass spectrometry bioanalysis: comparison of three tandem mass spectrometric techniques for monitoring plasma phospholipids, the effect of mobile phase composition on phospholipids elution and the association of phospholipids with matrix effects, Rapid Communications in Mass Spectrometry 23 (2009) 2125-2138.
[182] E.J. Lesnefsky, M.S.K. Stoll, P.E. Minkler, C.L. Hoppel, Separation and Quantitation of Phospholipids and Lysophospholipids by High-Performance Liquid Chromatography, Analytical Biochemistry 285 (2000) 246-254.
[183] M. Malavolta, F. Bocci, E. Boselli, N.G. Frega, Normal phase liquid chromatography–electrospray ionization tandem mass spectrometry analysis of phospholipid molecular species in blood mononuclear cells: application to cystic fibrosis, Journal of Chromatography B 810 (2004) 173-186.
[184] J. McHowat, J.H. Jones, M. H. Creer, Gradient elution reversed-phase chromatographic isolation of individual glycerophospholipid molecular species, Journal of Chromatography B: Biomedical Sciences and Applications 702 (1997) 21-32.
[185] T. Nakamura, D.L. Bratton, R.C. Murphy, Analysis of Epoxyeicosatrienoic and Monohydroxyeicosatetraenoic Acids Esterified to Phospholipids in Human Red Blood Cells by Electrospray Tandem Mass Spectrometry, JOURNAL OF MASS SPECTROMETRY 32 (1997) 888-896.
[186] M. Schwalbe-Herrmann, J. Willmann, D. Leibfritz, Separation of phospholipid classes by hydrophilic interaction chromatography detected by electrospray ionization mass spectrometry, Journal of Chromatography A 1217 (2010) 5179-5183.
[187] B. Fuchs, U. Jakop, F. Goritz, R. Hermes, T. Hildebrandt, J. Schiller, K. Muller, MALDI-TOF "fingerprint" phospholipid mass spectra allow the differentiation between ruminantia and feloideae spermatozoa, Theriogenology 71 (2009) 568-575.
[188] F.F. Hsu, J. Turk, Characterization of cardiolipin from Escherichia coli by electrospray ionization with multiple stage quadrupole ion-trap mass spectrometric analysis of [M-2H+Na](-) ions, Journal of the American Society for Mass Spectrometry 17 (2006) 420-429.
[189] F.F. Hsu, J. Turk, E.R. Rhoades, D.G. Russell, Y.X. Shi, E.A. Groisman, Structural characterization of cardiolipin by tandem quadrupole and multiple-stage quadrupole ion-trap mass spectrometry with electrospray ionization, Journal of the American Society for Mass Spectrometry 16 (2005) 491-504.
[190] J.M. Deeley, M.C. Thomas, R.J.W. Truscott, T.W. Mitchell, S.J. Blanksby, Identification of Abundant Alkyl Ether Glycerophospholipids in the Human Lens

by Tandem Mass Spectrometry Techniques, Analytical Chemistry 81 (2009) 1920-1930.

[191] H.Y. Yin, B.E. Cox, W. Liu, N.A. Porter, J.D. Morrow, G.L. Milne, Identification of intact oxidation products of glycerophospholipids in vitro and in vivo using negative ion electrospray iontrap mass spectrometry, Journal of mass spectrometry 44 (2009) 672-680.

[192] F.-F. Hsu, J. Turk, Electrospray ionization with low-energy collisionally activated dissociation tandem mass spectrometry of glycerophospholipids: Mechanisms of fragmentation and structural characterization, Journal of Chromatography B 877 (2009) 2673-2695.

[193] C.M. Spickett, A. Reis, A.R. Pitt, Identification of oxidized phospholipids by electrospray ionization mass spectrometry and LC-MS using a QQLIT instrument, Free Radical Biology and Medicine 51 (2011) 2133-2149.

[194] F.-F. Hsu, J. Turk, Studies on Phosphatidylserine by Tandem Quadrupole and Multiple Stage Quadrupole Ion-Trap Mass Spectrometry with Electrospray Ionization: Structural Characterization and the Fragmentation Processes, Journal of the American Society for Mass Spectrometry 16 (2005) 1510-1522.

[195] L.C. Green, D.A. Wagner, J. Glogowski, P.L. Skipper, J.S. Wishnok, S.R. Tannenbaum, Analysis of nitrate, nitrite, and [15N]nitrate in biological fluids, Analytical Biochemistry 126 (1982) 131-138.

[196] G.O. Fruhwirth, A. Loidl, A. Hermetter, Oxidized phospholipids: From molecular properties to disease, Biochimia et Biophysica Acta 1772 (2007) 718-736.

[197] V.N. Bochkov, O.V. Oskolkova, K.G. Birukov, A.L. Levonen, C.J. Binder, J. Stockl, Generation and Biological Activities of Oxidized Phospholipids, Antioxidants & Redox Signaling 12 (2010) 1009-1059.

[198] H. Bayir, B. Fadeel, M.J. Palladino, E. Witasp, I.V. Kurnikov, Y.Y. Tyurina, V.A. Tyurin, A.A. Amoscato, J. Jiang, P.M. Kochanek, S.T. DeKosky, J.S. Greenberger, A.A. Shvedova, V.E. Kagan, Apoptotic interactions of cytochrome c: Redox flirting with anionic phospholipids within and outside of mitochondria, Biochimica et Biophysica Acta (BBA) - Bioenergetics 1757 648-659.

[199] T. Matsura, A. Togawa, M. Kai, T. Nishida, J. Nakada, Y. Ishibe, S. Kojo, Y. Yamamoto, K. Yamada, The presence of oxidized phosphatidylserine on Fas-mediated apoptotic cell surface, Biochimica et Biophysica Acta (BBA) - Molecular and Cell Biology of Lipids 1736 (2005) 181-188.

[200] Z.Q. Guan, Discovering novel brain lipids by liquid chromatography/tandem mass spectrometry, Journal of Chromatography B-Analytical Technologies in the Biomedical and Life Sciences 877 (2009) 2814-2821.

[201] M.E. Greenberg, M. Sun, R. Zhang, Oxidized phosphatidylserine-CD36 interactions play an essential role in macrophage-dependent phagocytosis of apoptotic cells, JEM 203 (2006) 2613-2625.

[202] P. Spiteller, W. Kern, J. Reiner, G. Spiteller, Aldehydic lipid peroxidation products derived from linoleic acid, Biochimica Et Biophysica Acta-Molecular and Cell Biology of Lipids 1531 (2001) 188-208.

[203] O.I. Shadyro, I.L. Yurkova, M.A. Kisel, O. Brede, J. Arnhold, Radiation-induced fragmentation of cardiolipin in a model membrane, International Journal of Radiation Biology 80 (2004) 239-245.

[204] O. Shadyro, I. Yurkova, M. Kisel, O. Brede, J. Arnhold, Formation of phosphatidic acid, ceramide, and diglyceride on radiolysis of lipids: Identification by MALDI-TOF mass spectrometry, Free Radical Biology and Medicine 36 (2004) 1612-1624.
[205] E.R. Stadtman, B.S. Berlett, Fenton Chemistry, The Journal of Biological Chemistry 256 (1991) 1701-17211.
[206] A. Reis, P. Domingues, A.J.V. Ferrer-Correia, M.R.M. Domingues, Tandem mass spectrometry of intact oxidation products of diacylphosphatidylcholines: evidence for the occurrence of the oxidation of the phosphocholine head and differentiation of isomers, Journal of Mass Spectrometry 39 (2004) 1513-1522.
[207] G. Xu, M.R. Chance, Hydroxyl radical-mediated modification of proteins as probes for structural proteomics, Chem. Rev. 107 (2007) 3514-3543.
[208] E.R. Stadtman, R.L. Levine, Free radical-mediated oxidation of free amino acids and amino cid residues in proteins, Amino Acids 25 (2003) 207-218.
[209] M.J. Davies, Protein and peptide alkoxyl radicals can give rise to C-terminal decarboxylation and backbone cleavage, Archives of Biochemistry and Biophysics 336 (1996) 163-172.
[210] J.G. Kay, S. Grinstein, Sensing Phosphatidylserine in Cellular Membranes, Sensors 11 (2011) 1744-1755.
[211] M.L. Bader Lange, G. Cenini, M. Piroddi, H. Mohmmad Abdul, R. Sultana, F. Galli, M. Memo, D.A. Butterfield, Loss of phospholipid asymmetry and elevated brain apoptotic protein levels in subjects with amnestic mild cognitive impairment and Alzheimer disease, Neurobiology of Disease 29 (2008) 456-464.
[212] K.J. Barnham, C.L. Masters, A.I. Bush, Neurodegenerative diseases and oxidative stress, Nature Reviews Drug Discovery 3 (2004) 205-214.
[213] R.M. Adibhatla, J.F. Hatcher, Altered lipid metabolism in brain injury and disorders, Sub-cellular biochemistry 49 (2008) 241-268.
[214] P.B.L. Pun, M.P. Murphy, Pathological significance of mitochondrial glycation, International journal of cell biology 2012 (2012) 843505-843505.
[215] S. Takeda, N. Sato, K. Uchio-Yamada, K. Sawada, T. Kunieda, D. Takeuchi, H. Kurinami, M. Shinohara, H. Rakugi, R. Morishita, Diabetes-accelerated memory dysfunction via cerebrovascular inflammation and A beta deposition in an Alzheimer mouse model with diabetes, Proceedings of the National Academy of Sciences of the United States of America 107 (2010) 7036-7041.
[216] A. Ravandi, A. Kuksis, N.A. Shaikh, Glycated lipids present in LDL cause increased oxidation susceptibility: A novel role for glucose in LDL oxidation, Clinical Chemistry 44 (1998) A73-A73.
[217] T. Melo, R.A. Videira, S. André, E. Maciel, C.S. Francisco, A.M. Oliveira-Campos, L.M. Rodrigues, M.R.M. Domingues, F. Peixoto, M. Manuel Oliveira, Tacrine and its analogues impair mitochondrial function and bioenergetics: a lipidomic analysis in rat brain, Journal of Neurochemistry 120 (2012) 998-1013.
[218] A. Ahmad, N. Rasheed, N. Banu, G. Palit, Alterations in monoamine levels and oxidative systems in frontal cortex, striatum, and hippocampus of the rat brain during chronic unpredictable stress, Stress (Amsterdam, Netherlands) 13 (2010) 355-364.
[219] G. Lucca, C.M. Comim, S.S. Valvassori, G.Z. Reus, F. Vuolo, F. Petronilho, F. Dal-Pizzol, E.C. Gavioli, J. Quevedo, Effects of chronic mild stress on the oxidative parameters in the rat brain, Neurochemistry International 54 (2009) 358-362.

[220] V.B. O'Donnell, Mass spectrometry analysis of oxidized phosphatidylcholine and phosphatidylethanolamine, Biochimica et Biophysica Acta (BBA) - Molecular and Cell Biology of Lipids 1811 (2011) 818-826.
[221] R.G. Salomon, Structural Identification and Cardiovascular Activities of Oxidized Phospholipids, Circulation Research 111 (2012) 930-946.
[222] C.M. Spickett, A.R. Pitt, A.J. Brown, Direct observation of lipid hydroperoxides in phospholipid vesicles by electrospray mass spectrometry, Free Radical Biology and Medicine 25 (1998) 613-620.
[223] C. Mylonas, D. Kouretas, Lipid peroxidation and tissue damage, In Vivo 13 (1999) 295-309.
[224] D.R. Santinha, D.R. Marques, E.A. Maciel, C.S.O. Simoes, S. Rosa, B.M. Neves, B. Macedo, P. Domingues, M.T. Cruz, M.R.M. Domingues, Profiling changes triggered during maturation of dendritic cells: a lipidomic approach, Analytical and Bioanalytical Chemistry 403 (2012) 457-471.
[225] S.K. Adeniyijones, M.L. Karnovsky, Oxidative decarboxylation of free and peptide-linked amino-acids in phagocytizing guinea-pig granulocytes, Journal of Clinical Investigation 68 (1981) 365-373.
[226] A. Bruni, E. Bigon, A. Battistella, E. Boarato, L. Mietto, G. Toffano, Lysophosphatidylserine as histamine releaser in mice and rats, Inflammation Research 14 (1984) 619-625.
[227] S.C. Frasch, D.L. Bratton, Emerging roles for lysophosphatidylserine in resolution of inflammation, Progress in Lipid Research 51 (2012) 199-207.
[228] T. Sugo, H. Tachimoto, T. Chikatsu, Y. Murakami, Y. Kikukawa, S. Sato, K. Kikuchi, T. Nagi, M. Harada, K. Ogi, M. Ebisawa, M. Mori, Identification of a lysophosphatidylserine receptor on mast cells, Biochemical and Biophysical Research Communications 341 (2006) 1078-1087.
[229] K. Yea, J. Kim, S. Lim, T. Kwon, H.S. Park, K.S. Park, P.-G. Suh, S.H. Ryu, Lysophosphatidylserine regulates blood glucose by enhancing glucose transport in myotubes and adipocytes, Biochemical and Biophysical Research Communications 378 (2009) 783-788.
[230] N. Ahmed, P.J. Thornalley, Advanced glycation endproducts: what is their relevance to diabetic complications?, Diabetes, Obesity and Metabolism 9 (2007) 233-245.
[231] T. Miyazawa, K. Nakagawa, S. Shimasaki, R. Nagai, Lipid glycation and protein glycation in diabetes and atherosclerosis, Amino Acids 42 (2012) 1163-1170.
[232] A. Goldin, J.A. Beckman, A.M. Schmidt, M.A. Creager, Advanced Glycation End Products: Sparking the Development of Diabetic Vascular Injury, Circulation 114 (2006) 597-605.
[233] J.-L. Wautier, A.M. Schmidt, Protein Glycation: A Firm Link to Endothelial Cell Dysfunction, Circulation Research 95 (2004) 233-238.
[234] D.R. Santinha, M. Luísa Dória, B.M. Neves, E.A. Maciel, J. Martins, L. Helguero, P. Domingues, M. Teresa Cruz, M. Rosário Domingues, Prospective phospholipid markers for skin sensitization prediction in keratinocytes: A phospholipidomic approach, Archives of Biochemistry and Biophysics 533 (2013) 33-41.
[235] T. Melo, E.M.P. Silva, C. Simoes, P. Domingues, M.R.M. Domingues, Photooxidation of glycated and non-glycated phosphatidylethanolamines monitored by mass spectrometry, Journal of mass spectrometry 48 (2013) 68-78.

[236] E. Maciel, R. Faria, D. Santinha, M.R.M. Domingues, P. Domingues, Evaluation of oxidation and glyco-oxidation of 1-palmitoyl-2-arachidonoyl-phosphatidylserine by LC–MS/MS, Journal of Chromatography B 929 (2013) 76-83.
[237] G. Xu, M.R. Chance, Hydroxyl radical-mediated modification of proteins as probes for structural proteomics, Chemical Reviews 107 (2007) 3514-3543.
[238] J. Wang, Y.-M. Lu, B.-Z. Liu, H.-Y. He, Electrospray positive ionization tandem mass spectrometry of Amadori compounds, Journal of mass spectrometry 43 (2008) 262-264.
[239] J.R. Requena, M.U. Ahmed, C.W. Fountain, T.P. Degenhardt, S. Reddy, C. Perez, T.J. Lyons, A.J. Jenkins, J.W. Baynes, S.R. Thorpe, Carboxymethylethanolamine, a biomarker of phospholipid modification during the maillard reaction in vivo, Journal of Biological Chemistry 272 (1997) 17473-17479.
[240] N. Shoji, K. Nakagawa, A. Asai, I. Fujita, A. Hashiura, Y. Nakajima, S. Oikawa, T. Miyazawa, LC-MS/MS analysis of carboxymethylated and carboxyethylated phosphatidylethanolamines in human erythrocytes and blood plasma, Journal of Lipid Research 51 (2010) 2445-2453.
[241] T. Matsura, B.F. Serinkan, J. Jiang, V.E. Kagan, Phosphatidylserine peroxidation/externalization during staurosporine-induced apoptosis in HL-60 cells, Febs Letters 524 (2002) 25-30.
[242] R.N. da Silva, A.C. Silva, E. Maciel, C. Simoes, S. Horta, P. Laranjeira, A. Paiva, P. Domingues, M.R.M. Domingues, Evaluation of the capacity of oxidized phosphatidylserines to induce the expression of cytokines in monocytes and dendritic cells, Archives of Biochemistry and Biophysics 525 (2012) 9-15.
[243] B. Fadeel, D. Xue, V. Kagan, Programmed cell clearance: Molecular regulation of the elimination of apoptotic cell corpses and its role in the resolution of inflammation, Biochemical and Biophysical Research Communications 396 (2010) 7-10.
[244] A.A. Shvedova, C. Kommineni, B.A. Jeffries, V. Castranova, Y.Y. Tyurina, V.A. Tyurin, E.A. Serbinova, J.P. Fabisiak, V.E. Kagan, Redox cycling of phenol induces oxidative stress in human epidermal keratinocytes, Journal of Investigative Dermatology 114 (2000) 354-364.
[245] A.A. Shvedova, J.Y. Tyurina, K. Kawai, V.A. Tyurin, C. Kommineni, V. Castranova, J.P. Fabisiak, V.E. Kagan, Selective peroxidation and externalization of phosphatidylserine in normal human epidermal keratinocytes during oxidative stress induced by cumene hydroperoxide, Journal of Investigative Dermatology 118 (2002) 1008-1018.
[246] V.M. Schoop, N. Mirancea, N.E. Fusenig, Epidermal organization and differentiation of HaCaT keratinocytes in organotypic coculture with human dermal fibroblasts, Journal of Investigative Dermatology 112 (1999) 343-353.
[247] P. Boukamp, R.T. Petrussevska, D. Breitkreutz, J. Hornung, A. Markham, N.E. Fusenig, Normal keratinization in a spontaneously immortalized aneuploid human keratinocyte cell-line, Journal of Cell Biology 106 (1988) 761-771.
[248] J. O'Brien, I. Wilson, T. Orton, F. Pognan, Investigation of the Alamar Blue (resazurin) fluorescent dye for the assessment of mammalian cell cytotoxicity, European Journal of Biochemistry 267 (2000) 5421-5426.
[249] E. Maciel, R.N. da Silva, C. Simões, T. Melo, R. Ferreira, P. Domingues, M.R.M. Domingues, Liquid chromatography–tandem mass spectrometry of

phosphatidylserine advanced glycated end products, Chemistry and Physics of Lipids 174 (2013) 1-7.
[250] S. Betigeri, A. Thakur, K. Raghavan, Use of 2,2′-Azobis(2-Amidinopropane) Dihydrochloride as a Reagent Tool for Evaluation of Oxidative Stability of Drugs, Pharmaceutical Research 22 (2005) 310-317.
[251] U. Leiter, T. Eigentler, C. Garbe, Epidemiology of skin cancer, Adv Exp Med Biol 810 (2014) 120-140.
[252] D.L. Mitchell, A.A. Fernandez, Different types of DNA damage play different roles in the etiology of sunlight-induced melanoma, Pigment Cell & Melanoma Research 24 (2011) 119-124.
[253] D. Mitchell, A. Fernandez, The photobiology of melanocytes modulates the impact of UVA on sunlight-induced melanoma, Photochemical & Photobiological Sciences 11 (2012) 69-73.
[254] A.Z. Fernandis, M.R. Wenk, Lipid-based biomarkers for cancer, Journal of Chromatography B: Analytical Technologies in the Biomedical and Life Sciences 877 (2009) 2830-2835.
[255] M. Hilvo, C. Denkert, L. Lehtinen, B. Müller, S. Brockmöller, T. Seppänen-Laakso, J. Budczies, E. Bucher, L. Yetukuri, S. Castillo, E. Berg, H. Nygren, M. Sysi-Aho, J.L. Griffin, O. Fiehn, S. Loibl, C. Richter-Ehrenstein, C. Radke, T. Hyötyläinen, O. Kallioniemi, K. Iljin, M. Orešič, Novel theranostic opportunities offered by characterization of altered membrane lipid metabolism in breast cancer progression, Cancer Research 71 (2011) 3236-3245.
[256] P.V. Escribá, J.M. González-Ros, F.M. Goñi, P.K.J. Kinnunen, L. Vigh, L. Sánchez-Magraner, A.M. Fernández, X. Busquets, I. Horváth, G. Barceló-Coblijn, Membranes: A meeting point for lipids, proteins and therapies: Translational Medicine, Journal of Cellular and Molecular Medicine 12 (2008) 829-875.
[257] M.P. Wymann, R. Schneiter, Lipid signalling in disease, Nat Rev Mol Cell Biol 9 (2008) 162-176.
[258] A.Z. Fernandis, M.R. Wenk, Lipid-based biomarkers for cancer, Journal of Chromatography B 877 (2009) 2830-2835.
[259] A. Carpinteiro, C. Dumitru, M. Schenck, E. Gulbins, Ceramide-induced cell death in malignant cells, Cancer Letters 264 (2008) 1-10.
[260] T.L. Yuan, L.C. Cantley, PI3K pathway alterations in cancer: Variations on a theme, Oncogene 27 (2008) 5497-5510.
[261] R.W. Ledeen, G. Wu, Thematic Review Series: Sphingolipids. Nuclear sphingolipids: metabolism and signaling, Journal of Lipid Research 49 (2008) 1176-1186.
[262] J. Suburu, Y.Q. Chen, Lipids and prostate cancer, Prostaglandins & Other Lipid Mediators 98 (2012) 1-10.
[263] E. Ackerstaff, K. Glunde, Z.M. Bhujwalla, Choline phospholipid metabolism: A target in cancer cells?, Journal of Cellular Biochemistry 90 (2003) 525-533.
[264] N. Panupinthu, H.Y. Lee, G.B. Mills, Lysophosphatidic acid production and action: Critical new players in breast cancer initiation and progression, British Journal of Cancer 102 (2010) 941-946.
[265] Z. Shen, M. Wu, P. Elson, A.W. Kennedy, J. Belinson, G. Casey, Y. Xu, Fatty acid composition of lysophosphatidic acid and lysophosphatidylinositol in plasma from patients with ovarian cancer and other gynecological diseases, Gynecologic Oncology 83 (2001) 25-30.

[266] M.L. Dória, A.S. Ribeiro, J. Wang, C.Z. Cotrim, P. Domingues, C. Williams, M.R. Domingues, L.A. Helguero, Fatty acid and phospholipid biosynthetic pathways are regulated throughout mammary epithelial cell differentiation and correlate to breast cancer survival, The FASEB Journal (2014).

[267] E.O. Aboagye, Z.M. Bhujwalla, Malignant transformation alters membrane choline phospholipid metabolism of human mammary epithelial cells, Cancer Research 59 (1999) 80-84.

[268] Y. Ohkawa, S. Miyazaki, K. Hamamura, M. Kambe, M. Miyata, O. Tajima, Y. Ohmi, Y. Yamauchi, K. Furukawa, Ganglioside GD3 enhances adhesion signals and augments malignant properties of melanoma cells by recruiting integrins to glycolipid-enriched microdomains, Journal of Biological Chemistry 285 (2010) 27213-27223.

[269] K. Hamamura, K. Furukawa, T. Hayashi, T. Hattori, J. Nakano, H. Nakashima, T. Okuda, H. Mizutani, H. Hattori, M. Ueda, T. Urano, K.O. Lloyd, Ganglioside GD3 promotes cell growth and invasion through p130Cas and paxillin in malignant melanoma cells, Proceedings of the National Academy of Sciences of the United States of America 102 (2005) 11041-11046.

[270] S.A. Saddoughi, P. Song, B. Ogretmen, Roles of bioactive sphingolipids in cancer biology and therapeutics, Sub-cellular biochemistry 49 (2008) 413-440.

[271] S. Riedl, B. Rinner, M. Asslaber, H. Schaider, S. Walzer, A. Novak, K. Lohner, D. Zweytick, In search of a novel target - Phosphatidylserine exposed by non-apoptotic tumor cells and metastases of malignancies with poor treatment efficacy, Biochimica et Biophysica Acta - Biomembranes 1808 (2011) 2638-2645.

[272] M.L. Dória, C.Z. Cotrim, C. Simões, B. Macedo, P. Domingues, M.R. Domingues, L.A. Helguero, Lipidomic analysis of phospholipids from human mammary epithelial and breast cancer cell lines, Journal of Cellular Physiology 228 (2013) 457-468.

[273] M.L. Dória, Z. Cotrim, B. MacEdo, C. Simões, P. Domingues, L. Helguero, M.R. Domingues, Lipidomic approach to identify patterns in phospholipid profiles and define class differences in mammary epithelial and breast cancer cells, Breast Cancer Research and Treatment 133 (2012) 635-648.

[274] K. Rass, J. Reichrath, UV Damage and DNA Repair in Malignant Melanoma and Nonmelanoma Skin Cancer, in: J. Reichrath (Ed.), Sunlight, Vitamin D and Skin Cancer, Springer New York, 2008, pp. 162-178.

[275] D. Leszczynski, S. Fagerholm, K. Leszczynski, The Effects of the Broadband UVA Radiation on Myeloid Leukemia Cells: The Possible Role of Protein Kinase C in Mediation of UVA-lnduced Effects, Photochemistry and Photobiology 64 (1996) 936-942.

[276] E.G. Bligh, W.J. Dyer, A rapid method of total lipid extraction and purification, Can J Biochem Physiol 37 (1959) 911-917.

[277] E. Maciel, B.M. Neves, D. Santinha, A. Reis, P. Domingues, M. Teresa Cruz, A.R. Pitt, C.M. Spickett, M.R.M. Domingues, Detection of phosphatidylserine with a modified polar head group in human keratinocytes exposed to the radical generator AAPH, Archives of Biochemistry and Biophysics 548 (2014) 38-45.

[278] R. Ferreira, G. Guerra, A.I. Padrao, T. Melo, R. Vitorino, J.A. Duarte, F. Remiao, P. Domingues, F. Amado, M.R. Domingues, Lipidomic characterization of streptozotocin-induced heart mitochondrial dysfunction, Mitochondrion 13 (2013) 762-771.

[279] C. Simões, P. Domingues, R. Ferreira, F. Amado, J.A. Duarte, R. Vitorino, M.J. Neuparth, C. Nunes, C. Rocha, I. Duarte, M.R. Domingues, Remodeling of liver phospholipidomic profile in streptozotocin-induced diabetic rats, Archives of Biochemistry and Biophysics 538 (2013) 95-102.

[280] S. Aued-Pimentel, J.H. Lago, M.H. Chaves, E.E. Kumagai, Evaluation of a methylation procedure to determine cyclopropenoids fatty acids from Sterculia striata St. Hil. Et Nauds seed oil, J Chromatogr A 1054 (2004) 235-239.

[281] P.K. Smith, R.I. Krohn, G.T. Hermanson, A.K. Mallia, F.H. Gartner, M.D. Provenzano, E.K. Fujimoto, N.M. Goeke, B.J. Olson, D.C. Klenk, Measurement of protein using bicinchoninic acid, Analytical Biochemistry 150 (1985) 76-85.

[282] I. Romero-Calvo, B. Ocon, P. Martinez-Moya, M.D. Suarez, A. Zarzuelo, O. Martinez-Augustin, F.S. de Medina, Reversible Ponceau staining as a loading control alternative to actin in Western blots, Analytical Biochemistry 401 (2010) 318-320.

[283] N. Zaidi, L. Lupien, N.B. Kuemmerle, W.B. Kinlaw, J.V. Swinnen, K. Smans, Lipogenesis and lipolysis: The pathways exploited by the cancer cells to acquire fatty acids, Progress in Lipid Research 52 (2013) 585-589.

[284] E. Rysman, K. Brusselmans, K. Scheys, L. Timmermans, R. Derua, S. Munck, P.P. Van Veldhoven, D. Waltregny, V.W. Daniels, J. Machiels, F. Vanderhoydonc, K. Smans, E. Waelkens, G. Verhoeven, J.V. Swinnen, De novo lipogenesis protects cancer cells from free radicals and chemotherapeutics by promoting membrane lipid saturation, Cancer Res 70 (2010) 8117-8126.

[285] L.N. Andrade, T.M. de Lima, R. Curi, A.M. Castrucci, Toxicity of fatty acids on murine and human melanoma cell lines, Toxicol In Vitro 19 (2005) 553-560.

[286] M.J. Newman, Inhibition of carcinoma and melanoma cell growth by type 1 transforming growth factor beta is dependent on the presence of polyunsaturated fatty acids, Proc Natl Acad Sci U S A 87 (1990) 5543-5547.

[287] Y.-A. Moon, N.A. Shah, S. Mohapatra, J.A. Warrington, J.D. Horton, Identification of a Mammalian Long Chain Fatty Acyl Elongase Regulated by Sterol Regulatory Element-binding Proteins, Journal of Biological Chemistry 276 (2001) 45358-45366.

[288] A. Kihara, Very long-chain fatty acids: elongation, physiology and related disorders, Journal of Biochemistry 152 (2012) 387-395.

[289] G. Balogh, M. Péter, G. Liebisch, I. Horváth, Z. Török, E. Nagy, A. Maslyanko, S. Benkő, G. Schmitz, J.L. Harwood, L. Vígh, Lipidomics reveals membrane lipid remodelling and release of potential lipid mediators during early stress responses in a murine melanoma cell line, Biochimica et Biophysica Acta (BBA) - Molecular and Cell Biology of Lipids 1801 (2010) 1036-1047.

[290] M. Beloueche-Babari, V. Arunan, L.E. Jackson, N. Perusinghe, S.Y. Sharp, P. Workman, M.O. Leach, Modulation of melanoma cell phospholipid metabolism in response to heat shock protein 90 inhibition, 2010.

[291] T.E. Merchant, P. Meneses, L.W. Gierke, W. Den Otter, T. Glonek, 31P Magnetic resonance phospholipid profiles of neoplastic human breast tissues, British Journal of Cancer 63 (1991) 693-698.

[292] M. Sterin, J.S. Cohen, I. Ringel, Hormone sensitivity is reflected in the phospholipid profiles of breast cancer cell lines, Breast Cancer Research and Treatment 87 (2004) 1-11.

[293] O.T.T. Le, T.T.N. Nguyen, S.Y. Lee, Phosphoinositide turnover in Toll-like receptor signaling and trafficking, BMB Reports 47 (2014) 361-368.
[294] A.K. Ferreira, R. Meneguelo, F.L. Marques, A. Radin, O.M. Filho, S.C. Neto, G.O. Chierice, D.A. Maria, Synthetic phosphoethanolamine a precursor of membrane phospholipids reduce tumor growth in mice bearing melanoma B16-F10 and in vitro induce apoptosis and arrest in G2/M phase, Biomed Pharmacother 66 (2012) 541-548.
[295] A. Cör, J. Pižem, N. Gale, The expression of Bcl-2 and pro-caspase 3 in head and neck sqamous cell carcinoma, ZDRAV VESTN 71 (2002) III-39-43.
[296] T. Takata, F. Tanaka, T. Yamada, K. Yanagihara, Y. Otake, Y. Kawano, T. Nakagawa, R. Miyahara, H. Oyanagi, K. Inui, H. Wada, Clinical significance of caspase-3 expression in pathologic-stage I, nonsmall-cell lung cancer, Int J Cancer 96 Suppl (2001) 54-60.
[297] R.P. Wong, W.P. Tsang, P.Y. Chau, N.N. Co, T.Y. Tsang, T.T. Kwok, p53-R273H gains new function in induction of drug resistance through down-regulation of procaspase-3, Mol Cancer Ther 6 (2007) 1054-1061.
[298] F. Ponten, B. Berne, Z.P. Ren, M. Nister, J. Ponten, Ultraviolet light induces expression of p53 and p21 in human skin: effect of sunscreen and constitutive p21 expression in skin appendages, J Invest Dermatol 105 (1995) 402-406.
[299] D. Vucic, H.R. Stennicke, M.T. Pisabarro, G.S. Salvesen, V.M. Dixit, ML-IAP, a novel inhibitor of apoptosis that is preferentially expressed in human melanomas, Current Biology 10 (2000) 1359-1366.
[300] P.M. Henson, D.L. Bratton, V.A. Fadok, Apoptotic cell removal, Current Biology 11 (2001) R795-R805.
[301] J. Savill, V. Fadok, Corpse clearance defines the meaning of cell death, Nature 407 (2000) 784-788.
[302] A. Devitt, O.D. Moffatt, C. Raykundalia, J.D. Capra, D.L. Simmons, C.D. Gregory, Human CD14 mediates recognition and phagocytosis of apoptotic cells, Nature 392 (1998) 505-509.
[303] C.A. Ogden, A. DeCathelineau, P.R. Hoffmann, D. Bratton, B. Fadok, V.A. Ghebrehiwet, P.M. Henson, C1q and mannose binding lectin engagement of cell surface calreticulin and CD91 initiates macropinocytosis and uptake of apoptotic cells, Journal of Experimental Medicine 194 (2001) 781-795.
[304] N. Platt, H. Suzuki, Y. Kurihara, T. Kodama, S. Gordon, Role for the class A macrophage scavenger receptor in the phagocytosis of apoptotic thymocytes in vitro, Proceedings of the National Academy of Sciences of the United States of America 93 (1996) 12456-12460.
[305] Y. Ren, R.L. Silverstein, J. Allen, J. Savill, CD36 gene transfer confers capacity for phagocytosis of cells undergoing apoptosis, Journal of Experimental Medicine 181 (1995) 1857-1862.
[306] M.L. Albert, S.F.A. Pearce, L.M. Francisco, B. Sauter, P. Roy, R.L. Silverstein, N. Bhardwaj, Immature dendritic cells phagocytose apoptotic cells via αvβ 5 and CD36, and cross-present antigens to cytotoxic T lymphocytes, Journal of Experimental Medicine 188 (1998) 1359-1368.
[307] S. Krahling, M.K. Callahan, P. Williamson, R.A. Schlegel, Exposure of phosphatidylserine is a general feature in the phagocytosis of apoptotic lymphocytes by macrophages, Cell Death and Differentiation 6 (1999) 183-189.

[308] K. Asano, M. Miwa, K. Miwa, R. Hanayama, H. Nagase, S. Nagata, M. Tanaka, Masking of phosphatidylserine inhibits apoptotic cell engulfment and induces autoantibody production in mice, Journal of Experimental Medicine 200 (2004) 459-467.

[309] V.N. Bochkov, Inflammatory profile of oxidized phospholipids, Thrombosis and Haemostasis 97 (2007) 348-354.

[310] G. Subbanagounder, Y. Deng, C. Borromeo, A.N. Dooley, J.A. Berliner, R.G. Salomon, Hydroxy alkenal phospholipids regulate inflammatory functions of endothelial cells, Vascular Pharmacology 38 (2002) 201-209.

[311] G. Subbanagounder, N. Leitinger, D.C. Schwenke, J.W. Wong, H. Lee, C. Rizza, A.D. Watson, K.F. Faull, A.M. Fogelman, J.A. Berliner, Determinants of bioactivity of oxidized phospholipids - Specific oxidized fatty acyl groups at the sn-2 position, Arteriosclerosis Thrombosis and Vascular Biology 20 (2000) 2248-2254.

[312] A.A. Korotaeva, L.M. Samokhodskaya, V.N. Bochkov, Inhibition of bacterial lipopolysaccharide-induced inflammatory effects by lipid peroxidation products, Biochemistry (Moscow) Supplement Series B: Biomedical Chemistry 1 (2007) 225-229.

[313] T. Harel-Adar, T.B. Mordechai, Y. Amsalem, M.S. Feinberg, J. Leor, S. Cohen, Modulation of cardiac macrophages by phosphatidylserine-presenting liposomes improves infarct repair, Proceedings of the National Academy of Sciences (2011).

[314] M. Yeom, D.-H. Hahm, B.-J. Sur, J.-J. Han, H.-J. Lee, H.-I. Yang, K.S. Kim, Phosphatidylserine inhibits inflammatory responses in interleukin-1β–stimulated fibroblast-like synoviocytes and alleviates carrageenan-induced arthritis in rat, Nutrition Research 33 (2013) 242-250.

[315] H.M. Ma, Z. Wu, H. Nakanishi, Phosphatidylserine-containing liposomes suppress inflammatory bone loss by ameliorating the cytokine imbalance provoked by infiltrated macrophages, Laboratory Investigation 91 (2011) 921-931.

[316] Y. Aramaki, R. Matsuno, S. Tsuchiya, Involvement of p38 MAP Kinase in the Inhibitory Effects of Phosphatidylserine Liposomes on Nitric Oxide Production from Macrophages Stimulated with LPS, Biochemical and Biophysical Research Communications 280 (2001) 982-987.

[317] Y. Aramaki, F. Nitta, R. Matsuno, Y. Morimura, S. Tsuchiya, Inhibitory Effects of Negatively Charged Liposomes on Nitric Oxide Production from Macrophages Stimulated by LPS, Biochemical and Biophysical Research Communications 220 (1996) 1-6.

[318] R. Friedl, I. Pichler, P. Spieckermann, T. Moeslinger, Oxidized phospatidylcholine but not native phosphatidylcholine inhibits inducible nitric oxide synthase in RAW 264.7 macrophages, Life Sciences 78 (2006) 1586-1591.

[319] M. Seyerl, S. Blüml, S. Kirchberger, V.N. Bochkov, O. Oskolkova, O. Majdic, J. Stöckl, Oxidized phospholipids induce anergy in human peripheral blood T cells, European Journal of Immunology 38 (2008) 778-787.

[320] A.A. Birukova, P. Fu, S. Chatchavalvanich, D. Burdette, O. Oskolkova, V.N. Bochkov, K.G. Birukov, Polar head groups are important for barrier-protective effects of oxidized phospholipids on pulmonary endothelium, American Journal of Physiology - Lung Cellular and Molecular Physiology 292 (2007) L924-L935.

[321] F. Aktan, iNOS-mediated nitric oxide production and its regulation, Life Sciences 75 (2004) 639-653.

[322] Z. Guan, S.Y. Buckman, L.D. Springer, A.R. Morrison, Both p38αMAPK and JNK/SAPK Pathways Are Important for Induction of Nitric-oxide Synthase by Interleukin-1β in Rat Glomerular Mesangial Cells, Journal of Biological Chemistry 274 (1999) 36200-36206.